BB-3.4.3-5-101

EVALUATION OF AS-203 LOW GRAVITY ORBITAL EXPERIMENT

13 JANUARY 1967

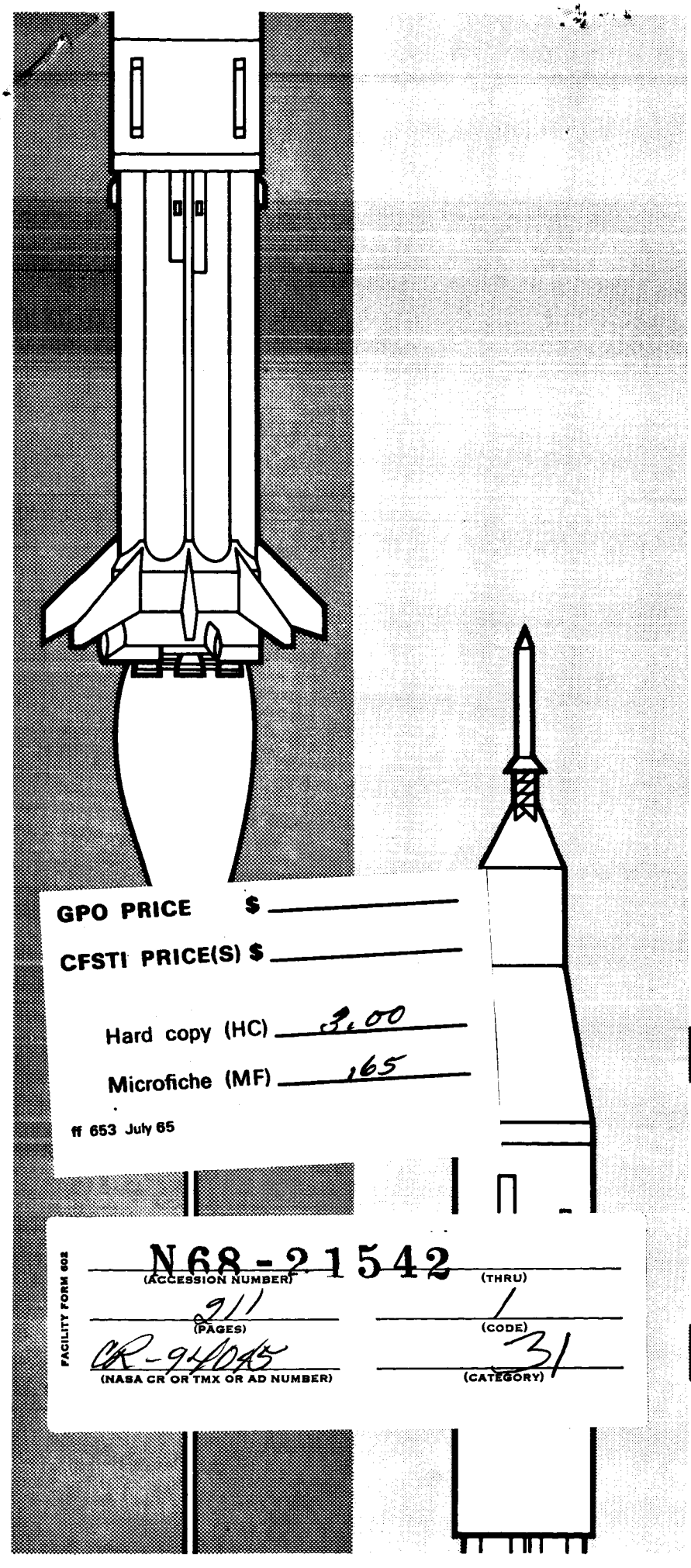

CONTRACT NAS8-4016
SCHEDULE II, VEHICLE SYSTEMS INTEGRATION

SPACE DIVISION CHRYSLER CORPORATION

TECHNICAL REPORT HSM-R421-67 BB-3.4.3-5-101

EVALUATION OF AS-203

LOW GRAVITY ORBITAL EXPERIMENT

CONTRACT NAS8-4016
SCHEDULE II, VEHICLE
SYSTEMS INTEGRATION

13 January 1967

FLUID MECHANICS AND THERMODYNAMICS RESEARCH SECTION

SYSTEMS SIMULATION AND INTEGRATION BRANCH

SPACE DIVISION CHRYSLER CORPORATION

HUNTSVILLE OPERATIONS

ABSTRACT

This report presents the orbital flight results and detailed evaluation of the low gravity liquid hydrogen experiments conducted on the Saturn IB vehicle AS-203. The performance of various S-IVB stage subsystems and special low gravity instrumentation was also evaluated. This experiment verified that satisfactory performance can be obtained from the Saturn V/S-IVB propellant control and J-2 engine thermal conditioning systems. Additional information on heat transfer in a closed container and fluid behavior during rapid tank depressurization is also presented.

TABLE OF CONTENTS

TABLE OF CONTENTS (Cont'd)

LIST OF ILLUSTRATIONS

LIST OF ILLUSTRATIONS (Cont'd)

LIST OF ILLUSTRATIONS (Cont'd)

LIST OF ILLUSTRATIONS (Cont'd)

LIST OF ILLUSTRATIONS (Cont'd)

LIST OF ILLUSTRATIONS (Cont'd)

LIST OF TABLES

SUMMARY

The Saturn IB vehicle AS-203 was launched into a nominal 100 nautical mile circular earth orbit on July 5, 1966. The primary purpose of the flight was to verify the performance of the S-IVB propellant control systems and the propulsion engine chilldown systems in a low gravity environment by executing a programmed sequence of events designed to closely simulate the Saturn V Lunar Mission. The flight data have been evaluated to (1) determine the vehicle and propellant conditions actually experienced during the flight, (2) verify that the Saturn V Lunar Mission was adequately simulated and that the S-IVB systems performed satisfactorily under the simulated conditions, and (3) determine significant results concerning basic fluid behavior and heat transfer under reduced gravity conditions. The results of the evaluation are presented in detail in this report.

The vehicle acceleration level during the various experiment events was of the same approximate magnitude as expected during similar events on the Saturn V mission. In general, the flight demonstrated that the slosh baffle, deflector, and other devices added for propellant control performed adequately. The liquid hydrogen was maintained in the desired location in the tank at all times, and only vapor was vented during the portion of the flight that simulated the Saturn V mission. The performance of the systems that thermally condition the J-2 engine feed lines and engine hardware was verified for both liquid oxygen and liquid hydrogen. The flight also provided significant data and information concerning the rapid depressurization of a cryogenic (hydrogen) tank in a low gravity environment, the behavior of liquid hydrogen when all vehicle longitudinal thrusting is terminated, and the pressure rise rate in a closed hydrogen container in space.

The following specific conclusions are based on the detailed evaluation of the flight data.

1. Liquid dynamic phenomena, such as sloshing, are amplified when the vehicle acceleration is reduced, but these disturbances can be controlled by baffles and the proper timing of the thrust changes.

2. The low level acceleration presently designed for the Saturn V/S-IVB stage is sufficient for maintaining propellant control during orbital flight.

3. The chilldown experiments demonstrated that the Saturn V/S-IVB main propulsion engine can be adequately conditioned for orbital restart.

4. The liquids and/or gases returned to the main propellant tanks by the present engine thermal conditioning system do not noticeably disturb the liquid position in those tanks.

5. The presence of liquid in the engine suction ducts during the orbital coast phase of the mission was unexpected and substantially aided the chill of the engine feed systems.

6. The hydrogen thermal conditioning system operates satisfactorily with zero net positive suction head for the recirculation pump.

7. During the orbital phase of the mission, the vehicle showed a tendency to pitch nose up, even when longitudinal thrusting was terminated. This behavior could not be adequately explained.

8. The free coast experiment demonstrated that the drag force acting on the vehicle caused the liquid propellants to move toward the forward end of the tanks. The low level acceleration subsequently applied to the vehicle was adequate for resettling the liquid.

9. Rapid depressurization of a cryogenic tank containing saturated propellants under low gravity conditions causes a severe disturbance of the liquid surface thereby creating conditions that could result in loss of control of the liquid position in the tank.

10. The non-propulsive vent system produced a torque on the vehicle that greatly increased attitude control system activity. However, the vent system unbalanced thrust was within design tolerance.

11. The liquid hydrogen boiloff during orbital flight indicates that the S-IVB fuel tank effective sidewall thermal conductivity is considerably greater than the design value.

12. Commonly accepted free convection heat transfer correlations may be used with reasonable confidence at reduced gravity conditions.

13. The TV was invaluable in determining the behavior of the fluid in a low gravity environment. It would have been extremely difficult to reconstruct the propellant motions solely on the basis of data from other instrumentation.

14. Instrumentation indicated a considerable loss of helium from the LOX tank pressurant bottles immediately after J-2 cutoff and during the fourth revolution. The reason for this loss could not be explained. A similar loss on the Saturn V/S-IVB stage could be detrimental to the success of the mission.

15. **An unexpected cycling of the S-IVB continuous vent regulator valve occurred throughout the orbital phase of the flight. These oscillations did not affect the valve's specified function. However, the valve was not designed to withstand the large number of cycles experienced during this flight. Therefore, a modification or redesign of the valve should be considered.**

16. The quality meter installed in the S-IVB continuous vent line did not yield data that were useful in the evaluation of the fluid quality being vented from the fuel tank. The meter did respond to changes in fluid conditions, and, if modified, it may be useful for similar applications in the future.

17. Three types of experimental low gravity vapor-liquid sensors were installed in the S-IVB fuel tank. The only type of sensor that operated satisfactorily in a low gravity environment was the variable resistance type transducer employed in the Centaur vehicle. Both the Douglas and Transonics designed capacitance type transducers failed to indicate the change from wet to dry conditions within a reasonable time.

18. The performance of 119 of the 129 pressure sensors on the S-IVB stage was satisfactory throughout the flight. Three sensors failed prior to liftoff and seven others failed during boost flight. The most critical of these failures was the J-2 engine fuel pump inlet pressure sensor which apparently read erroneously during S-IVB powered flight.

19. Of the 207 temperature sensors on the S-IVB stage, four failed prior to liftoff, one during powered flight, and four during the orbital period. None of these failures were critical.

20. The fifteen fluid temperature sensors modified to prevent liquid trapping under low gravity conditions were more reliable in indicating surrounding fluid temperature than were the unmodified sensors. The modified temperature sensors were also more useful in distinguishing liquid from vapor than any of the vapor-liquid sensors except the Centaur design.

21. The low gravity longitudinal accelerometer located in the AS-203 Instrument Unit failed early in the first orbit. However, data were received during the first pass over the Canary Islands that agreed reasonably well with the vehicle acceleration calculated from continuous vent data.

This evaluation was performed for the Fluid Mechanics and Thermodynamics Branch, Propulsion Division, Propulsion and Vehicle Engineering Laboratory of the Marshall Space Flight Center, under Schedule II, Modification 292, MSFC-1, Change Order Amendment 21, Contract NAS8-4016.

SECTION I. INTRODUCTION

The present concept of the Saturn Apollo mission requires that the Saturn V/S-IVB stage must coast for an extended period in earth orbit and then restart to place the Apollo in a translunar trajectory. To accomplish this particular mission, the propellant location must be controlled in a low gravity environment for periods of up to 4 1/2 hours, and the J-2 engine propellant feed systems must be thermally conditioned prior to restart. One requirement for propellant control is dictated by the necessity for pressure relief of the hydrogen tank during the orbital coast period. Thus, the propellant must be maintained away from the vent outlet to prevent entrainment of liquid in the vent flow. A second requirement for propellant control is established by the necessity to minimize disturbances to the vehicle that may impose excessive demands on the control system. Such disturbances may be caused by large amplitude liquid motion following sudden changes in vehicle acceleration or by unbalanced vent forces. Still a third requirement arises from the necessity to provide liquid at the engine suction ducts prior to the restart. The thermal conditioning of the J-2 engine is complicated by the two-phase flow problem and the complex geometry of the system. Ground tests indicated that the system could probably be adequately conditioned in the orbital environment within the required time duration. However, extrapolation of ground test performance data to the low gravity conditions experienced in orbit was a questionable procedure.

Data on many fluid behavioral phenomena in a low gravity environment are relatively limited and are, for the most part, based upon scale model tests in facilities providing low gravity test durations of only a few seconds. The model tests have provided valuable data on fundamental laws and the scaling parameters applicable to various individual phenomena. However, in the full scale vehicle many phenomena occur simultaneously and are further influenced by the particular vehicle hardware configuration and transient operating characteristics. It is not possible to adequately duplicate all phenomena that may be present and simultaneously superimpose the vehicle transients in model tests. For this reason, a full scale orbital test was considered essential to confirm the design of the S-IVB propellant control and J-2 engine thermal conditioning systems. The AS-203 vehicle was designated for this purpose.

The Saturn IB/S-IVB vehicle AS-203 was launched from Cape Kennedy on July 5, 1966, into a nominal 100 nautical mile circular earth orbit and successfully executed a programmed sequence of events designed primarily to simulate the orbital phase of the Saturn V Lunar Mission. In addition, the flight provided substantial additional data concerning the behavior of a cryogenic liquid in a reduced gravity environment.

SECTION II. BACKGROUND

A. EXPERIMENT OBJECTIVES

The AS-203 experiment had two basic objectives:

1. The primary objective of the flight was to verify the low gravity performance of the S-IVB propellant control and engine thermal conditioning systems required for the Saturn V Lunar Mission.

2. A secondary objective was to obtain data on heat transfer and fluid behavior under reduced gravity conditions that would be applicable to other vent systems and to the design of future cryogenic stages.

B. VEHICLE MODIFICATIONS

To accomplish the objectives of the flight, a standard Saturn IB vehicle was modified by replacing the Apollo command and service modules with an aerodynamic nose cone (see figure II-1). The vehicle payload was the liquid remaining in the S-IVB propellant tanks at insertion into orbit. Payload limitations of the Saturn IB vehicle would not permit restarting the J-2 engine or delivering Saturn V propellant loads into orbit. Since the problems associated with hydrogen were believed to be more critical than with oxygen, it was decided to duplicate the Saturn V hydrogen tank liquid level and conditions as closely as possible. This was accomplished by off-loading the LOX tank so that at insertion into orbit only 5,000 lb of LOX and 19,100 lb of LH_2 remained in the tanks. The corresponding liquid levels are shown in figure II-2. The LOX residual provided a liquid depth of about seven inches above the recirculation pump inlet. Several systems were added to the S-IVB stage and many modifications were made to provide the capability of performing the Saturn V orbital functions. The new systems and modifications are also shown in figure II-2 and will be discussed in the following paragraphs.

To obtain the desired data, additional instrumentation and a TV system were installed in the hydrogen tank of the S-IVB stage. The instrumentation added to the S-IVB, in excess of the normal R & D flight instrumentation, included:

57 temperature sensors	3 calorimeters	Power
9 pressure sensors	1 voltage indicator	to
7 liquid-vapor sensors	1 amperage indicator	TV
4 event indicators	1 quality meter	System
5 accelerometers (located in I. U.)		

Figure II-3 shows the location and type of all instrumentation in the S-IVB propellant tanks and propellant systems. Figure II-4 shows the location of the temperature sensors on the hydrogen tank sidewall. Additional descriptions of the AS-203 peculiar instrumentation are given by reference 1. Section VIII of this report discusses certain significant operational characteristics of some of the instruments that were observed during the flight.

The TV system consisted of two cameras mounted in the manhole cover of the liquid hydrogen tank providing real time TV coverage at the rate of 30 frames per second. The television system was considered mandatory to the success of the orbital experiment. Therefore, two cameras were included in the TV system primarily for increased reliability. The field of view of the cameras overlapped with the LH_2 suction duct being visible in both. Camera number one failed prior to liftoff. The viewing angles of camera number two are shown in figure II-5. The ground stations receiving the TV picture were Corpus Christi, Texas, the Kennedy Space Center, Bermuda, and Carnarvon, Australia. The TV reception areas of the first three stations mentioned overlapped giving a continuous coverage from Corpus Christi to Bermuda (about 14 minutes) on most passes. The maximum continuous telemetry reception time was slightly longer (about 17 minutes) beginning at Guaymas, Mexico, and lasting through Bermuda. Because of this extended continuous coverage, most of the flight events were programmed to occur as the vehicle passed over the North American Continental area.

To control the propellant, the vehicle was positively accelerated from liftoff until the end of the second orbit. During S-IB/S-IVB separation, the acceleration was provided by solid propellant ullage rockets whose firing time overlapped thrust tailoff on the S-IB stage and thrust buildup on the S-IVB stage. A hydrogen tank continuous vent system and a LOX ullage thruster system were added to the S-IVB stage to provide axial thrusting during the orbital phase of the flight. Passive control devices such as a baffle, a liquid deflector, and a special fuel suction duct anti-vortex unit were also added to the hydrogen tank. Table II-1 summarizes the modifications and/or new systems added to the S-IVB-203 stage and indicates the purpose of each.

C. SEQUENCE OF EVENTS

The vehicle was launched at 14:53:16 GMT on July 5, 1966, into a nominal 100 nautical mile circular earth orbit. In orbit, the vehicle was maintained in a velocity orientation (longitudinal axis perpendicular to local vertical) with the nose cone in the direction of flight and stage position I toward the earth at all times. The basic sequence of events following insertion, the time at which the various events occurred, and the tracking station coverage are presented by figure II-6. Reference 2 gives a more detailed sequence of events and also indicates programmed alternate sequences that would have been

employed if a failure occurred making completion of the primary sequence impossible. The entire planned primary sequence was successfully completed and none of the alternate sequences were utilized. The times given in figure II-6 are the actual times at which the events occurred. The orbital insertion occurred 2.8 seconds earlier than planned and a 48-second program update was made on the third pass over Carnarvon.

At insertion into orbit, the vehicle acceleration was reduced in steps. As the J-2 engine thrust decayed, auxiliary thrusting was initiated that produced a nominal acceleration of 5×10^{-4} g's. On the Saturn V vehicle this thrust is provided by two 70 lb Gemini ullage engines. Those engines are not present on the Saturn IB/S-IVB stage and the thrust on AS-203 was obtained by venting the LOX tank residual gases for 77 seconds after insertion into orbit. Prior to closing the LOX ullage thruster system, the continuous vent system was opened. The hydrogen gases were vented through the continuous vent system to produce a continuous longitudinal acceleration having a minimum value of 2×10^{-5} g's. The major concern during the orbital insertion phase of the mission was the behavior of the liquid when the vehicle acceleration was suddenly reduced.

Following orbital insertion, the continuous vent remained open, and the vehicle coasted with no events planned until the first pass over the United States. The mission objectives during the coast period were to determine if the small continuous venting acceleration could maintain control of the propellants and to obtain data on the orbital sloshing of the liquid hydrogen resulting from the action of the attitude control system. Toward the end of the first orbit, a chill of the engine feed lines and engine components was conducted on both the liquid oxygen and hydrogen sides. The chilldown experiment lasted for about five minutes. During the chill, the hydrogen venting was terminated and the fuel tank was partially repressurized to obtain a net positive suction head for the recirculation pump. While the hydrogen venting was suspended, the LOX thruster system was used to provide vehicle acceleration. Besides confirming the ability of the chill systems to thermally condition the engine feed systems, this test also provided data on the disturbances in the main propellant tanks caused by the gas or liquids being returned from the recirculation systems. The second orbit was similar to the first except that only a hydrogen feed system chill was conducted. The second hydrogen system chill was conducted without repressurizing the tank. This test concluded the experiments related to the Saturn V/S-IVB.

During the last two orbits, experiments were performed to obtain data applicable to an alternate venting system and to the design of future cryogenic stages. The exact experiments performed were a test to observe the behavior of liquid hydrogen when vehicle longitudinal thrust is terminated, rapid depressurization of the hydrogen tank in a low gravity environment, and a test to determine the rate of pressure rise in a closed cryogenic container in space.

TABLE II-1. S-IVB-203 STAGE MODIFICATIONS

Modification	Purpose
a. Continuous vent system	Provide longitudinal acceleration during orbital coast to maintain LH_2 in settled condition.
b. LOX ullage thruster system	Provide ullage thrust to simulate the Saturn V S-IVB 70 lb_f ullage control engines.
c. LH_2 tank anti-slosh baffle	Minimize LH_2 sloshing during powered flight, orbital insertion, and orbital coast.
d. LH_2 tank liquid deflector	Deflect LH_2 away from forward end of tank.
e. LOX tank anti-slosh baffle	Minimize LOX sloshing during powered flight.
f. Television systems	Provide real time visual monitoring of LH_2 behavior.
g. Manhole cover (redesigned)	Provide mounting area for television systems.
h. Instrumentation sensors	Provide additional data on vehicle condition and various fluid phenomena.
i. Instrumentation probe support structure	Mounting area for measurement sensors in LH_2 tank.
j. Helium repressurization sphere (ambient)	Provide LH_2 tank repressurization for simulated engine restart.
k. Aluminized mylar insulation on forward dome	Temperature regulation.
l. Additional batteries	Increase power capacity to satisfy television system and additional instrumentation requirements.
m. Anti-vortex assembly with movable top	Reduce suction duct blowback at J-2 cutoff, release trapped vapor in fuel suction duct.
n. LH_2 tank grid system	Provide reference markings on tank wall to assist in visual observations.
o. Deflector baffle cloth streamers	Assist in visual observations.

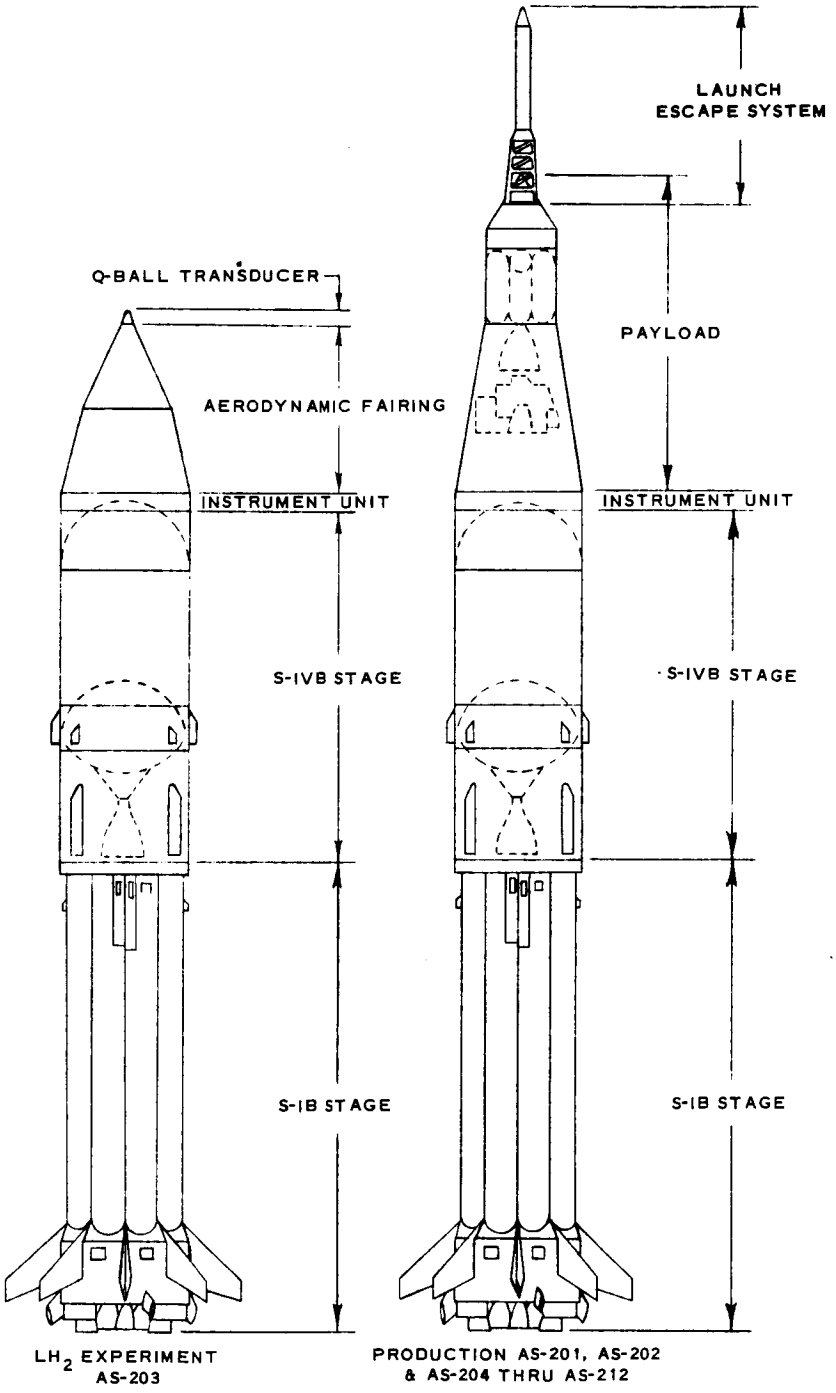

FIGURE II-1 AS-203 AND STANDARD SATURN IB VEHICLE CONFIGURATIONS

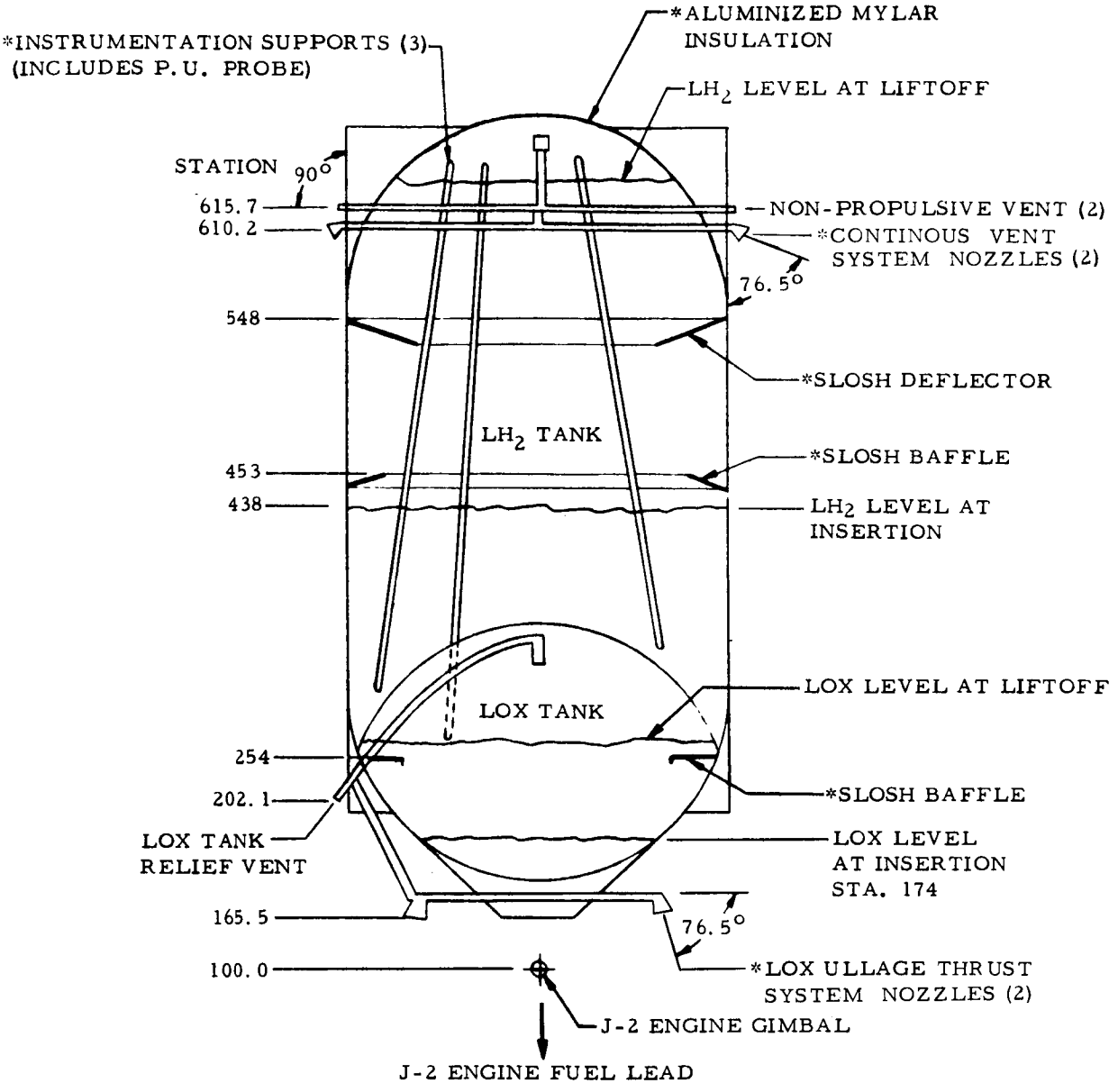

FIGURE II-2 SCHEMATIC OF S-IVB-203 STAGE MODIFICATIONS

FOLDOUT FRAME 1

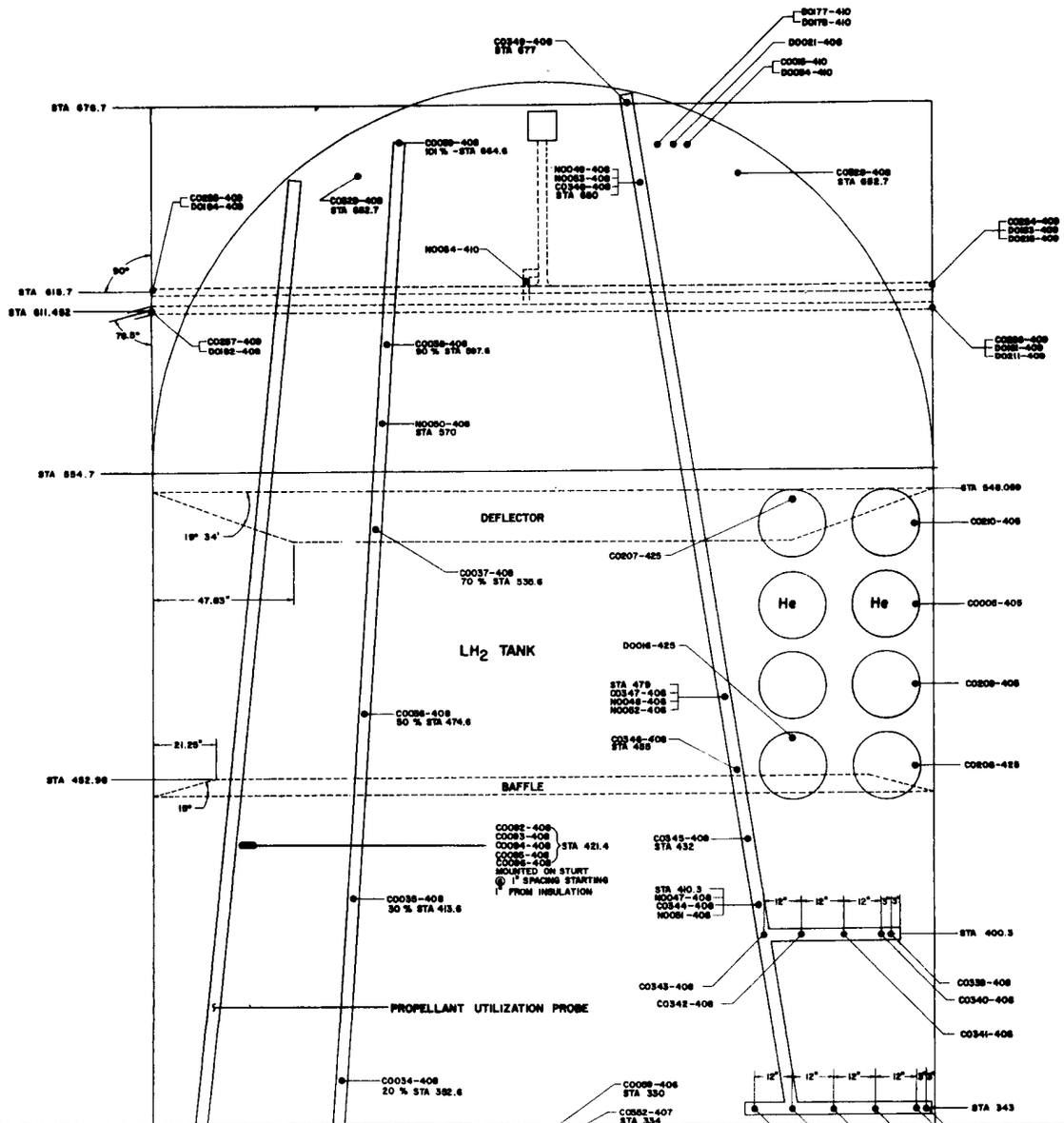

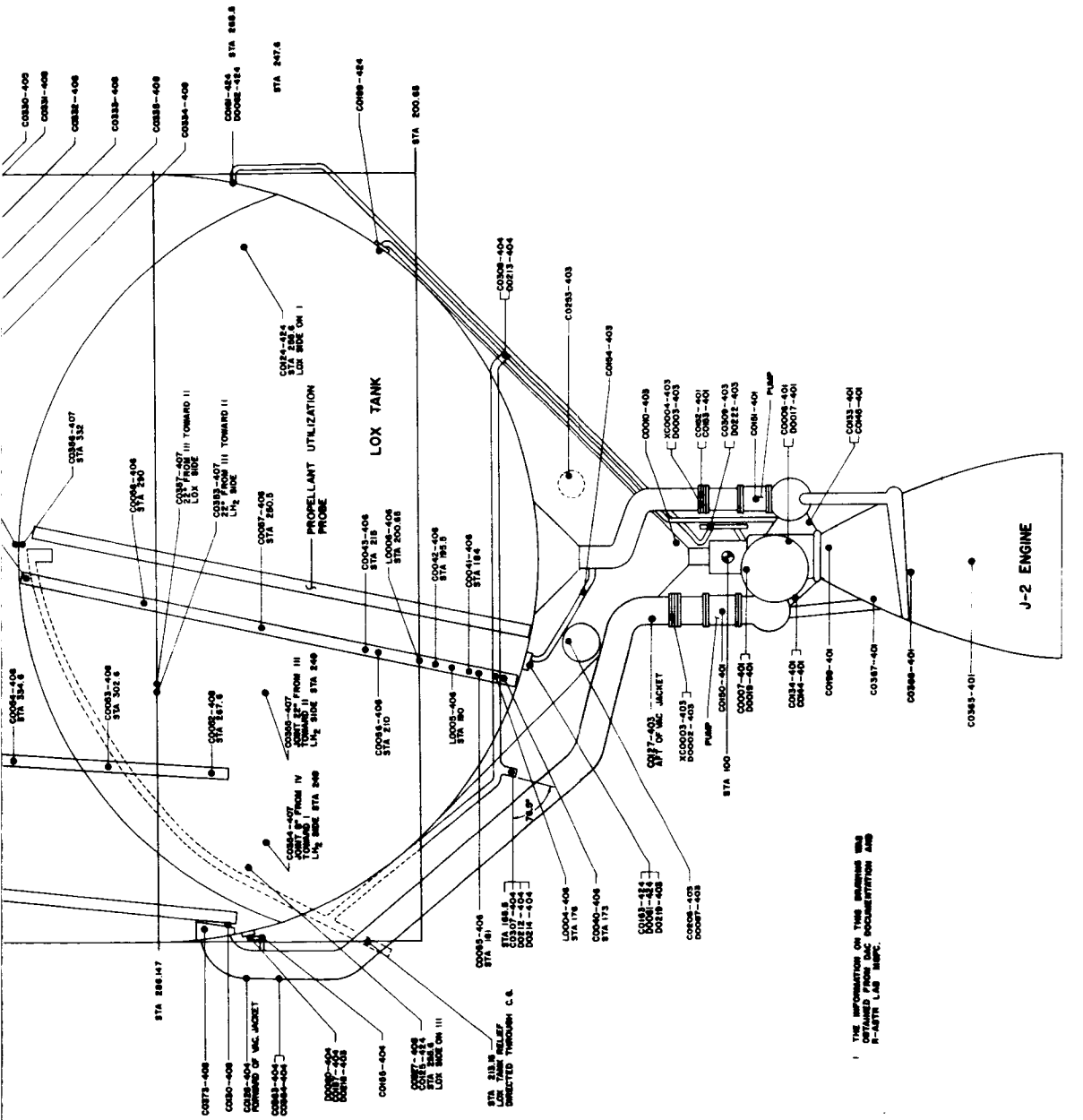

FIGURE II-3 S-IVB-203 INSTRUMENTATION SCHEMATIC

FOLDOUT FRAME 2

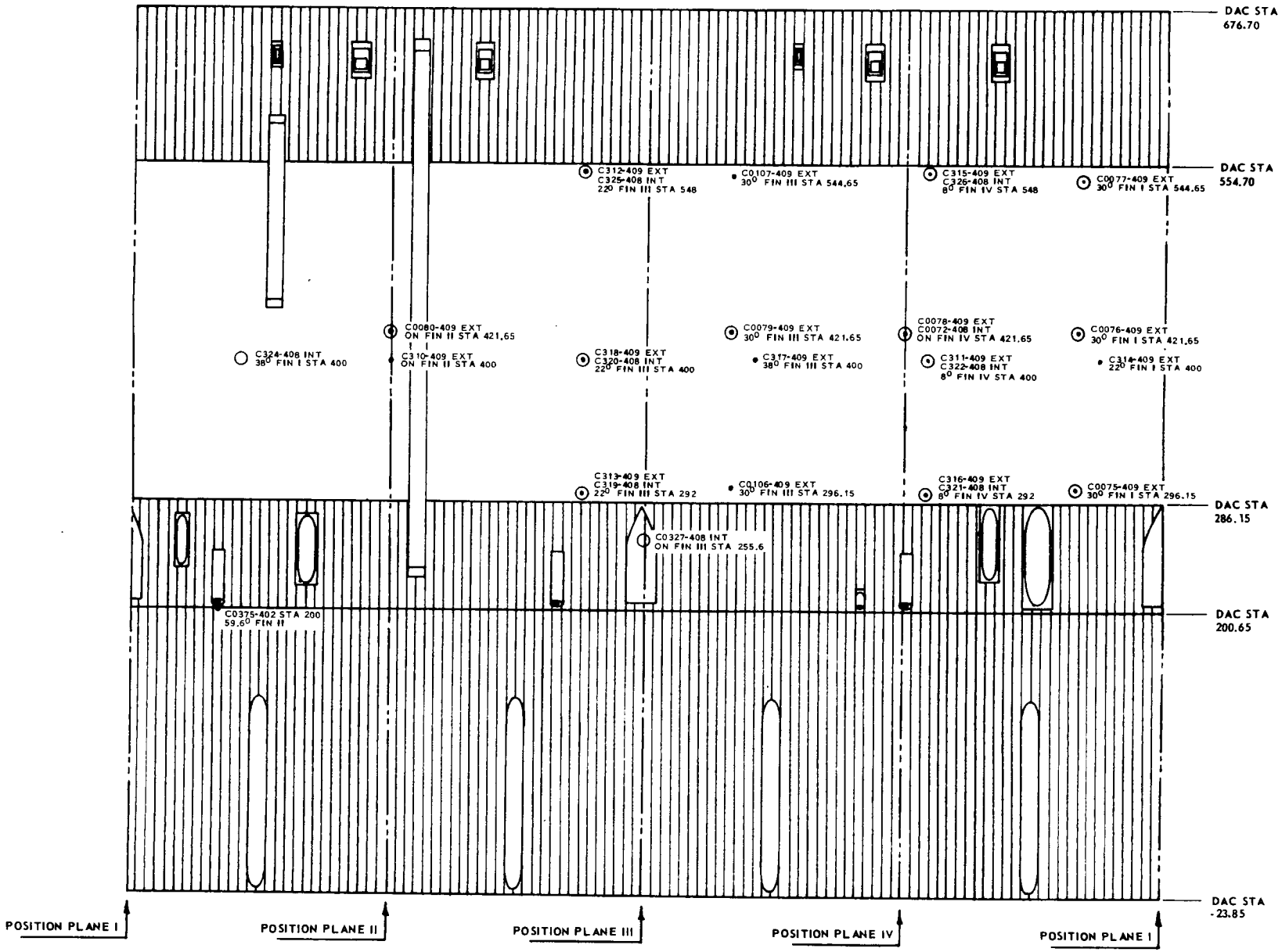

FIGURE II-4 S-IVB-203 FUEL TANK SIDEWALL INSTRUMENTATION SCHEMATIC

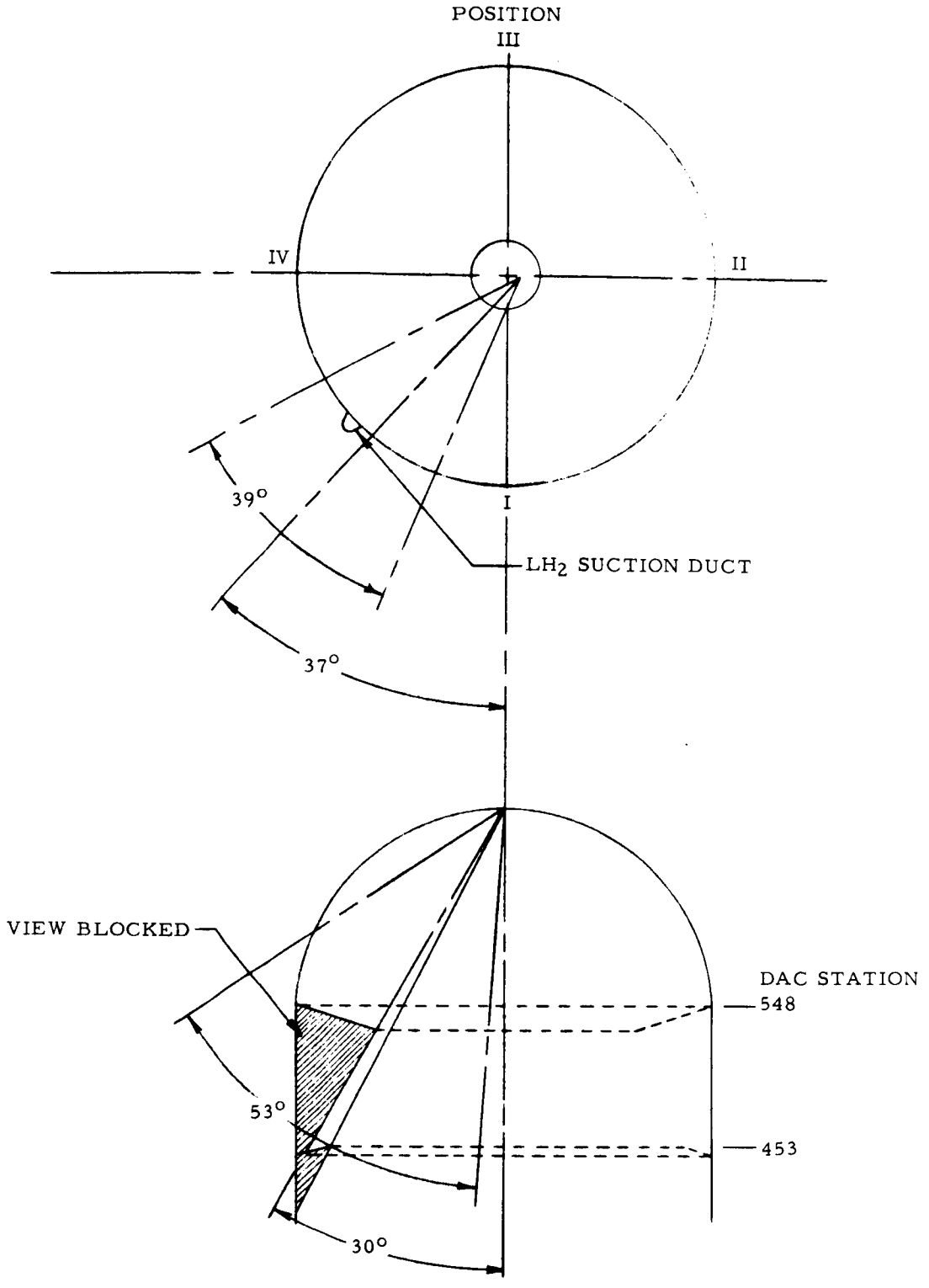

FIGURE II-5 TELEVISION VIEWING ANGLES (CAMERA #2)

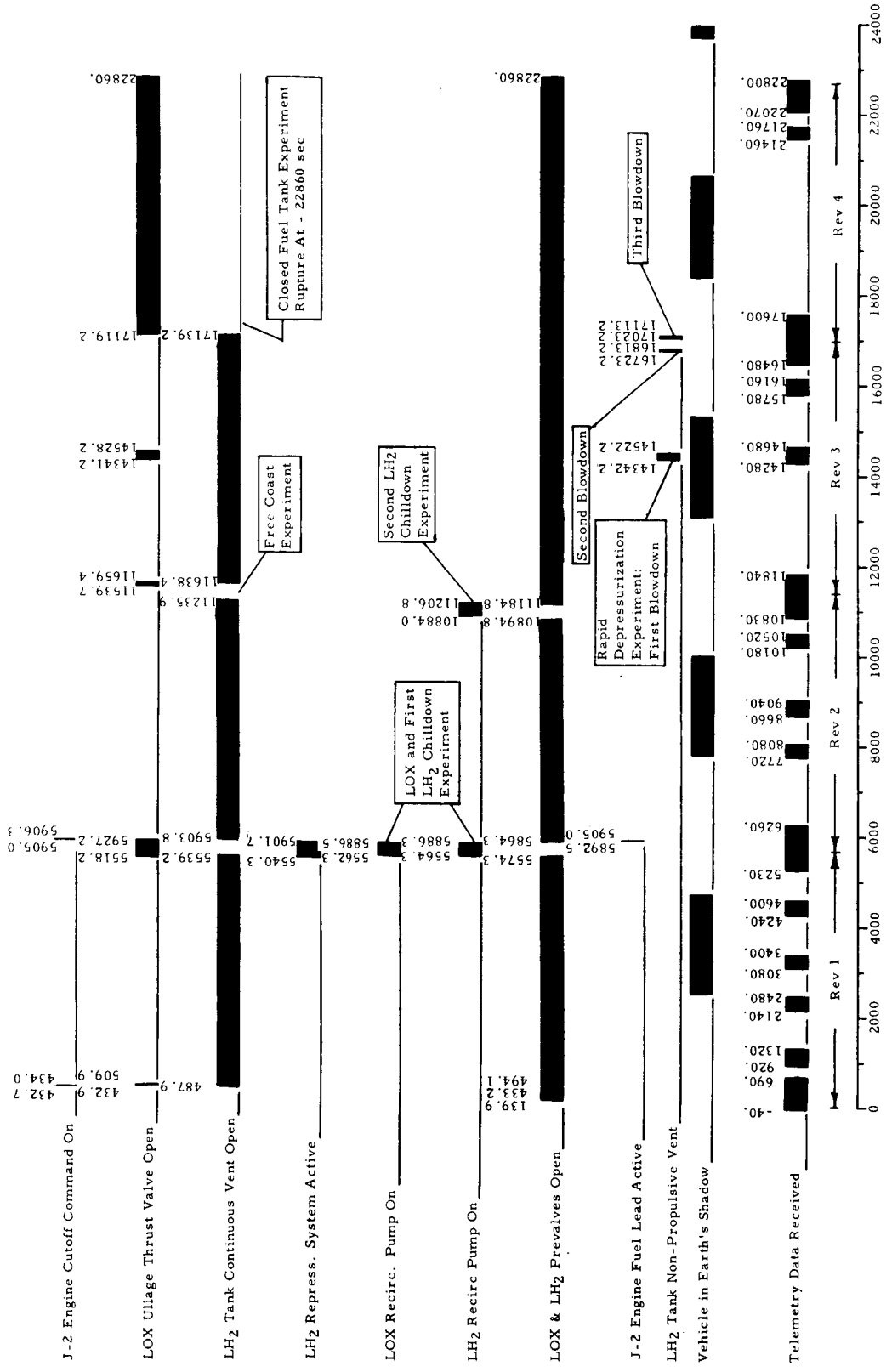

FIGURE II-6 SEQUENCE OF EVENTS, AS-203 LIQUID HYDROGEN ORBITAL EXPERIMENT

SECTION III. LIQUID DYNAMICS

Simple analyses and drop tower experiments have shown that following a sudden reduction of acceleration forces, liquid motions will be amplified. That is, any motion developed in the liquid mass under conditions of high acceleration will persist with increased amplitude when the acceleration is suddenly reduced. In addition, energy inputs to the liquid from various sources at J-2 engine shutdown may contribute to the resulting motion under the reduced gravity conditions. Prior to the AS-203 flight, it was suspected that one of the most severe low gravity propellant behavior problems would be controlling the liquid during the sudden decrease in vehicle acceleration at orbital insertion. Possible sources of liquid motion or energy input to the liquid during ascent and/or at J-2 shutdown are:

1. Propellant sloshing (major source)
2. Thermal convective patterns
3. Valve closure (back flow through suction duct)
4. Structural relaxation
5. Liquid compression
6. APS operation to correct for shutdown disturbances

Certain of the modifications described in section II and shown in figure II-2 were made to the S-IVB stage specifically for the purpose of minimizing and controlling the liquid motions arising from these energy sources.

A. BOOST FLIGHT

The propellant sloshing and thermal convection patterns developed in the liquid during powered flight represent potentially significant sources of motion within the liquid. Although this evaluation was primarily concerned with the orbital phase of the AS-203 flight, it is of interest to briefly review the propellant dynamics during powered flight since they establish the conditions contributing to the liquid dynamics at insertion.

At insertion into orbit the liquid hydrogen level was about ten inches below the slosh baffle attachment point (STA 448). Large amplitude propellant sloshing occurred during powered flight, but as the liquid drained past the

baffle (at about 270 seconds) the sloshing amplitude was damped as can be seen from the amplitude histories shown in figure III-1. However, in the 18 seconds of powered flight during which the liquid level was below the baffle, the slosh amplitude again increased. Immediately prior to J-2 engine cutoff, the first mode sloshing had a peak-to-peak amplitude of approximately three inches and a frequency of 0.80 cps. The LH_2 sloshing frequency during S-IVB powered flight is shown by figure III-2. The measured values of liquid frequency and amplitude at J-2 engine cutoff represent a maximum liquid velocity at the tank wall at that time of approximately 7.5 in./sec.

The additional instrumentation added to the LH_2 tank included three temperature rakes for the purpose of measuring sidewall boundary layer profiles under low gravity conditions. The presence of a temperature profile would indicate liquid motion toward the surface within the boundary layer. As shown by figure II-3, there was a three-inch gap between the tank wall and the first temperature sensor on the rakes. During powered flight, the temperature rakes did not indicate a significant radial temperature gradient in the liquid. Calculations show that under the combined conditions of heat flux and acceleration experienced during powered flight, the maximum expected boundary layer thickness would be approximately three inches. On the basis of the data from the temperature rakes, no specific conclusions can be made as to the nature of the sidewall boundary layer or that a boundary layer even existed. However, there are other indications that a boundary layer of some form was present. There was a general heating of the liquid bulk and the gradual development of a warmer layer near the liquid surface (see figure VII-1). The presence of the surface stratification, the fact that the liquid bulk temperature increased with time, and the absence of detectable radial temperature gradients all substantiate the presence of convective currents in the liquid during powered flight.

B. ORBITAL INSERTION

1. Fuel Tank

At insertion into orbit the longitudinal acceleration of the vehicle decreased from 3.6 g's to 6.1×10^{-4} g's. Immediately after insertion into orbit the television picture showed two separate flow patterns developing in the liquid hydrogen. Using the television picture, with verification from the associated telemetry data, a graphical reconstruction of the flow patterns is possible (see figure III-3). The major flow pattern, as viewed from above, appeared to be a movement of the entire liquid surface from right to left in the TV picture. It is believed that this flow, as determined by the surface light reflections, was a large amplitude slosh wave which had transverse motion and was moving up the left side of the tank. This wave was produced

from the boost slosh wave whose amplitude was magnified by the sudden reduction in body forces. In the television picture the surface tilted and sloshed to the left, where it remained for a short duration. A column of liquid was then observed to enter the field of view from the left. The column of liquid was moving at an angle toward the top of the tank at an average velocity of between 1.0 and 1.5 feet per second. The liquid was evidently part of the slosh wave that had been deflected by the slosh baffle. Similar liquid behavior has been observed in model testing in the Marshall Space Flight Center Drop Tower Facility. Portions of the liquid column continued past the deflector and then broke into pieces that fell back to the bottom of the tank.

The second major flow pattern observed at insertion into orbit was liquid flow up the tank wall. This flow hit the baffle and spilled around it in the form of many individual particles and columns. Most of these liquid fragments continued vertically at an average velocity of one-half foot per second and hit the underside of the deflector where they were stopped. Since this flow was detected only by the television, it is uncertain whether the flow pattern was annular or local in nature. If the flow pattern was local, it was probably caused by a flow surge from the fuel suction duct (located directly in view of the TV camera) at J-2 engine cutoff. The prevalve in the fuel suction duct closed 0.5 sec after the engine main fuel valve closed. The data sampling rate (one data point per second) was insufficient to determine if the suction line pressure rose high enough to cause a flow surge back into the tank before the prevalve could close. If the flow pattern was annular, this disturbance could have been caused by either thermal boundary layer amplification, structural relaxation of the tank walls, or both.

The following specific events associated with the flow patterns were observed from the video tape and fuel tank instrumentation at the times indicated. The times are referenced from J-2 engine cutoff signal (432.7 seconds after liftoff).

a. The baffle was wetted by liquid flowing up near the wall at approximately 6 seconds. The baffle area within the field of view appeared to be uniformly wetted.

b. Asymmetrical movement of the propellant surface was detected at approximately 14 seconds. The direction of motion appeared to be toward the side of the tank out of the field of view (between positions II and III).

c. A small portion of the liquid, independent of this asymmetrical movement, wetted the underside of the nylon cloth deflector at approximately 21 seconds. This wetting was a result of liquid

fragments hitting the underside of the deflector and consisted only of spotting.

d. The asymmetrical movement of the propellant, apparently deflected by the baffle, came back into view of the TV camera at approximately 23 seconds after J-2 engine cutoff. At this time, a significant volume of liquid appeared to pass through the center opening of the deflector in a direction opposite to that previously noted on the free surface of the liquid below the baffle. Because of the angular relationship of the instrumentation probes with respect to one another and the uncertainty as to the exact direction of the deflected wave with respect to the probes, it is impossible to describe the deflected wave accurately on the basis of instrumentation. Figure III-3 shows a sketch of the deflected wave based on the television observation.

e. The television further indicated that the forward motion of the deflected liquid ceased at approximately 61 seconds.

f. The liquid began to settle at 73 seconds and gradually receded over the top of the deflector. A large quantity of liquid was distributed between the baffle and the deflector at this time. No further disturbances of the liquid were noted when the vehicle acceleration level was reduced further to 2.5×10^{-4} g's by closing of the LOX ullage thrusting system at 77 seconds.

g. The portion of the deflector within the field of vision was clear of liquid at approximately 91 seconds.

h. At 145 seconds after J-2 engine cutoff, all of the liquid was apparently positioned below the baffle where it remained.

i. The liquid surface was relatively quiescent until the warmer liquid at the surface became saturated and began boiling at 166 seconds. A vapor fog began to appear in the ullage at 191 seconds.

j. The instrumentation indicated the following significant events. The ullage temperature sensor (C346) at station 455, indicated the presence of liquid from about 20 seconds until 40 seconds after J-2 engine cutoff which confirms the TV observation that liquid was above the baffle. The temperature sensor (C347) and liquid vapor sensors (N048, N052) at STA 479 all indicated wetting at approximately the same time and for the same duration as C346. The 70 percent ullage temperature measurement (C037) at STA 535.6 (near the center clearance of the deflector)

indicated cooling beginning at about 50 seconds, probably due to the proximity of the deflected liquid. It appears that C037 was not actually contacted by liquid because it did not experience the sudden drop to liquid temperature characteristic of wetted sensors. The 50 percent ullage sensor (C036) at STA 474.6 began cooling at about 55 seconds and dropped sharply to liquid temperature at about 70 seconds. The sensor continued to indicate liquid temperature until loss of telemetry signal by Bermuda. This is not consistent with the television observation (see item h) and may represent trapping of liquid by the instrument (see Section VIII-6). No temperature measurements or liquid vapor sensors forward of, and including N050 (station 570), indicated wetting by liquid hydrogen. Measurement number C345 at station 432 (below the quiescent liquid level) showed the presence of ullage gas from 47 seconds until 76 seconds. The inside wall temperature measurements C325 and C326 located at station 548 (attach plane of the deflector) indicated liquid temperatures from 27 seconds until 97 seconds and from 37 seconds until 252 seconds, respectively.

The orbital insertion phase of the AS-203 experiment indicated that the position of the liquid hydrogen was successfully controlled by the particular combination of propellant control devices employed. Though some liquid hydrogen was deflected into the ullage region, the quantity was extremely small relative to the bulk of liquid in the tank. The mass of the deflected liquid is estimated to be only 50 lb_m, with the major portion of the liquid propellant (19,100 lb_m) being maintained in a settled condition. No problems concerning the control of the propellant at orbital insertion were indicated that could impair the success of the Saturn V mission.

2. Sequencing of Longitudinal Accelerations

A second factor that may have contributed to the successful control of the liquid at orbital insertion is the timing of the reductions in applied thrust. To lessen the severity of the liquid disturbances at insertion into orbit, the magnitude of thrust changes should be minimized. However, the liquid disturbance can also be reduced, theoretically, by properly timing the thrust changes. The thrust changes on AS-203 were timed to minimize liquid disturbances.

The engineering reasoning that determined the specific sequencing of the longitudinal thrust on AS-203 was first proposed in reference 3. Since the exact position of the slosh wave cannot be precisely determined or controlled, it was concluded that the J-2 engine cutoff could not be timed to minimize slosh amplification. Therefore, it was assumed that the slosh wave would be in the worst position for amplification (horizontal wave, which

gives maximum vertical velocities), and all subsequent thrusts were sequenced to produce minimum amplification. If the wave was in a position other than that for maximum amplification at J-2 engine cutoff, the subsequent thrust timings would not be correct, but the resulting amplification would still be less than the worst case.

Since it had been decided that the vehicle would be positively accelerated in the longitudinal direction at all times, the applied thrustings must overlap. To minimize amplification, any increase in longitudinal acceleration caused by the overlapping thrust should occur when the slosh wave is horizontal, to avoid increasing the potential energy of the fluid. All thrust decreases should occur when the slosh wave has its maximum wall displacement and, therefore, minimum vertical velocity. To determine the quarter and half cycle multiples for timing, a simple first mode slosh model was postulated using the natural frequency of a liquid column without considering coupling with the control system, vehicle, etc. At insertion into orbit, the boost slosh wave amplified as previously described. However, no amplification could be detected when the thrust level was further reduced to the continuous venting level. During the orbital coast phase of the mission, the timing of the thrust increases and decreases were based on similar reasoning. No amplifications were apparent due to changes in the longitudinal acceleration levels during orbital coast, although it is possible that there were changes not large enough to be detected by the TV and the instrumentation. Data from full-scale flights using different timing philosophies will be required before a complete evaluation of sequencing methods can be made.

3. Oxygen Tank

Due to the relatively small amount of instrumentation in the oxidizer tank, the liquid oxygen dynamics at insertion into orbit could not be defined as well as in the fuel tank. A rapid pressure decay detected in the oxidizer feed line (D003) indicated that liquid had surged back into the tank after the main engine oxidizer valve was closed. This surge was detected immediately after engine cutoff by two temperature sensors (C042 and C043) located 20 and 39 inches above the mean liquid level. The flow into the tank was stopped by the closing of the prevalve one-half second after J-2 engine cutoff. Approximately 80 seconds after engine cutoff, liquid was again detected as high as 39 inches above the mean liquid level by three temperature sensors (C041, C042, C043) and one liquid-vapor sensor (L005). It is felt that the last liquid detected was caused by a slosh wave. However, telemetry was lost before a slosh frequency could be established.

C. ORBITAL COAST

Limited data on sloshing in orbit was obtained from the temperature measurements in the hydrogen tank. These measurements showed regular fluctuations such as might be expected if they were being intermittently wetted. This behavior could be detected only when the fuel tank was closed and the liquid was subcooled. During those times, the vehicle was being accelerated by the LOX ullage thrust system. Whenever the continuous vent system was open, the hydrogen tank was saturated and no temperature fluctuations could be detected. Also, the period of oscillation at the continuous venting acceleration level was so long that a continuous data record of approximately 1000 seconds would have been required to detect the oscillations and such data were not available.

Figure III-5 shows the periods of oscillation that were obtained from the temperature measurements and gives a comparison with the first mode natural frequency predicted by the methods of reference 4. The data scatter at the higher acceleration is believed to be due to the fact that the response times of some of the temperature sensors were apparently large compared to the slosh period. Since the temperature measurements were not located ideally for slosh detection, it is difficult to determine the exact slosh amplitudes. Approximate maximum and minimum amplitudes have been evaluated by the Aero-Astrodynamics Laboratory of MSFC. These amplitudes are given in Table III-1.

There was not sufficient liquid oxygen in the tank during orbit to sustain any large amplitude sloshing, and the smaller amplitudes could not be detected.

TABLE III-1

HYDROGEN SLOSH AMPLITUDE

Tracking Station	Acceleration (g's)	Maximum Amplitude (in.)	Minimum Amplitude (in.)
KSC Orbit 1	4×10^{-4}	34	2
Guaymas Orbit 4	8×10^{-5}	89	21

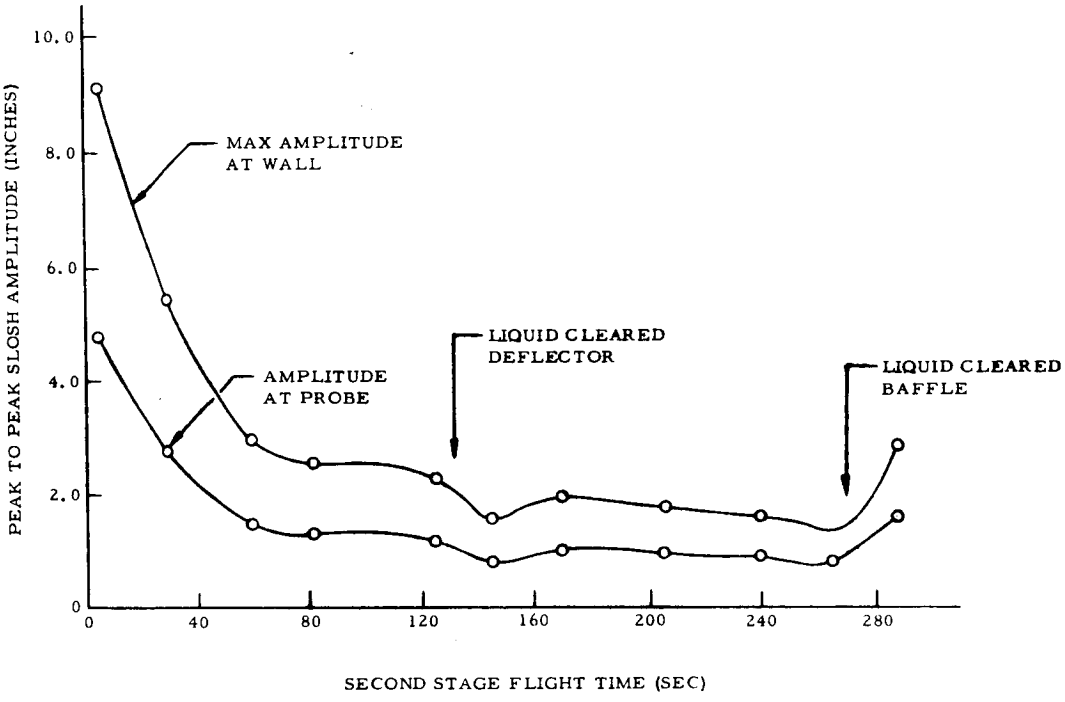

FIGURE III-1 LIQUID HYDROGEN SLOSH AMPLITUDE DURING S-IVB POWERED FLIGHT

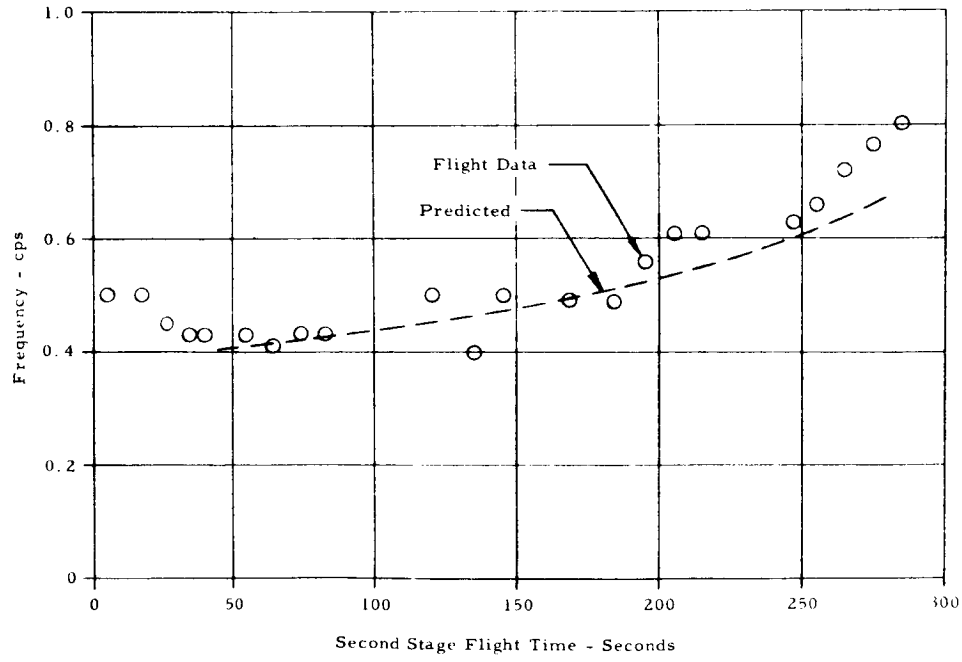

FIGURE III-2 LIQUID HYDROGEN SLOSH FREQUENCY DURING S-IVB POWERED FLIGHT

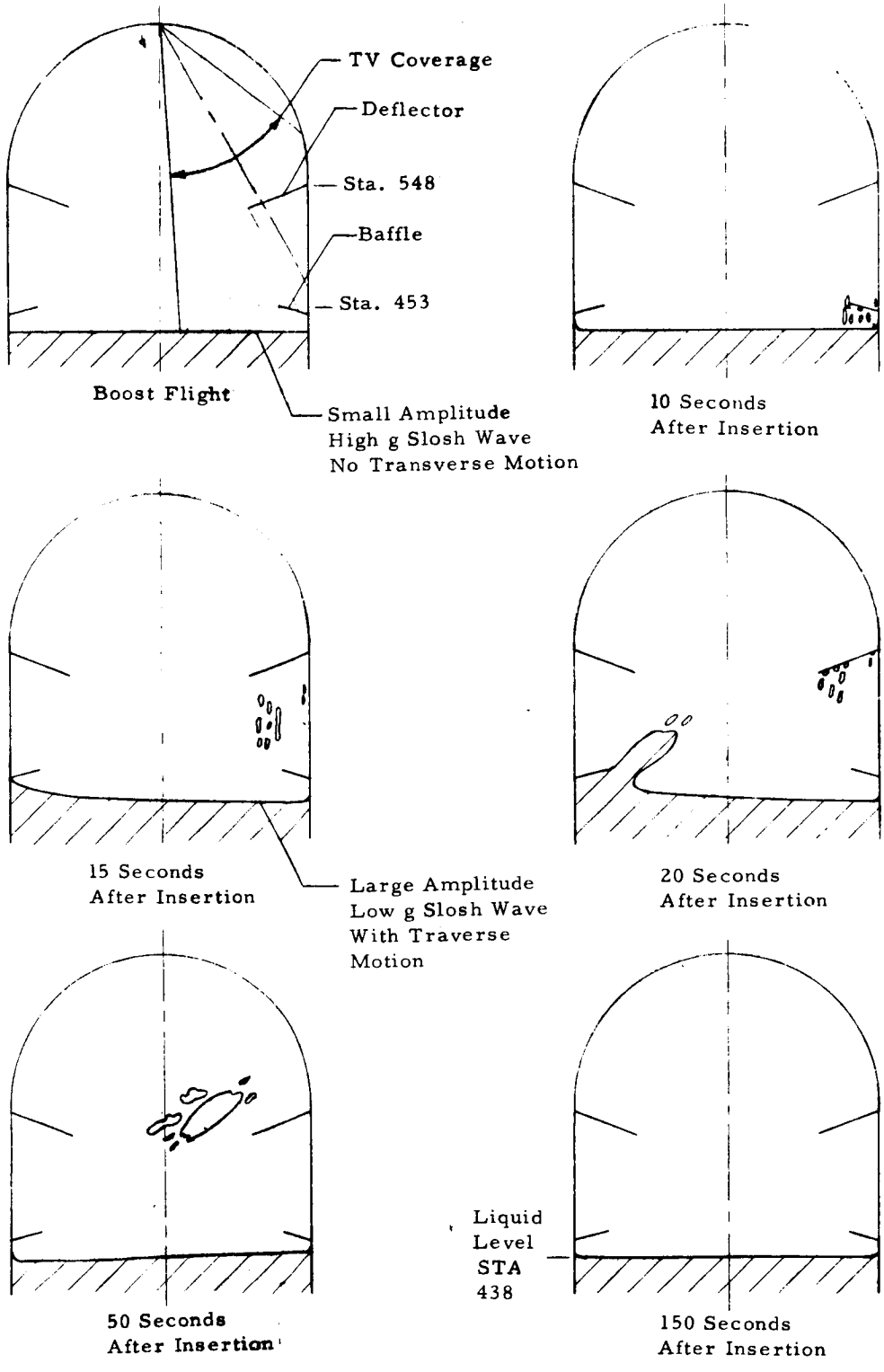

FIGURE III-3 SCHEMATIC OF LIQUID MOTION FOLLOWING ORBITAL INSERTION

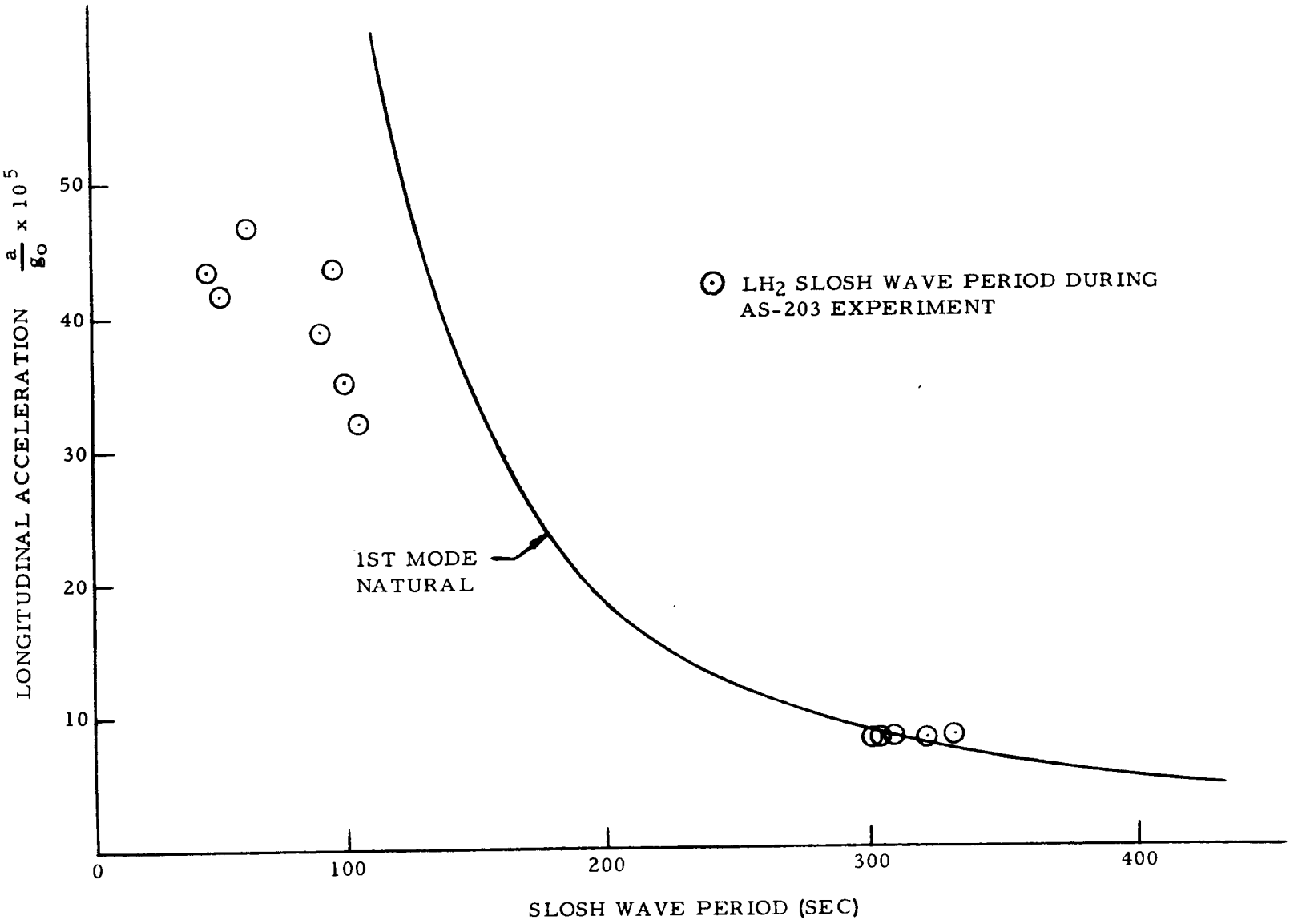

FIGURE III-4 LIQUID HYDROGEN SLOSH PERIOD DURING ORBITAL COAST

SECTION IV. PROPELLANT CONTROL DURING ORBITAL FLIGHT

A. VENT SYSTEM DESCRIPTIONS

Propellant control during the orbital phase of the experiment was achieved by maintaining a continuous low-level acceleration on the vehicle. This acceleration was produced by venting ullage gases through the hydrogen continuous vent (CV) system and/or the LOX ullage thruster (LUT) system. The CV system is not a standard system on the Saturn IB/S-IVB stage, but was added to the S-IVB-203 to perform the same general function as its intended function on the Saturn V/S-IVB stage. The continuous vent system contains a variable area regulator valve that was opened and closed on command according to the programmed sequence of events. The valve has a fixed maximum flow area at inlet pressures greater than 20.5 psia and a fixed minimum flow area at inlet pressures less than 20.0 psia. Ideally, the flow area varies smoothly between the maximum and minimum area when the inlet pressure is between 20.5 and 20.0 psia. The purpose of the regulator valve is to maintain the hydrogen saturation pressure at approximately 20 psia while still providing adequate axial thrust for continuous propellant control. The ullage gas flow from the fuel tank is split between two branches and then discharged through two nozzles directed aft at an angle of 76.5^{o} from the vehicle longitudinal axis (see figures IV-1 and IV-2). This nozzle cant angle was selected to produce the same net acceleration as designed for the Saturn V/S-IVB continuous vent system. Except for the overboard nozzle cant angle, the system is identical to the Saturn V system.

The LUT system provided a means of controlling the propellants at main engine cutoff to minimize the effects of various liquid dynamics phenomena that might result in excessive control disturbances or venting of liquid. It also served to maintain the propellants in a settled condition during the J-2 engine chilldown sequence. This system is unique with the AS-203 vehicle. It was designed to perform the same function as the two 70-lb thrust ullage motors of the Saturn V/S-IVB auxiliary propulsion system. The nominal design acceleration level of the LUT system is approximately 5×10^{-4} g's. The system consists of a shutoff valve and two discharge nozzles directed aft at an angle of 13.5^{o} with respect to the vehicle longitudinal axis (see figures IV-1 and IV-2).

Both the fuel and oxidizer tanks on the S-IVB stage are equipped with a pressure relief vent system. The relief valves will open and close automatically to prevent the fuel and oxidizer tank pressures from exceeding 42 and 44 psia, respectively. The relief valves may also be opened and closed on

command to obtain a rapid depressurization of the tanks. The vent flow through the fuel tank relief system is directed through two discharge orifices, diametrically opposed, at the vehicle outer skin such that the thrust produced is theoretically non-propulsive. The fuel tank relief valve acted on pressure demand during S-IVB powered flight (154 to 225 seconds after liftoff) and on command during the rapid fuel tank depressurization tests (Section VI-B). The vent flow through the LOX tank relief system is discharged through a single port. The thrust produced from the LOX tank relief system is directed through the vehicle center of gravity thereby creating no torques on the vehicle. The LOX tank relief valve was not required to function during the flight.

B. LOX ULLAGE THRUSTER SYSTEM PERFORMANCE

The LUT system was employed five times during the experiment. The system was opened for 77.0 seconds at orbital insertion, for 409.0 seconds during the J-2 engine chilldown experiment, for 119.7 seconds at the end of the free coast experiment, for 187.0 seconds during the first fuel tank rapid depressurization test, and for 1.5 hours during the closed fuel tank experiment. The LUT system performed exceptionally well throughout the flight.

The LOX tank pressure history during orbit is shown in figure IV-3. Throughout most of the first orbit the measured LOX tank pressure was slightly lower than predicted. During the initial ullaging sequence (432 seconds to 509 seconds after liftoff) the tank pressure decreased approximately at the predicted rate. The measured initial ullage pressure was lower than the predicted pressure at insertion, thereby resulting in a lower than predicted ullage pressure when the initial sequence was terminated. At the initiation of the second ullaging sequence, which occurred concurrently with the first J-2 engine chilldown, the LOX recirculation pump added gaseous oxygen to the tank, resulting in a significant amount of repressurization. Consequently, the ullage pressure was approximately 3 psi higher than predicted at the termination of ullaging and remained higher thereafter. Although the actual pressure level was slightly higher than predicted during most of the flight, the slope of the predicted curve generally agrees well with the data. Because conditions in the LOX tank were particularly suited to the establishment of convective currents (cold common bulkhead and uninsulated lower bulkhead), ullage heating effects were considered in the preflight predictions. Estimates of the heating rates were based upon commonly accepted heat transfer correlations evaluated at the reduced gravity levels. The results indicate that this approach was reasonably valid.

The mass flow rate and thrust produced by the LUT system was calculated using the measured temperatures (C307 and C308) and pressures (D212 and D213) immediately upstream of the LUT system discharge nozzles. The

critical flow parameter and thrust coefficient were calculated using the procedure described in reference 5 and assuming that shifting equilibrium flow conditions existed. To simplify the calculations, it was further assumed that the helium in the LOX tank at orbital insertion was completely vented before any GOX was discharged. This assumption could cause a significant error in the calculated vent flow rates. However, the calculated thrust will not vary more than $\pm$ 5 percent regardless of whether helium or GOX is being vented. Figures IV-4 and IV-5 show the calculated mass flow and thrust from the LUT system during the AS-203 flight.

C. CONTINUOUS VENT SYSTEM PERFORMANCE

The CV system was functioning continually during the first three orbits of the flight except for relatively short time intervals immediately following insertion, during the first J-2 engine chilldown, and during the free coast experiment. At the end of the third orbit the continuous vent valve was closed and remained closed thereafter. The measured fuel tank pressure history (figure IV-6) indicates that the regulator valve maintained the fuel tank at approximately 20 psia until near the end of the third orbit when the blowdown sequence reduced the pressure below the 20 psia level. The regulator valve began operating in a regulating mode for the first time at approximately 800 seconds after liftoff. When operating in a regulating mode, the valve oscillated with frequencies ranging from 2 to 30 cycles per minute. Although, undesirable, the oscillation did not produce any noticeably adverse conditions during the flight. However, the problem should be investigated and corrected to insure that this type of operation will not be prejudicial to the performance of subsequent vehicles. The regulator valve oscillation problem is discussed in greater detail in Section VIII-C.

The pressure rise shown by the flight data at approximately 5900 seconds resulted from the combined effects of repressurization and ullage heating with the tank vents closed. The effect of this pressure rise on the CV system performance is apparent for only a short duration after the system is again opened. The second pressure rise, occurring at approximately 11,200 seconds, is a result of ullage heating during the time that the tank was closed for the free liquid experiment. The rapid pressure rise from approximately 17,200 seconds to 22,500 seconds occurred while the tank was closed during the fourth orbit and is also primarily a result of ullage heating. The pressure rise rate and ullage heating rate during the fourth orbit are discussed in greater detail in Sections VI-C and VII of this report.

The mass flow rate and thrust from the CV system were calculated using the measured temperatures (C256 and C257) and pressure (D181) (D182 failed) upstream of the discharge nozzles. Typical plots of pressure and temperature upstream of the continuous vent discharge nozzles at various

times during the flight are shown in figures IV-7, IV-8, and IV-9. The fluctuations of the pressure and temperature are a result of the regulator valve oscillation. These plots were taken at times when the tank thermodynamic conditions were quasi-steady state. To obtain the average vent flow and thrust during the time the regulator valve was oscillating, integrated averaged values (over 100 to 300 seconds) of nozzle upstream pressure and temperature were employed in the calculations. Due to a calibration error in the nozzle upstream pressure measurement (D181), it was necessary to reduce all measured values by 0.5 psi before calculating mass flow and thrust. Figures IV-10 and IV-11 give the calculated average values of continuous vent mass flow rate and thrust during the orbital period. Also shown on these figures are the various assumptions and equations used in making the calculations.

D. ORBITAL VEHICLE ACCELERATION

The transient acceleration of the AS-203 vehicle was calculated by dividing the total axial force applied to the stage at any time by the vehicle mass. The mass of the vehicle at any time was obtained by subtracting the accumulated vented mass (other mass losses were negligible) from the mass of the vehicle at insertion (58, 700 lb_m). The accumulated vented mass was obtained by integrating the continuous vent, LOX ullage thrust system, and the non-propulsive vent system mass flow rates (see figures IV-4, IV-10, and VI-4). The accumulated vented mass from the various vent systems is shown in Figure IV-12. The total axial force applied to the stage is the summation of the axial thrust from the continuous vent and LOX ullage thrust systems minus the drag force. The total axial thrust of the LUT and CV systems is 97.2% and 23.3% of the thrust values shown by figures IV-5 and IV-11, respectively. A constant drag force of 0.11 lb_f was used in the vehicle acceleration calculations. Figure IV-13 shows the AS-203 calculated acceleration for the entire orbital period. Figures IV-14 and IV-15 show the vehicle acceleration on an expanded scale at orbital insertion, during first J-2 engine chilldown, at the end of the free coast experiment, and during the first fuel tank blowdown. The vehicle acceleration, as measured by a low gravity longitudinal accelerometer (measurement A008) during the first pass over the Canary Islands is also shown on figure IV-13. The measured acceleration values at the Canary Islands compare favorably with those based on the calculated vent thrust. However, the accelerometer failed before reaching Tananarive on the first orbit, and no further measured acceleration values were available throughout the remainder of the flight.

The vehicle acceleration level during the various experiment events was of the same approximate magnitude as expected during similar events on the Saturn V/S-IVB mission. The television coverage visibly indicated that the CV system thrust was adequate to maintain control of the liquid hydrogen

during the orbital coast period. Temperature and pressure data substantiated this fact. It is concluded that the CV system successfully demonstrated its ability to perform as required on the Saturn V/S-IVB stage. In addition, the LUT system demonstrated the capability of the Saturn V/S-IVB 70 lb_f ullage motors to perform as required with respect to the control of the propellants.

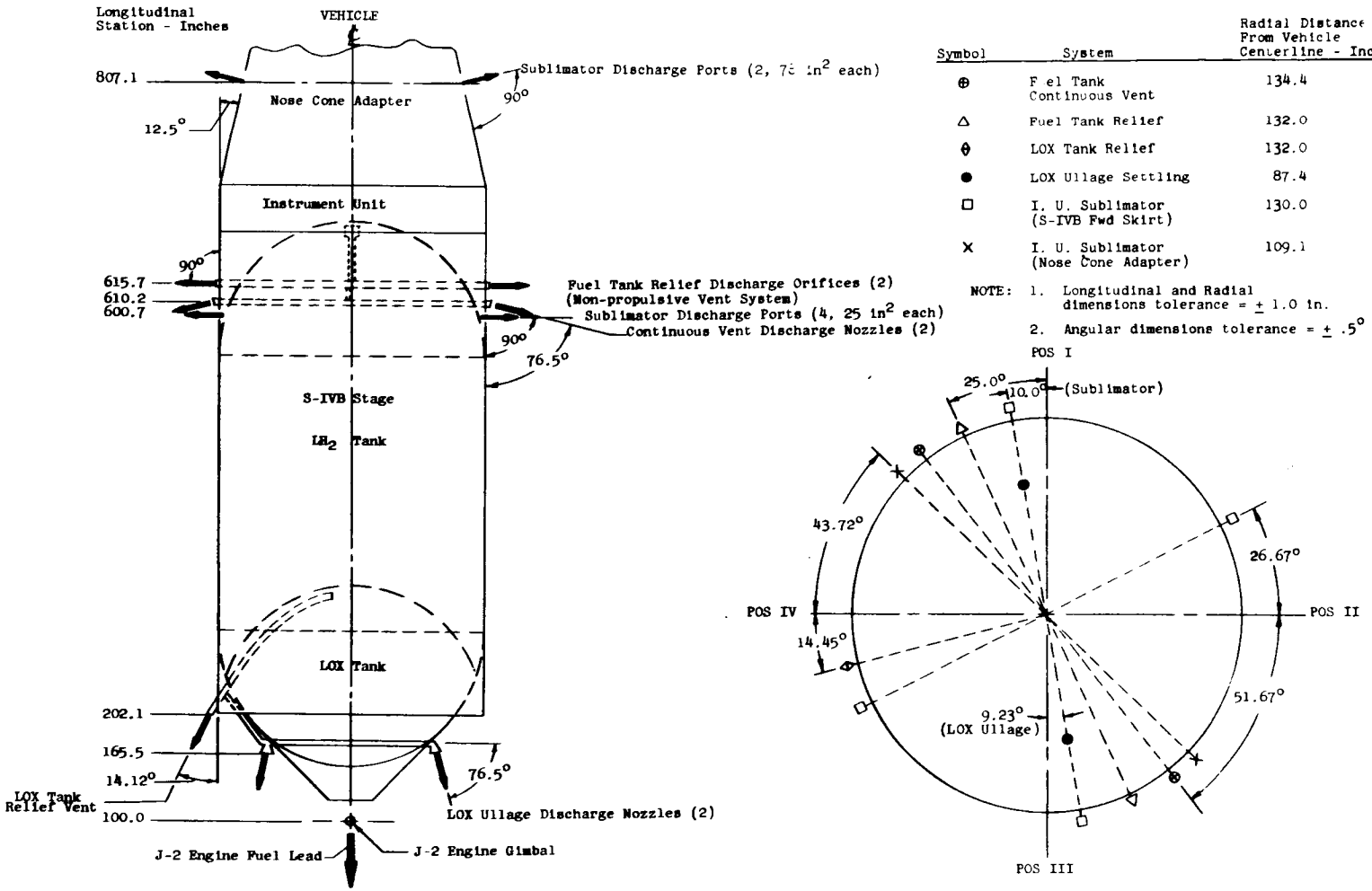

FIGURE IV-1 LOCATIONS OF S-IVB-203 VENT DISCHARGE PORTS

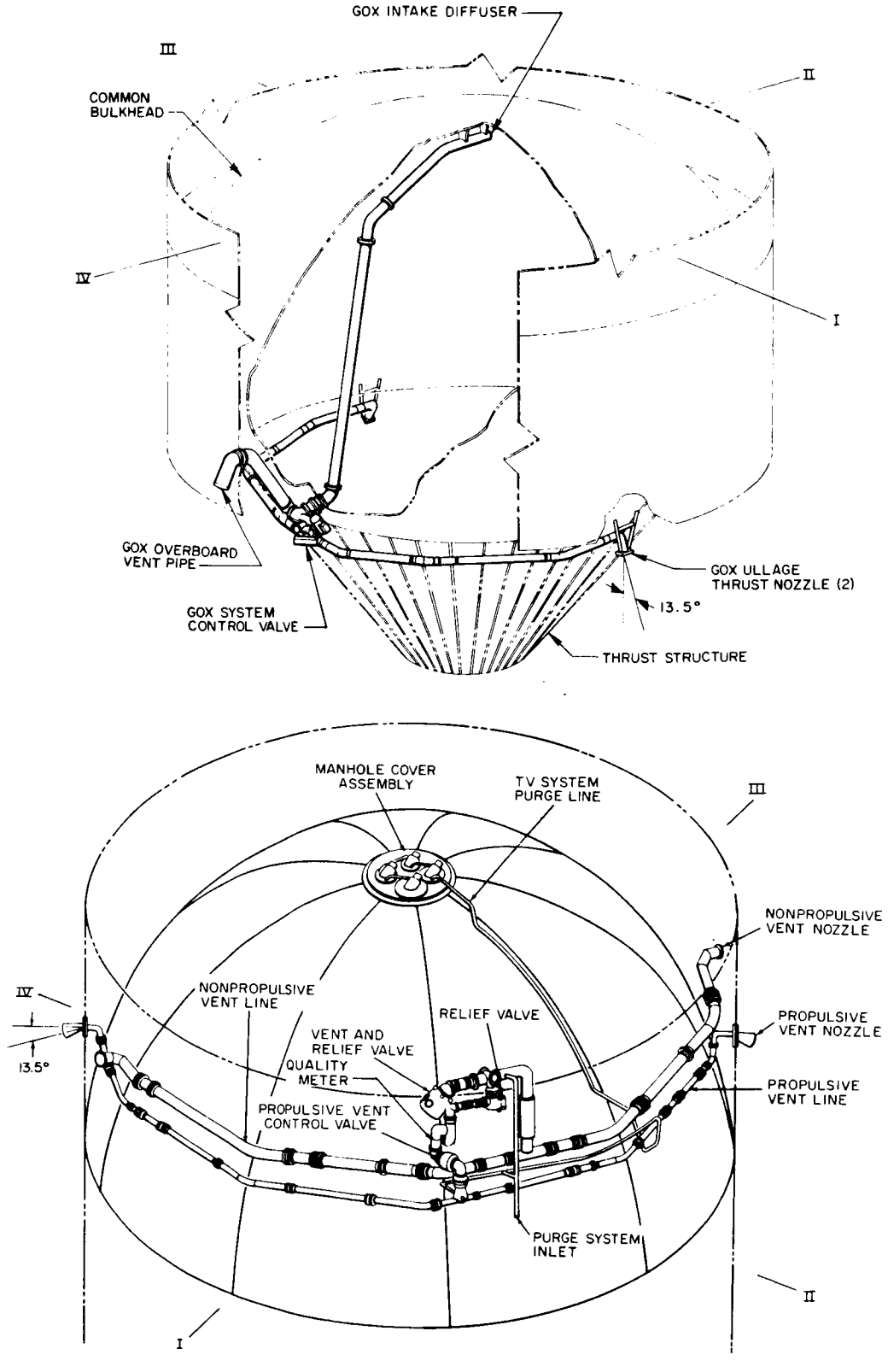

FIGURE IV-2 PICTORIAL SCHEMATIC OF S-IVB-203 VENT SYSTEMS

FIGURE IV-3 S-IVB LOX TANK PRESSURE DURING AS-203 FLIGHT

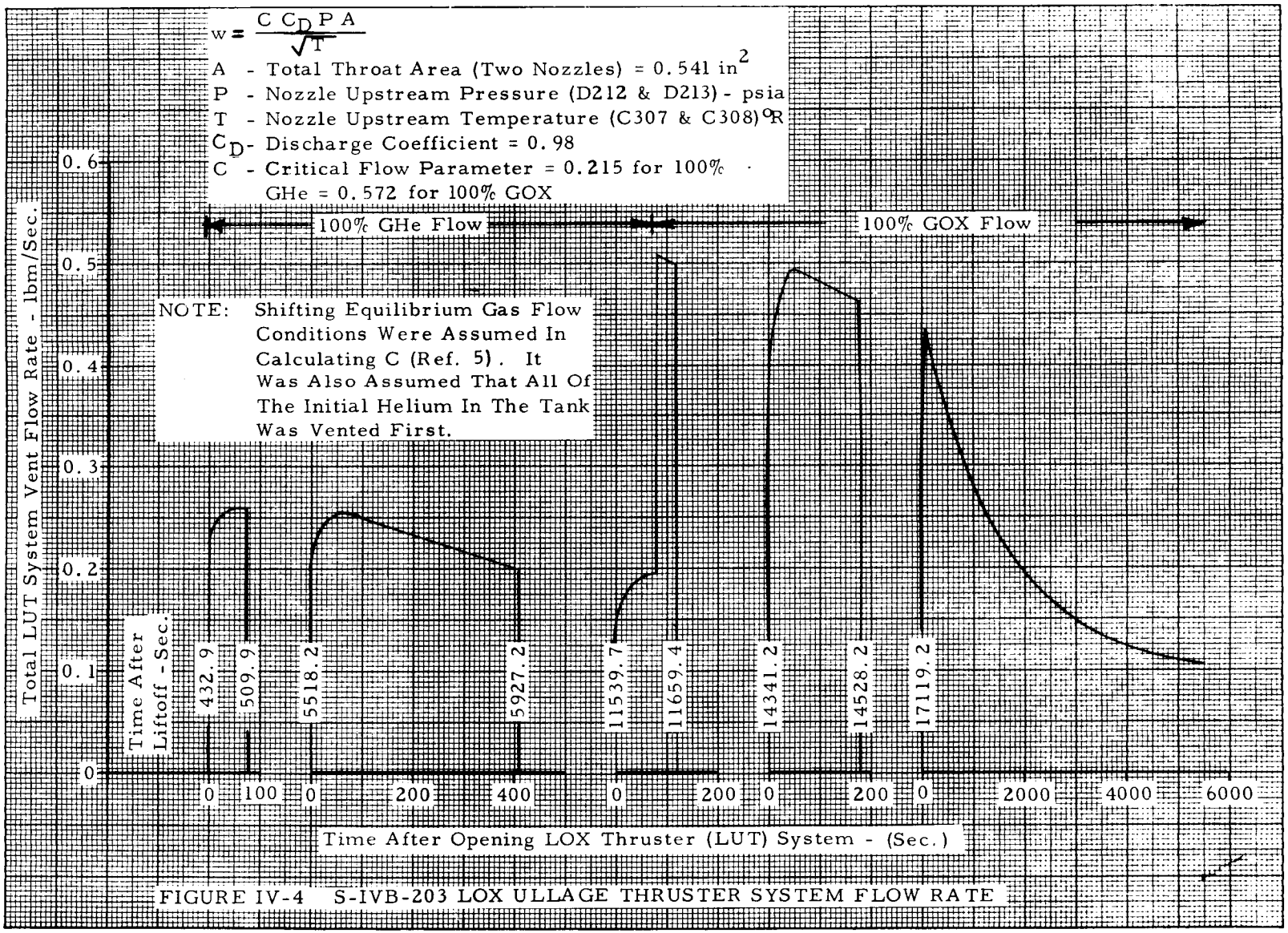

FIGURE IV-4 S-IVB-203 LOX ULLAGE THRUSTER SYSTEM FLOW RATE

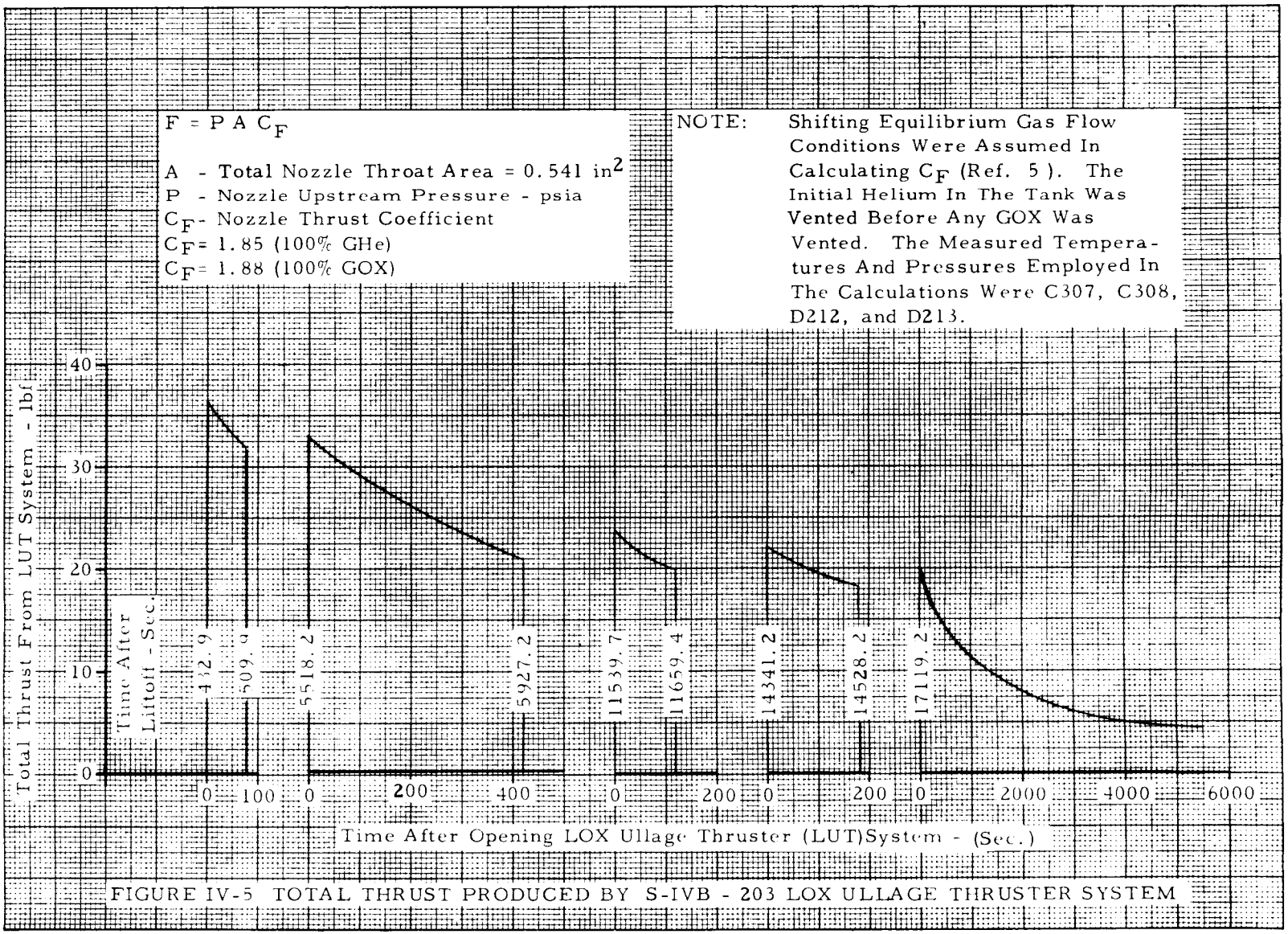

FIGURE IV-5 TOTAL THRUST PRODUCED BY S-IVB - 203 LOX ULLAGE THRUSTER SYSTEM

FIGURE IV-6 S-IVB FUEL TANK PRESSURE DURING AS-203 FLIGHT

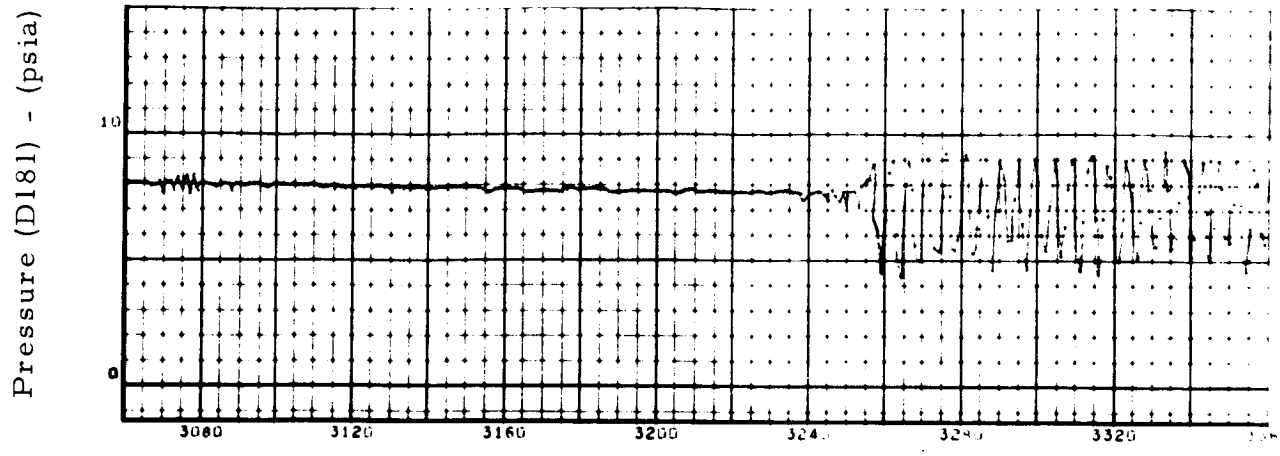

Time After Liftoff - (Sec.)

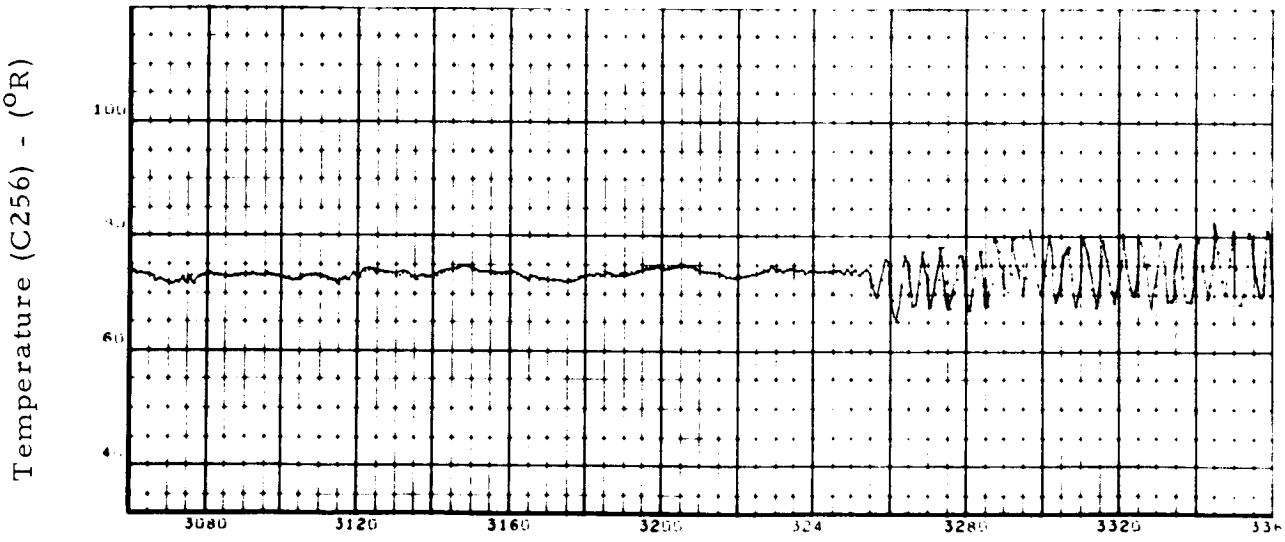

Time After Liftoff - (Sec.)

FIG. IV-7 TEMPERATURE AND PRESSURE UPSTREAM OF CONTINUOUS VENT NOZZLE - CARNARVON, FIRST REVOLUTION

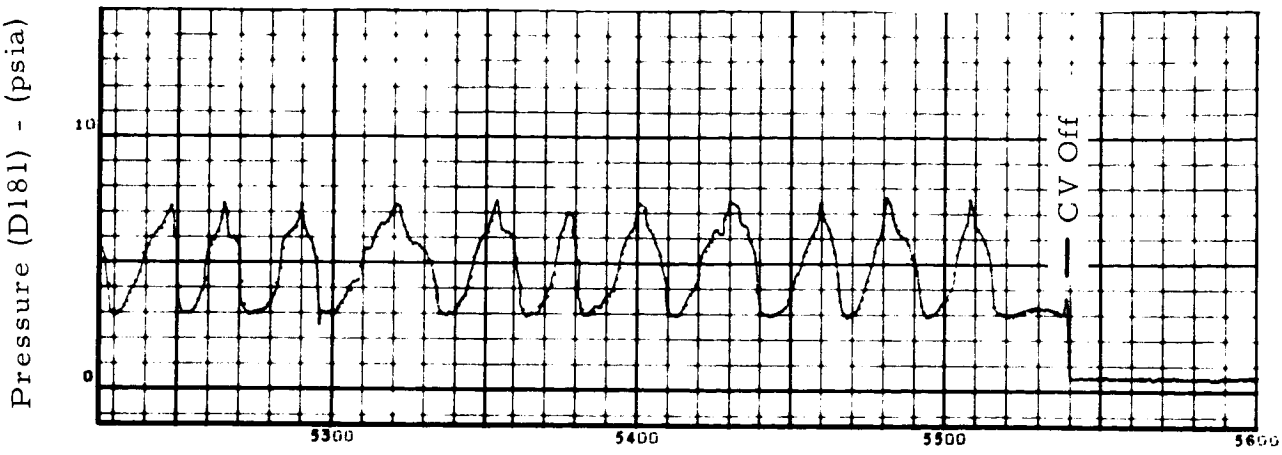

Time After Liftoff – (Sec.)

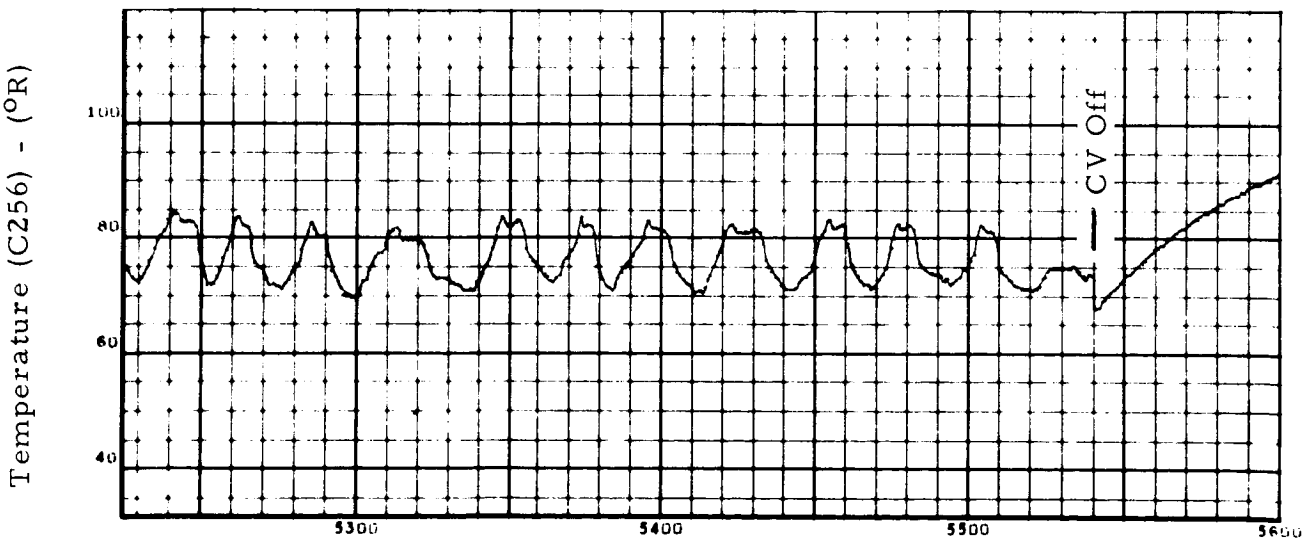

Time After Liftoff - (Sec.)

FIG. IV-8 TEMPERATURE AND PRESSURE UPSTREAM OF CONTINUOUS VENT NOZZLE- GUAYMAS, FIRST REVOLUTION

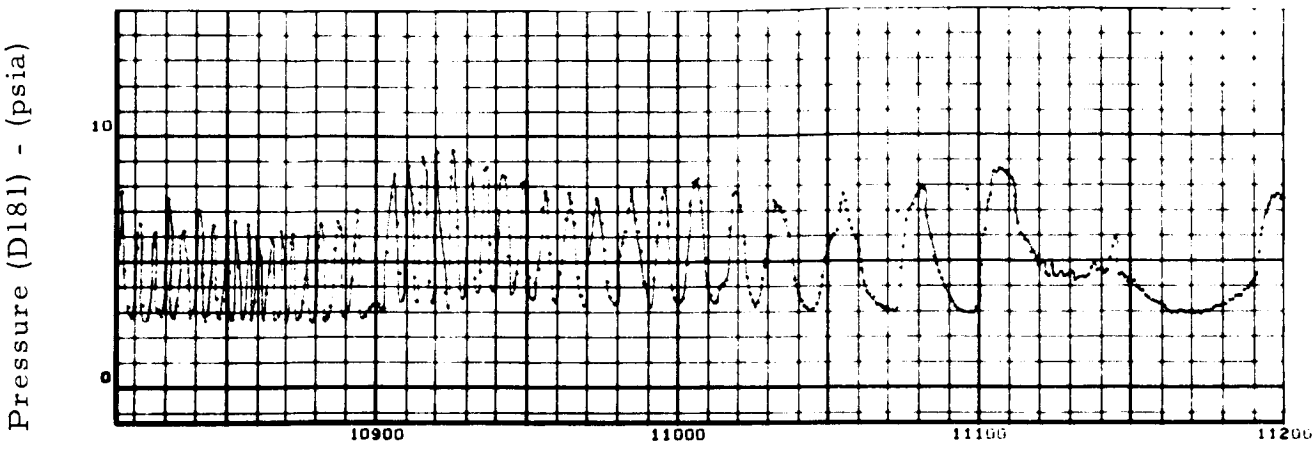

Time After Liftoff - (Sec.)

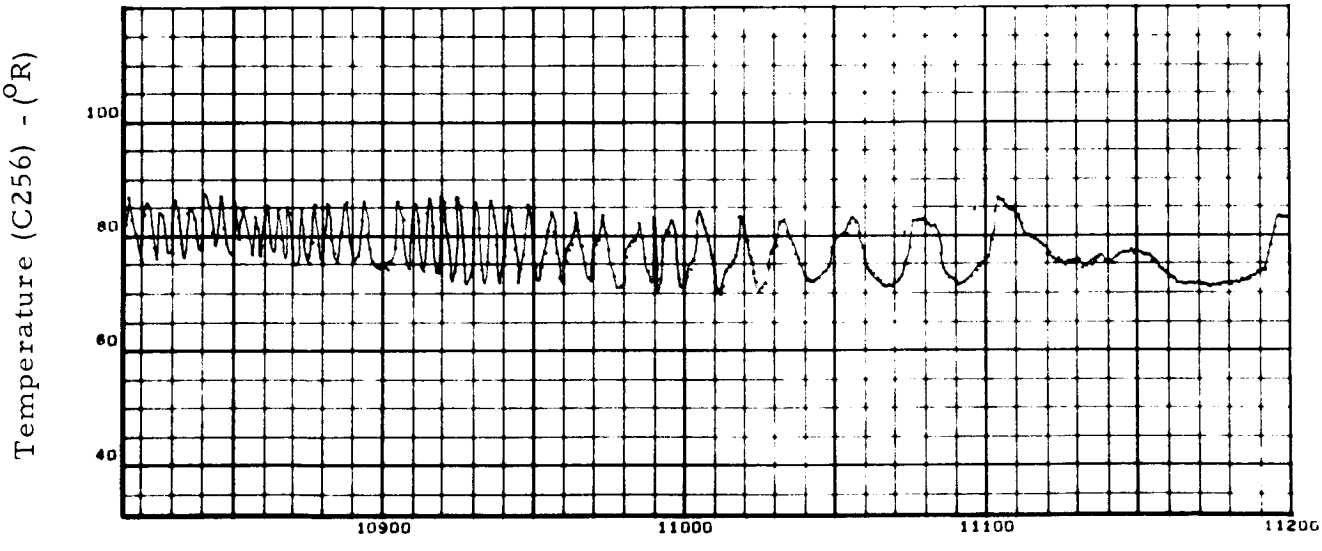

Time After Liftoff – (Sec.)

FIG. IV-9 TEMPERATURE AND PRESSURE UPSTREAM OF CONTINUOUS VENT NOZZLE - GUAYMAS, SECOND REVOLUTION

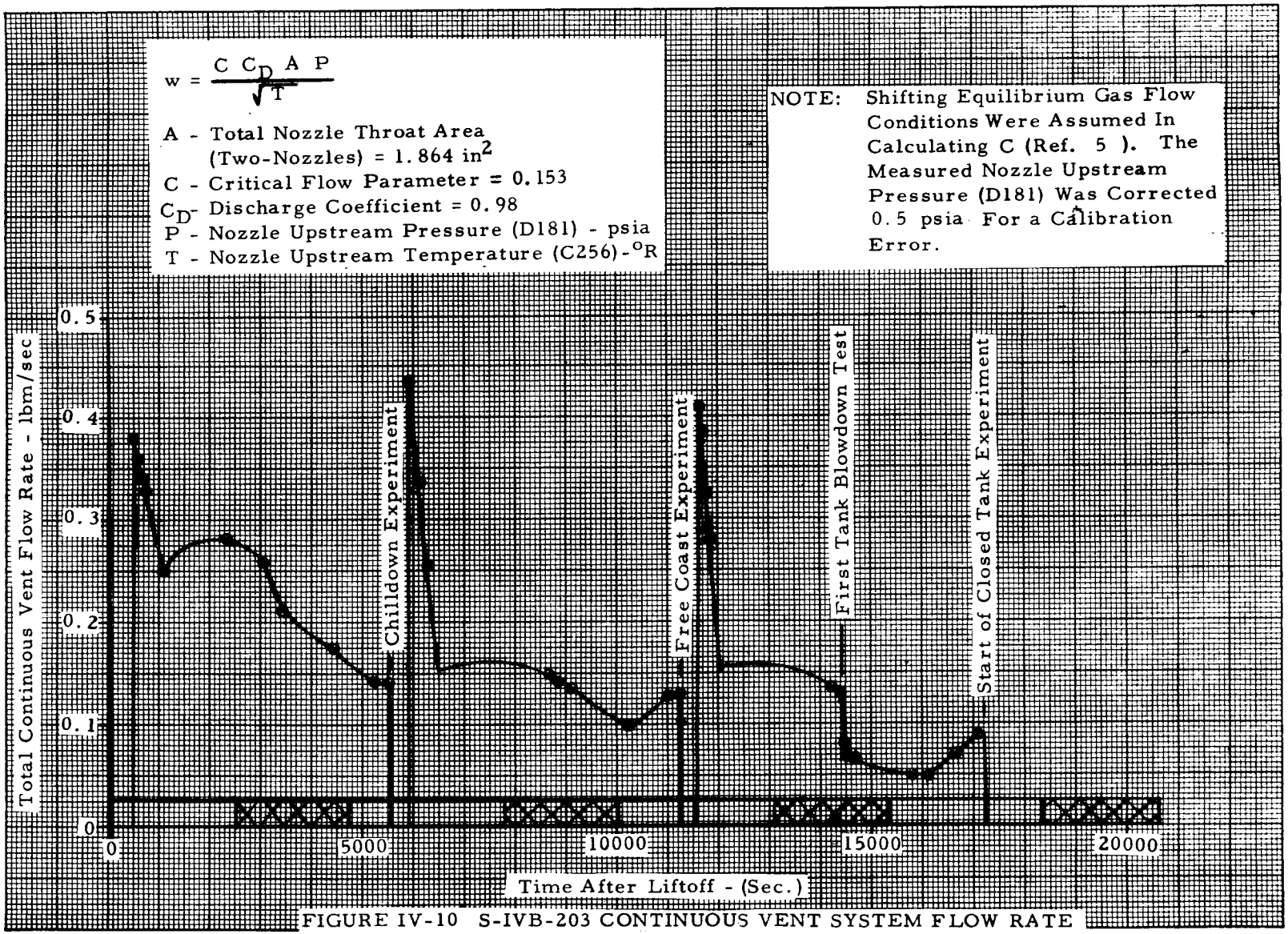

FIGURE IV-10 S-IVB-203 CONTINUOUS VENT SYSTEM FLOW RATE

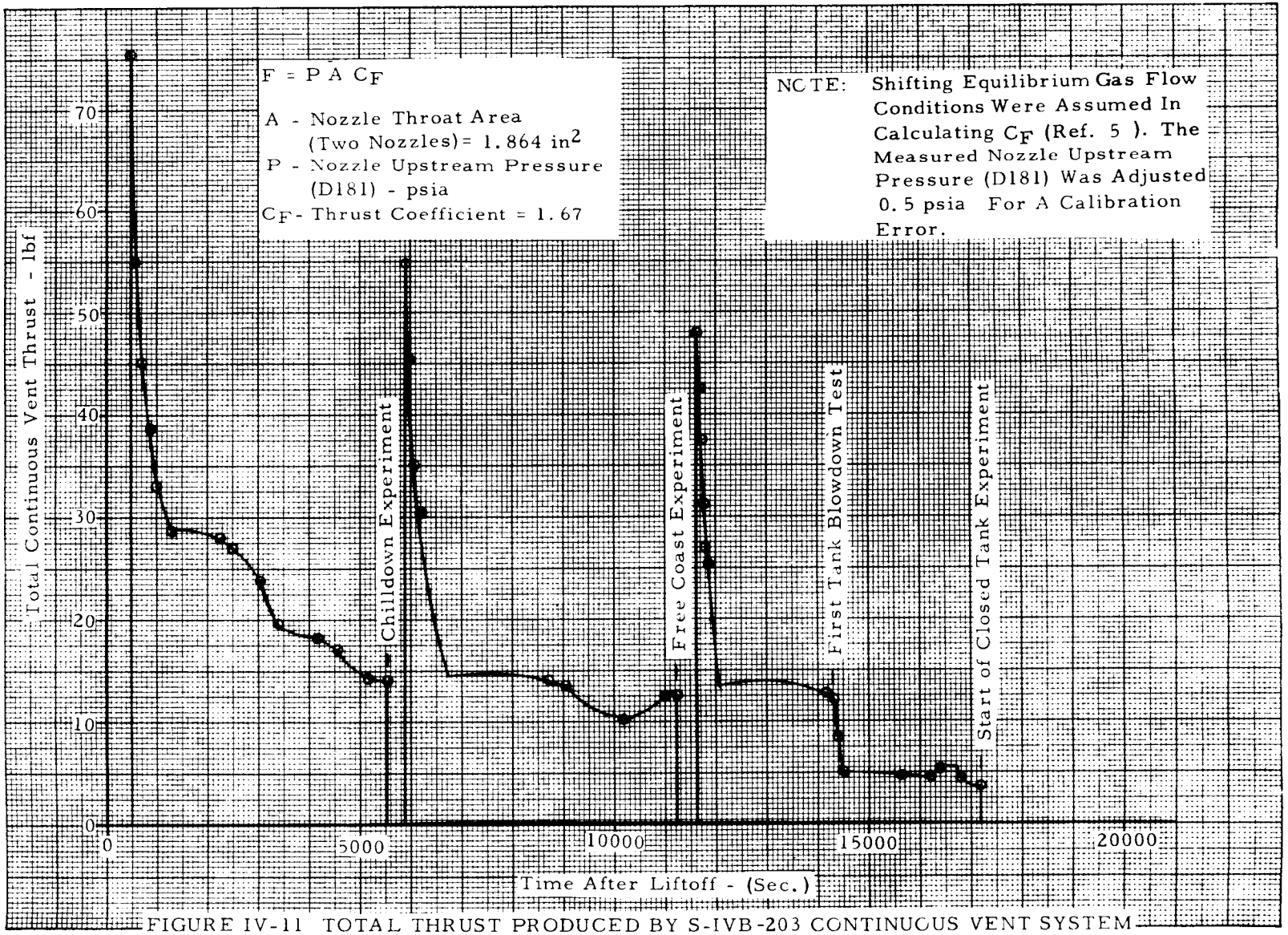

FIGURE IV-11 TOTAL THRUST PRODUCED BY S-IVB-203 CONTINUOUS VENT SYSTEM

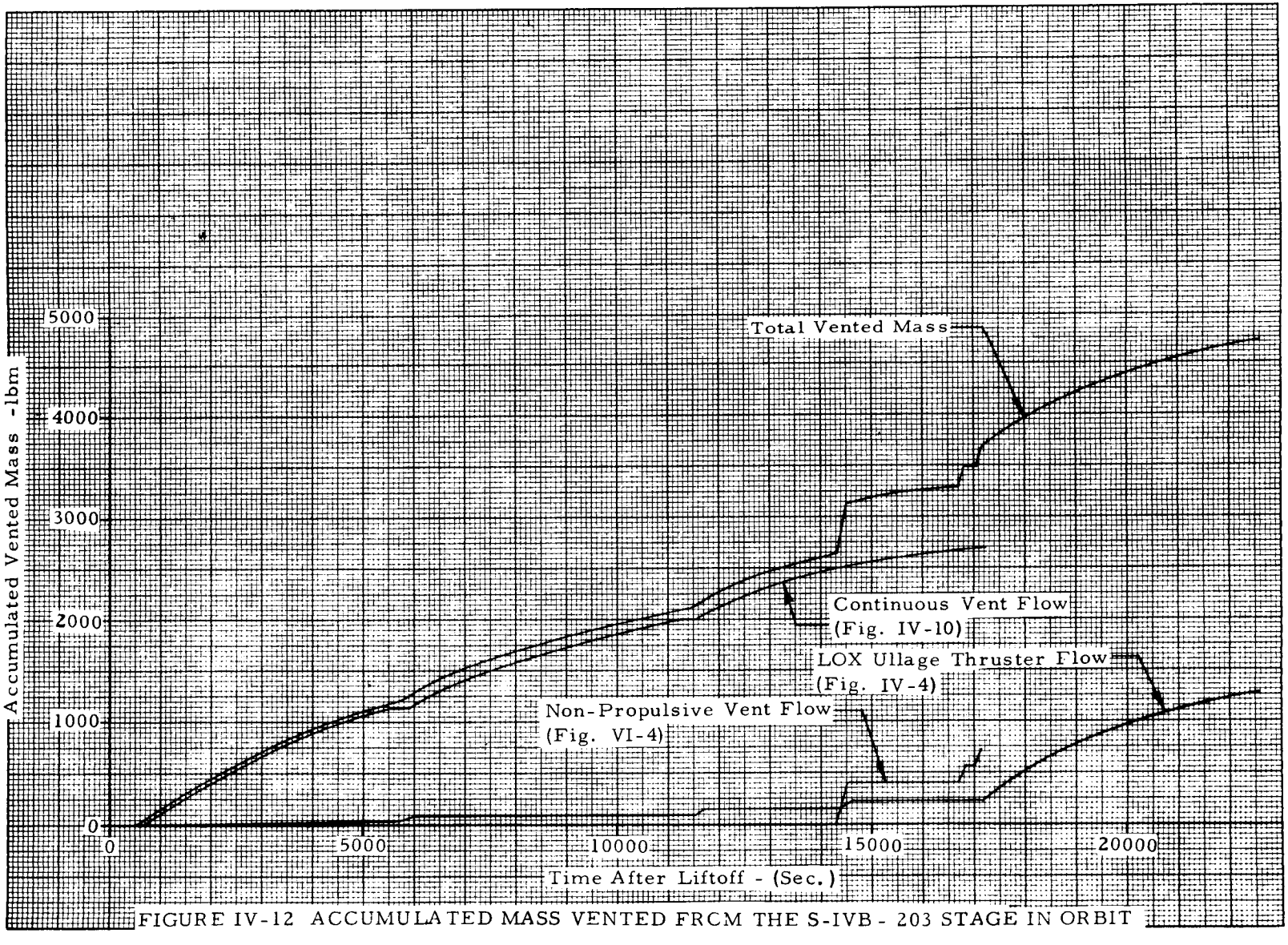

FIGURE IV-12 ACCUMULATED MASS VENTED FROM THE S-IVB - 203 STAGE IN ORBIT

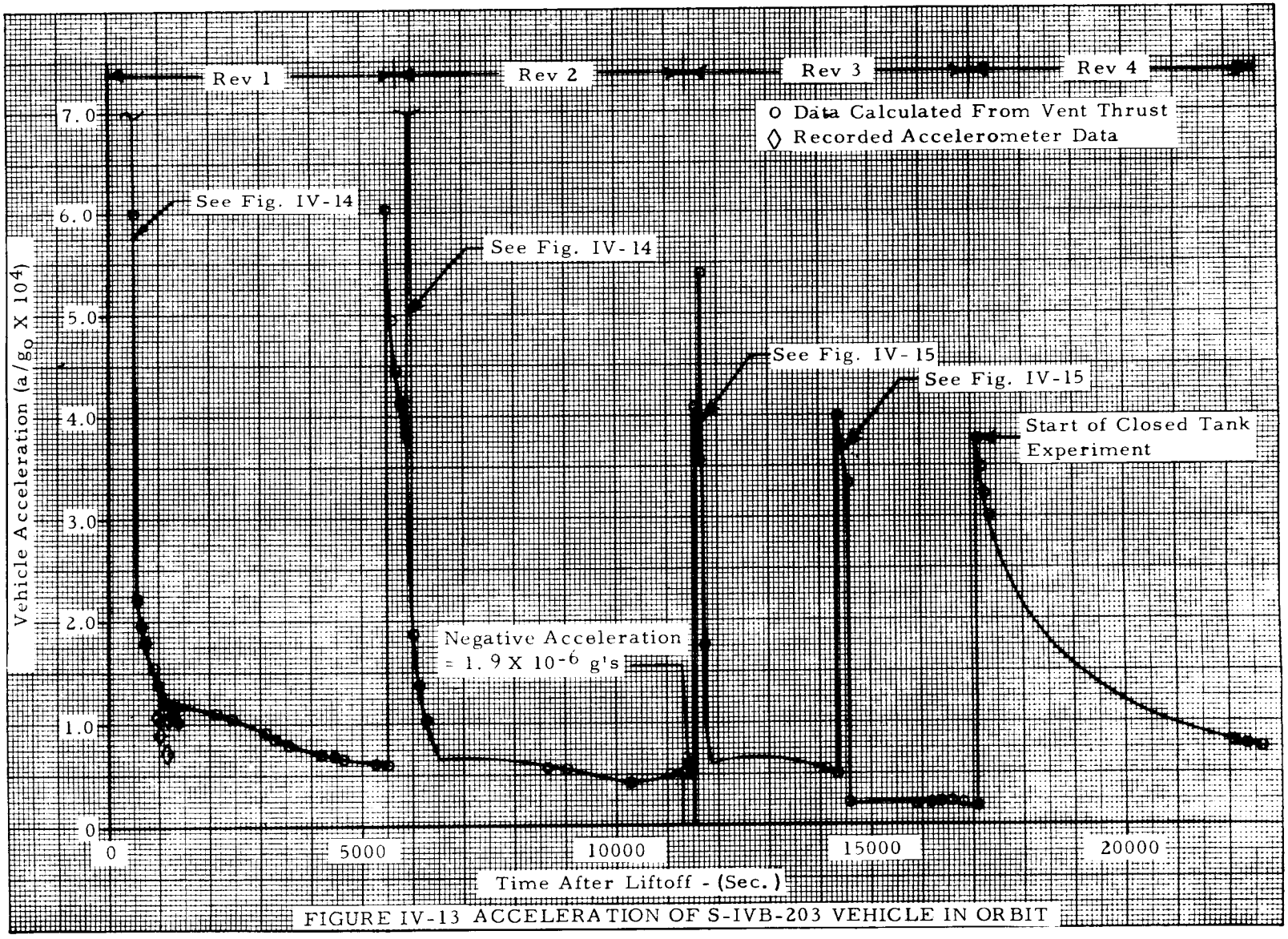

FIGURE IV-13 ACCELERATION OF S-IVB-203 VEHICLE IN ORBIT

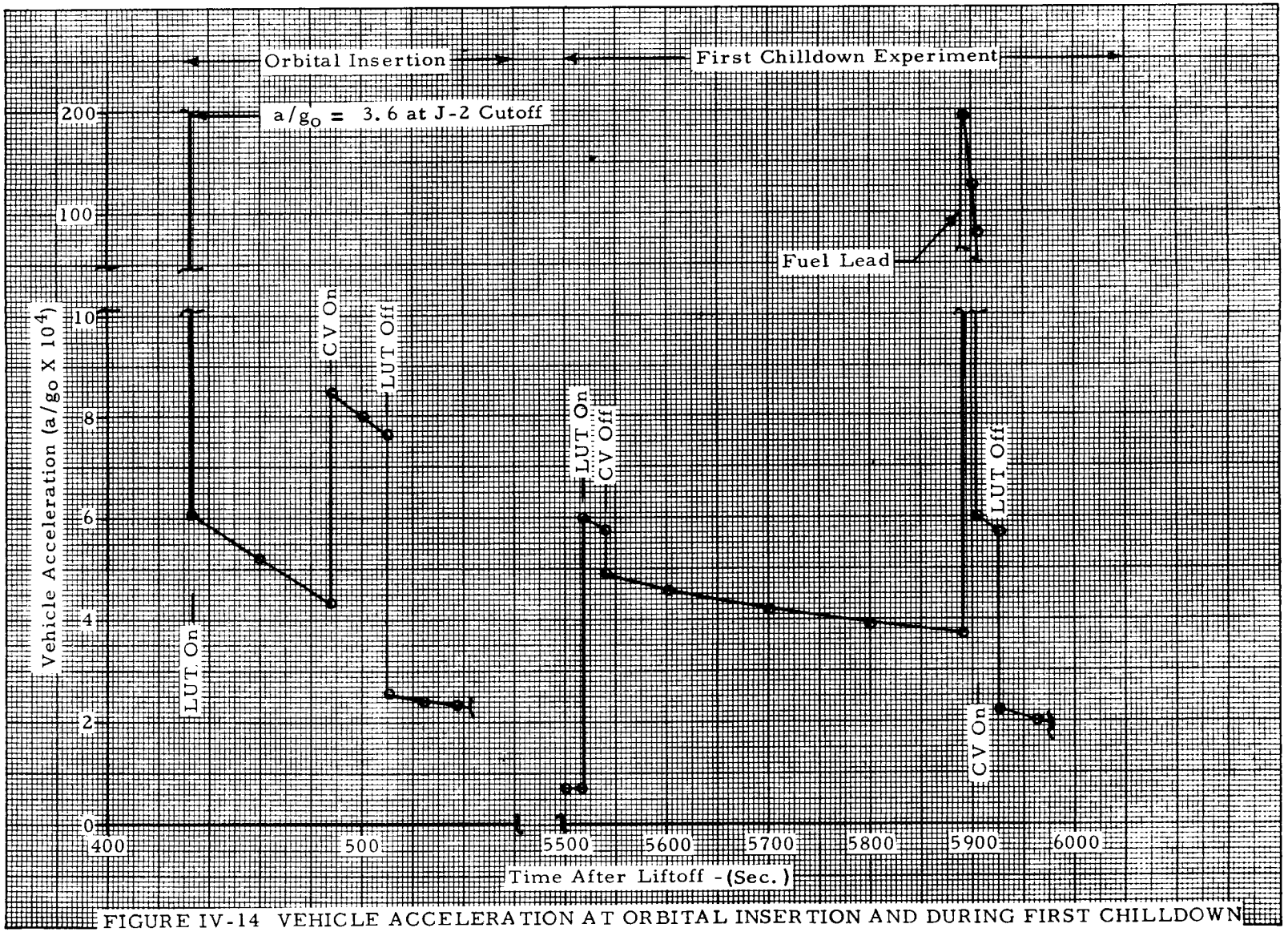

FIGURE IV-14 VEHICLE ACCELERATION AT ORBITAL INSERTION AND DURING FIRST CHILLDOWN

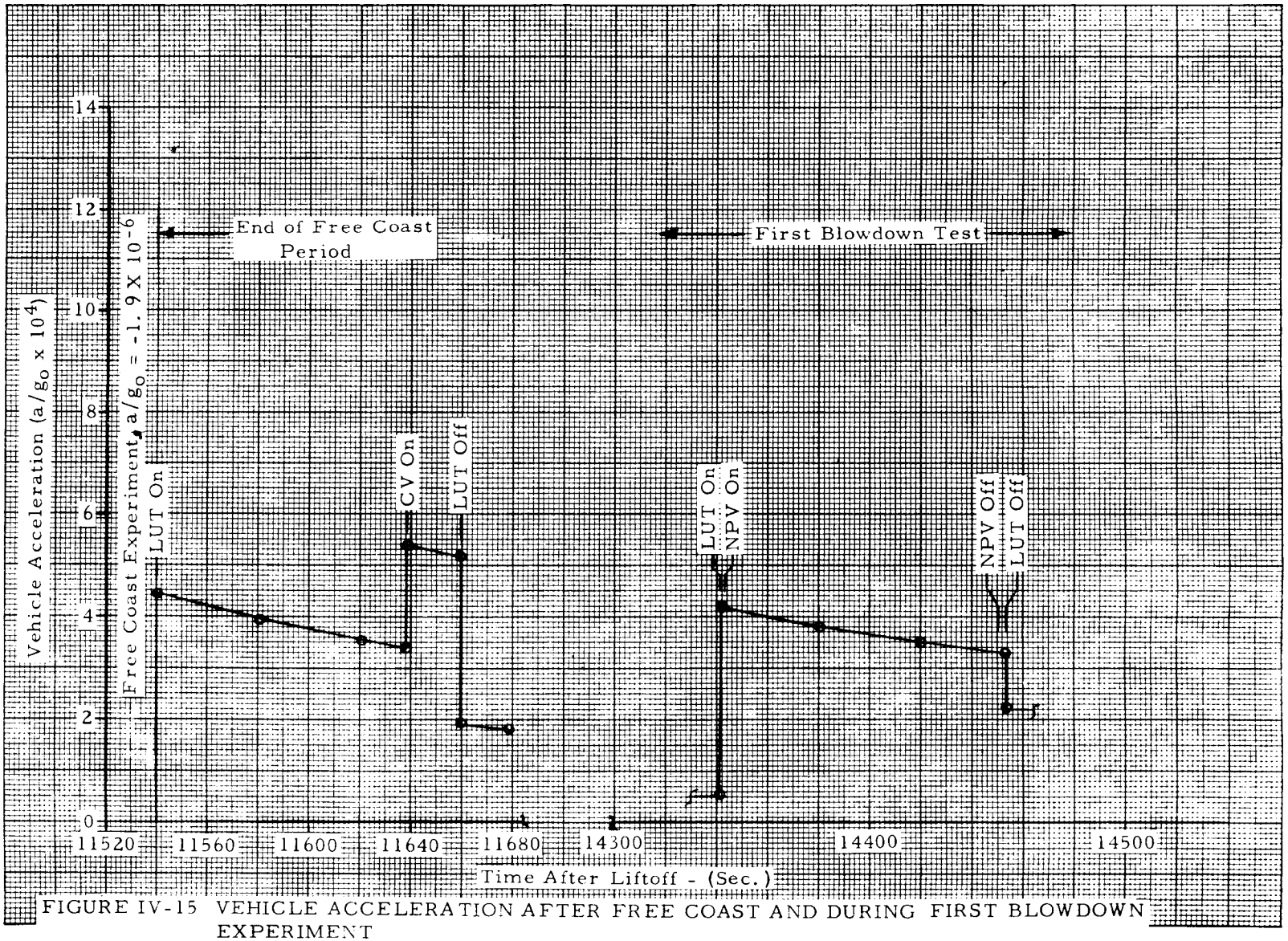

FIGURE IV-15 VEHICLE ACCELERATION AFTER FREE COAST AND DURING FIRST BLOWDOWN EXPERIMENT

SECTION V. J-2 ENGINE ORBITAL CHILLDOWN

One of the primary objectives of the AS-203 flight was to determine the ability of the S-IVB stage design to thermally condition the J-2 engine for orbital restart. The purpose of the engine chilldown is to remove heat from the propellant feed systems so that the cryogenic propellants are in the subcooled liquid state at the pump inlet when the engine is ignited. Figure V-1 is a schematic of the S-IVB chilldown systems and the associated instrumentation for the AS-203 flight. The system is chilled by pumping cryogenic liquid from the propellant tank through the suction duct, the engine pump, a bleed valve on the pump discharge, and into a line that returns the fluid to the lower portion of the propellant tank. One oxidizer and two fuel system chilldown experiments were conducted during the AS-203 flight. These experiments were successful and demonstrated techniques for thermally conditioning the J-2 engine in the orbital environment.

A. FIRST FUEL CHILLDOWN

The first hydrogen system chilldown was conducted during the final minutes of the first orbit, approximately 90 minutes after liftoff. During the first orbit, the liquid hydrogen had been maintained in the bottom of the fuel tank by the low-level acceleration produced by the continuous vent system. The chilldown experiment began when the LOX ullage thrusting (LUT) system was activated 5518.2 seconds after liftoff. The LUT system provided an average acceleration of approximately 4.4×10^{-4} g's during the chilldown experiment. The events that followed were:

1. 5539.2 seconds, continuous vent system closed.

2. 5540.3 seconds, fuel tank repressurization initiated.

3. 5564.3 seconds, fuel recirculation pump started (suction line prevalve was open).

4. 5574.3 seconds, suction line prevalve closed (beginning recirculation flow through engine).

5. 5864.3 seconds, suction line prevalve opened (stopping recirculation flow through engine).

6. 5886.3 seconds, fuel recirculation pump stopped.

7. 5892.5 seconds, main fuel shut-off valve opened (fuel lead).

8. 5903.8 seconds, continuous vent system opened.

9. 5905.0 seconds, main fuel shut-off valve closed.

10. 5927.2 seconds, LOX ullage thrusting system closed, ending the chilldown experiment.

The fuel tank repressurization began 1.1 seconds after the continuous vent system was closed. The fuel tank was repressurized with helium that had been stored at ambient temperature in a 4.5 ft^3 sphere at 3000 psia (reference 7). The helium pressure and temperature in the sphere during repressurization are shown in figures V-2 & V-3. The 7.9 lb_m of helium used for repressurization in combination with the ullage heating increased the fuel tank pressure from the initial value of 19.6 psia to 23 psia at the completion of the repressurization (figure V-4). Only about 0.5 psi is attributable to ullage heating. The liquid boiloff and ullage heating caused the tank pressure to continue to rise after the helium repressurization was completed. By the end of the chilldown experiment the tank pressure had risen to 25.8 psia. When the recirculation pump started the tank pressure was 21.6 psia, giving the recirculation pump an initial NPSH of 2.0 psid. The increasing tank pressure resulted in an NPSH of 6.2 psid at the conclusion of the chilldown. For the first 10 seconds, the recirculation pump operated with the prevalve open. This allowed the LH_2 to chilldown the by-pass line, and then flow back through the prevalve into the fuel tank, thus preventing severe initial pressure oscillations. When the prevalve closed, the fluid was forced through the suction duct, fuel pump, and the return line back into the tank.

The performance of the recirculation pump (figure V-5) during the first chilldown was very good. Except for a few points during the initial period of chilldown the pump operated above the pump characteristic (design) curve. During the initial period of chilldown the flowrate and pressure rise through the recirculation pump oscillated for 60 seconds before quasi-steady state conditions were obtained (figures V-6 and V-7). After the initial transient period the recirculation pump flowrate gradually increased until 60 seconds before the prevalve was opened, at which time the flowrate leveled off to 145 gpm.

The initial pressure rise of the recirculation pump (which is also the recirculation system pressure loss) reached 11 psid. As the boiling subsided and the fluid quality decreased, the pressure losses decreased to only 7.6 psid at the end of the chilldown. The fluid at the recirculation pump discharge was subcooled from 1°R when the prevalve closed to 2.9°R when the prevalve reopened (figure V-8).

During the fuel tank repressurization, the fluid in the fuel duct downstream of the prevalve was saturated (figure V-9). As the pressure in the suction line increased, the temperature increased, thereby indicating a predominately gaseous fluid. When the prevalve closed, the temperature continued to follow the pressure rise for approximately 4 seconds, after which the fluid began subcooling, indicating the presence of liquid hydrogen. When the recirculating flow through the engine was terminated by reopening the prevalve, the liquid had subcooled 3°R, and the heat absorbed by the fluid in passing through the prevalve bypass line was 0.54 Btu/sec.

The fluid at the fuel pump inlet was initially superheated (figures V-10 and V-11). However, the saturated fluid in the suction duct reached the fuel pump inlet only 5 seconds after the prevalve closed, and the fluid began subcooling 25 seconds later. After the liquid became subcooled, the fluid temperature at the fuel pump inlet decreased slowly until the recirculation flow was stopped. At that time the liquid was 1.8°R subcooled, and the heat absorbed by the fluid in passing through the suction line was 2.72 Btu/sec.

Downstream of the fuel pump the fluid was routed from the pump discharge line into the recirculation return line by the gas generator (G.G.) fuel bleed valve. At the end of the pump discharge line, where the main fuel shut-off valve was closed, there was no flow. A temperature sensor here showed saturated fluid for a short time at the start of chilldown, and then again just before the fuel lead near the end of the experiment (figure V-12). The fluid flowing through the G. G. fuel bleed valve became saturated 18 seconds after the prevalve closed, and began subcooling about 150 seconds later (figure V-13). The G.G. fuel bleed valve temperature measurement (C012) appears to be about 0.9°R too low. When the recirculation flow stopped, the liquid had subcooled 1.2°R, and the heat being absorbed by the fluid in passing through the fuel pump was 1.09 Btu/sec.

The fluid in the recirculation return line became saturated about 20 seconds after the prevalve closed and was saturated for the remainder of the chilldown. (See figures V-14, V-15, V-16 & V-17.)

The recirculating flow through the engine was terminated by the opening of the prevalve 290 seconds after it had been closed. This caused the recirculation flow to short circuit back through the prevalve and anti-vortex screen thereby chilling and removing any trapped vapor located within this region. The fluid immediately under the anti-vortex screen remained subcooled during the chilldown. However, when the prevalve opened the warmer fluid above the prevalve passed through, increasing the temperature at the anti-vortex screen to saturation. The wall temperature of the suction duct upstream of the prevalve was lowered 0.9°R (figure V-18) by the introduction of the cooler LH_2 from below the prevalve.

The fluid in the engine became saturated when the recirculation flow was terminated. Twenty seconds after the prevalve was opened, the recirculation pump was turned off and 10 seconds later the fuel lead was initiated. The fuel lead was accomplished by opening the main fuel shut-off valve and allowing the LH_2 to flow through the engine tubes and injector, and out of the bell for 12.5 seconds. The fuel lead is necessary for thermal conditioning of the thrust chamber in order to prevent pump stall during the start transients. The fuel lead replaced the saturated fluid in the fuel pump with subcooled liquid from the suction line and propellant tank (figures V-10 and V-12). An indication of the effect of the fuel lead was obtained from the thrust chamber nozzle temperature (C199). The nozzle temperature decreased from 440°R to 300°R after 8 seconds of fuel lead, and to 245°R after 12.5 seconds. For the 8 second fuel lead used on engines which will restart in orbit, the nozzle temperatures were within the allowable temperature range of 260°R to 320°R.

When the fuel lead ended the continuous vent was opened. Twenty-four seconds later the LOX ullage thrusting system was deactivated ending the first hydrogen chilldown experiment. A review of television pictures received during the chilldown indicated that very little surface disturbance was caused by the return flow into the fuel tank from the chilldown system. The fluid surface appeared to be rippled, but large gas bubbles were not observed breaking the surface. Calculations indicate that if all of the vapor produced during chilldown had remained below the liquid surface, the surface would have been displaced less than 4 inches. With the LH_2 completely bottomed, the mean fluid surface was estimated to be 24 inches below the top of the slosh baffle and no liquid was observed to rise above the baffle during the chilldown. This is verified by various temperature measurements. Temperature measurement C345, located 21 inches below the baffle, alternated between saturated and subcooled temperatures. Temperature measurement C346, located 3 inches above the baffle, responded instantaneously to tank pressure changes, indicating that it was above the liquid surface.

The results of ground test chilldowns conducted prior to the AS-203 flight, as well as the flight chilldowns, are shown in table V-1. The data shown in the table are compiled from references 8, 9, 10, and 11. Comparison of the flight chilldowns with the ground tests indicates that the ground environment was more severe on the operation of the chilldown system. As can be seen from a comparison of flowrates (figure V-19), the flow oscillations during the initial phases of the orbital chilldown were less severe than during a typical ground test. The more severe oscillations during the ground test were caused by the gravity feed of LH_2 into the suction ducts, whereas in the AS-203 flight the very low acceleration did not induce any significant velocity to the more dense liquid. The flowrate during the first orbital chilldown was more than was measured during any of the hot duct ground tests (figure V-20). This was primarily because much of the suction duct had already been chilled before the experiment began.

A comparison of the fuel pump discharge line wall temperature during the first orbital chilldown with the ground chilldowns (figure V-21) indicates that not only were the initial hardware temperatures lower for the orbital chilldown but the final temperatures were also lower. During the ground tests the final temperature was maintained relatively high by the formation of solid air on the external surfaces of the hardware. This condition was, of course, not experienced during the orbital chilldown. Although the ground chilldowns were conducted in an environment different from that of the orbital chilldown, the tests still provided a good estimate of the orbital results, a useful standard for comparison and an operational familiarization with the chilldown system.

The results of the first hydrogen chilldown experiment indicate that it was a complete success. The condition of the hydrogen at the fuel pump inlet, as well as the envelope of conditions required for engine start, is shown in figure V-22. Prior to the opening of the prevalve, engine start conditions were met. The opening of the prevalve reduced the local pressure at the fuel pump inlet and caused the fluid to become saturated. However, when the fuel lead was activated the fluid became subcooled almost immediately. The higher tank pressure planned for vehicles requiring actual engine restart will provide fuel pump inlet conditions well within the engine start requirements.

There are several other indications that the chilldown of the system was complete before the prevalve was opened. The flowrate through the system reached 145 gpm and leveled off 60 seconds before the prevalve opened. This flowrate was higher than measured during most ground chilldowns. For example, ground test 25X was well within engine start conditions, but the flowrate reached only 120 gpm (figure V-19) and the system pressure loss was 8.7 psid. Immediately prior to the first burn during the 203 acceptance test the flowrate was 143 gpm with subcooled liquid throughout the completely chilled system. Because the flowrate exceeded this value and leveled off during the orbital chilldown, the system appears to have been completely chilled.

Although the hardware was completely chilled, the system did not contain subcooled liquid throughout at the end of the first orbital chilldown (figure V-23). This saturated condition of the fluid in some parts of the system was caused by the small degree of liquid subcooling in the fuel tank and not by an excessive heating rate. The tank pressure achieved by the repressurization was less than will be produced on Saturn V vehicles. Therefore, the degree of subcooling was less than normal. The tank repressurization provided some subcooling, and the recirculation pump produced additional subcooling of the liquid. As the fluid passed through the chilldown system, the increase in fluid temperature due to heating and the decrease in saturation temperature due to the system pressure losses were sufficient to overcome the small amount of liquid subcooling and subsequently, caused the fluid to become

saturated downstream of the G.G. fuel bleed valve. After saturation conditions were reached the fluid temperature varied as a function of the local static pressure and not the heat input to the fluid. Although the fluid contained vapor, its quality was probably quite low as determined by the system pressure loss and the recirculation pump flowrate. The higher tank pressure of vehicles requiring engine restart will allow subcooled liquid to exist throughout the entire system.

When the propellant feed system is completely chilled, the flowrate will be a maximum and the pressure losses will be a minimum. Therefore, the flow parameter ($\Delta P/\dot{w}^2$) was used as an additional measure of the state of chill. Although the characteristic curve of individual pumps and other such variables can influence the results, the flow parameter gives a good measure of the state of chill. Figure V-24 shows the flow parameter for the flight chilldowns as well as for the ground test chilldowns. The lower curve is from the 203 acceptance test, first burn, in which the system was completely chilled. The upper curve is the approximate boundary below which the system, although not completely chilled, is chilled sufficiently for engine start conditions to be met if the local pressure is of sufficient magnitude. As can be seen from figure V-24, the first orbital chilldown was complete, lacking only the proper tank pressure for engine start conditions.

B. LOX SYSTEM CHILLDOWN

Concurrent with the first hydrogen chilldown, a LOX chilldown experiment was also conducted. The chilldown experiment was initiated by the activation of the LOX ullage thrusting system 5518.2 seconds after liftoff. The events which followed were:

1. 5539.2 seconds, continuous vent thruster system closed
2. 5562.3 seconds, LOX recirculation pump started (LOX prevalve open)
3. 5574.3 seconds, LOX prevalve closed (beginning recirculation flow through engine)
4. 5864.3 seconds, LOX prevalve opened (stopping flow through engine)
5. 5886.5 seconds, LOX recirculation pump stopped
6. 5903.8 seconds, continuous vent thruster system opened
7. 5927.2 seconds, LOX ullage thruster system closed (end of chilldown experiment)

During this particular flight abnormally severe operating conditions were imposed on the LOX chilldown system. However, the system operated satisfactorily, and no problems are anticipated during the orbital chilldown on vehicles requiring engine restart.

The abnormal conditions imposed during the AS-203 flight were the large LOX tank pressure decay during chilldown and the small quantity of LOX on board. Because propellant control was being maintained by the LOX ullage thruster system, the initial LOX tank ullage pressure of 35.2 psia decreased to 33.3 psia when the recirculation pump was started, and decreased further to 24.0 psia by the time the recirculation pump was stopped (figure V-25). The bulk temperature of the LOX in the tank was about 171°R, giving the LOX recirculation pump an initial NPSH of 11.6 psi. The pump NPSH decayed to a final value of only 0.7 psi. This condition will not exist on Saturn V vehicles.

The recirculation pump operated properly during the initial phases of the chilldown (5570 to 5630 seconds) as illustrated by the pump performance data shown on figure V-26. Near the end of the chilldown (5777 to 5830 seconds) the recirculation pump flowrate became unstable (figure V-27) and the pump performance became poor. This is not surprising because the small quantity of LOX in the tank resulted in a nominal liquid level only 7 inches above the recirculation pump impeller. The poor pump performance can be attributed to gas ingestion caused by either liquid vortexing or an uncovering of the pump inlet by a slosh wave. The theoretical period of LOX sloshing corresponds to the apparent period, and sloshing probably caused the gas ingestion. This problem will not exist on vehicles requiring engine restart since a much larger quantity of LOX will be on board.

During the chilldown, the recirculation pump provided flowrates up to 42 gpm (figure V-27) and a pressure rise of up to 14 psid (figure V-28). The LOX at the recirculation pump discharge was subcooled 12°R about 20 seconds after the prevalve closed (figure V-29). However, because of the decaying tank pressure, it was only 5°R subcooled when the prevalve opened ending the flow through the engine.

The upper limit of the LOX pump inlet temperature measurement was 2°R below the LOX bulk temperature. Therefore, LOX pump inlet temperature data were not obtained. Instead, the G.G. LOX bleed valve temperature, measured downstream of the LOX pump, was used to indicate the state of chill (figure V-30). The saturation temperature based on the pressure at the G.G. LOX bleed valve (figure V-31) was derived from the LOX pump inlet pressure as discussed in reference 12. The LOX at the bleed valve reached a maximum of 6.2°R subcooled; but, because of the LOX tank ullage pressure decay, the fluid was subcooled only 2.8°R when the prevalve opened. The heat absorbed by the LOX between the recirculation pump discharge and the G.G. LOX bleed

valve was 1.9 Btu/sec at the end of the chilldown. The LOX pump discharge temperature was quite similar to the G.G. LOX bleed valve temperature (figure V-32) although the LOX was bled from the discharge line upstream of the LOX pump discharge measurement.

The fluid at the tank inlet of the recirculation return line became saturated 15 seconds after the prevalve closed (figure V-33 and V-34). It reached a maximum of 2.7°R subcooled, but by the time the prevalve opened it was only slightly subcooled (about 0.8°R). The heat absorbed in the recirculation return line at the end of chilldown was about 1.7 Btu/sec. The total heat leak into the LOX at the end of chilldown was 3.6 Btu/sec.

The LOX flowthrough the engine was stopped after 290 seconds by the opening of the prevalve. With the prevalve open, the LOX flows back through the prevalve into the LOX tank, chilling the volume above the prevalve and clearing it of vapor. Twenty seconds after the prevalve opened the recirculation pump was turned off.

The fluid conditions required at the LOX pump inlet for engine start are shown by figure V-35. Fluid conditions at both the recirculation pump discharge and the gas generator LOX bleed valve immediately prior to prevalve opening are shown. The fluid condition at the LOX pump inlet is between these points. This indicates that although the start conditions did not exist, the LOX was subcooled and a higher tank pressure would have produced start conditions.

On vehicles requiring an engine restart the higher tank pressures planned plus the lower LOX bulk temperature (due to the larger quantity of LOX) will produce fluid conditions well within the J-2 engine start requirements.

C. SECOND FUEL CHILLDOWN

A contingency hydrogen chilldown was conducted near the end of the second orbit (about 3 hours after liftoff). The primary purpose of the experiment was to determine if the recirculation pump would operate under the low acceleration level of the continuous vent system (5.5×10^{-5} g's), with zero pump NPSH. The operation of the recirculation pump under these conditions would permit the propellant feed system to be chilled without requiring an auxiliary setting system during the chilldown sequence (such as the LUT system employed during the first orbital chilldown or the 70-lb settling engines employed on the Saturn V/S-IVB). The second fuel chilldown experiment was successful, and provided a contingency technique for thermally conditioning the J-2 engine in the orbital environment.

During the second hydrogen chilldown, the fuel tank was not repressurized. The continuous vent system operated during the entire experiment, and the

hydrogen in the tank remained saturated at 19.5 psia (figure V-36). Except for the fact that no fuel tank repressurization or fuel lead was used during the second hydrogen chilldown, the sequence of events was a repeat of the first hydrogen chilldown.

1. 10884.8 seconds, recirculation pump started (prevalve open)

2. 10894.8 seconds, prevalve closed (flow through engine began)

3. 11184.8 seconds, prevalve opened (ending flow through engine)

4. 11206.8 seconds, recirculation pump stopped (end of experiment)

When the recirculation pump started, the prevalve was open. The fluid at the recirculation pump discharge was initially superheated, but became saturated as soon as the pump was activated (figure V-37). The initial flow through the recirculation pump chilled down the bypass line and flowed back through the prevalve and anti-vortex screen into the tank. Ten seconds after the recirculation pump was activiated the prevalve closed directing the flow through the suction duct to the engine. The recirculation pump provided alternately saturated and subcooled fluid throughout the remainder of the chilldown experiment. Initially, the recirculation pump pressure rise varied between 3 and 10 psi (figure V-38), with large flow oscillations between 5 and 140 gpm (figure V-39). During the last 35 seconds before the prevalve opened, however, both the pressure rise and the flowrate appeared to become more stable. The pressure rise leveled off at about 7.9 psid with spikes down to 6.5 and up to 8.7 psid, and the flowrate leveled off at an average value of about 118 gpm with oscillations down to 75 and up to 130 gpm.

The fluid in the upper portion of the suction duct, which was saturated at the initiation of chilldown, become subcooled 60 seconds after the prevalve closed (figure V-40). Thereafter, it did not remain subcooled, but varied from saturated to subcooled because of the pressure oscillations from the recirculation pump.

The fuel pump inlet, which was initially superheated, became saturated 2 seconds after the prevalve closed (figures V-41 and V-42). Unlike the upper portion of the suction duct, the fluid at the fuel pump inlet did not become subcooled during the contingency chilldown.

The fluid passing through the G.G. fuel bleed valve became saturated 17 seconds after the prevalve opened and was saturated for the remainder of the chilldown (figure V-43). The fluid at the recirculation return line (tank inlet) became saturated 27 seconds after the prevalve opened (figures V-44 and V-45).

Because subcooled liquid was present only in the upper portion of the suction duct and quality throughout the system was unknown, the heat absorbed by the fluid could not be determined.

Although subcooled liquid was present only in the upper portion of the suction duct during the chilldown, all indications are that the propellant feed system hardware was sufficiently chilled such that a higher tank pressure would have provided engine start conditions. At the end of the chilldown the flow parameter (figure V-24) indicated that the system was almost completely chilled. The chilldown of the fuel pump discharge line was similar to the first orbital chilldown and indicated the same final temperature as obtained during the first chilldown (figure V-21).

The recirculation pump operated successfully under the low acceleration, zero NPSH, conditions. Although its performance was substantially reduced (figure V-5), it provided sufficient flow for the chilldown process. The accumulated flow during the second chilldown was less than during the first chilldown. However, the accumulated flow was still greater than was achieved during a typical ground chilldown (S-IVB-25X) (figure V-46).

Although the contingency chilldown successfully chilled the propellant feed system hardware, the cryogen itself must also be properly conditioned to meet engine start requirements. On vehicles requiring an engine restart, the removal of the saturated cryogen from the propellant feed system could be accomplished within a 50-second time interval during the propellant tank repressurization prior to engine ignition.

D. HARDWARE HEATING CONDITIONS DURING ORBIT

At the beginning of the chilldown experiments, the propellant feed system hardware temperatures were lower than had been anticipated. Two conditions contributed to these low temperatures. The first was a recirculation of propellants through the engine pumps that occurred just after main engine cutoff (MECO) at insertion. The prevalves closed 0.5 seconds after MECO, trapping liquid propellants in the suction ducts and the engine. Heat from the turbines was conducted through the pumps and into the liquid. The heat input to the liquid in the suction ducts caused it to expand through the engine pumps and through the recirculation return line back into the propellant tank. The failure of the shutoff valve on the fuel recirculation pump allowed an additional 26.6 lb_m of LH_2 to enter the suction duct after MECO (figures V-47 & V-48). The prevalves were opened 60 seconds after MECO. However, enough liquid was present at the fuel pump inlet to maintain saturation conditions until loss of telemetry signal 225 seconds after engine shutdown (figure V-49). The fuel pump discharge line wall temperature remained low ($46^{\circ}R$) for 135 seconds after engine shutdown (figure V-50). When the first chilldown was conducted at

the end of the first orbit the fluid at the fuel pump inlet was superheated, but the fuel pump discharge line wall temperature had risen to only 280°R which was the maximum value measured during the flight. If the chilldown had not been conducted until the end of the third orbit as is the normal case, it is expected that the temperature would have been about 400°R based on extrapolation of the pre-chilldown temperature slope. This is still approximately 50°R to 100°R less than originally estimated for the hardware temperatures at the initiation of chilldown.

Following MECO, the fluid in the LOX suction duct remained subcooled for 90 seconds. The LOX pump discharge temperature was still saturated when the telemetry signal was lost. The shutoff valve on the LOX recirculation pump was closed at MECO, and no additional LOX was supplied to the system. The artificial circulation of propellants through the chilldown system immediately after insertion removed a significant quantity of heat from the warm turbines, thereby reducing the heat soak through during orbital coast and subsequently the chilldown requirements.

The second condition that contributed to lower hardware temperatures was the presence of saturated fluid in the suction ducts throughout the entire orbital period. Heating during the orbital period was expected to produce a vapor filled duct, resulting in relatively high hardware temperatures. However, the unexpected presence of saturated fluid maintained the hardware temperatures lower than anticipated. The top of the anti-vortex screen in the suction duct had been redesigned to open in a low-gravity environment to reduce its tendency to trap vapor. Analyses conducted prior to the flight indicated that a large bubble could form in the line as a result of the coalescence of hydrogen bubbles formed by boiling in the duct. Such a single large bubble could not be removed from the duct by the continuous vent acceleration. Thus, even with the redesigned anti-vortex screen, there was a possibility that vapor could be trapped in the suction duct. Apparently the prevailing environmental conditions were such that the formation of a large bubble did not occur and liquid remained in the fuel suction duct.

The fluid under the anti-vortex screen in the fuel tank (figure V-51) was saturated or subcooled throughout the entire flight. The saturated fluid maintained the low hardware temperatures as indicated by the LH_2 duct inner wall temperature measurement (figure V-52) and the LH_2 prevalve by-pass line outer wall temperature (figure V-53), both of which decreased during the flight. These temperatures indicate that the first chilldown was more severe than the second. The fluid temperature just downstream of the prevalve is shown by figure V-54. Except during the final two blowdowns at the end of the third orbit, saturated or subcooled fluid was present during the entire flight. Although no temperature sensors were in the LOX suction duct, there are indications (from C004) that saturated fluid also remained in this duct throughout the flight.

The relatively low hardware temperatures at the initiation of the chilldown sequence reduced the orbital chilldown requirements and contributed to the success of the chilldown experiments. These low initial temperatures are also expected to reduce the chilldown requirements on vehicles requiring engine restart.

TABLE V-1

RESULTS OF S-IVB FUEL FEED SYSTEM CHILLDOWN EXPERIMENTS

RUN #	IDENT	PFRPI psia	PFPI psia	TFRPI °R	TFRPO °R	TFPIS °R	TFPI °R	(TFPI-TFRPO) °R	$\dot{w}_c$ lb_m/sec	Q_1 (FRPD to FPI) Btu/sec.	(TFTS-TFPI) °R	NPSH RPI psid	PRPΔP psid	TGGFBV °R	Subcooled at GGFBV	Subcooled at MFSOV	(TGGFBV-TFPI) °R	Q_2 (FPI to GGFBV) Btu/sec.	REMARKS
203 1st Burn (L.P.)	X	16.0	25.0	(C-0052) 37.0	(C-0157) 38.3	40.0	(C-0658) 39.8 (C-0003) 39.8	N/A	1.035	N/A	N/A	1	9.2	(C-012) 39.2 (C-650) 39.7	No	No	N/A	N/A	Steady state flow conditions, complete chilldown but two phase at pump inlet
203 1st Burn (H.P.)	0	41.4	47.4	(C-0052) 37.0	(C-0157) 38.3	44.9	(C-0658) 41.2 (C-0003) 39.5	2.9 1.2	1.391	4.2	4.3	26	6.7	(C-012) 45.0 (C-650) 40.2	Yes (4.5°R)	No	7	2.4	Complete chilldown, liquid throughout system.
203 Acc (L.P.) 300 sec	◇	18.9	30.8*	38.1 E	40.4*	41.5*	(C-0003) 42.0	N/A	0.69*	N/A	N/A	1	11.7*	N/A	N/A	N/A	N/A	N/A	Oscillating flow throughout chilldown.
203 Acc (H.P.) 300 sec.	△	35.7	43.8	38.5 E	40.2*	44.2	(C-0003) 42.8	2.6	0.95	6.2	-.2	17	8.2	N/A	N/A	N/A	N/A	N/A	No oscillations chilled to pump but not throughout
S-IVB 17 300 sec.	○	15.2	25.1*	36.6 E	(C0157)* 37.2	40.0*	(C-0637) 40.8	N/A	1.00*	N/A	N/A	1	10.1*	37.6	No	Not Available	N/A	N/A	Flow oscillations two-phase at fuel pump inlet
S-IVB 17 920 sec.	▷	41.0	48.4	37.4 E	37.4	45.1	(C0637) 39.5	2.1	1.37	7.2	4.1	24.3	8.5	39.4	Yes E (2.5°R)	Not Available	N/A	N/A	Two-phase flow at return line exit
S-IVB 20 260 sec.	△	29.3	39.0	36.8 E	36.8	43.3	(C-0658) 42.0 (C-0637) 41.4	5.2 4.6	0.70	9.1 8.1	-.9 -.3	14	9.5	(C-012) 39.9 (C-650) 40.8	No	Not Available	N/A	N/A	No oscillations however flow still transient
S-IVB 20 480 sec	◇	29.4	37.1	36.8	36.8	42.9	(C-0658) 40.2 (C-0637) 39.6	3.4	1.00	8.5 7.0	.9 1.5	14	8.7	(C-012) 39.6 (C-650) 40.4	Yes (2.8°R)	Not Available	.2	.5	No oscillations but pump not chilled
S-IVB 21 300 sec	□	42.6	49.0	(C-5006) 37.5	36.7	45.2	(C-0658) 39.9 (C-0637) 39.1	3.2 2.4	1.293	10.36 7.77	4.1 4.9	26	7.2	(C-012) 41.3 (C-650) 42.0	Yes (2.3°R)	Yes (1.3°R)	2.2	7.12	Chilldown complete Sat. at return
S-IVB 24 300 sec	△	30.8	39.5*	(C-5006) 41.5	(C-640)* 39.9	43.4*	(C-637)* 43.1	N/A	.671	N/A	N/A	1	8.4	(C-012) 40.1 (C-650) 41.0	No	No	N/A	N/A	Flow oscillating chilldown not complete
S-IVB 25 300 sec.	□	36.1	44.0	36.5 E	36.5	44.2	40.0	3.5	.96	8.3	2.6	19	8.3	(C-012) 41.6 (C-650) 42.1	Yes (1.5°R)	Yes (1.0°R)	2.0	6.4	Chilldown complete Sat. at return
S-IVB 25X 300 sec	△	37.5	45.5	36.8 E	(C-640) 37.0	44.5	(C-637) 40.0 (C-658) 40.3	3.0 3.3	1.102	8.26 9.13	3.0 2.7	22	8.7	(C-012) 41.6 (C-650) 42.1	Yes (1.7°R)	Yes (1.4°R)	1.8	5.0	Chilldown complete no oscillations Sat. at return.
S-IVB 26 300 sec	◇	36.2	43.2	(C-30067) 37.3	35.5	44.1	(C-658) 37.3	1.8	1.15 E	5.2	5.4	19.6	7.8	(C-012) 36.8	Yes	Yes (1.5°R)	N/A	N/A	Cold duct chill corrected temps show subcooled at RRL tank inlet.
S-IVB 27 300 sec	○	35.7	42.3	36.0 E	36.0	43.9	(C-658) 37.4	1.4	1.4 F	4.9	5.3	24	6.4	(C-012) 36.0	Yes (6.5°R)	Yes (1.2°R)	N/A	N/A	Oscillations (2b0 sec'd) Sat at return, cold duct chill
203 Flight 1st. chill	●	(D021) 25.5	(D002) 33.	39.2 E	(C-0157) 39.2	41.9 (from D002)	(C003) 40.1	0.9	(F005) 1.45	3.3	-.2	6.2	7.6	(C012) 40.4	(C012) Yes (1.2°R)	(C134) No	39.5-40.3	1.1	Complete chilldown higher tank pressure required for start
203 Flight 2nd chill	◇	(D021) 19.5	(D002) 27.5	38.3 E	(C157) 39.3	(fromD002) 40.7	(C003) 40.1	.8	(F005) 1.16	N/A	N/A	0.	7.9	(C012) 39.4	No	No	N/A	N/A	System sufficiently chilled. Higher tank pressure required for start

* Averaged Value E Calculated Value

TABLE V-1
(continued)

Definition of Symbols Used

PFRPI - Pressure - Fuel Recirculation Pump Inlet

PFPI - Pressure - Fuel Pump Inlet

TFRPI - Temperature - Fuel Recirculation Pump Inlet

TFRPO - Temperature - Fuel Recirculation Pump Outlet

TFPIS - Saturation Temperature-Fuel Pump Inlet

TFPI - Temperature - Fuel Pump Inlet

$\dot{w}_c$ - Recirculation Flowrate

Q - Heat Absorbed by Fluid

TFTS - Saturation Temp. in Fuel Tank

NPSH - Net Positive Suction Pressure

PRPΔP - Fuel Recirculation Pump Pressure Rise

TGGFBV - Temperature - Gas Generator Fuel Bleed Valve

GGFBV - Gas Generator Fuel Bleed Valve

MFSOV - Main Fuel Shutoff Valve

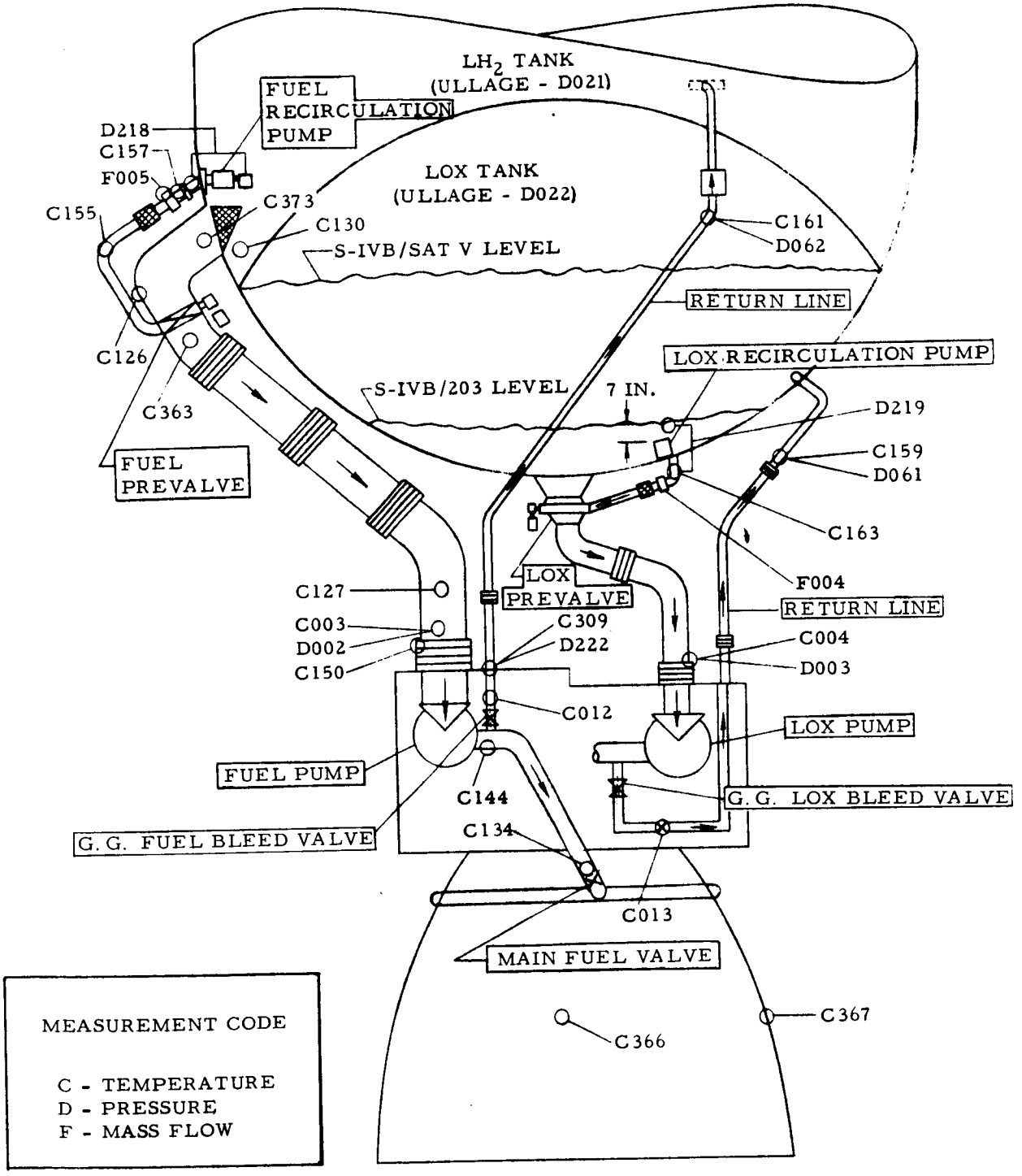

FIGURE V-1 SCHEMATIC OF J-2 ENGINE CHILLDOWN SYSTEM

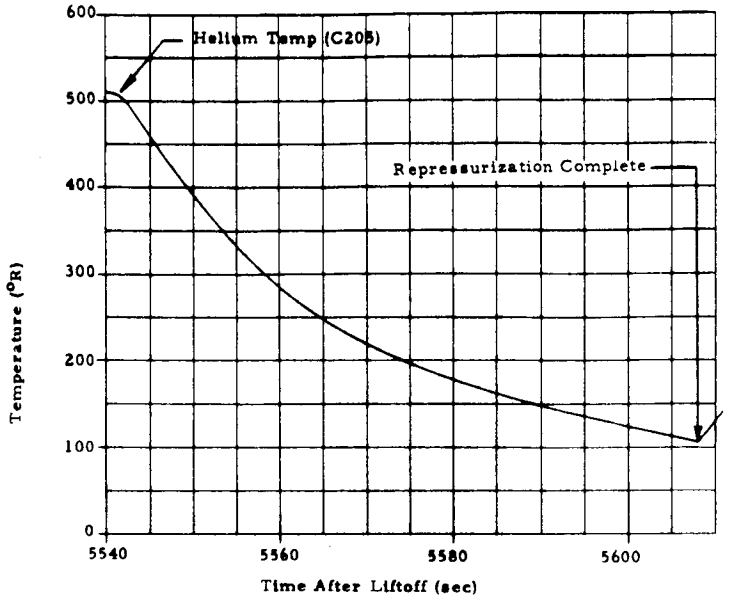

FIGURE V-2 HELIUM TEMPERATURE IN STORAGE BOTTLE DURING FUEL TANK REPRESSURIZATION

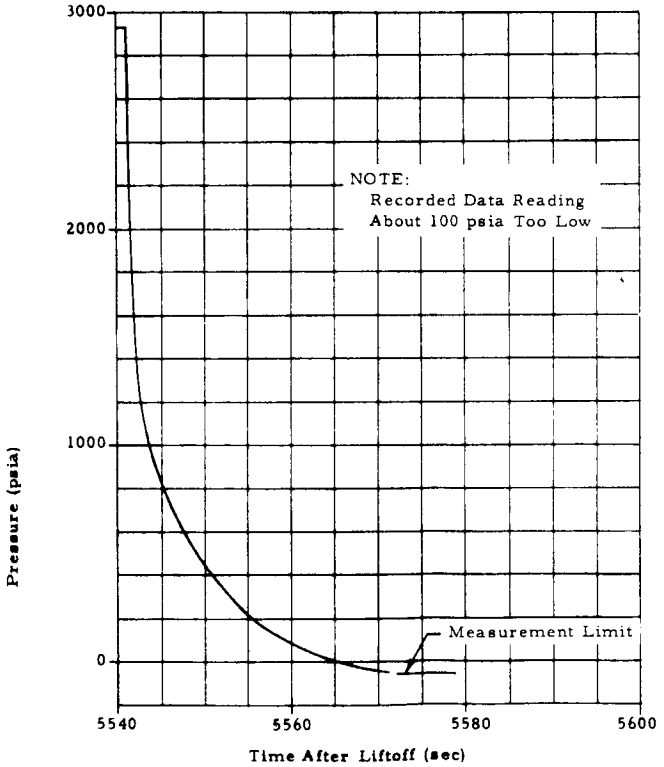

FIGURE V-3 HELIUM STORAGE BOTTLE PRESSURE DURING FUEL TANK REPRESSURIZATION

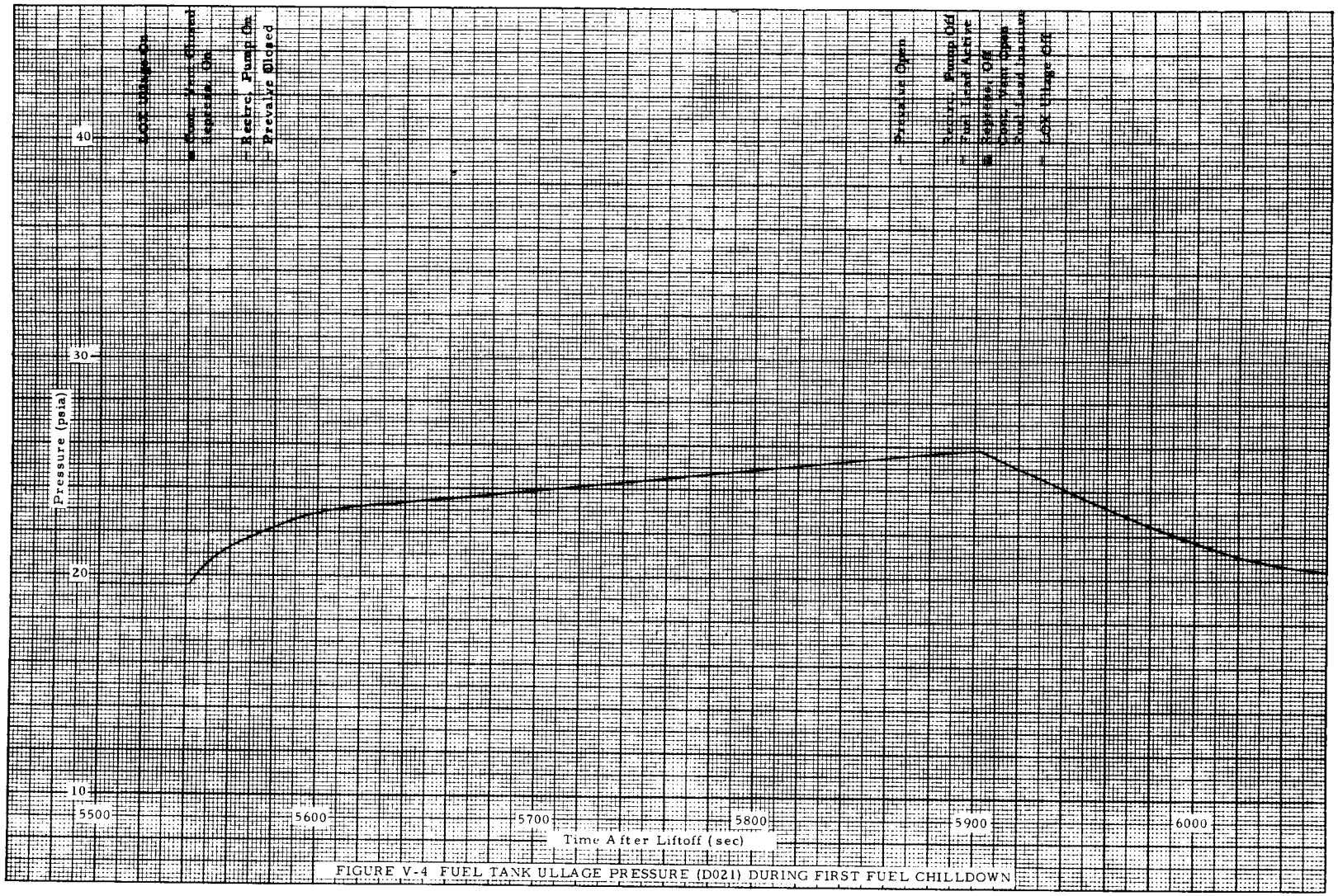

FIGURE V-4 FUEL TANK ULLAGE PRESSURE (D021) DURING FIRST FUEL CHILLDOWN

NOTE: DATA POINTS AT 10 SECOND INTERVALS DURING CHILLDOWN

× FIRST CHILLDOWN - 2.0 TO 6.2 PSID NPSH

○ SECOND CHILLDOWN - ZERO NPSH

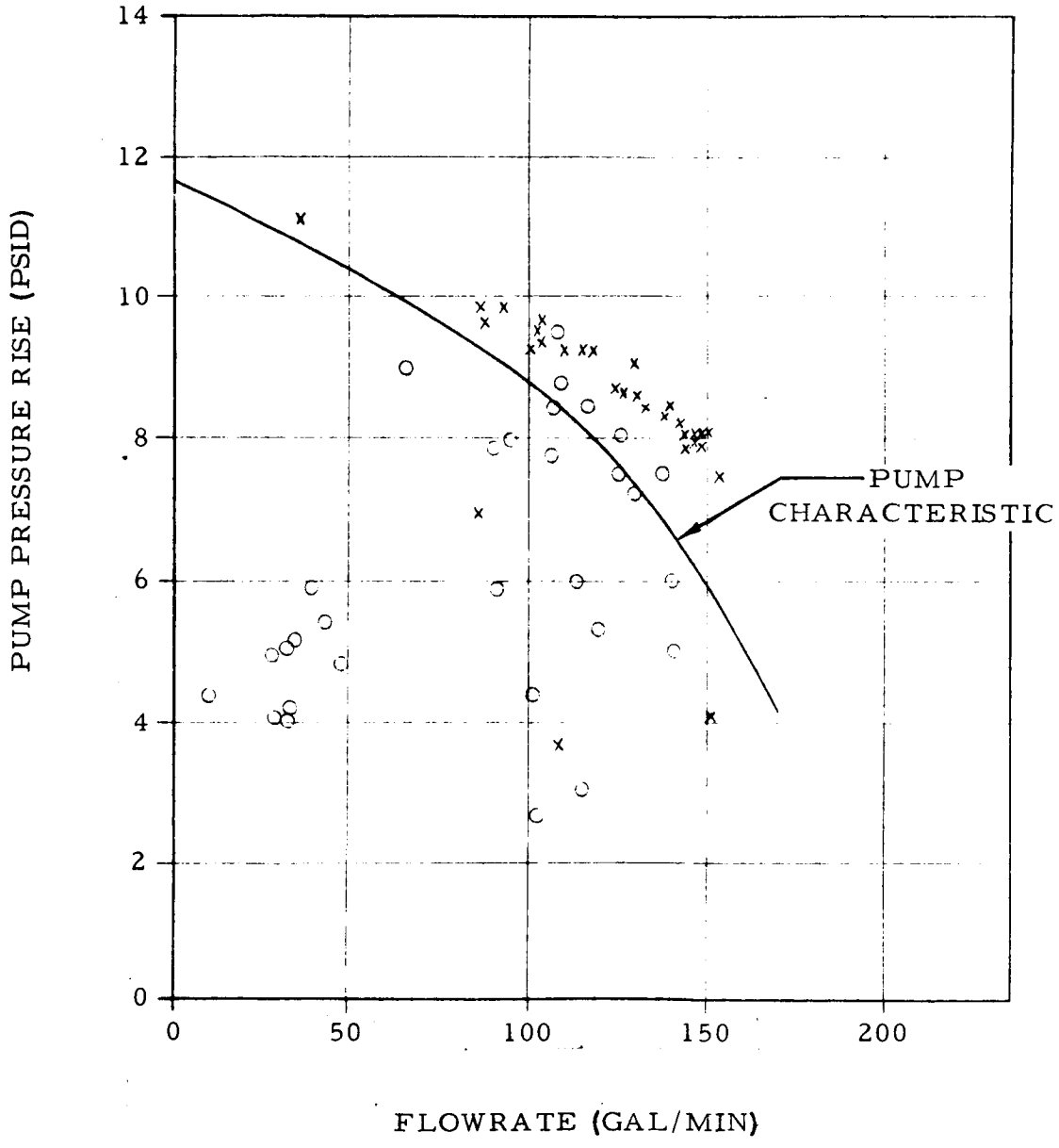

FIGURE V-5 FUEL RECIRCULATION PUMP PERFORMANCE

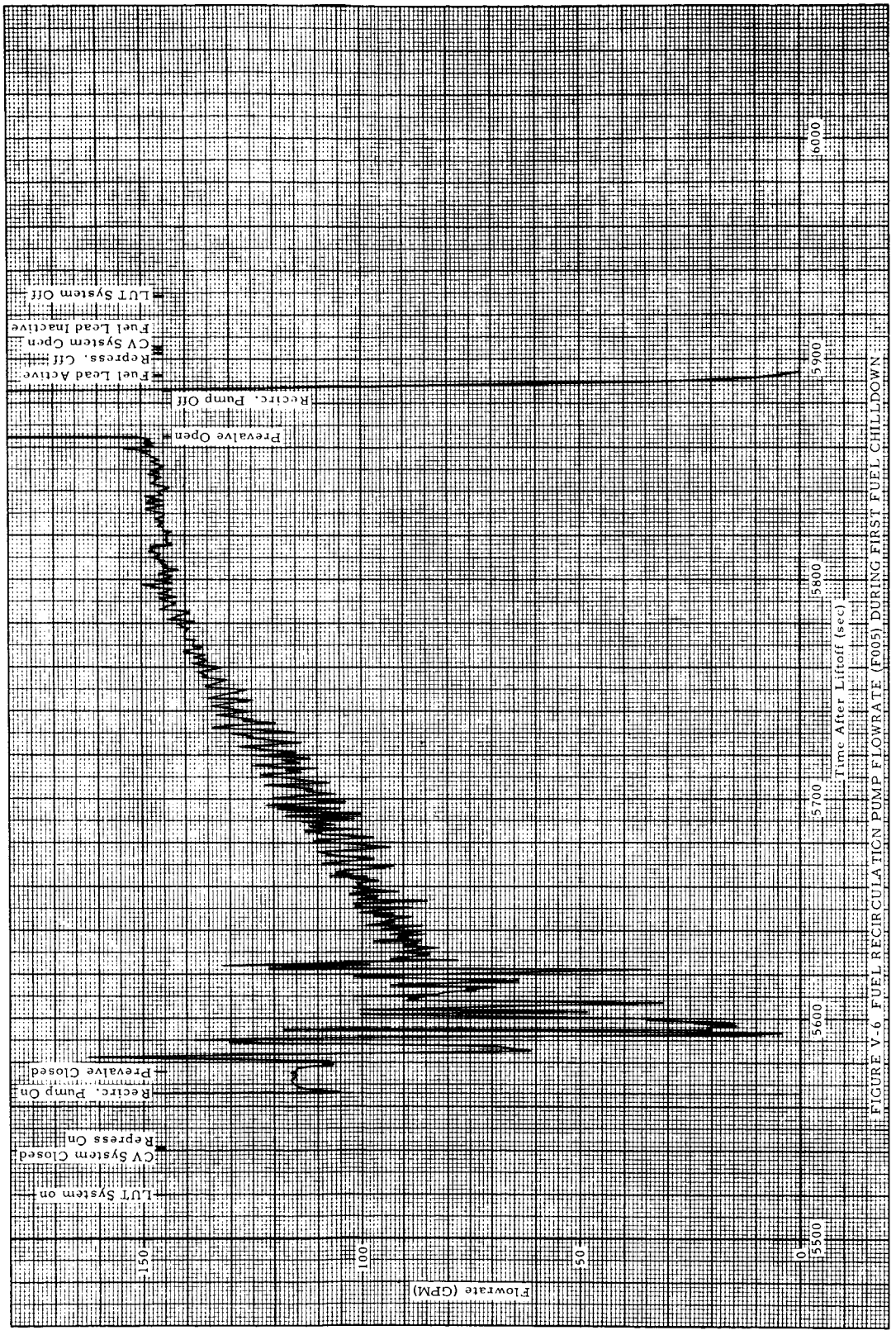

FIGURE V-6 FUEL RECIRCULATION PUMP FLOWRATE (F005) DURING FIRST FUEL CHILLDOWN

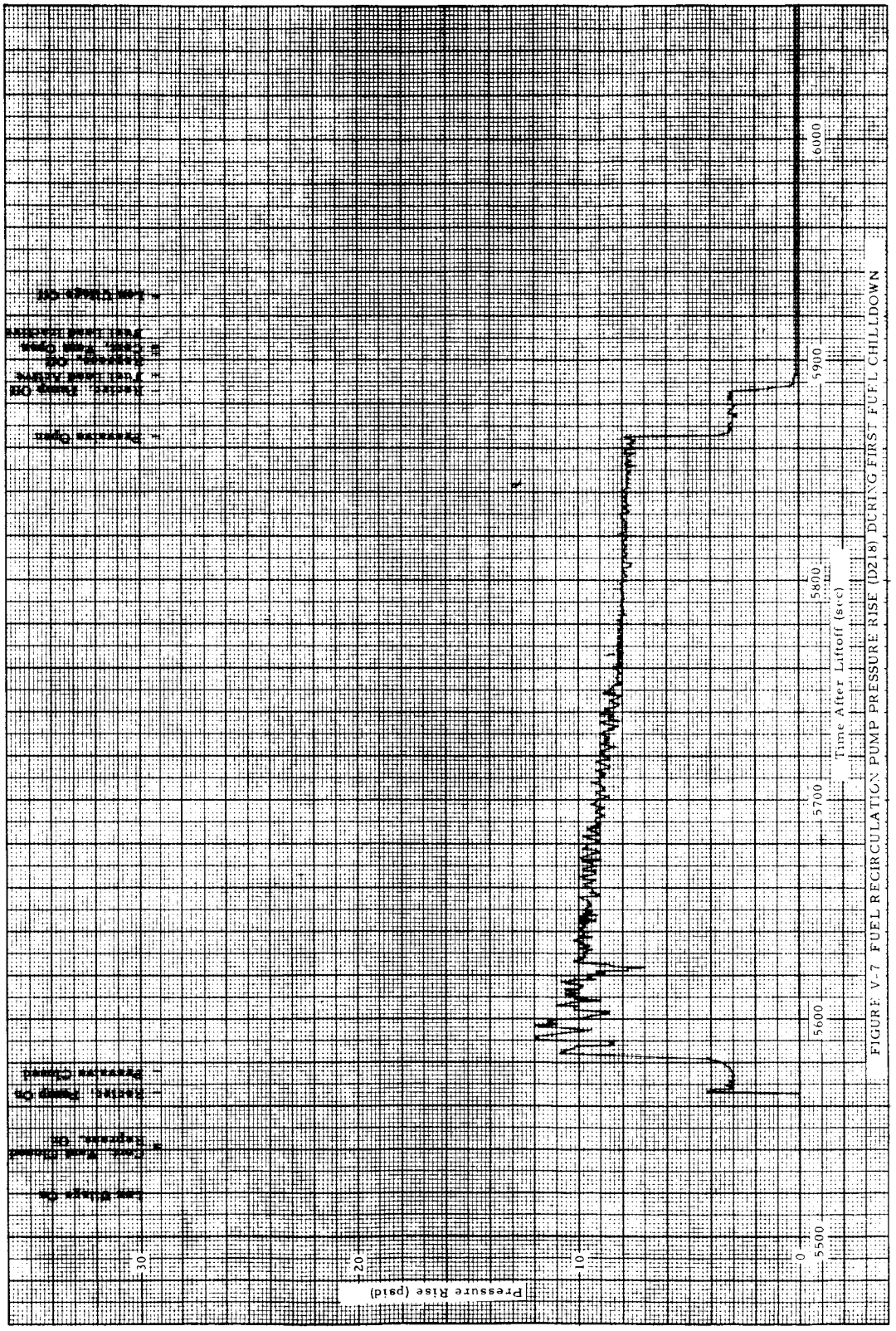

FIGURE V-7 FUEL RECIRCULATION PUMP PRESSURE RISE (D218) DURING FIRST FUEL CHILLDOWN

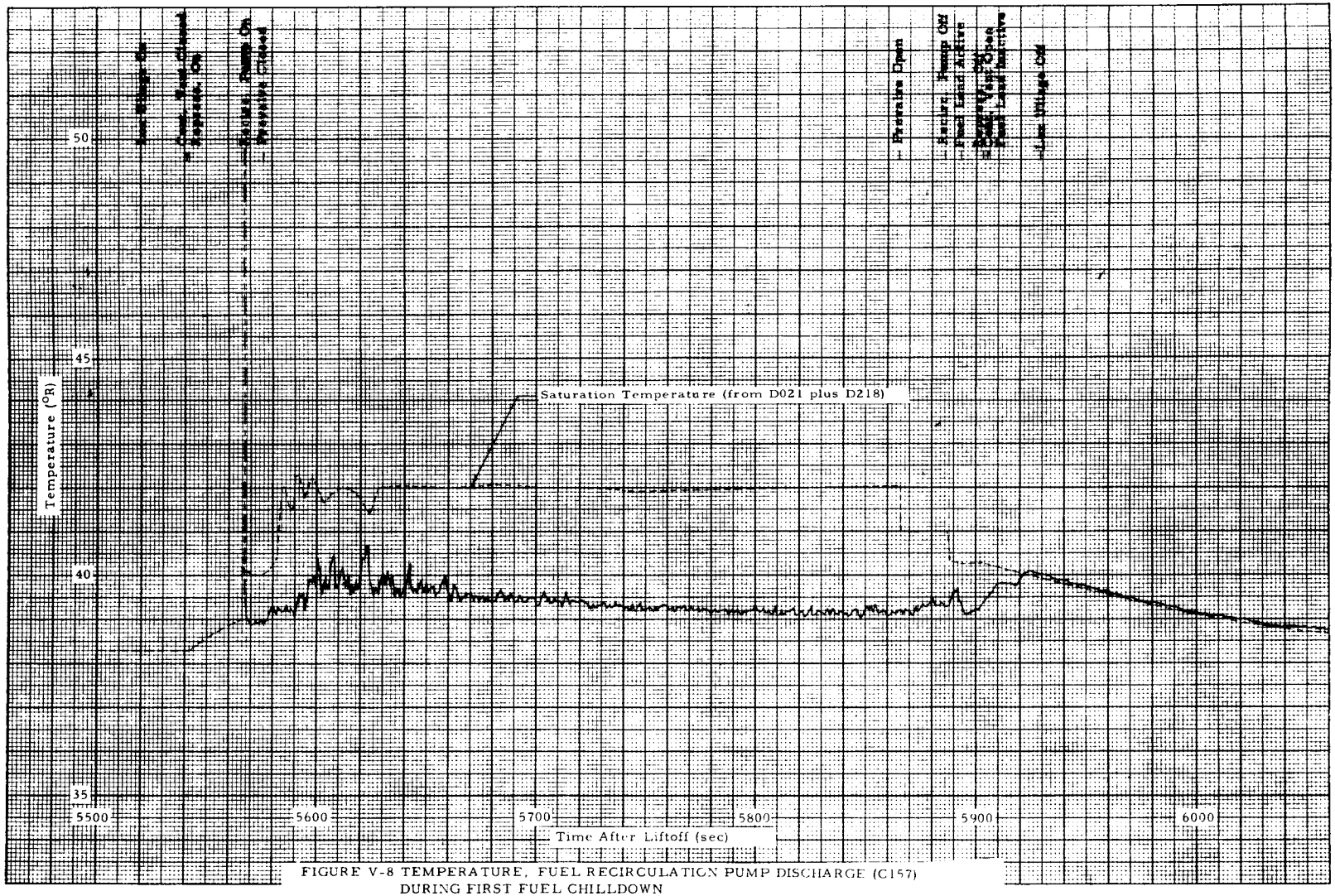

FIGURE V-8 TEMPERATURE, FUEL RECIRCULATION PUMP DISCHARGE (C157) DURING FIRST FUEL CHILLDOWN

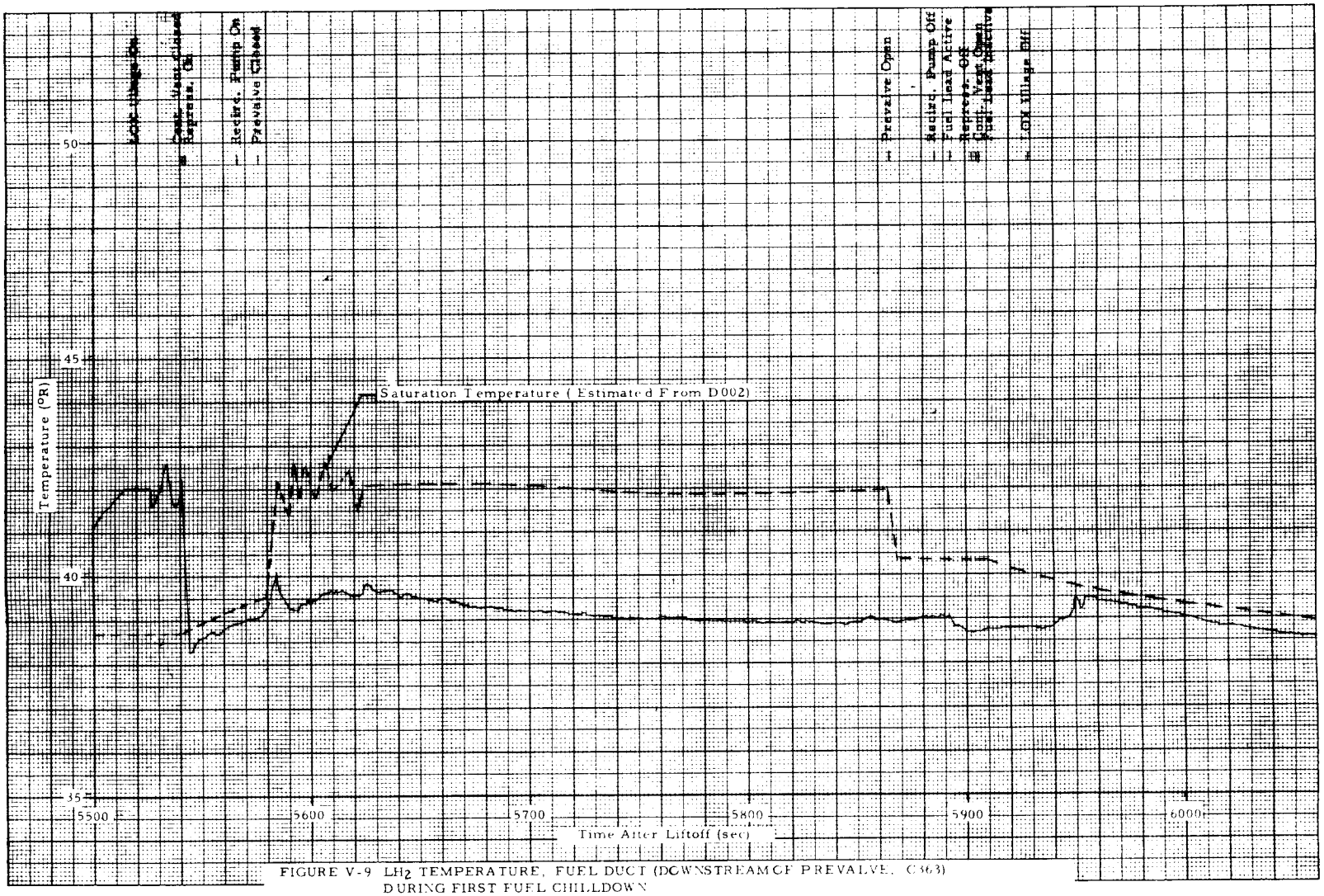

FIGURE V-9 LH_2 TEMPERATURE, FUEL DUCT (DOWNSTREAM OF PREVALVE, C663) DURING FIRST FUEL CHILLDOWN

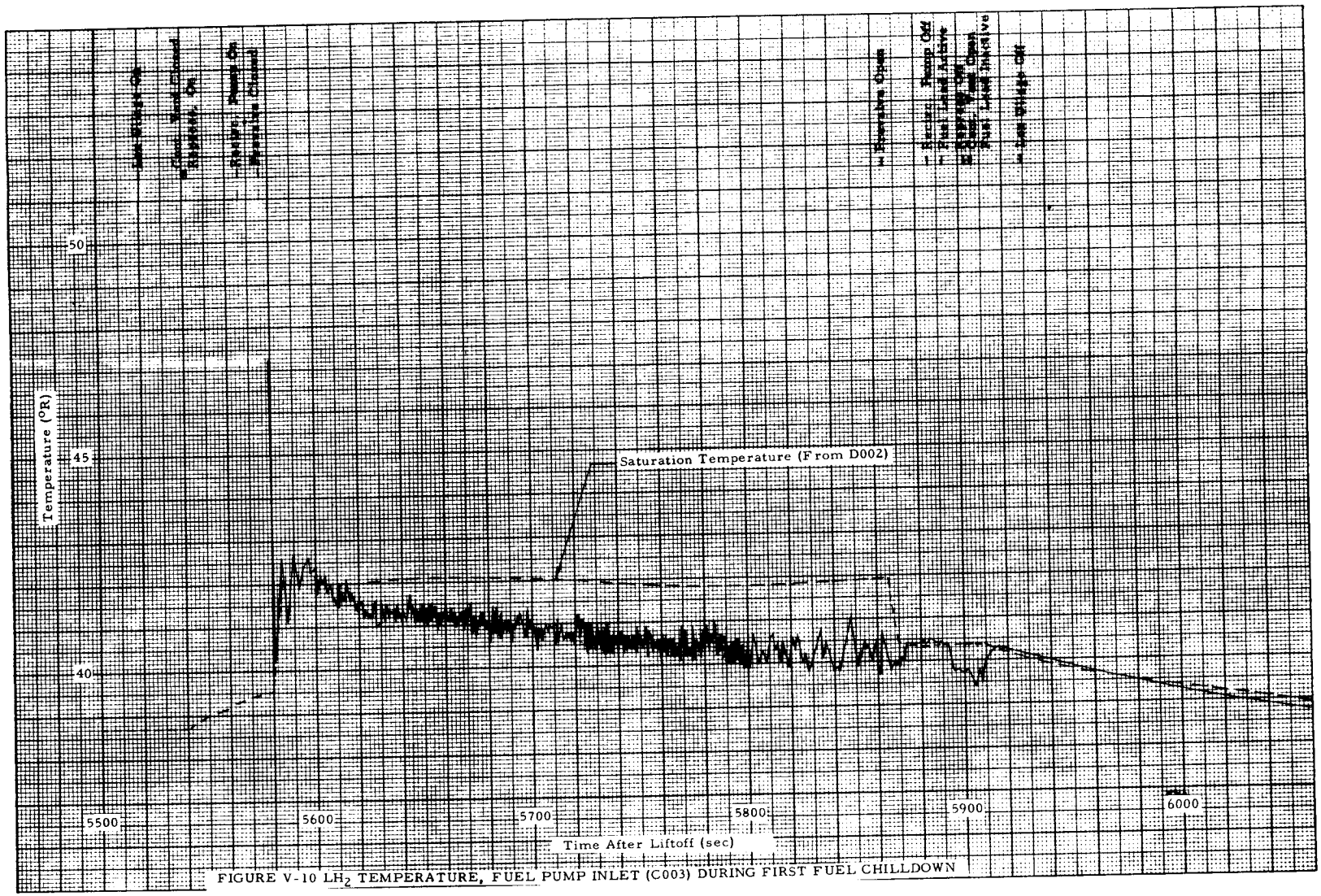

FIGURE V-10 LH_2 TEMPERATURE, FUEL PUMP INLET (C003) DURING FIRST FUEL CHILLDOWN

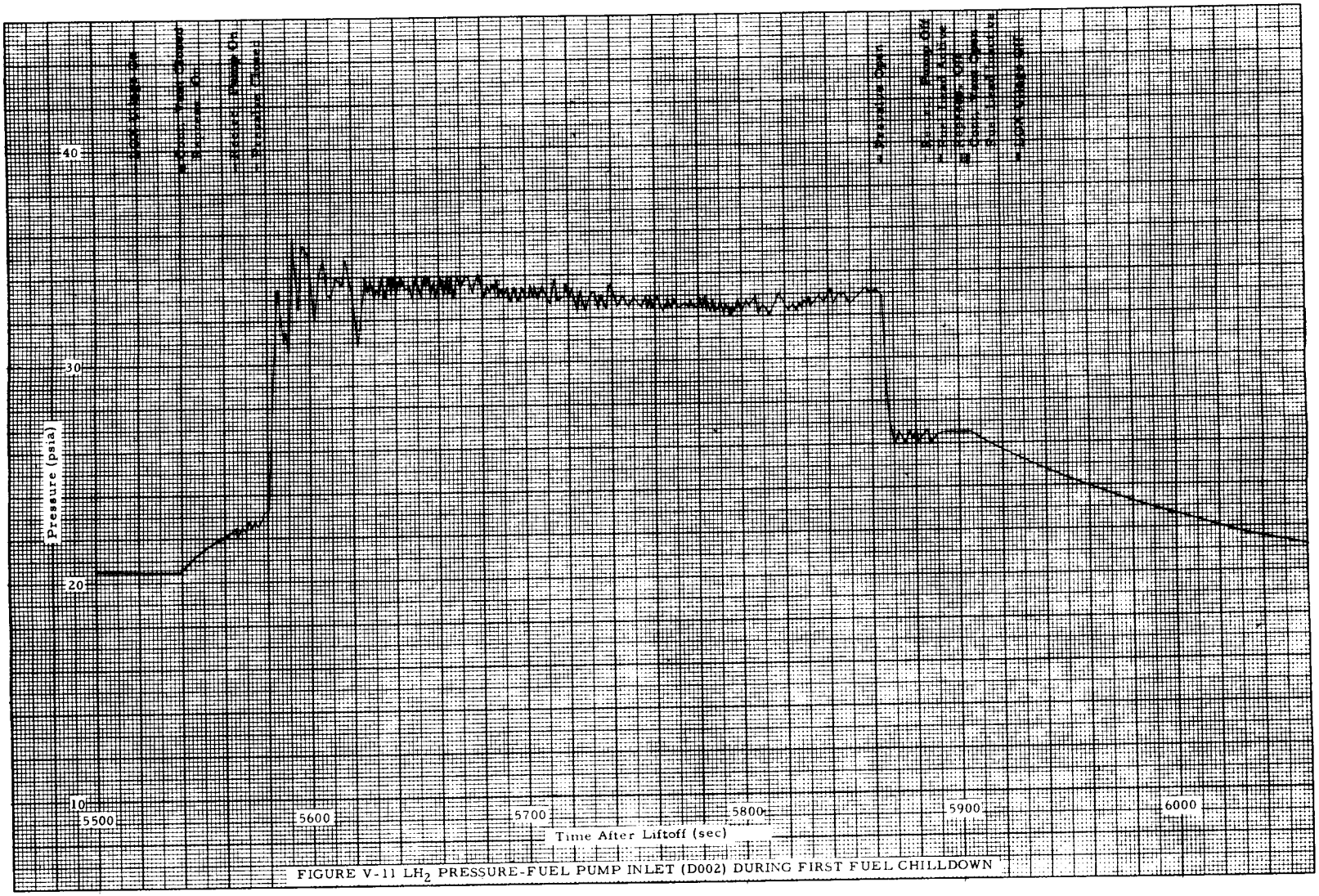

FIGURE V-11 LH_2 PRESSURE-FUEL PUMP INLET (D002) DURING FIRST FUEL CHILLDOWN

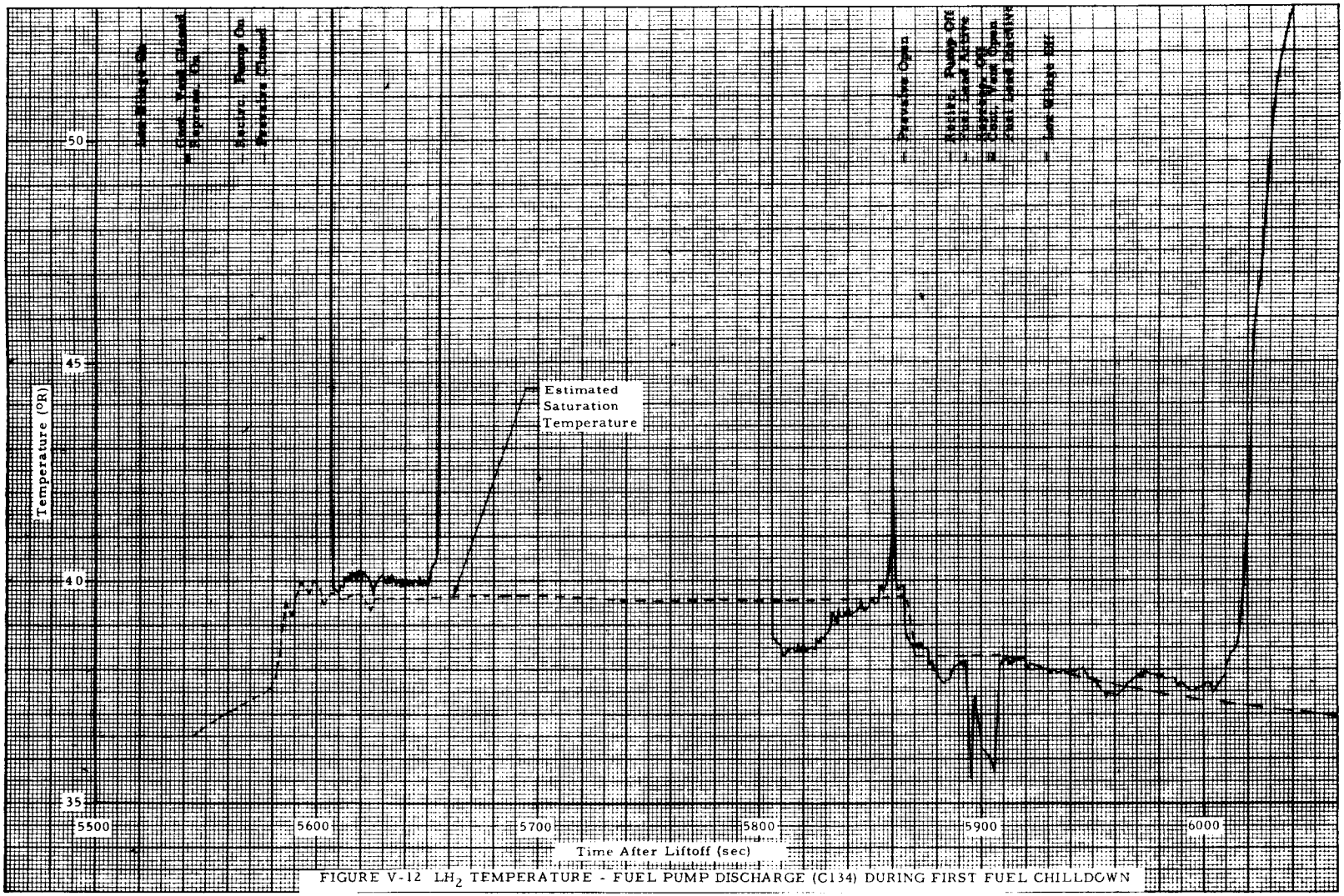

FIGURE V-12 LH_2 TEMPERATURE - FUEL PUMP DISCHARGE (C134) DURING FIRST FUEL CHILLDOWN

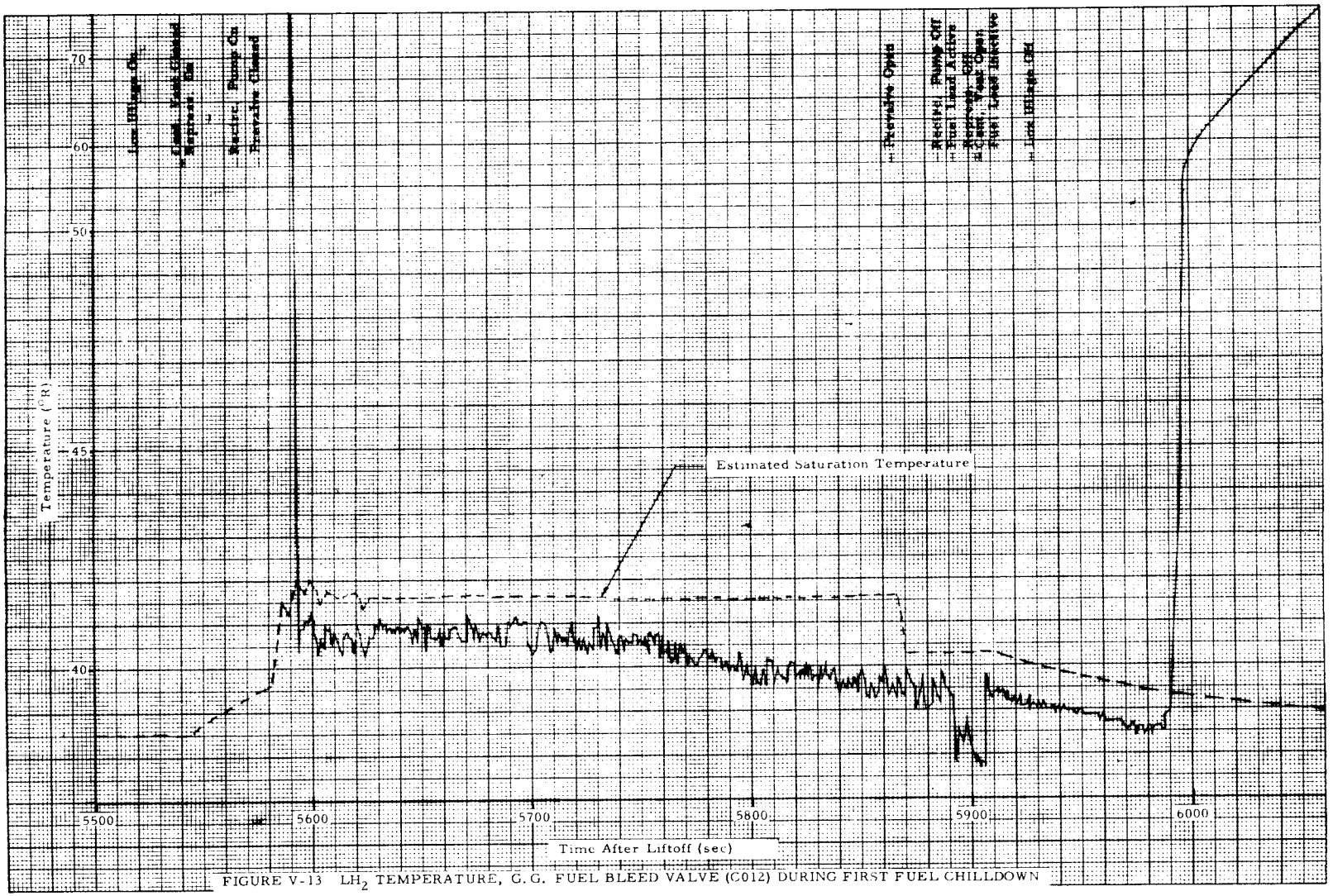

FIGURE V-13 LH_2 TEMPERATURE, G.G. FUEL BLEED VALVE (C012) DURING FIRST FUEL CHILLDOWN

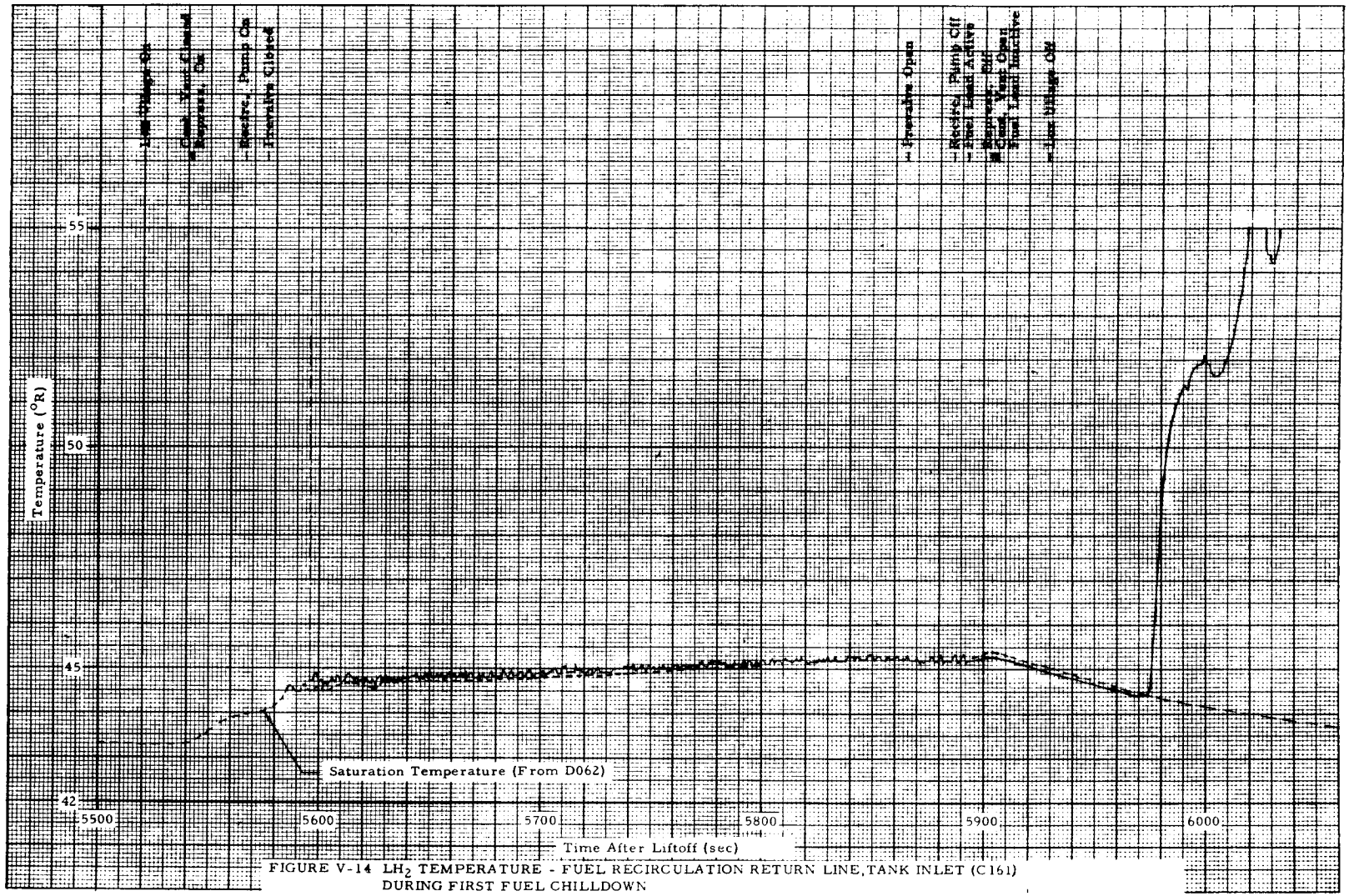

FIGURE V-14 LH_2 TEMPERATURE - FUEL RECIRCULATION RETURN LINE, TANK INLET (C161) DURING FIRST FUEL CHILLDOWN

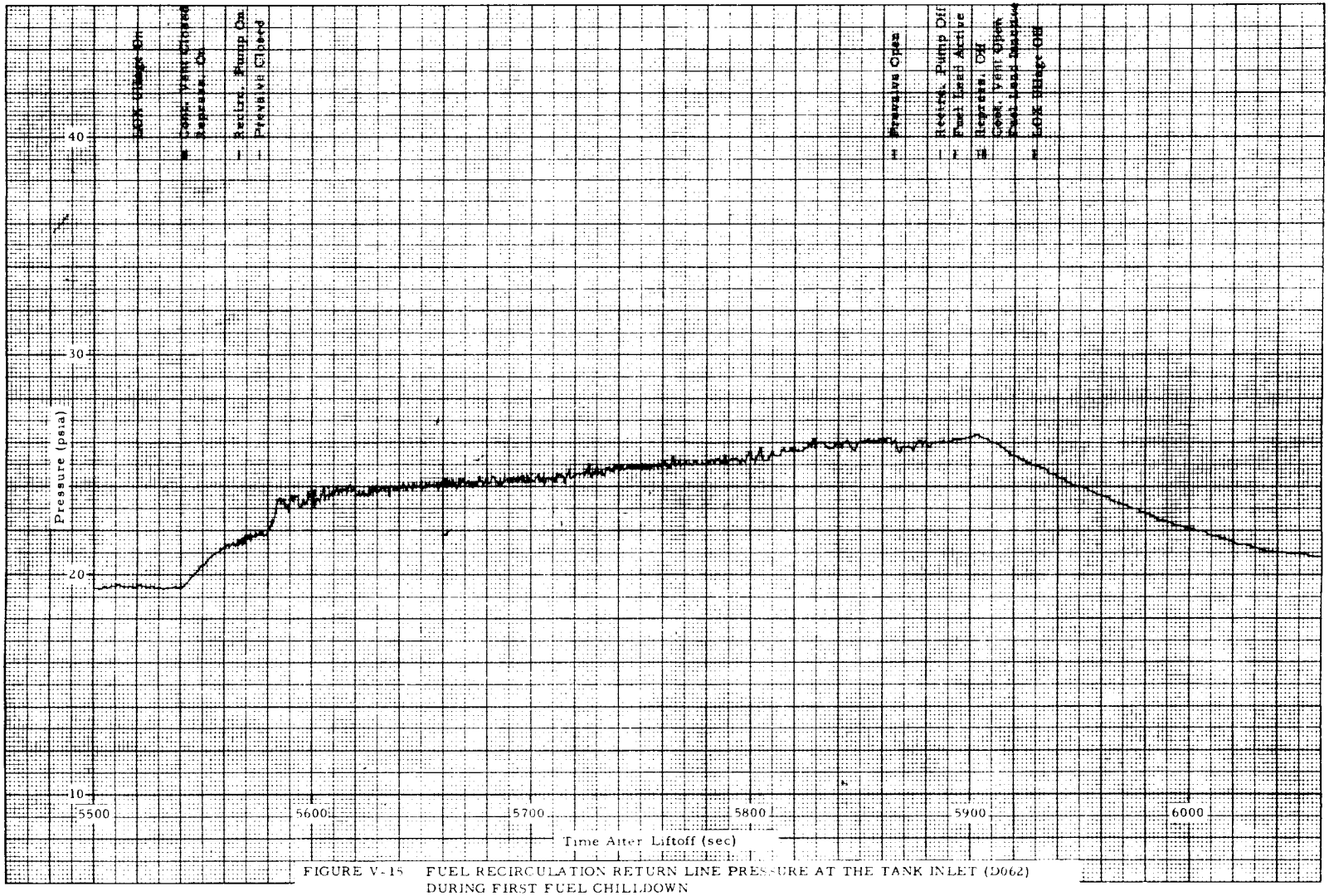

FIGURE V-15 FUEL RECIRCULATION RETURN LINE PRESSURE AT THE TANK INLET (D062) DURING FIRST FUEL CHILLDOWN

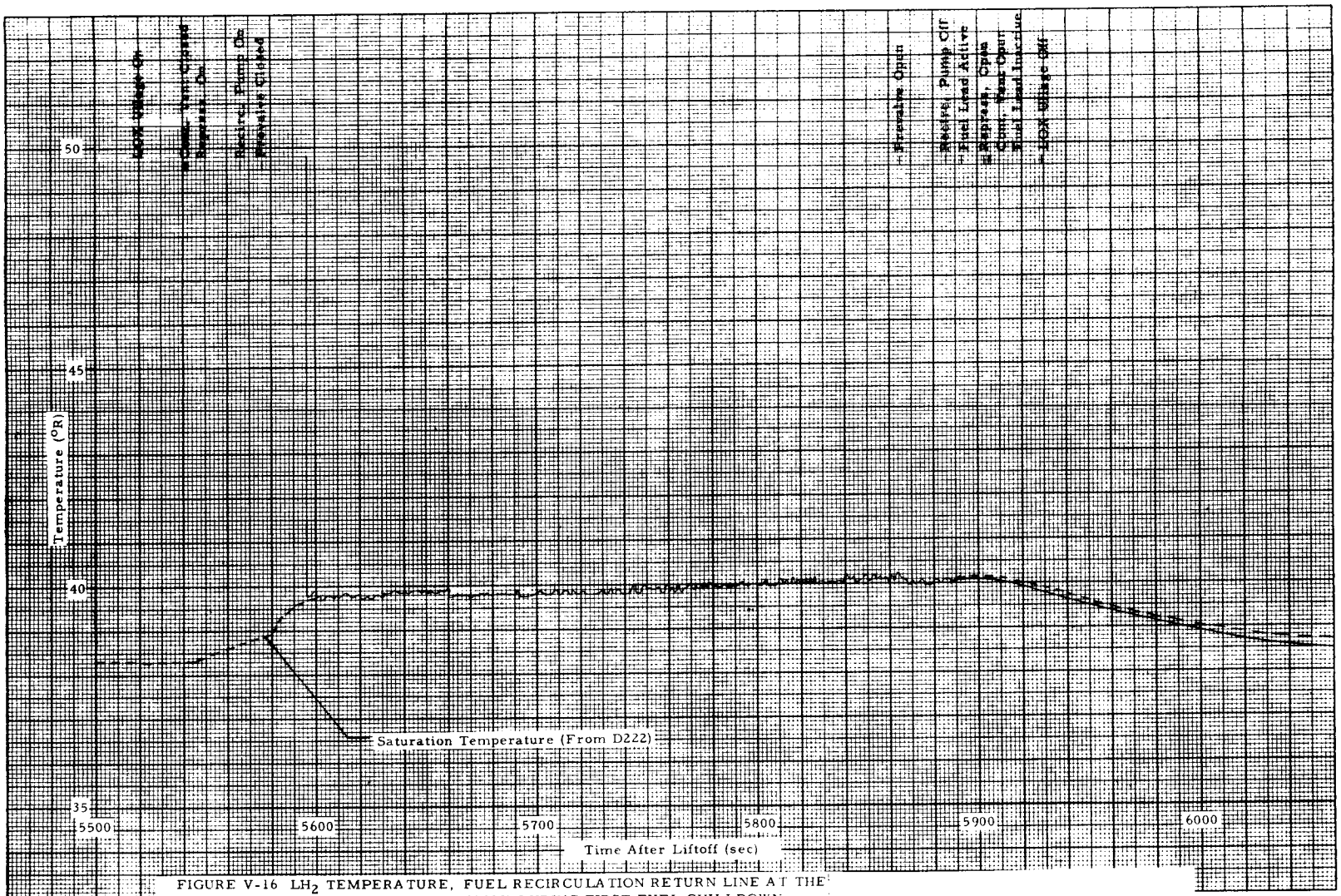

FIGURE V-16 LH_2 TEMPERATURE, FUEL RECIRCULATION RETURN LINE AT THE CUSTOMER CONNECT (C309) DURING FIRST FUEL CHILLDOWN

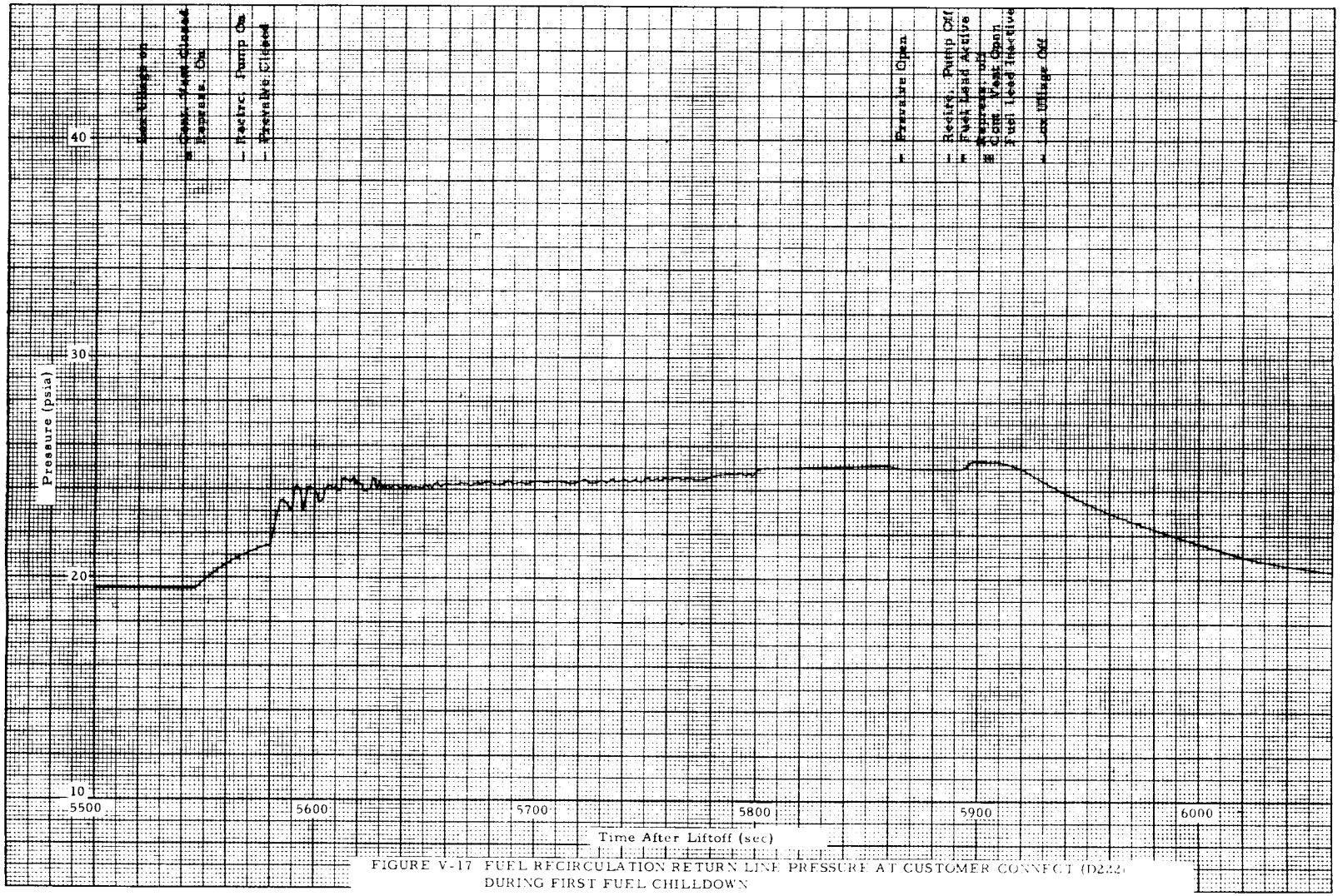

FIGURE V-17 FUEL RECIRCULATION RETURN LINE PRESSURE AT CUSTOMER CONNECT (D222) DURING FIRST FUEL CHILLDOWN

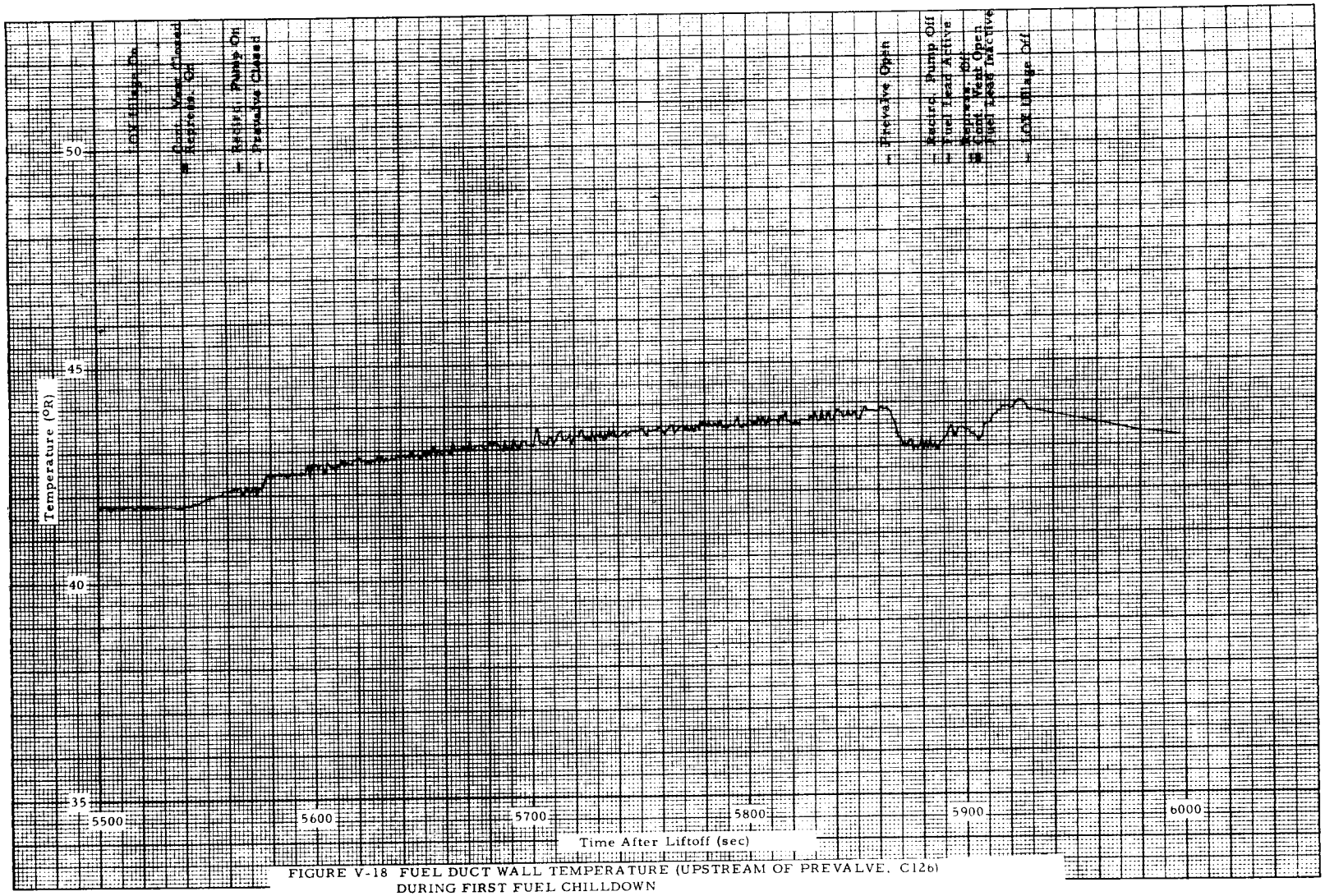

FIGURE V-18 FUEL DUCT WALL TEMPERATURE (UPSTREAM OF PREVALVE, C12b) DURING FIRST FUEL CHILLDOWN

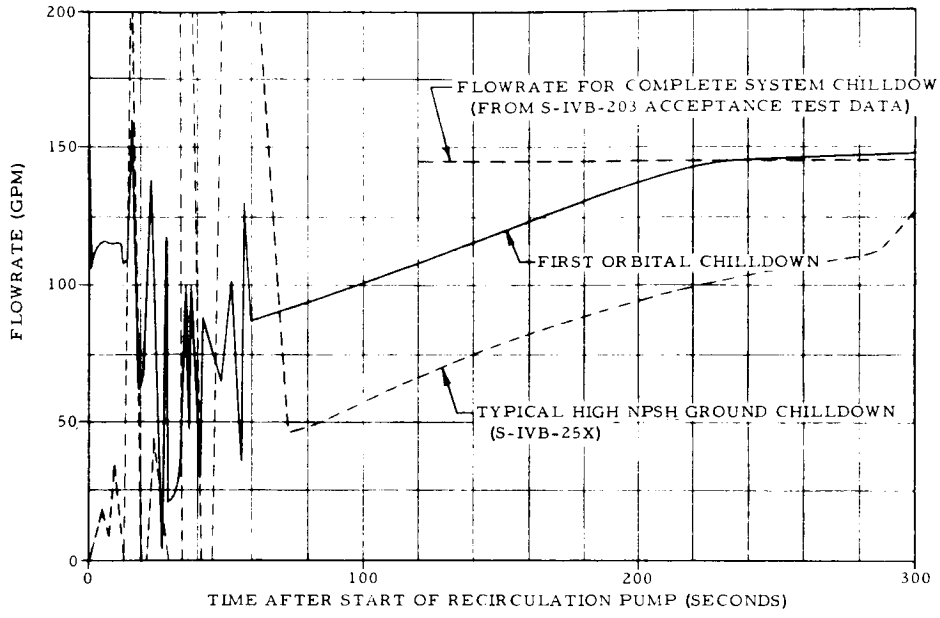

FIGURE V-19 FUEL RECIRCULATION PUMP FLOW RATES

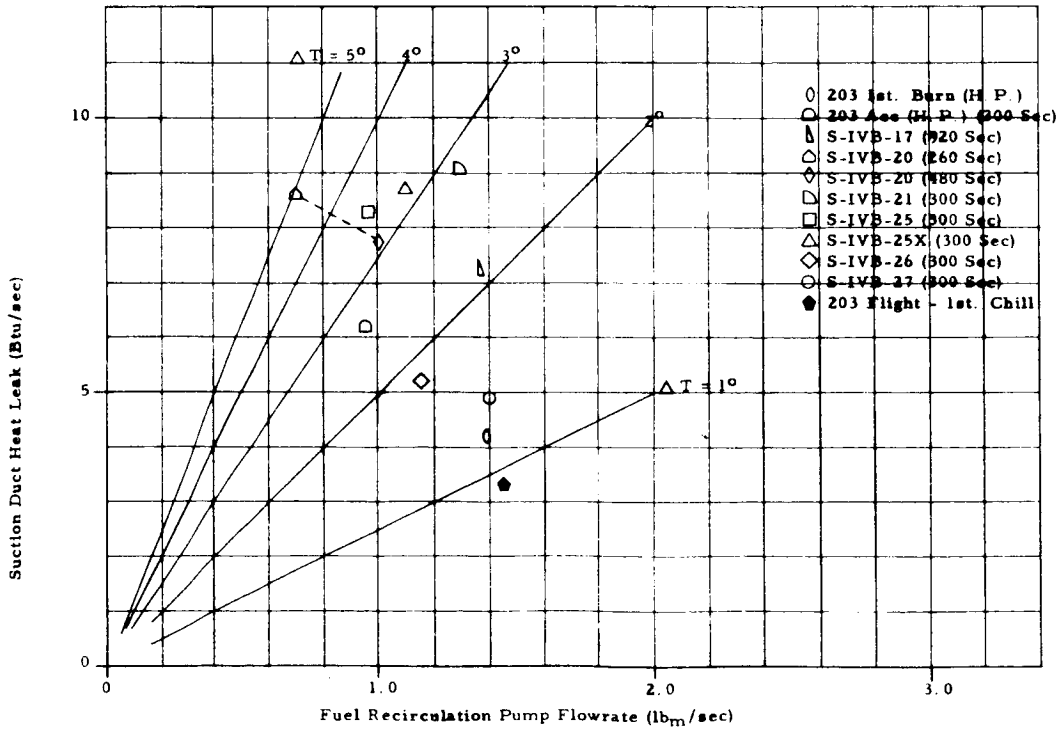

FIGURE V-20 S-IVB SUCTION DUCT HEAT LEAK DURING CHILLDOWN EXPERIMENTS

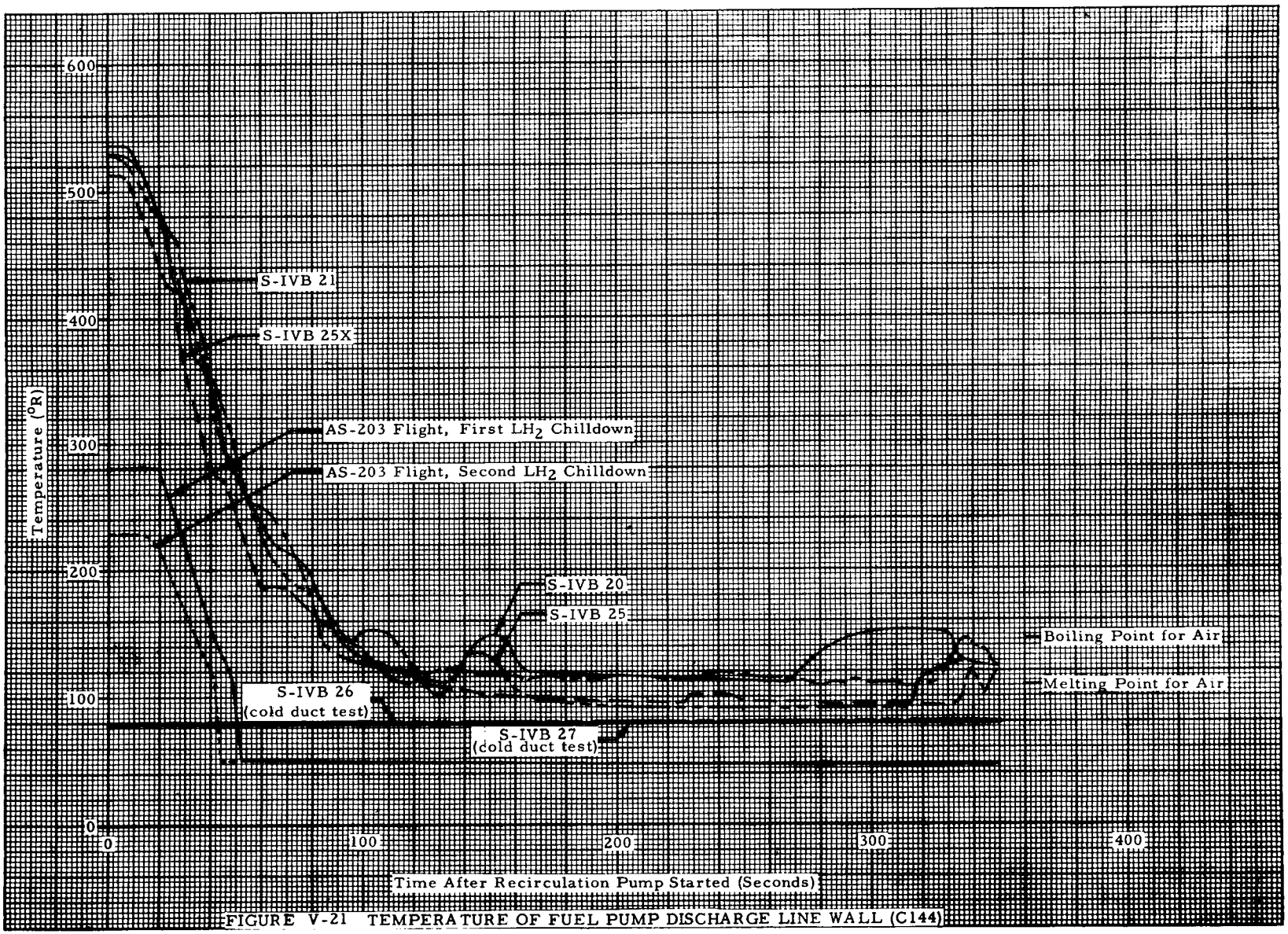

FIGURE V-21 TEMPERATURE OF FUEL PUMP DISCHARGE LINE WALL (C144)

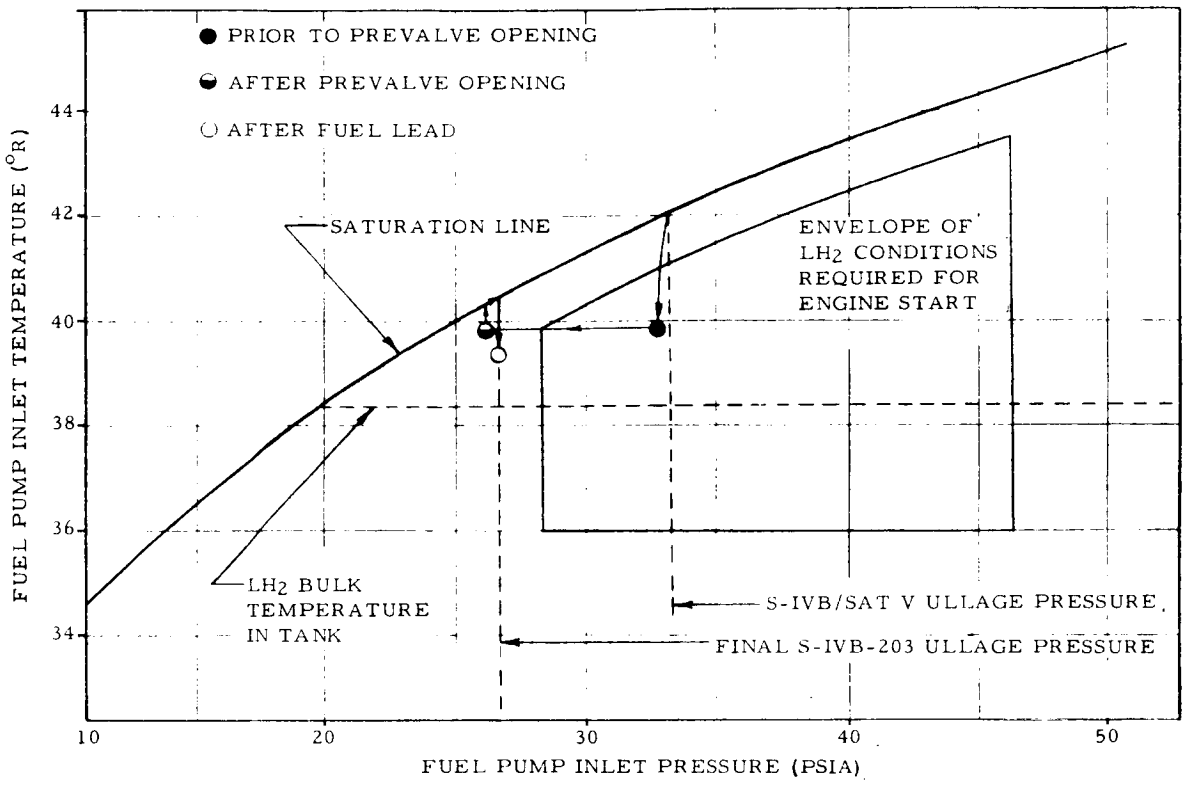

FIGURE V-22 CONDITION OF LH_2 AT FUEL PUMP INLET DURING FIRST FUEL CHILLDOWN

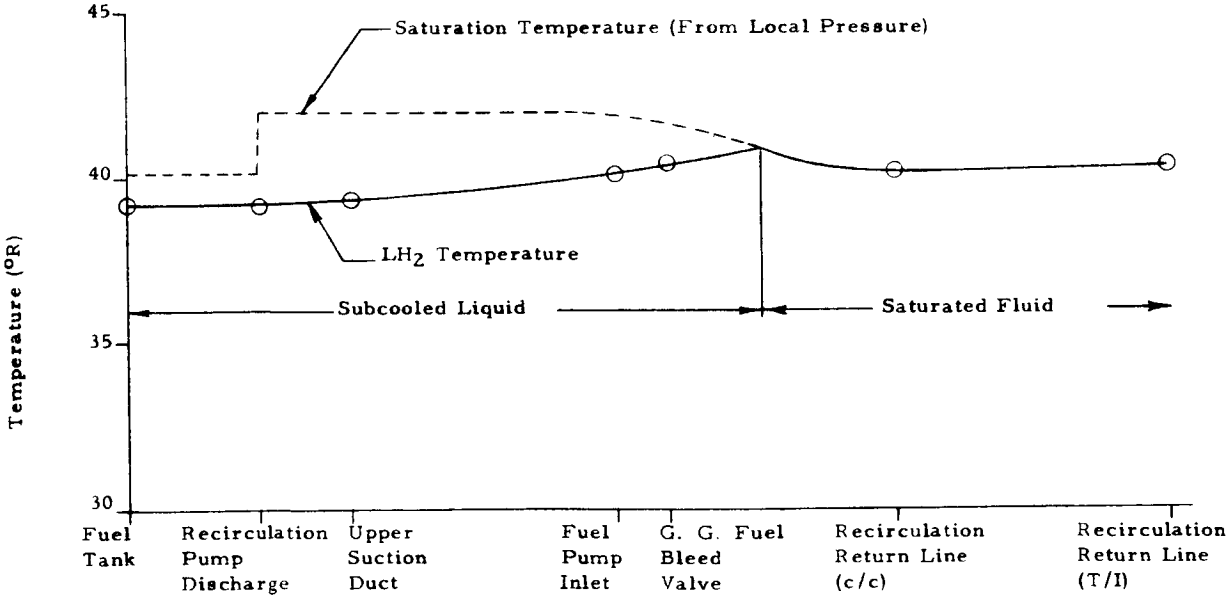

FIGURE V-23 LH_2 TEMPERATURE IN CHILLDOWN SYSTEM AT END OF FIRST ORBITAL CHILLDOWN

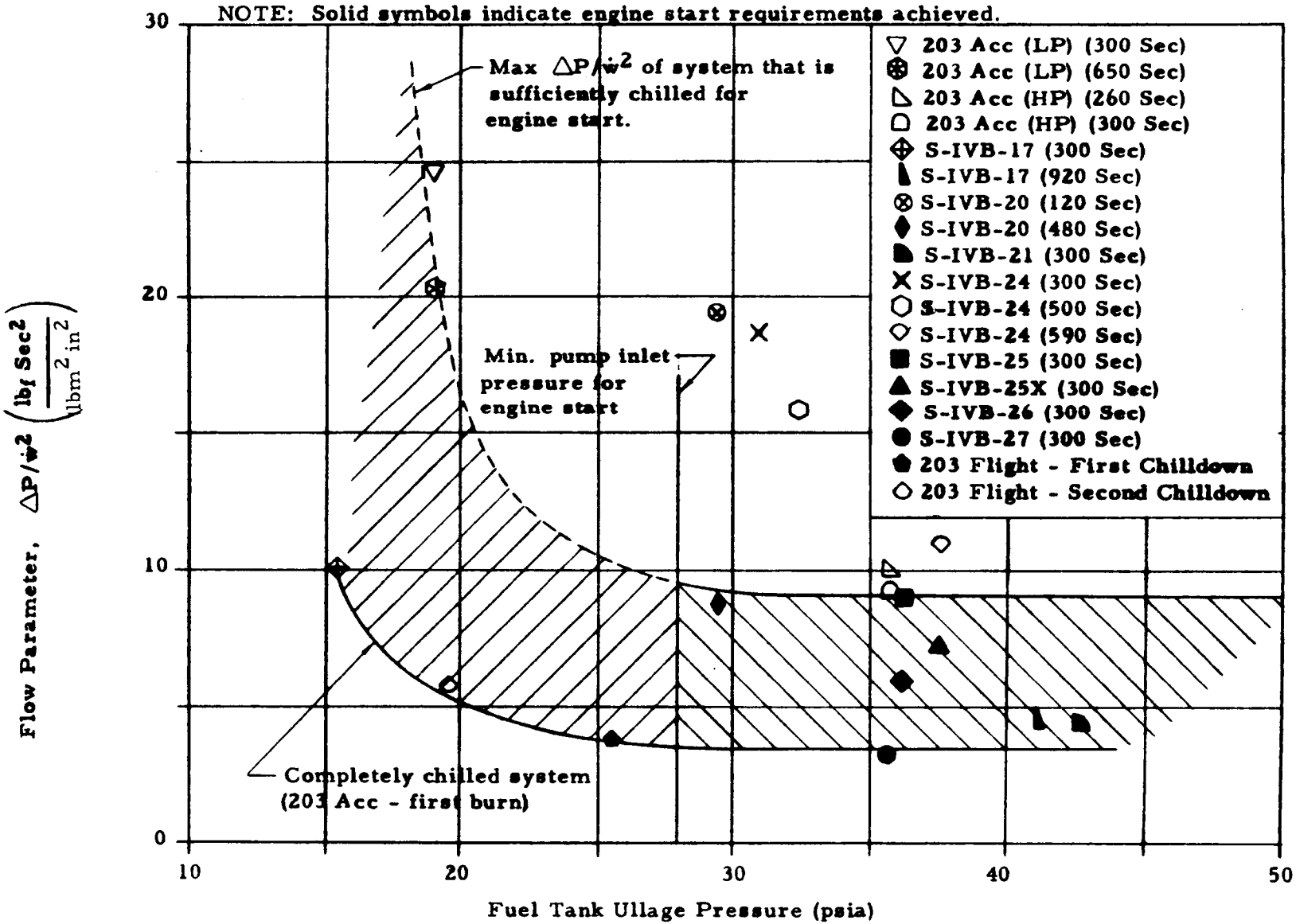

FIGURE V-24 STATE OF CHILLDOWN DURING S-IVB CHILLDOWN EXPERIMENTS

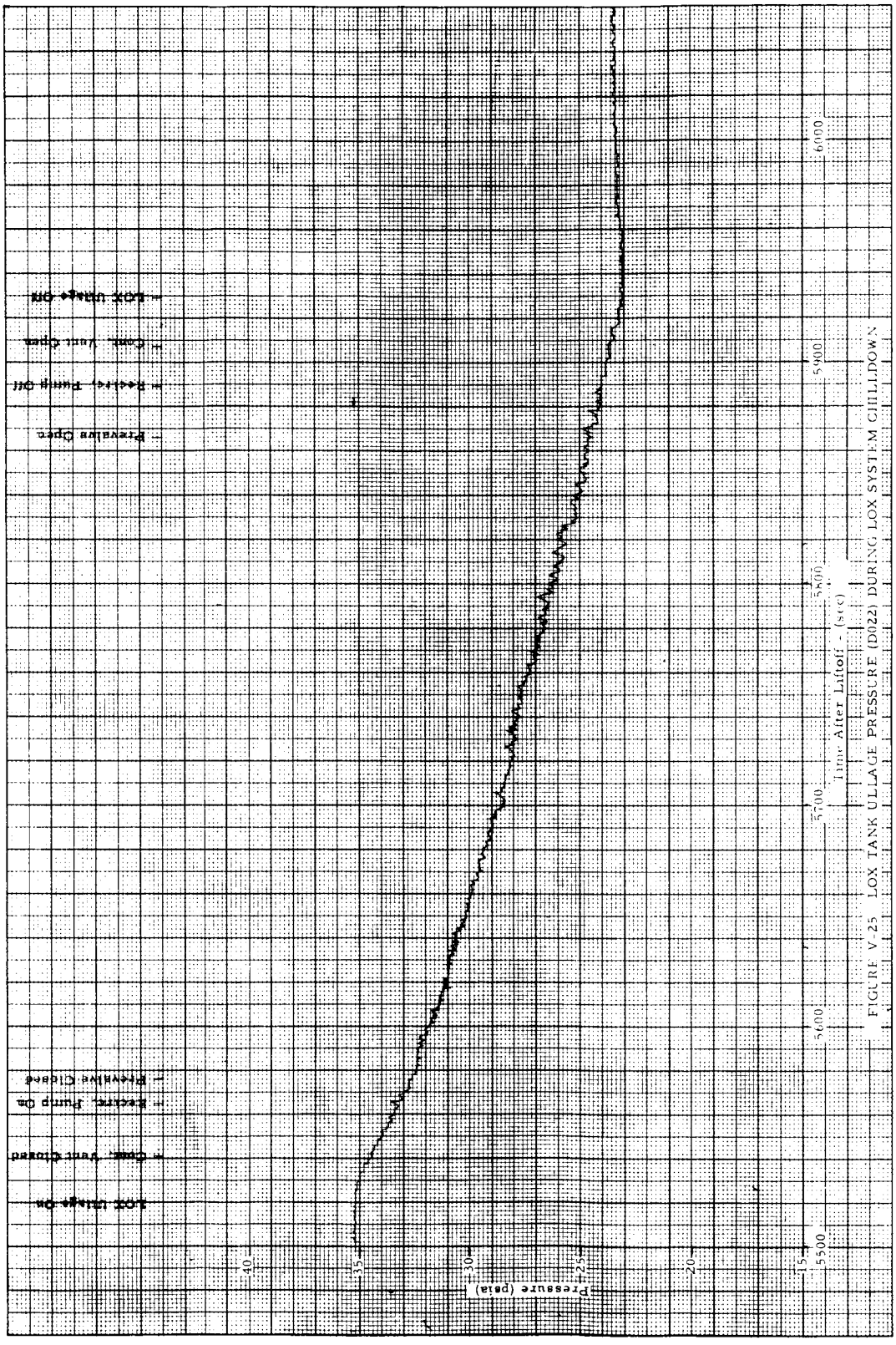

FIGURE V-25 LOX TANK ULLAGE PRESSURE (D022) DURING LOX SYSTEM CHILLDOWN

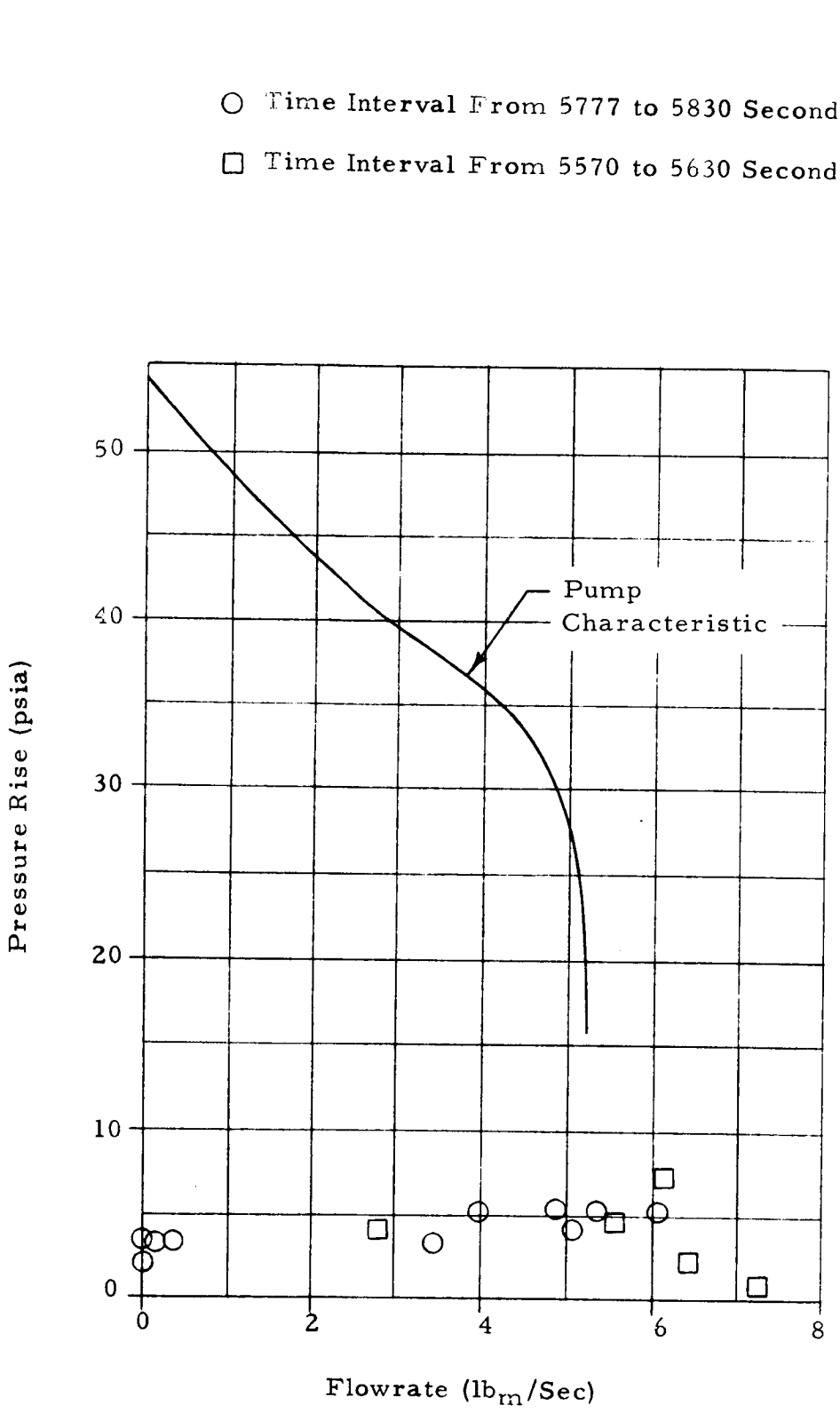

FIGURE V-26 S-IVB - 203 FLIGHT - LOX RECIRCULATION PUMP PERFORMANCE

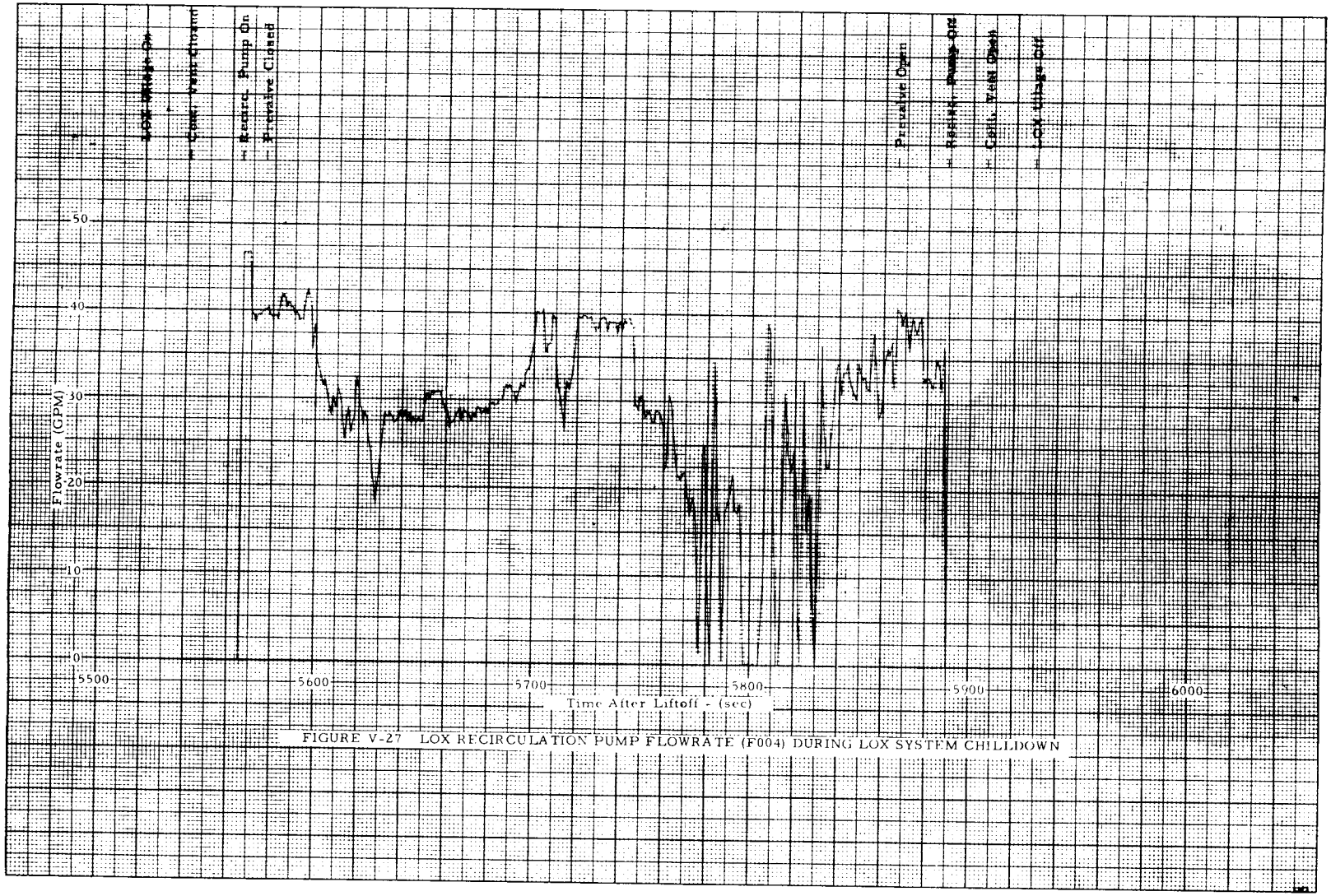

FIGURE V-27 LOX RECIRCULATION PUMP FLOWRATE (F004) DURING LOX SYSTEM CHILLDOWN

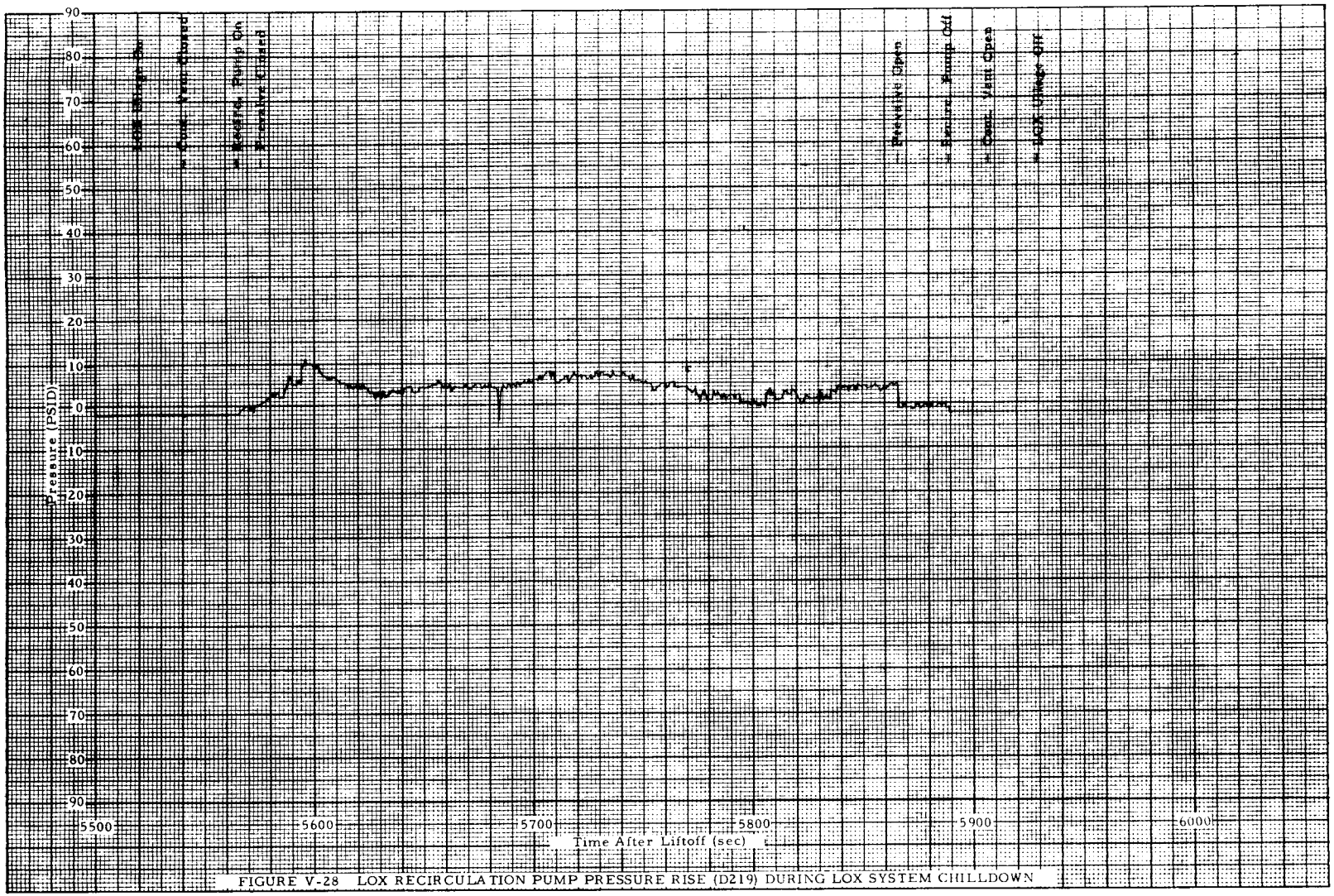

FIGURE V-28 LOX RECIRCULATION PUMP PRESSURE RISE (D219) DURING LOX SYSTEM CHILLDOWN

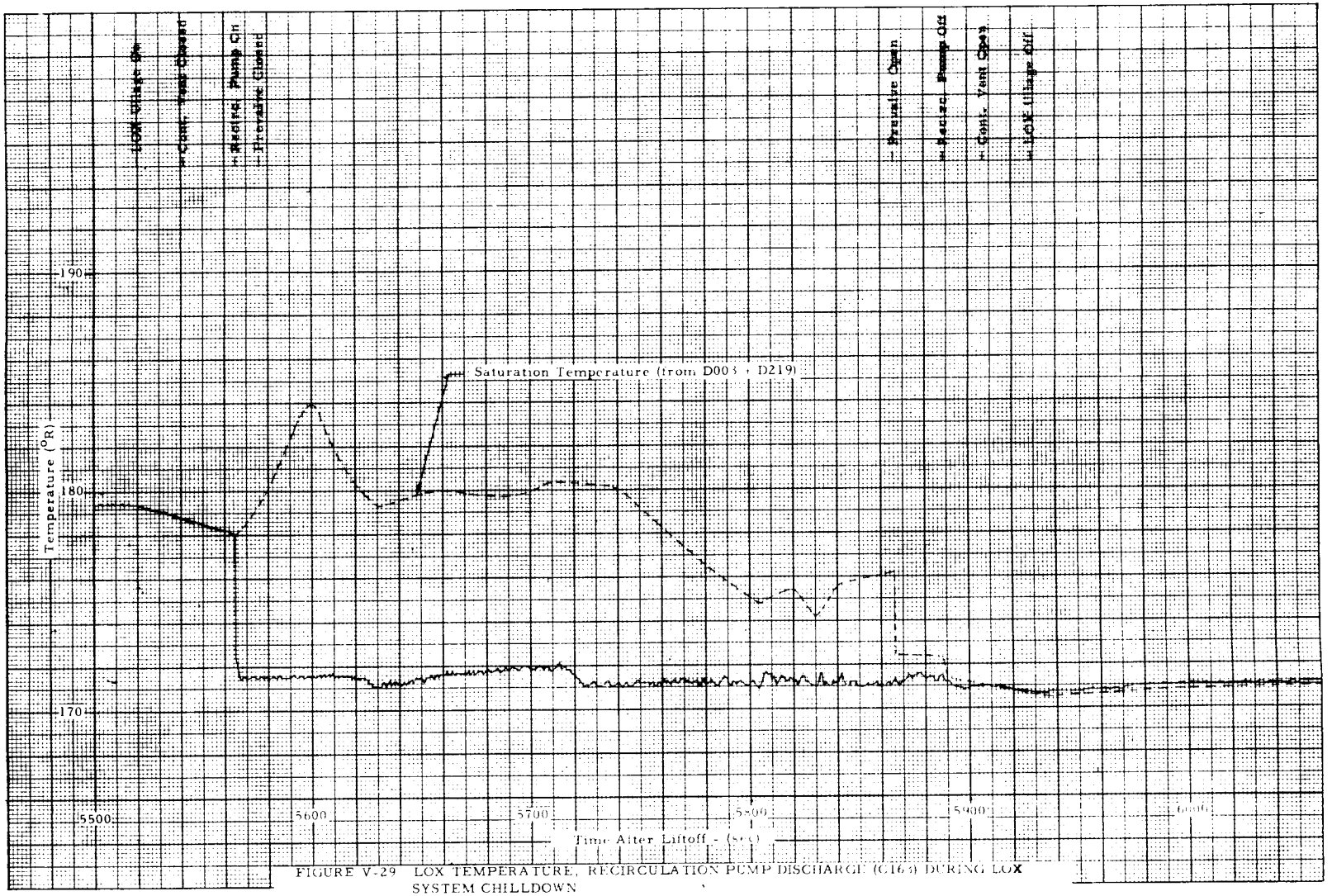

FIGURE V-29 LOX TEMPERATURE, RECIRCULATION PUMP DISCHARGE (C163) DURING LOX SYSTEM CHILLDOWN

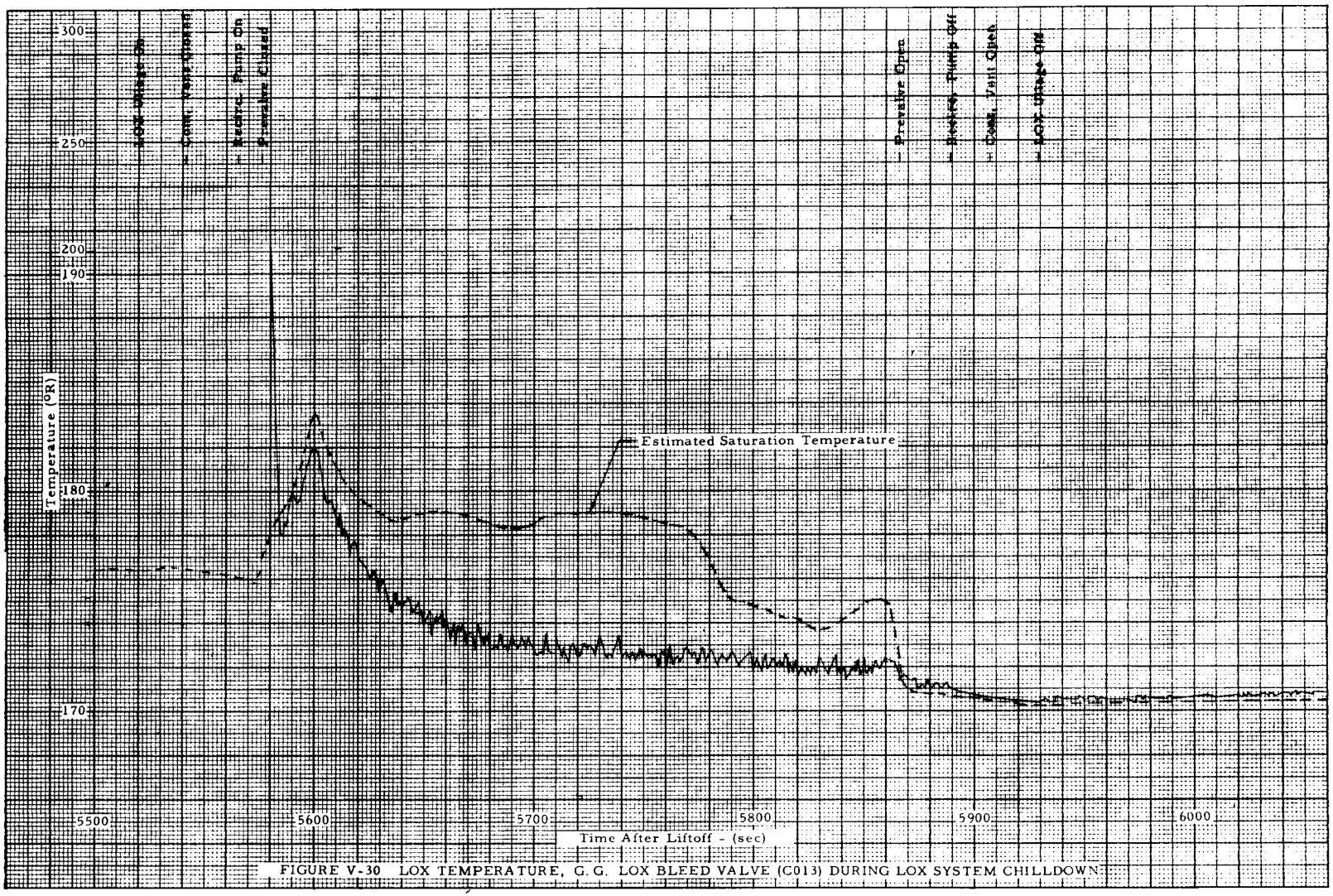

FIGURE V-30 LOX TEMPERATURE, G.G. LOX BLEED VALVE (C013) DURING LOX SYSTEM CHILLDOWN

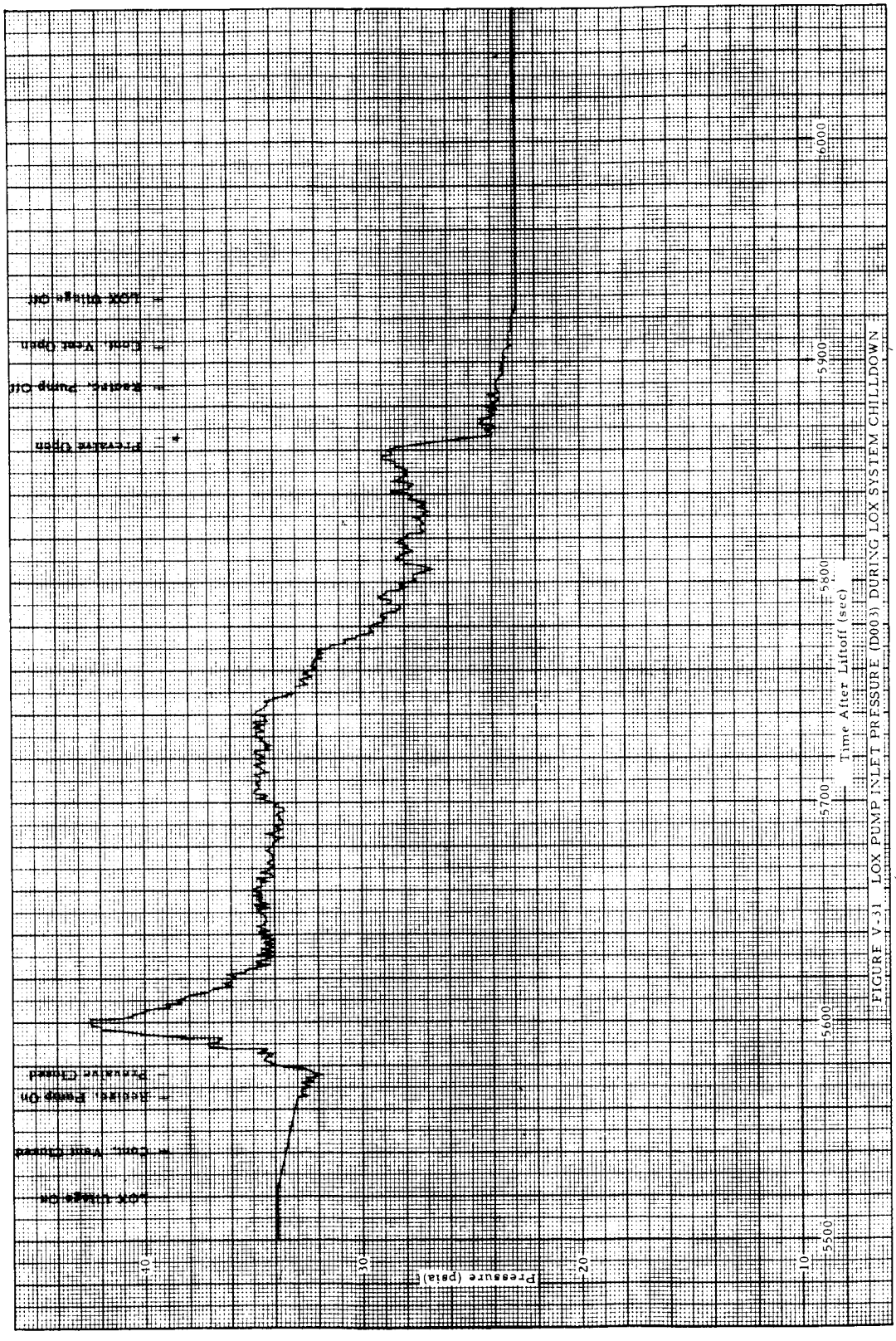

FIGURE V-31 LOX PUMP INLET PRESSURE (D003) DURING LOX SYSTEM CHILLDOWN

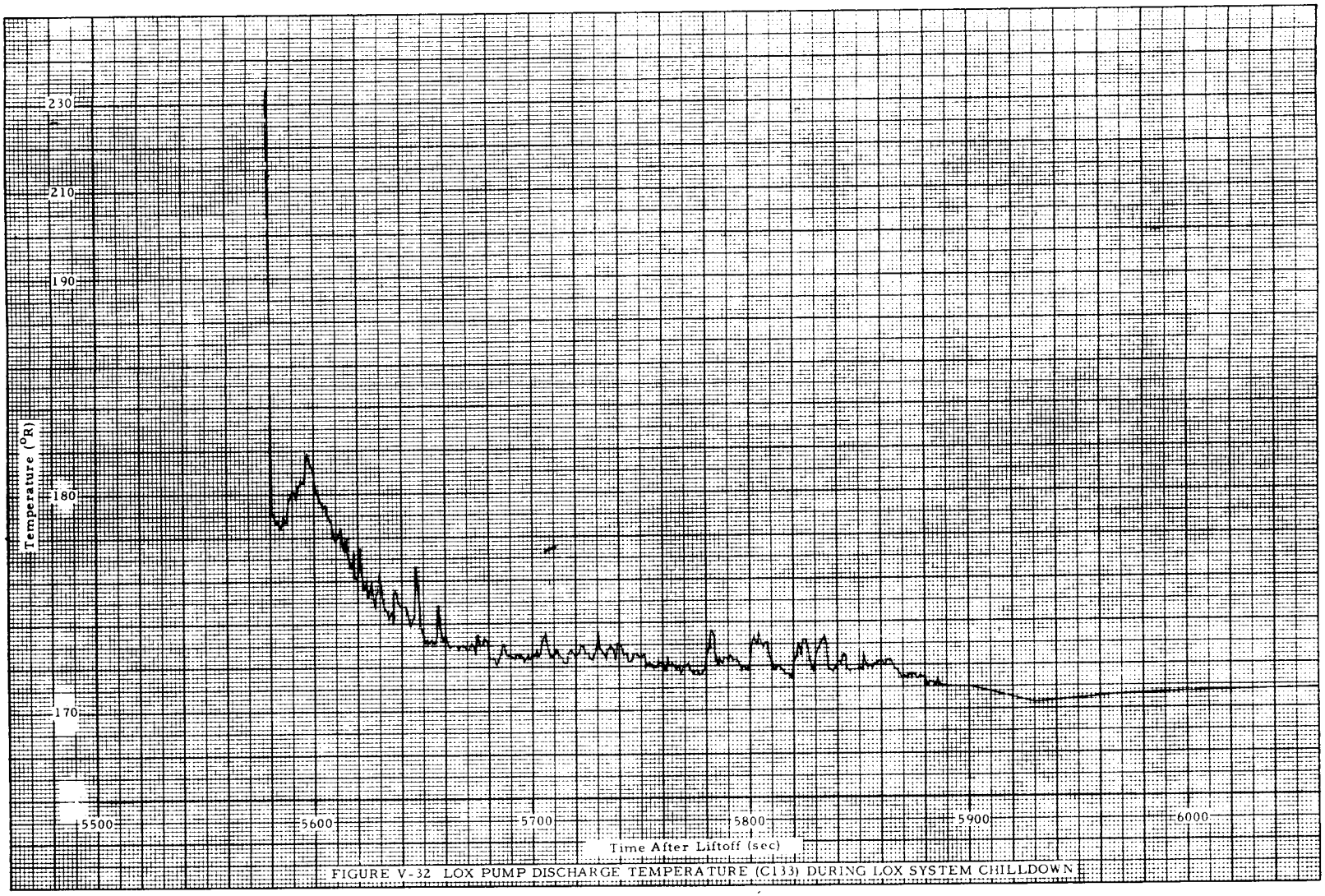

FIGURE V-32 LOX PUMP DISCHARGE TEMPERATURE (C133) DURING LOX SYSTEM CHILLDOWN

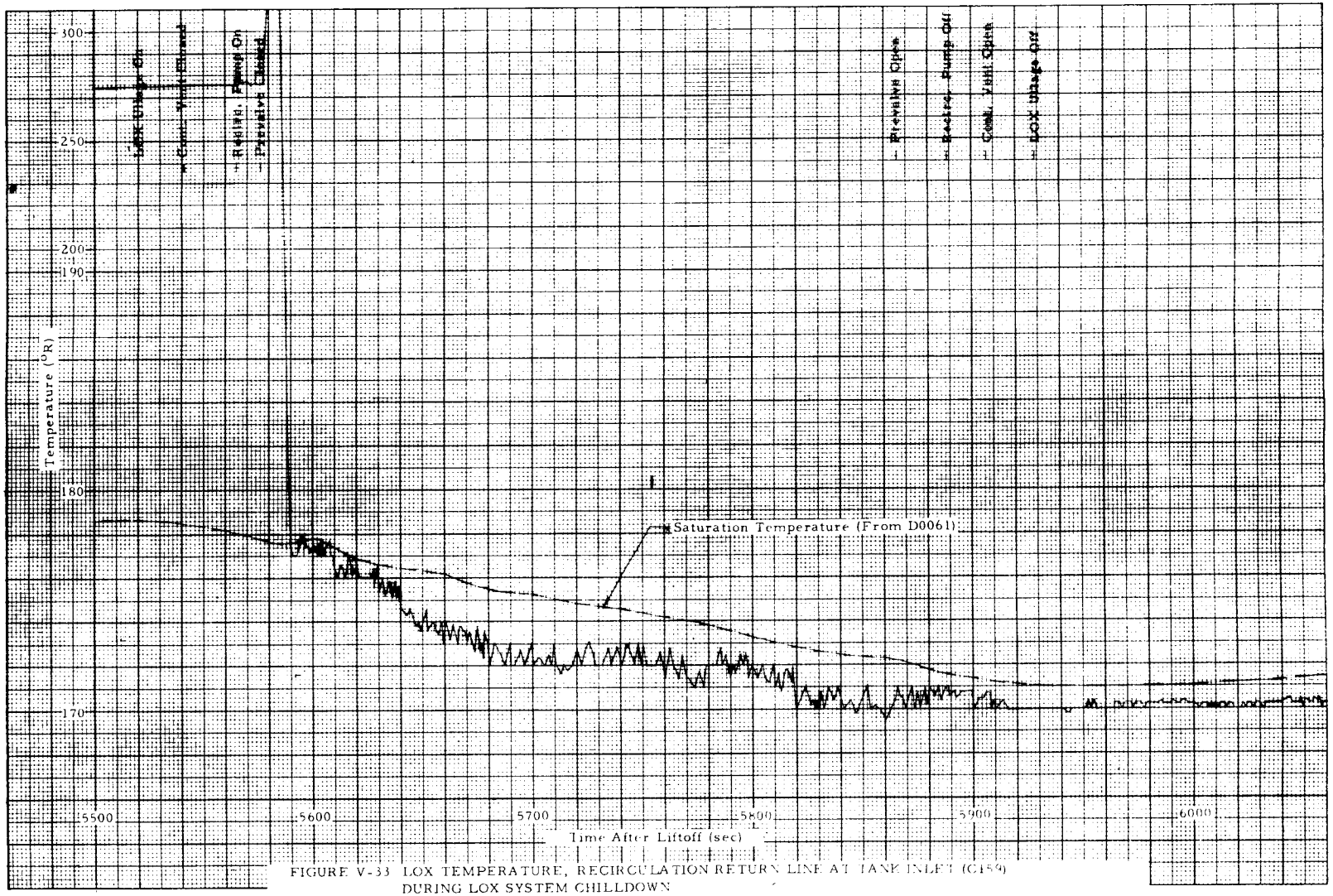

FIGURE V-33 LOX TEMPERATURE, RECIRCULATION RETURN LINE AT TANK INLET (C159) DURING LOX SYSTEM CHILLDOWN

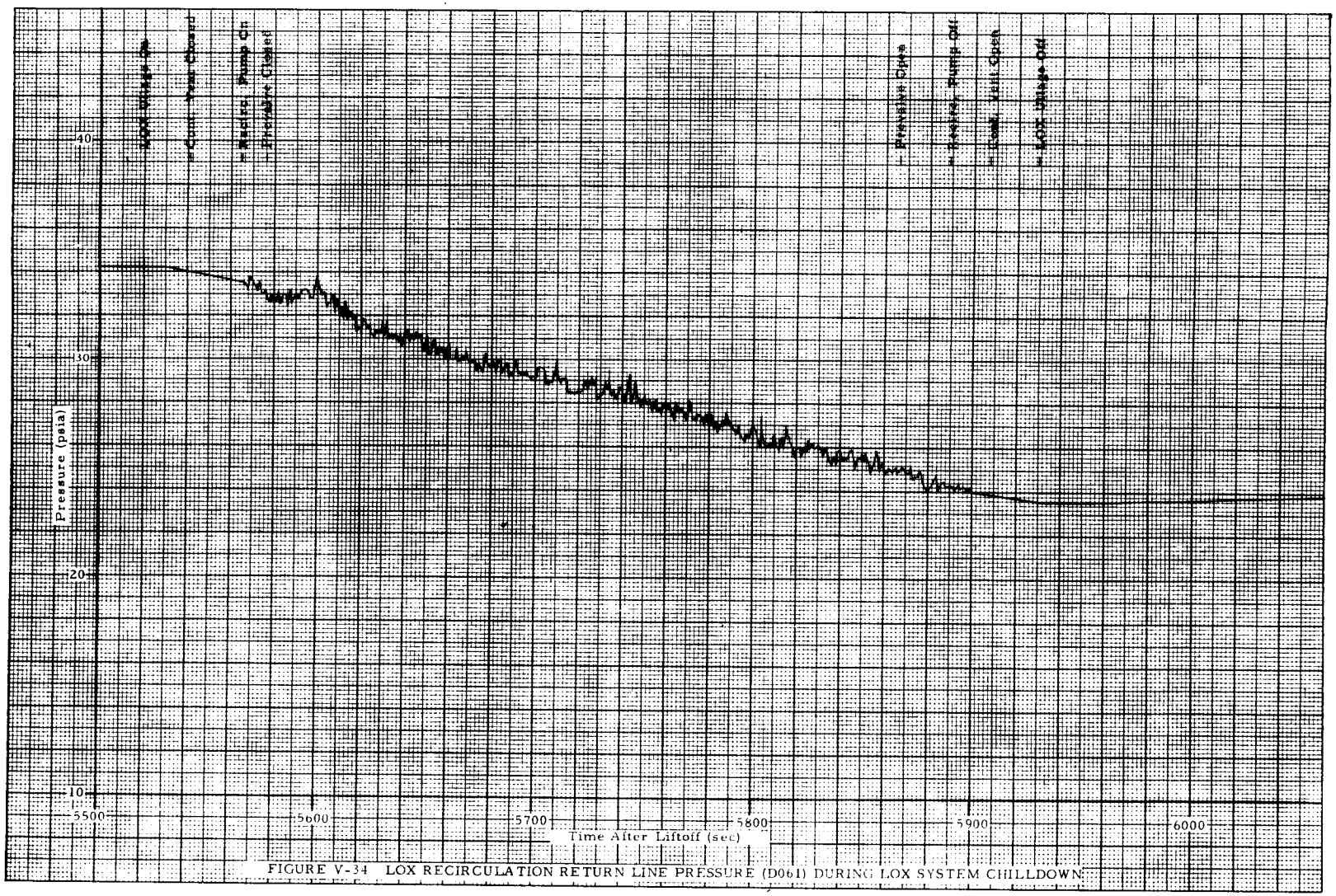

FIGURE V-34 LOX RECIRCULATION RETURN LINE PRESSURE (D061) DURING LOX SYSTEM CHILLDOWN

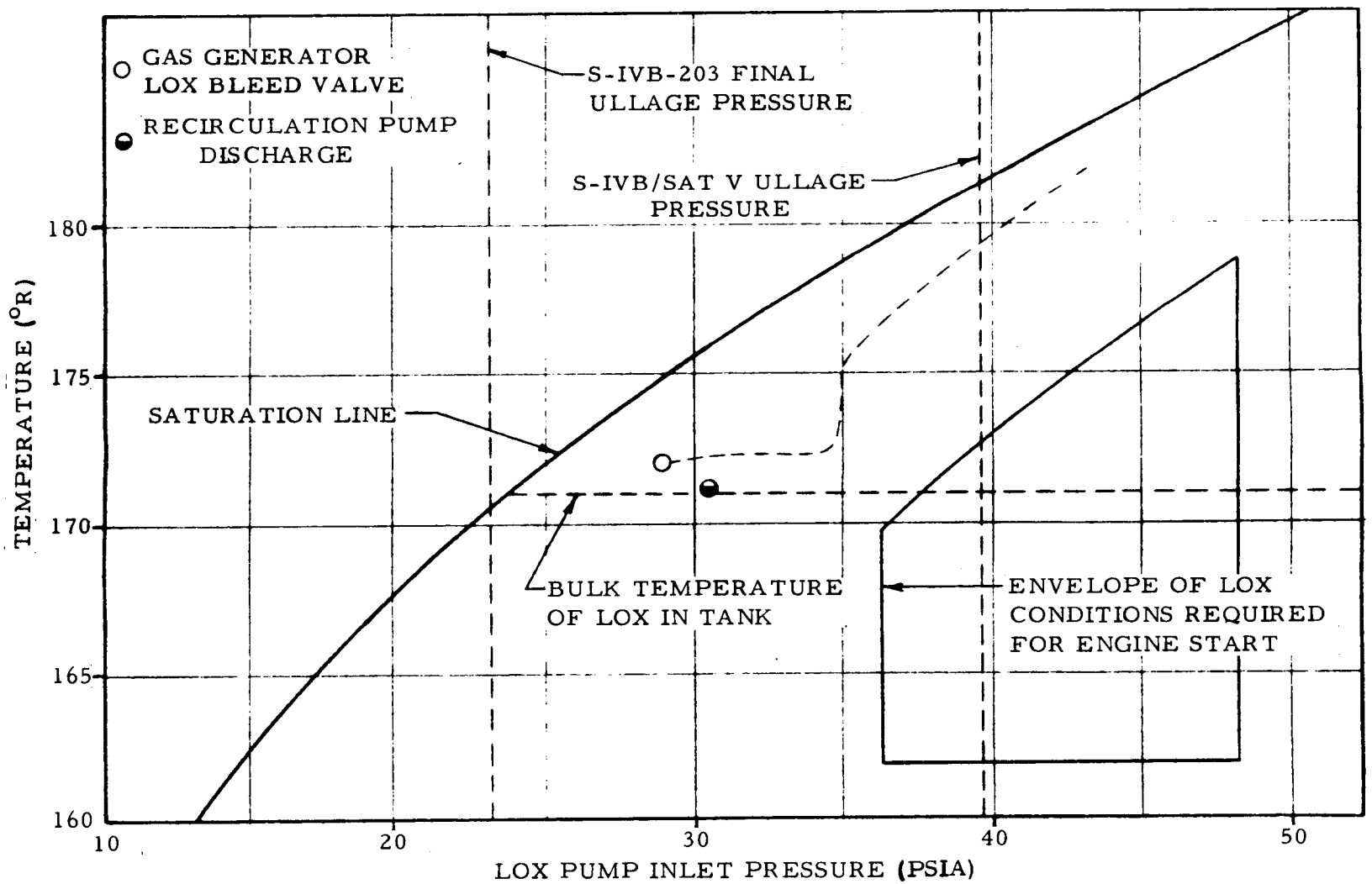

FIGURE V-35 CONDITION OF LOX PRIOR TO PREVALVE OPENING DURING OXIDIZER SYSTEM CHILL DOWN

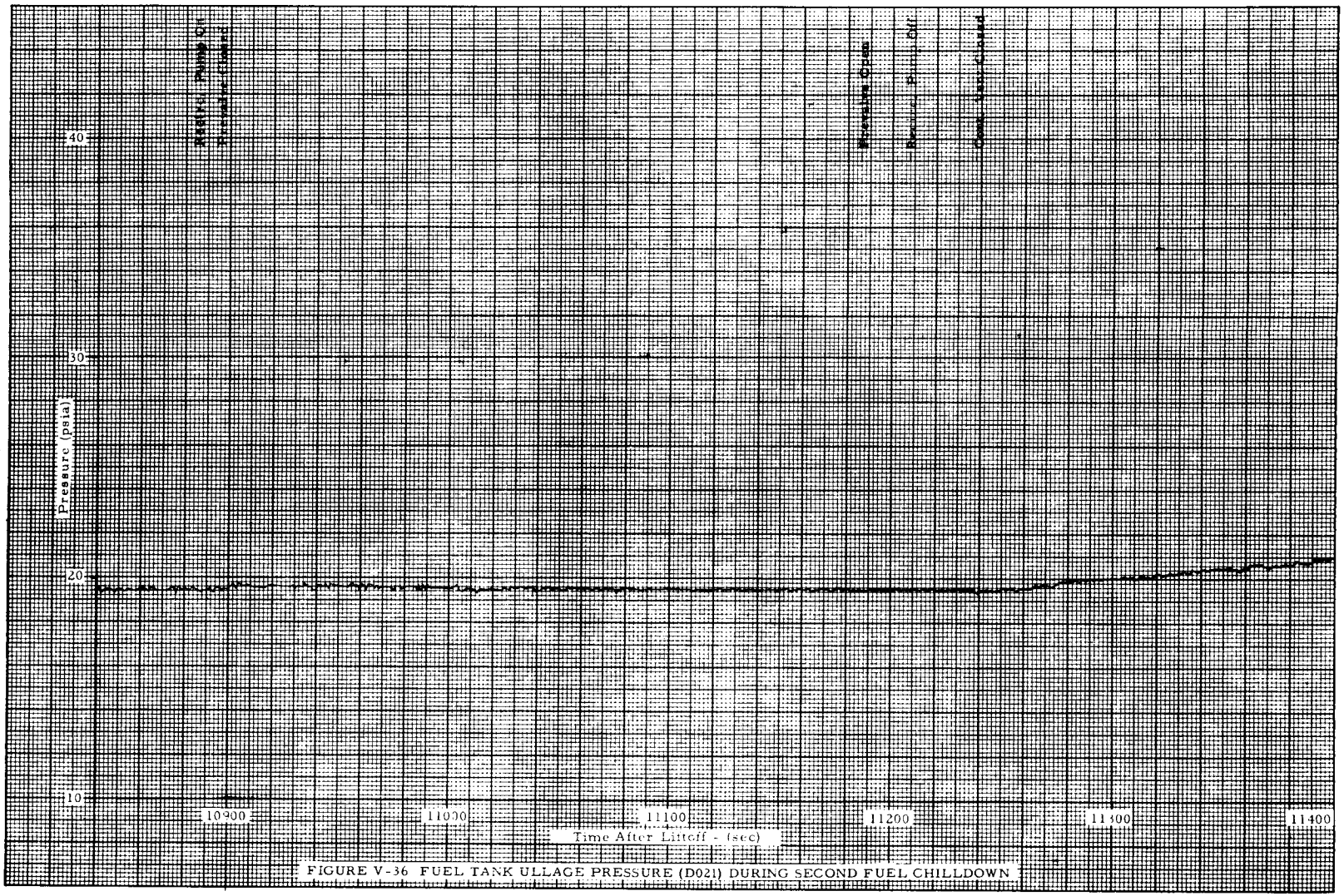

FIGURE V-36 FUEL TANK ULLAGE PRESSURE (D021) DURING SECOND FUEL CHILLDOWN

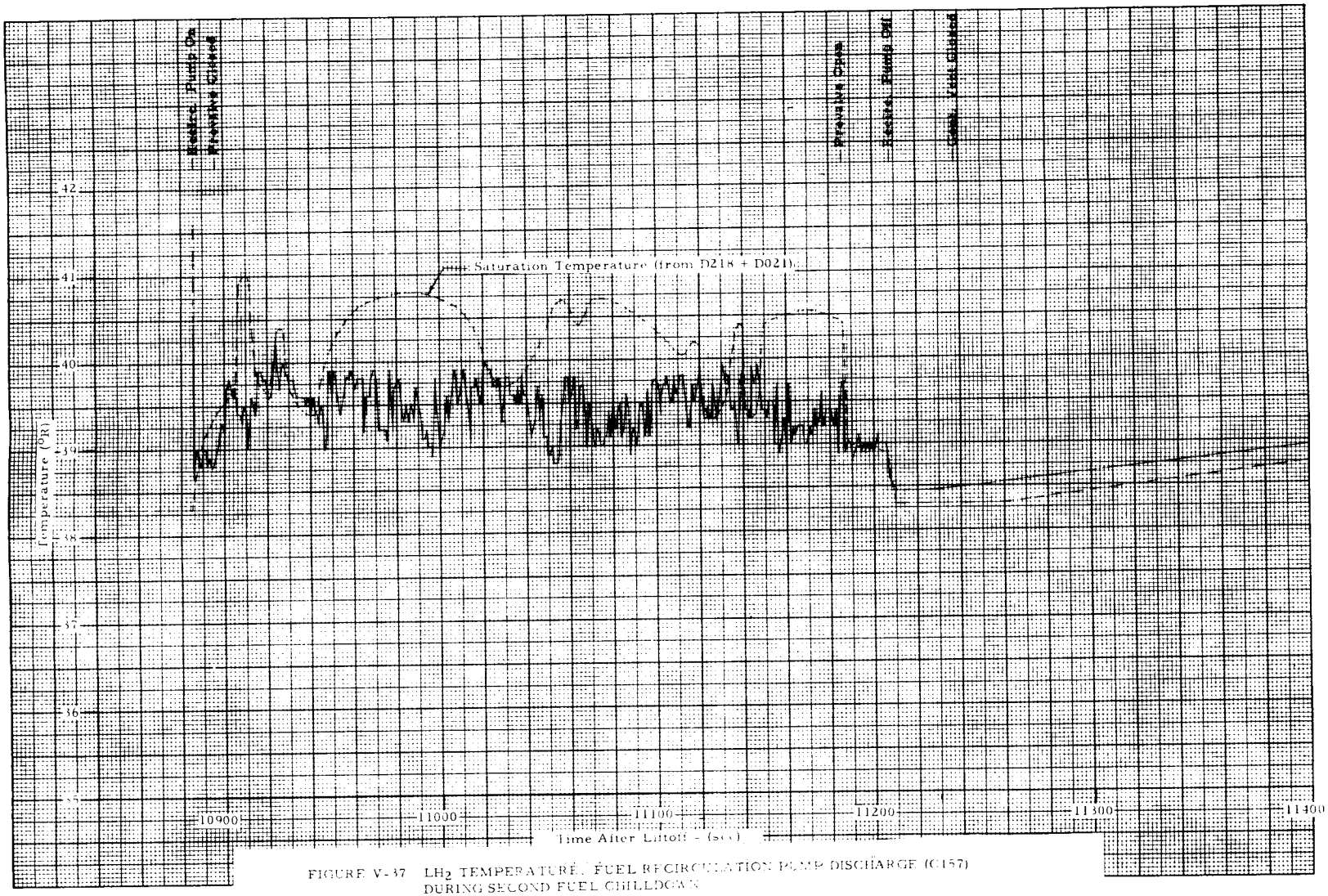

FIGURE V-37 LH_2 TEMPERATURE, FUEL RECIRCULATION PUMP DISCHARGE (C157) DURING SECOND FUEL CHILLDOWN

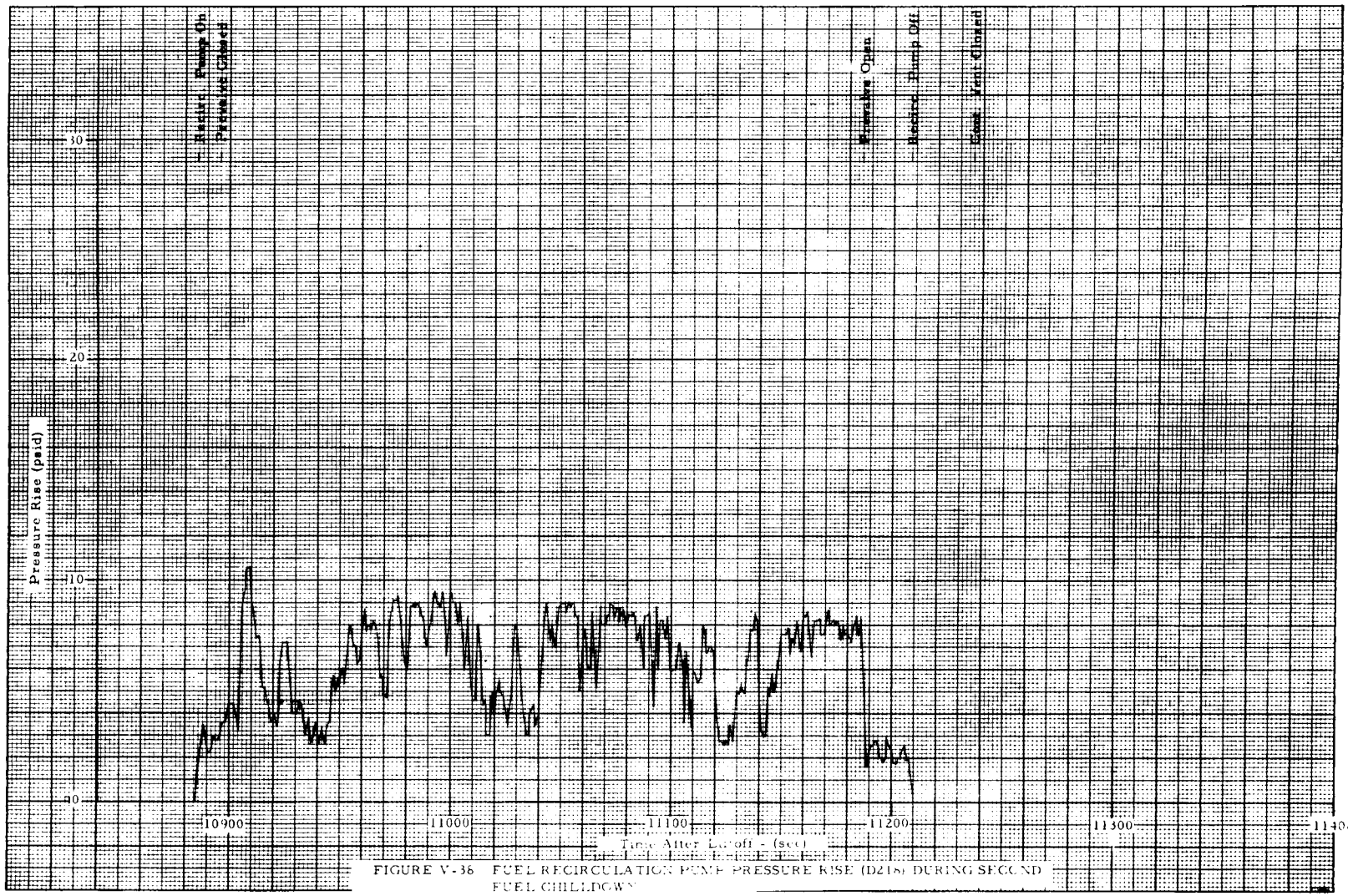

FIGURE V-36 FUEL RECIRCULATION PUMP PRESSURE RISE (D218) DURING SECOND FUEL CHILLDOWN

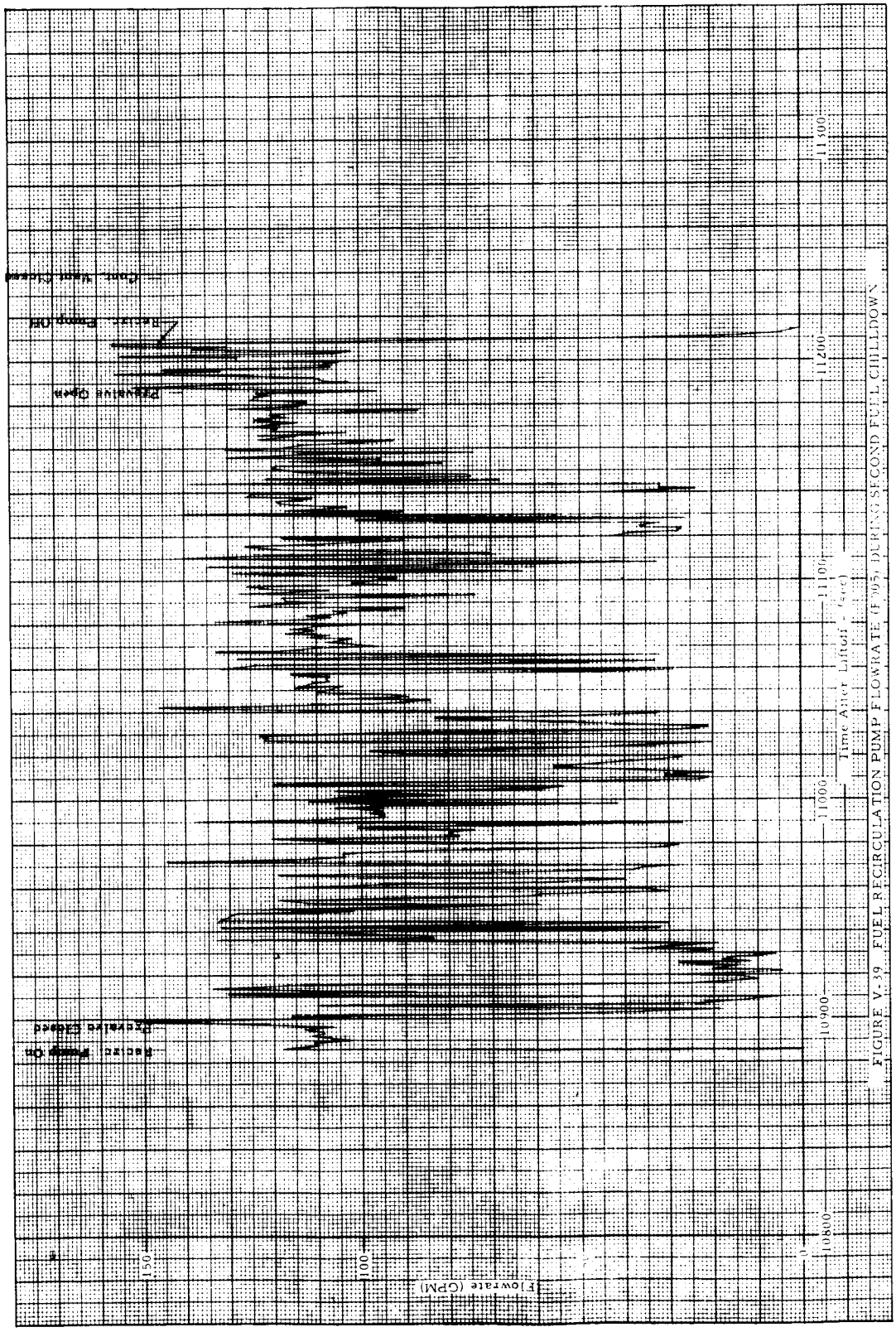

FIGURE V-39 FUEL RECIRCULATION PUMP FLOWRATE (F-905) DURING SECOND FUEL CHILLDOWN

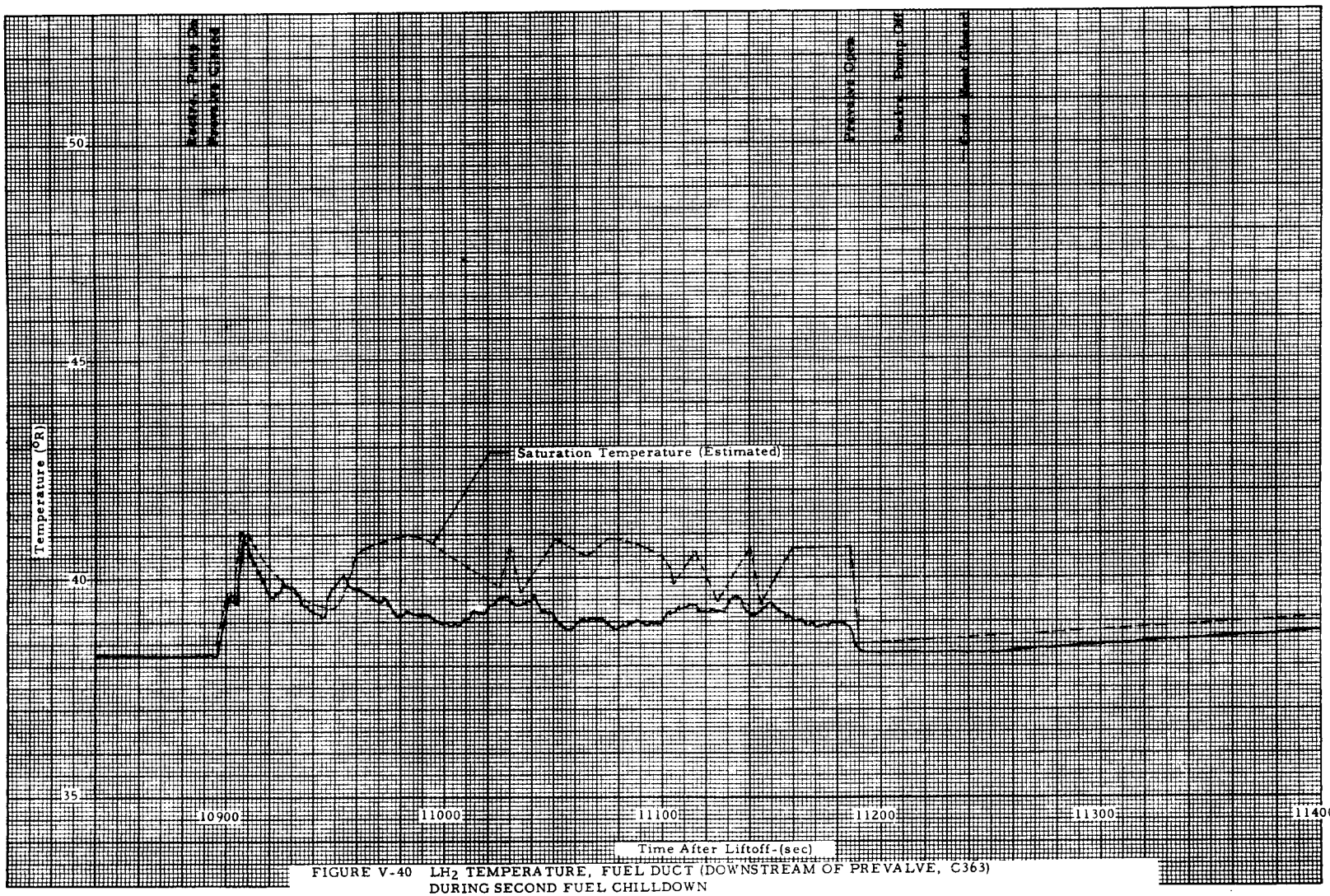

FIGURE V-40 LH_2 TEMPERATURE, FUEL DUCT (DOWNSTREAM OF PREVALVE, C363) DURING SECOND FUEL CHILLDOWN

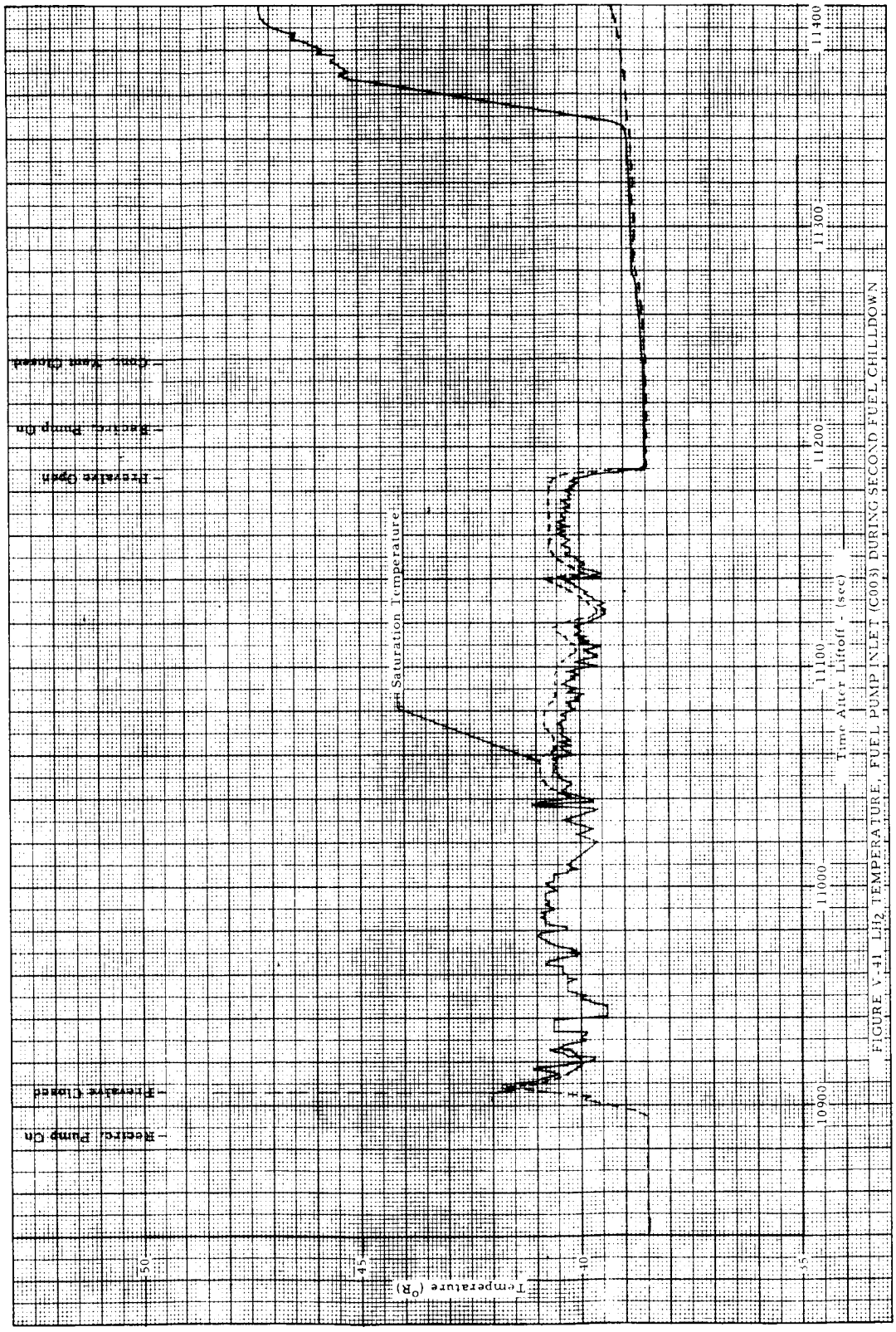

FIGURE V-41 LH_2 TEMPERATURE, FUEL PUMP INLET (C003) DURING SECOND FUEL CHILLDOWN

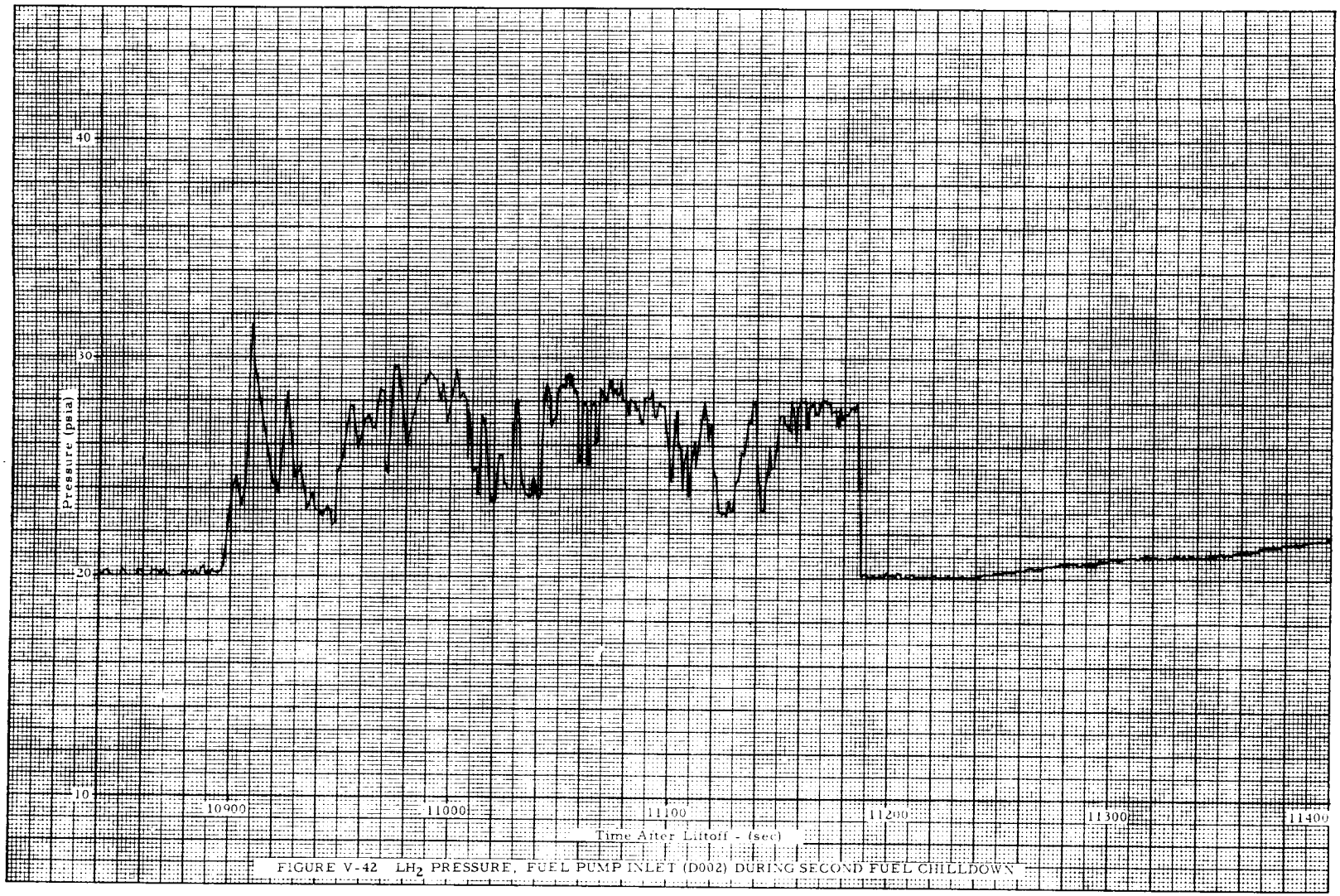

FIGURE V-42 LH_2 PRESSURE, FUEL PUMP INLET (D002) DURING SECOND FUEL CHILLDOWN

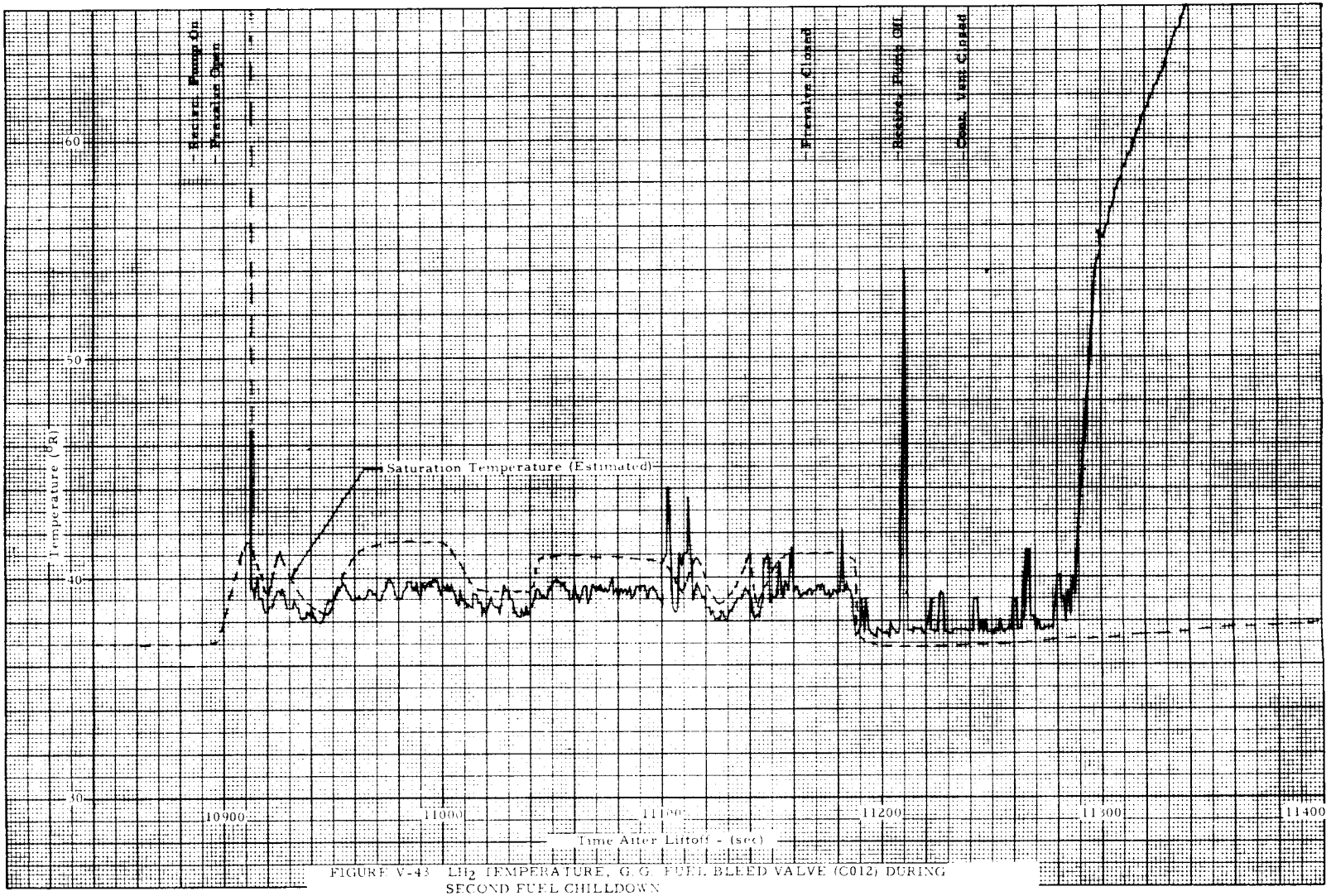

FIGURE V-43 LH_2 TEMPERATURE, G.G. FUEL BLEED VALVE (C012) DURING SECOND FUEL CHILLDOWN

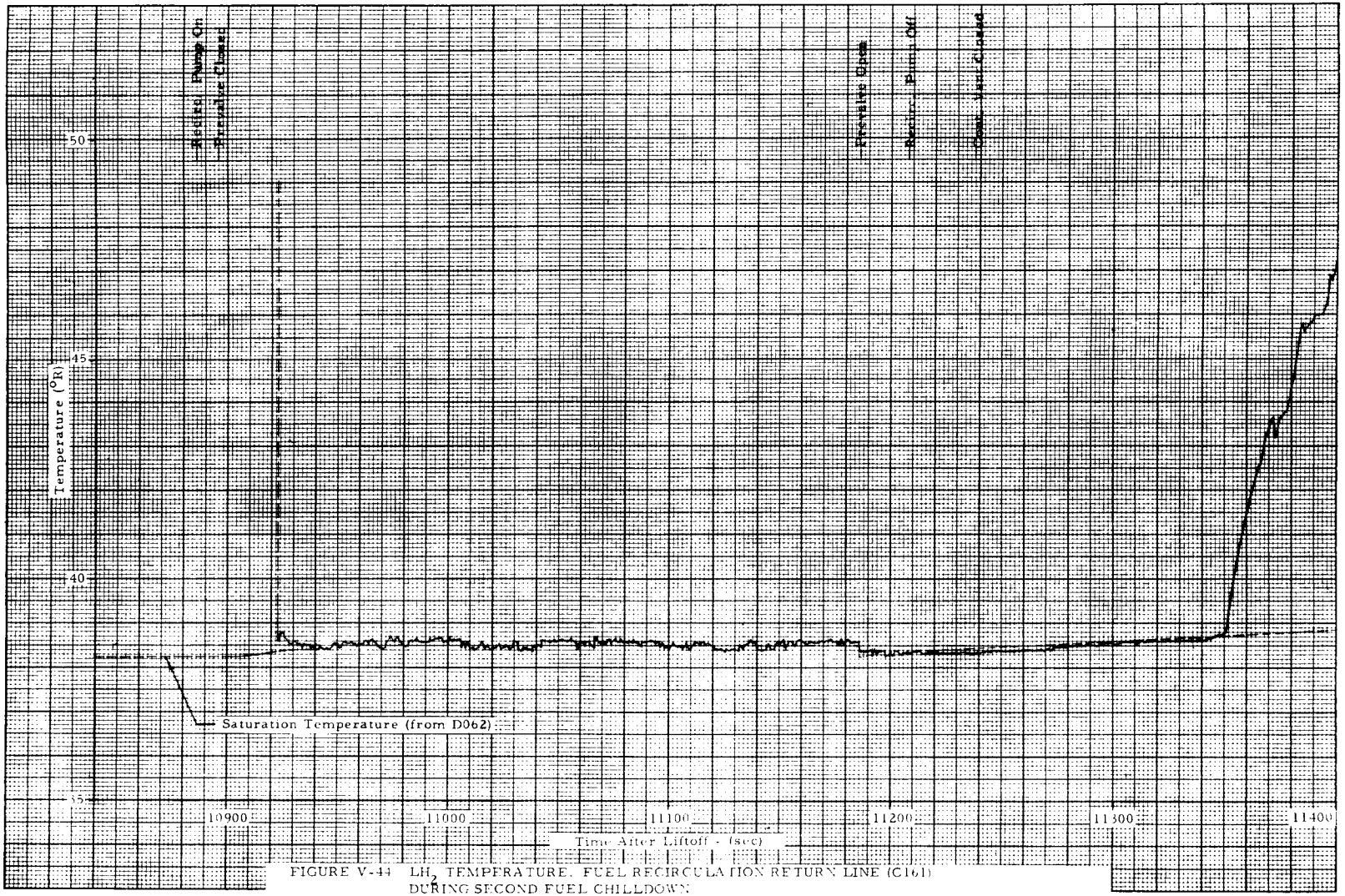

FIGURE V-44 LH_2 TEMPERATURE, FUEL RECIRCULATION RETURN LINE (C161) DURING SECOND FUEL CHILLDOWN

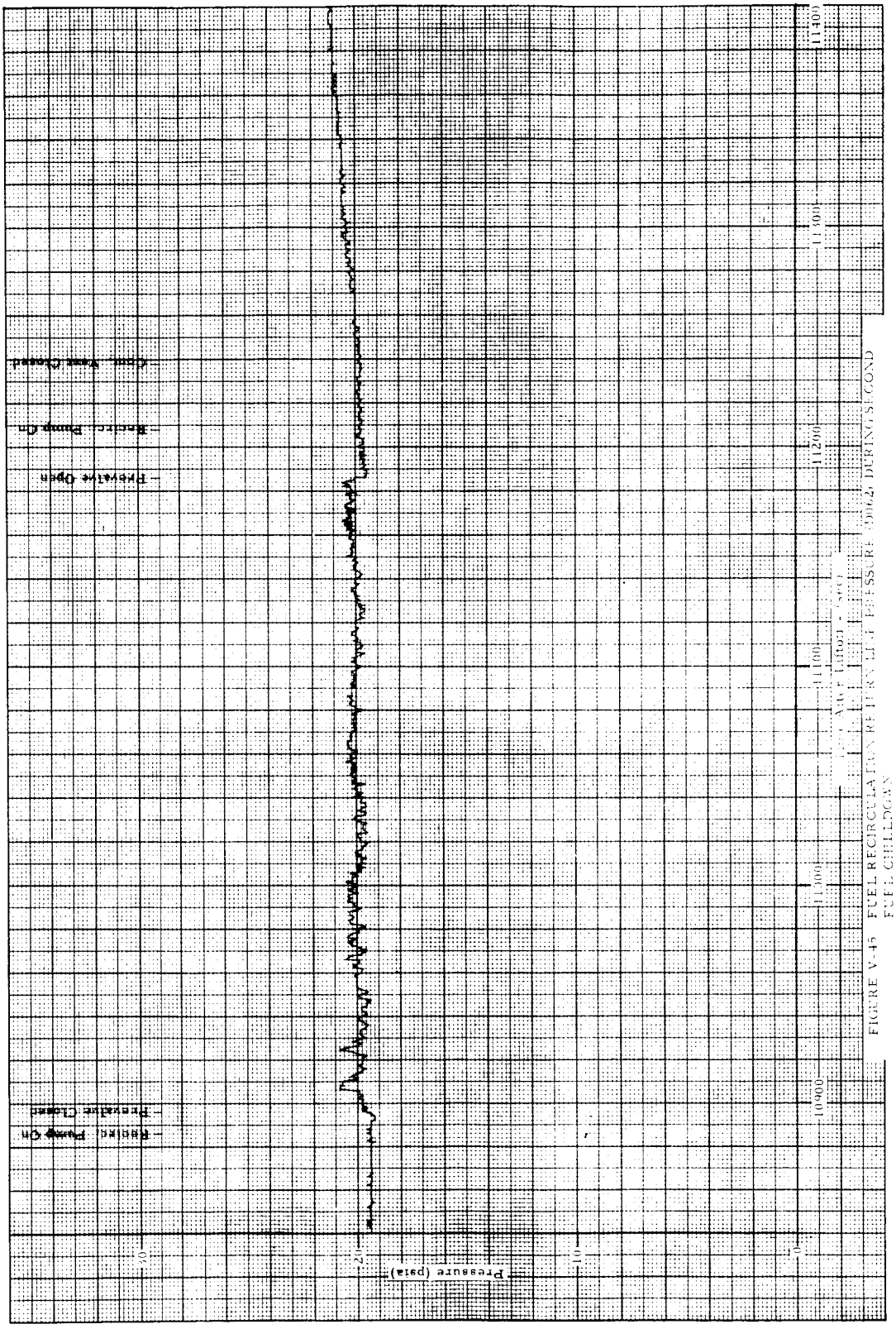

FIGURE V-45 FUEL RECIRCULATION RETURN LINE PRESSURE 09:42 DURING SECOND FUEL CHILLDOWN

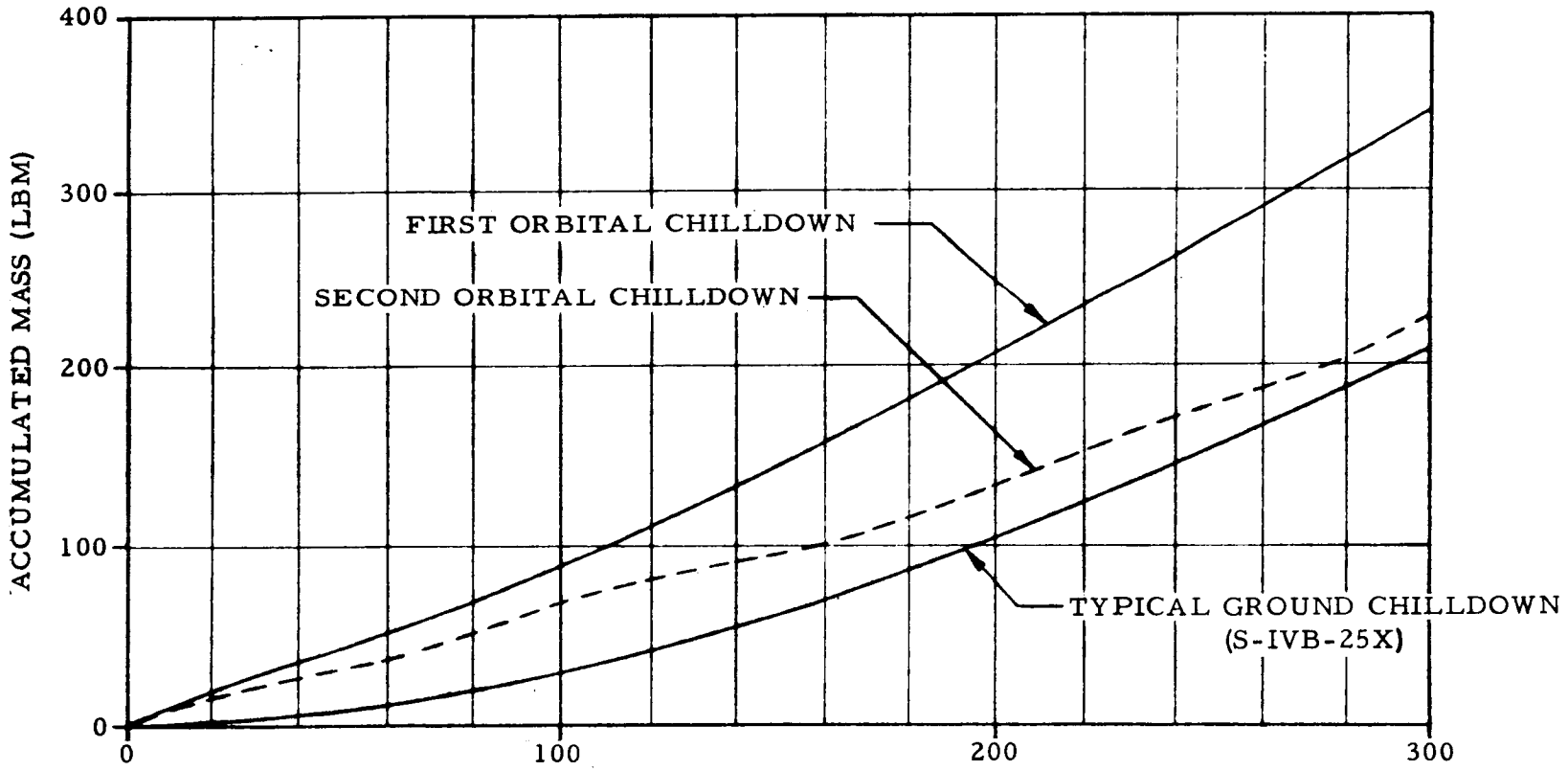

FIGURE V-46 ACCUMULATED MASS FLOW THROUGH FUEL RECIRCULATION PUMP

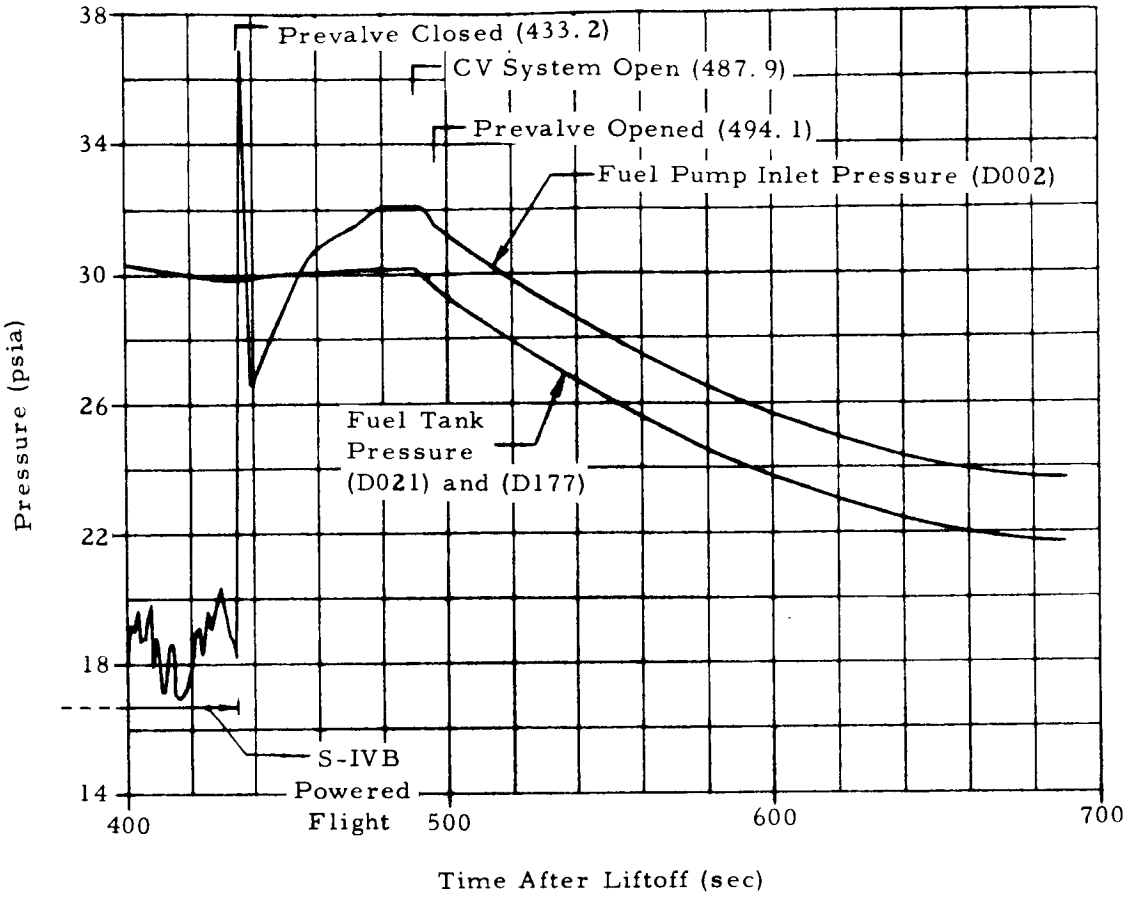

FIGURE V-47 FUEL TANK AND PUMP INLET PRESSURES AT INSERTION

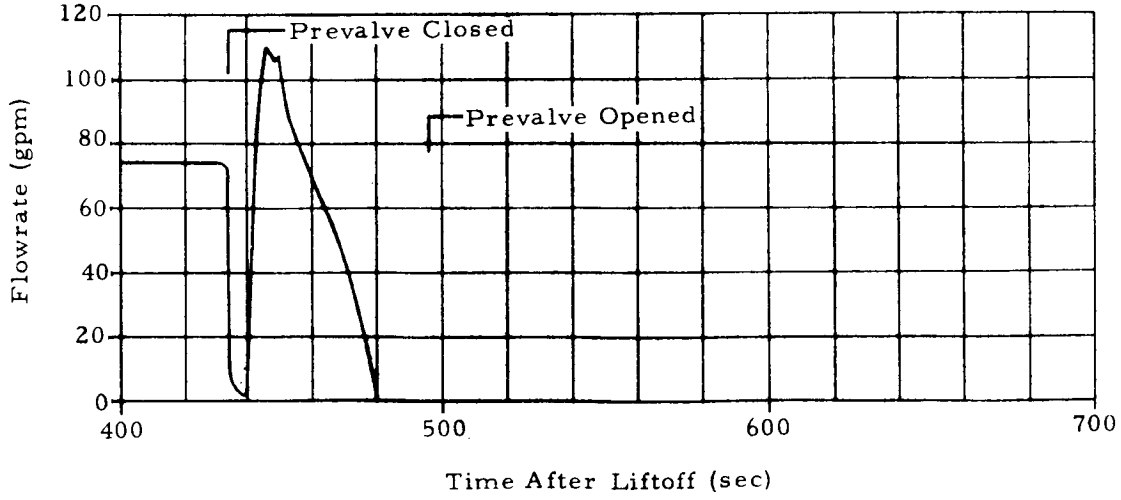

FIGURE V-48 FUEL RECIRCULATION PUMP FLOWRATE AT INSERTION

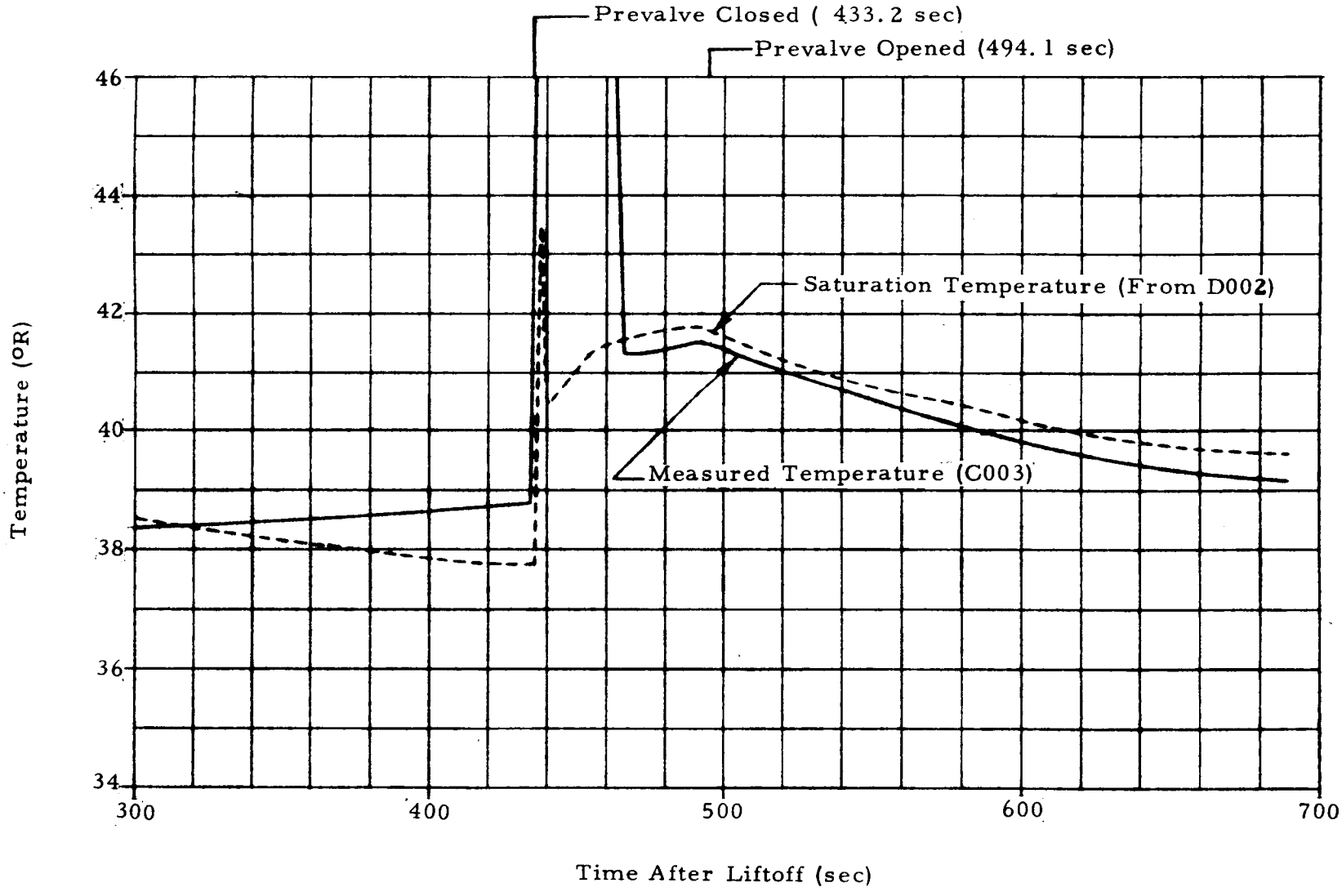

FIGURE V-49 FUEL PUMP INLET TEMPERATURE AT INSERTION

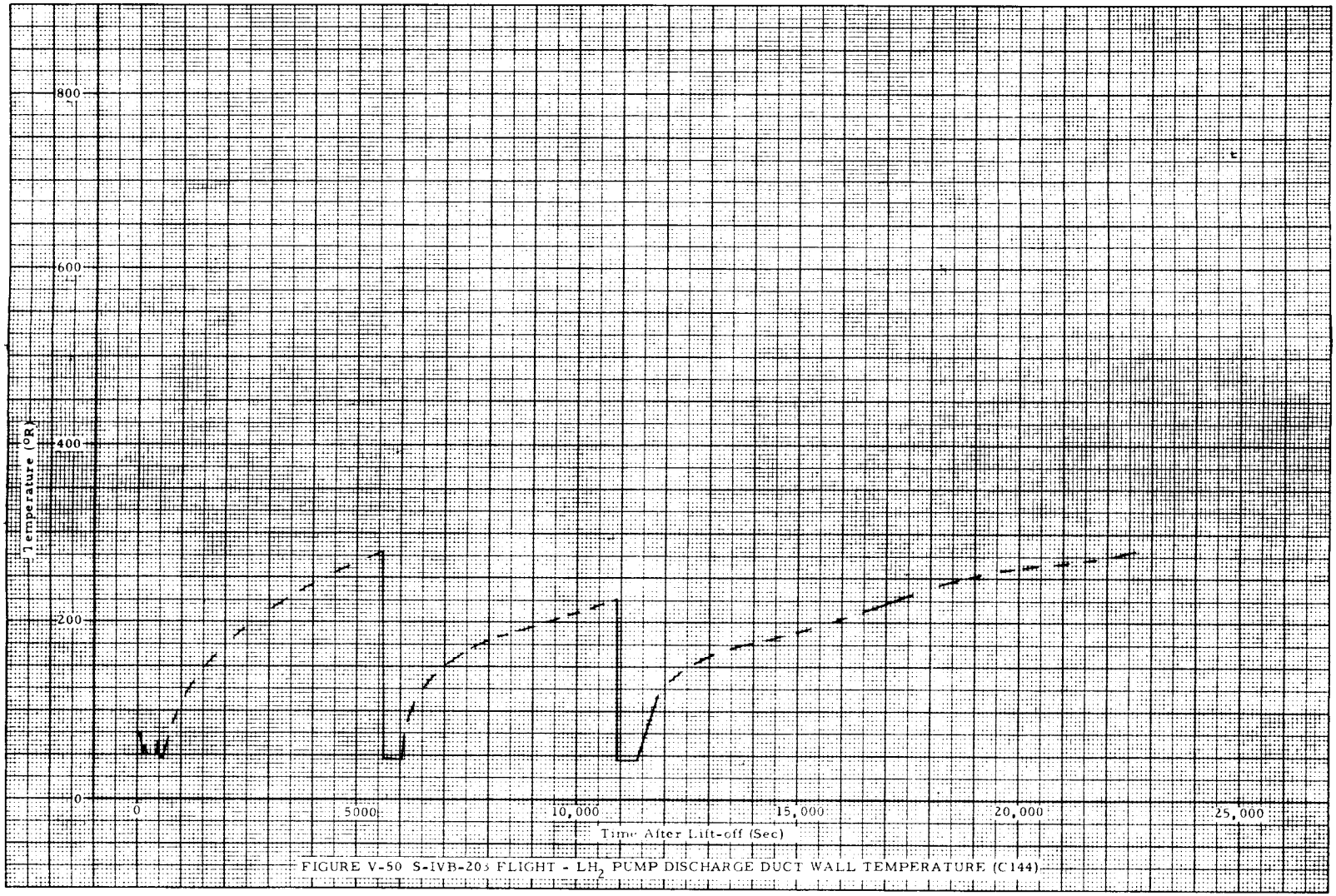

FIGURE V-50 S-IVB-203 FLIGHT - LH_2 PUMP DISCHARGE DUCT WALL TEMPERATURE (C144)

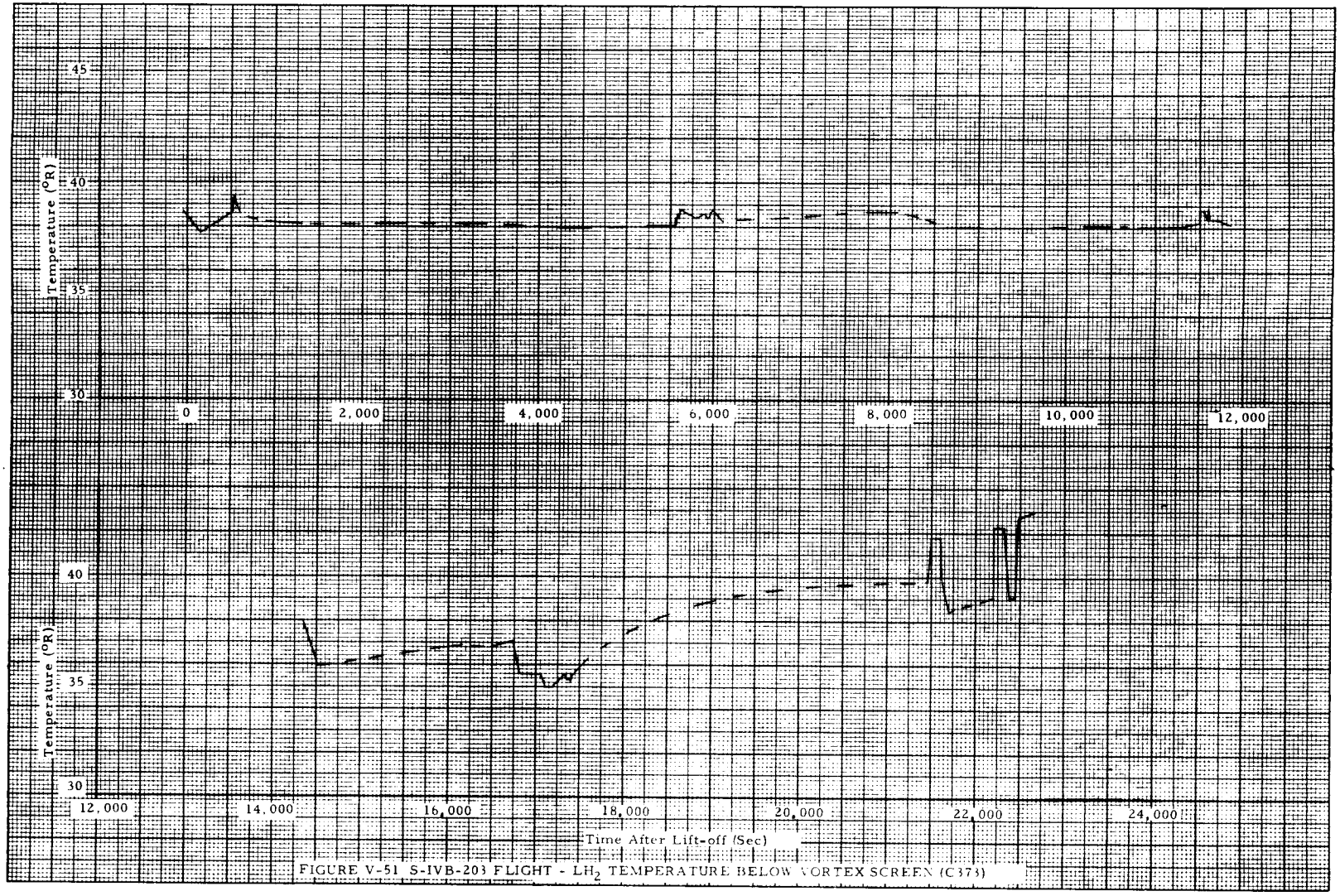

FIGURE V-51 S-IVB-203 FLIGHT - LH_2 TEMPERATURE BELOW VORTEX SCREEN (C373)

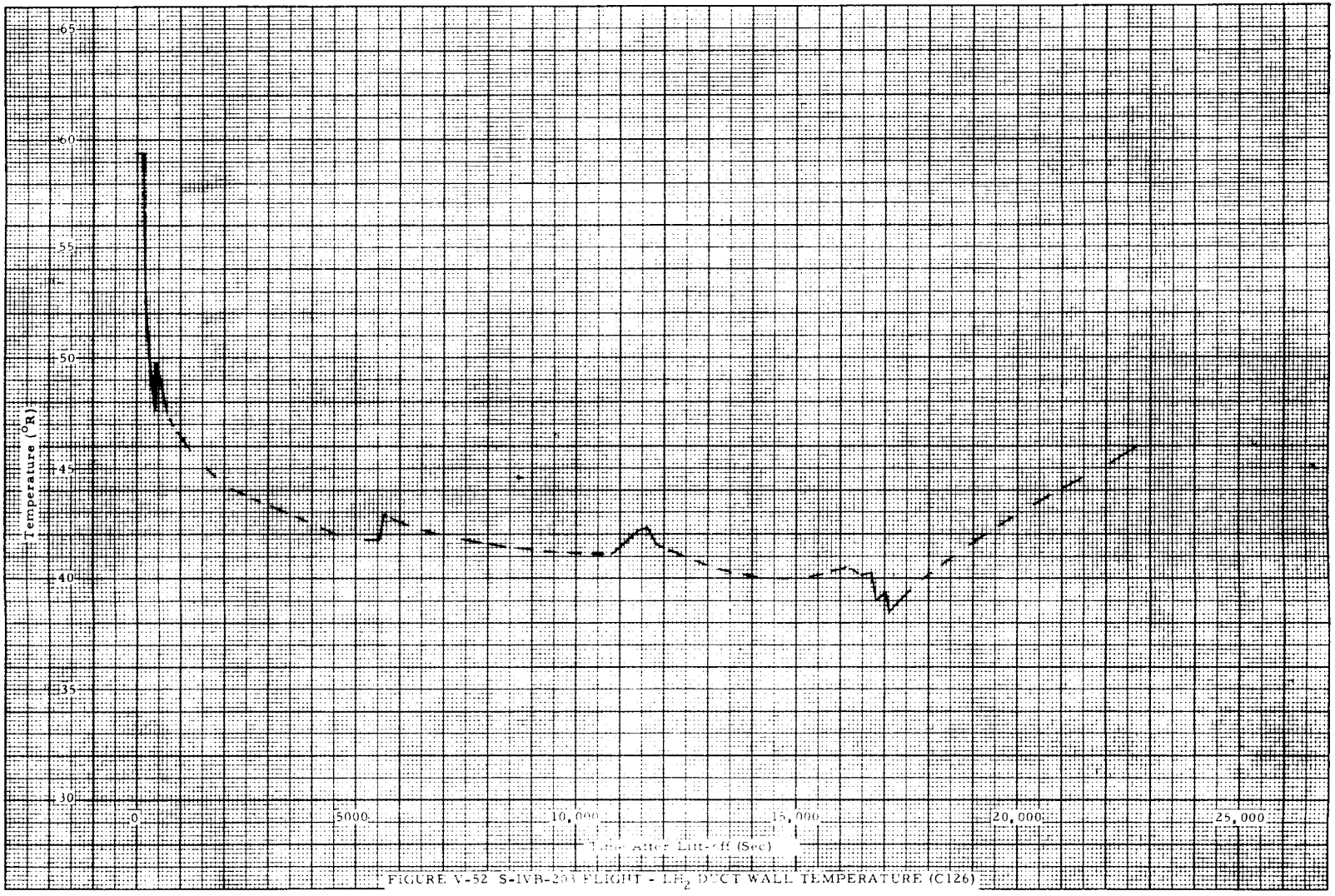

FIGURE V-52 S-IVB-203 FLIGHT - LH_2 DUCT WALL TEMPERATURE (C126)

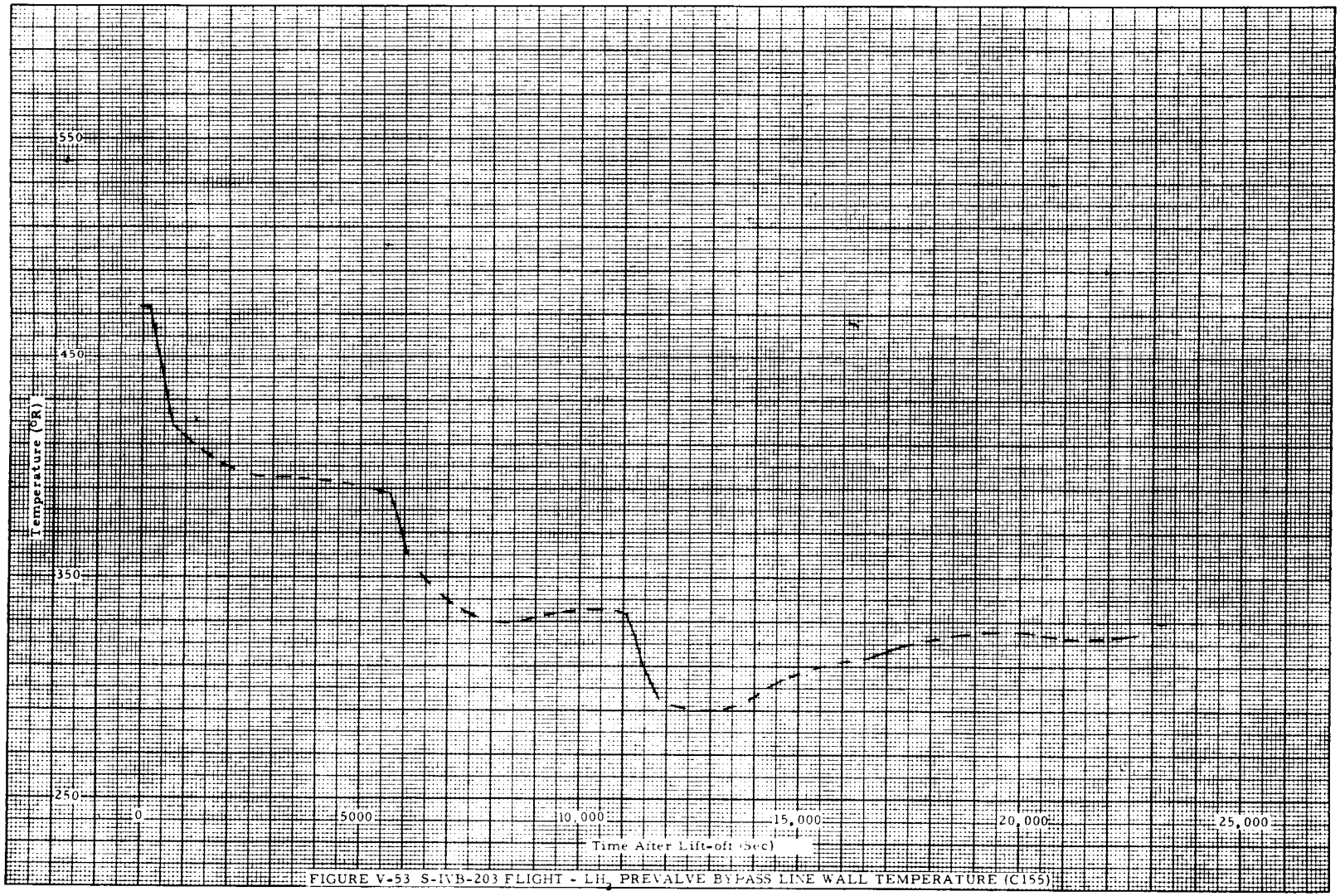

FIGURE V-53 S-IVB-203 FLIGHT - LH$_2$ PREVALVE BYPASS LINE WALL TEMPERATURE (C155)

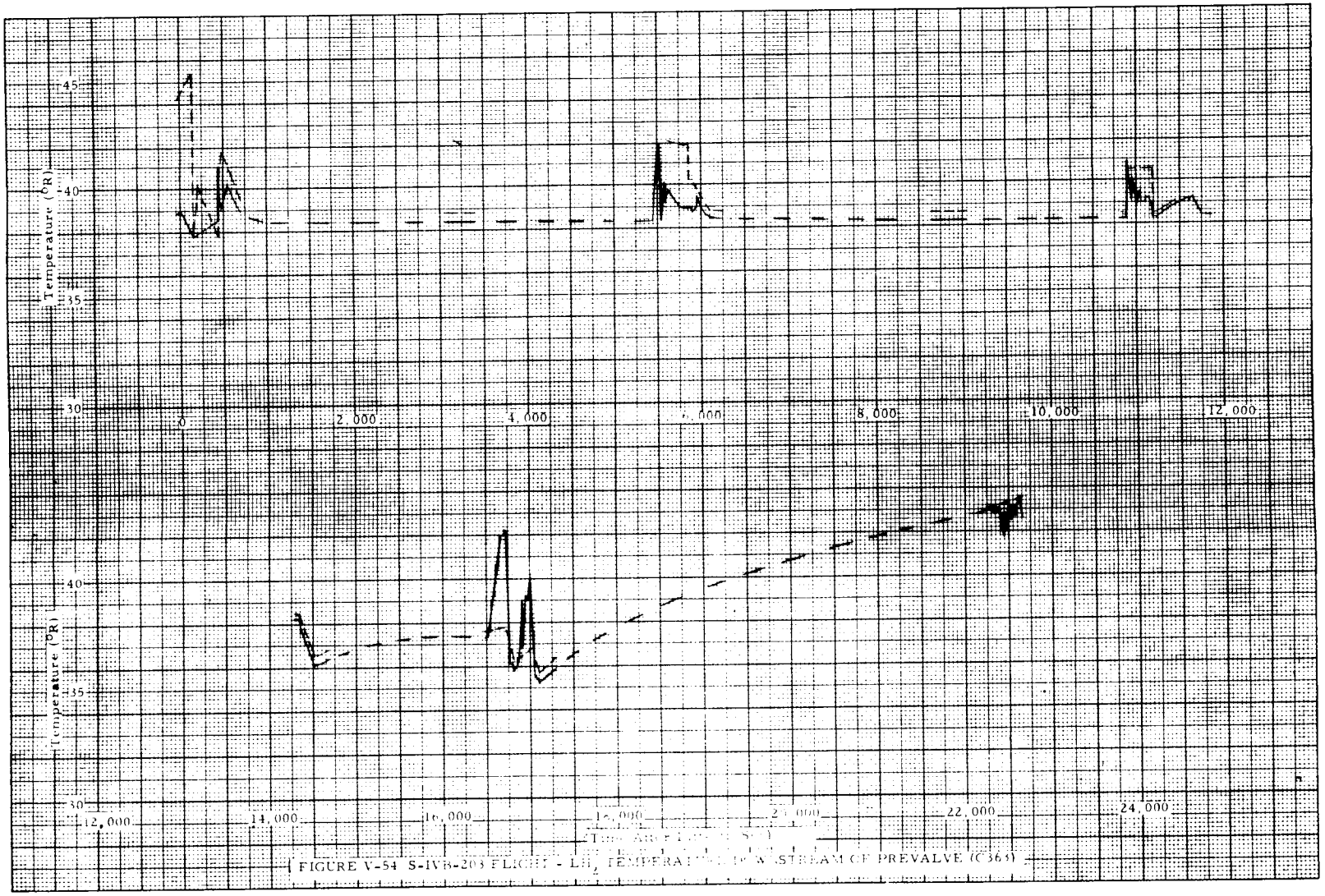

FIGURE V-54 S-IVB-203 FLIGHT - LH_2 TEMPERATURE IN A STREAM OF PREVALVE (C369)

SECTION VI. NON-SATURN V RELATED EXPERIMENTS

The second hydrogen system chilldown experiment concluded the Saturn V related experiments. The remainder of the flight was utilized to obtain data applicable to other types of vent systems and to the design of future cryogenic stages. The tests conducted during the final two orbits included the free coast experiment, rapid depressurization of the fuel tank, and the closed tank pressure rise experiment.

A. FREE COAST EXPERIMENT

Near the end of the second orbit, immediately following the second fuel system chilldown, the continuous vent valve was closed (11,237 seconds) allowing the vehicle to go into a free coast so that the only accelerations experienced by the vehicle were those resulting from the prevailing environment. The objective of this sequence was to observe the liquid behavior in the presence of a very low adverse acceleration. Aerodynamic drag on the vehicle produced a deceleration of approximately 1.9×10^{-6} g's with the liquid above the vapor with respect to the acceleration vector. This acceleration corresponds to a Bond number of approximately 7. According to theoretical analyses and drop tower experiments concerned with the liquid-vapor interface stability, the critical Bond number (based on tank radius) is well defined as 0.84. In the case of the S-IVB hydrogen tank, any negative acceleration greater than approximately 10^{-7} g's should unseat the propellant causing it to move to the forward end of the tank. The TV indicated that after the continuous vent valve was closed, the liquid began to flow forward along the tank walls. The average velocity of the liquid moving along the tank wall was approximately 0.04 ft/sec. The flow apparently advanced somewhat faster on the side of the tank next to the earth (position I). After approximately 3 minutes of coast the deflector near position I became wetted. Wetting of the deflector continued slowly toward position IV until the end of the coast period. A temperature sensor (C325), located just below the deflector attachment plane and near position III, showed a sharp drop in wall temperature near the end of the coast period, indicating that liquid had also risen to the deflector on the upper side (position III) of the tank.

The favoritism of the liquid motion toward one side of the tank may be explained by the fact that the vehicle was in a slightly nose-up attitude and the orbital drag was therefore greater on the side of the vehicle toward the earth. Bowman (reference 13) has shown that if the deceleration vector is not aligned with the axis of symmetry of the fluid container, the liquid will tend to flow up one side of the tank, as would be expected. The TV did not

reveal the formation of a liquid spike in the center of the tank (Helmholtz instability) as the liquid moved toward the forward dome. For the prevailing Bond number this observation is also consistent with Bowman's findings.

The forward motion of the liquid was arrested after five minutes (at 11,540 seconds) by the resumption of thrusting from the LOX ullage thruster system which applied a positive acceleration to the vehicle of about 4×10^{-4} g's. The liquid could be seen flowing back down the walls toward the bottom of the tank. The majority of the liquid had settled below the baffle within 90 seconds after resumption of thrusting. The continuous vent system was opened 99 seconds after initiation of settling and the LOX system was closed 21 seconds later. The prevailing acceleration following the closing of the LOX thrust system was 2×10^{-4} g's.

Thirty seconds after the LOX ullage thrust system was closed, several particles of liquid were observed moving forward near the center of the tank. A portion of this liquid passed the deflector before going out of view of the TV camera. It is believed that the motion of these particles was a result of (1) an amplification phenomenon when the thrust level was decreased to the continuous venting level and/or (2) a redirection of liquid momentum during the resettling process. The particles hit the internal surfaces of the forward dome and were vaporized. This vaporization, plus the passage of the liquid particles through the superheated ullage vapor, created a significant thermal gradient in the ullage which caused a wavy pattern (similar to that observed with a full tank of liquid) to appear on the TV picture. As the thermal gradient in the ullage subsequently decreased, the wavy pattern on the TV disappeared. This optical phenomenon is discussed further in Section VIII-A.

B. RAPID DEPRESSURIZATION OF FUEL TANK

Three separate blowdowns of the hydrogen tank were performed to observe the behavior of liquid hydrogen under the combined conditions of low gravity and rapid tank depressurization. The first blowdown occurred over Carnarvon, Australia, and lasted for a period of three minutes (14,342 - 14,522 seconds). The second and third blowdowns were each ninety seconds in duration (16,723 - 16,813 seconds and 17,023 - 17,113 seconds) and occurred during the third pass over the United States. All blowdowns were accomplished by venting fuel tank ullage gases through the non-propulsive vent (NPV) system.

The NPV system contains a vent valve that may be actuated either on command or by pressure demand. This valve acted on pressure demand during powered flight (154 to 225 seconds) and on command only during orbital flight. The system flow is directed through two discharge orifices,

diametrically opposed, at the vehicle outer skin such that the thrust produced is theoretically non-propulsive. Figures IV-1 and IV-2 show the location of the vent system with respect to the vehicle.

1. First Blowdown

During the first blowdown sequence, a positive acceleration of approximately 3.7×10^{-4} g's was maintained by thrusting from both the continuous vent system and the LOX ullage thruster system. The LOX ullage thruster system was opened at 14,341 seconds and remained open for 187 seconds. The rapid depressurization was initiated by opening the NPV system at 14,342 seconds.

Before the NPV system was opened the TV picture showed that the liquid was completely settled in the bottom of the tank. The liquid was saturated at about 20 psia. Thermocouples throughout the ullage (C038, C039, and C348), together with the continuous vent system line temperatures (C0256 and C0257), indicated that the ullage gas was superheated and under nearly steady-state continuous venting conditions. When the NPV system was opened, a white fog formed above the liquid obscuring the surface. This fog was caused by the recondensation of the gases above the liquid as the tank pressure dropped. The fog continued to develop and rise in the tank so that the entire tank interior was obscured within about one minute. Therefore, it was not possible to visually locate the liquid surface during this test. As the venting continued, the fog could be seen streaming past the TV lens toward the direction of the vent outlet. Two minutes and fifteen seconds after venting was initiated, nearly spherical liquid particles ranging in size from about one to six inches in diameter were observed moving past the TV lens, with estimated velocities as great as 1.5 ft/sec. This flow of liquid particles continued until the end of the depressurization test. The tank pressure at the end of the first blowdown was 14.2 psia. When the NPV system was closed, the fog began to clear and the liquid particles could be seen moving randomly about in the ullage above the liquid which had apparently remained settled. These conditions were virtually unchanged until the time of loss of the TV signal by Carnarvon approximately one minute later. Corpus Christi, Texas, acquired the vehicle one-half hour later and the liquid particles had resettled in the tank.

The existance of the liquid particles in the top of the tank as well as their relatively high velocity has not been conclusively explained. Three sources of particle energy were investigated in an attempt to explain this phenomenon.

a. Entrainment by flowing gas

b. Breakup of slosh waves

c. Boiling

A simplified analysis equating the gaseous drag forces and buoyancy forces to the gravity forces on a liquid particle indicates that under the prevailing fuel tank conditions, the maximum particle size that could have been entrained in the ullage stream was approximately one inch in diameter. The results of this analysis for the S-IVB fuel tank are shown by figure VI-1. The results show the maximum particle radius (assuming spherical particles) as a function of vehicle acceleration for various vent flow rates. The minimum acceleration experienced by the AS-203 vehicle during the blowdown sequences is also indicated on the figure. It is concluded that particles of the size actually observed could not have been entrained by the gas.

It is doubtful that the particles were formed by the breakup of slosh waves at the tank sidewall and baffles. No particles were formed under the low acceleration level just prior to the blowdown, and although there was increased attitude control system activity during the blowdown, the higher acceleration level provided by the LOX ullage thruster system should have reduced the slosh wave amplitude. The particles observed in the ullage at orbital insertion, which were almost certainly a result of slosh wave breakup, did not achieve either amplitudes or velocities as great as those observed during the blowdown sequences. In addition, the particles observed at orbital insertion moved in a much more orderly pattern than those observed during the blowdown. For these reasons it is doubtful that the particles originated from the breakup of slosh waves.

Since the movement of the observed liquid droplets was apparently not caused by either slosh waves or entrainment in the gas stream, it is believed that liquid boiling phenomena were the major contributing energy sources in accelerating the liquid particles. As the tank pressure was rapidly decreased a portion of the initially saturated liquid probably became superheated. It is likely that only a few nucleation sites were present in the center of the liquid, so that when the superheated liquid finally began to vaporize, the bubble growth rate was so rapid that a portion of the liquid near the surface was thrown into the ullage. The maximum liquid superheat that could have occurred between the start of the tank depressurization and the time that the first liquid droplets were observed 130 seconds later is about $1.7^{\circ}R$. No superheating was recorded on any of the temperature sensors within the liquid during the test. However, this would not be expected since the sensors represent a very good nucleation site.

2. Second and Third Blowdowns

Shortly after acquisition by Texas, the NPV system was again opened (16,723 seconds). The only vehicle thrusting during both the second and third blowdown sequences was provided by the continuous vent system. The acceleration level was approximately 2.0×10^{-5} g's. The tank pressure at initiation of the second blowdown was 17.1 psia, having risen 2.9 psi due to heat addition since Carnarvon. The TV pictures during the sequence showed events similar to those observed at Carnarvon; fog immediately obscured the liquid surface, and completely filled the tank within 60 seconds; and the first liquid particles were observed 30 seconds later. The fog was not as dense as had been observed at Carnarvon, but it was still impossible to determine the exact liquid level. The liquid location could not be determined by instrumentation, because the ullage gases were nearly saturated and temperature sensors were not effective in distinguishing liquid from vapor. Since it did not appear that large amounts of liquid were in the ullage, it was concluded that the major portion of liquid was still in the bottom of the tank. At the end of the 90 second venting period the NPV was closed and the tank pressure had decreased 3.8 psi to 13.3 psia.

The NPV remained closed for three minutes and thirty seconds. The TV viewing port became covered by a liquid film 40 seconds after the NPV was closed. Occasionally a portion of the viewing port would clear and the inside of the tank could be seen. During these brief glimpses, it appeared that liquid droplets were clinging to all of the internal tank surfaces.

When the NPV was again opened, the liquid film was blown off the TV viewing port. Since all of the gas being vented during this depressurization was essentially saturated, the tank pressure decreased by only 2.3 psi, from 14.5 to 12.2 psia. Kennedy Space Center received the TV picture until two minutes after the NPV system was closed. During this two minute interval, the conditions inside the tank remained almost unchanged. When the contents of the hydrogen tank were again seen at Texas one and one-half hours later, the liquid was settled below the baffle and calm. All of the liquid particles and droplets were gone and the internal surfaces of the tank above the liquid level were dry.

3. Vented Mass

An important objective of this particular experiment was to obtain an indication of the loss of liquid overboard, if any, as a result of rapid venting. A quality meter was installed in the continuous vent system to indicate the quality of the vented fluid. It is felt that the quality meter did not furnish data of acceptable accuracy. The performance of the quality meter is discussed in greater detail in Section VIII-D. Although the actual

vented liquid mass cannot be established, the temperatures in the vent lines can be used as an indication of the vented fluid conditions.

Figure VI-2 shows the fuel tank pressure (D021) and the pressure upstream of the NPV orifices (D184) during the blowdown sequences. Figure VI-3 shows the measured fluid temperature (C255) and hydrogen saturation temperature upstream of the NPV orifices. It can be seen from the latter figure that the vented fluid temperatures were superheated in the NPV system throughout all blowdown periods. It is very unlikely that the measured temperatures are in error since both thermocouples in the system (C254, C255) were indicating approximately the same temperature. Superheated vapor was also measured in the continuous vent system. Due to the turbulent flow conditions in the vent lines and the low incipient boiling temperature difference for liquid hydrogen, it is very unlikely that a significant amount of liquid hydrogen was vented overboard through either the NPV or CV system. It appears that some liquid did enter the CV system after the second blowdown (sharp decrease in CV fluid temperature). However, this liquid was probably evaporated by the hotter surrounding gas and vent line walls before reaching the overboard nozzles.

Figure VI-4 shows the transient mass flow rate from the NPV system during the three blowdown sequences. The mass flow rate was calculated using the measured temperatures (C254, C255) and pressures (D183, D184) upstream of the discharge orifices. Consistent with the conclusions of the previous paragraph, it was assumed that the vented fluid was 100% quality. The total mass vented during the blowdowns was 392 lb_m, 166 lb_m, and 168 lb_m for the first, second, and third tests, respectively. Also shown on figure VI-4 are the various assumptions and equations used in the calculations.

These tests indicated that the phenomena observed during the blowdowns should be further investigated before rapid venting of a cryogenic container in orbit is employed. During the Saturn V simulated mission the venting of the boiloff gases from the saturated liquid produced negligible disturbance of the liquid. The rapid venting during the blowdowns, in which the tank pressure dropped well below the initial liquid saturation pressure, produced rather severe liquid disturbances. No significant difference in the fluid behavior between the first and second blowdown tests could be detected, although there was an order of magnitude variation in the acceleration levels between the tests. The phenomena, therefore, appear to be primarily controlled by either, or both, the depressurization rate and the prevailing fluid conditions.

4. Vent System Thrust Unbalance

During the three blowdown sequences, it was observed that the auxiliary propulsion system engines were excessively active in providing control about the yaw axis, indicating a significant unbalanced force between the two sides of the non-propulsive vent system. During the first blowdown (180 second duration) the number two yaw engine in Module I (I_2) fired 29 times and the number two engine in Module III (III_2) fired 22 times. During the second blowdown, I_2 and III_2 fired 16 and 11 times, respectively, and during the third blowdown they fired 7 and 4 times, respectively. This firing frequency represents the highest APS activity during the entire flight, except at orbital insertion. Other than during the blowdown sequences, these particular engines were the least active of the APS system. The non-propulsive vent system ΔP measurement (D215) fluctuated rapidly and indicated a significant differential between the vent system branches during all three tests substantiating the fact that venting from the NPV system had produced an unbalanced force on the vehicle. The pressure differential during the blowdowns varied from zero to -0.40, -0.36, and -0.26 psi during the first, second, and third tests, respectively. Figure VI-5 illustrates the ΔP fluctuation during the first blowdown. The maximum unbalanced thrust resulting from the unbalanced pressure during the first blowdown is calculated to be about 3.85 lb_f.

C. CLOSED FUEL TANK EXPERIMENT

Early in the fourth revolution (at 17,139.2 sec) the fuel tank continuous vent system was closed for the remainder of the flight. The LOX ullage thruster system had been opened (at 17,119.2 sec) to provide a positive acceleration on the vehicle thereby maintaining the LH_2 settled during the experiment. The primary objective of the closed fuel tank experiment was to determine the pressure rise rate in the closed hydrogen tank in orbit. As a result of this experiment it was also possible to determine the differential pressure necessary to collapse the S-IVB stage common bulkhead.

1. Pressure Rise

The primary objective was to determine the rate of pressure increase in the orbiting S-IVB stage. This also allows the evaluation of the fluid heating rates in the low gravity environment. When the fuel tank vents were closed, approximately 16,000 lb_m of LH_2 remained in the tank and the tank pressure was 12.4 psia. The ullage pressure 5,360 seconds later (approximately one orbit) was 37.7 psia which represents a mean pressure rise rate of 17.0 psi/hr in the closed tank. The vehicle acceleration decreased from 3.7×10^{-4} g's at the beginning of the time period to 0.8×10^{-4} g's at the end.

The calculated pressure rise rate based upon the maximum predicted liquid heating rate and assuming homogeneous distribution of the heat input within the liquid bulk was only 3.2 psi/hr. The significantly higher measured pressure rise rate is attributed primarily to heating of the ullage gases. In addition, axial temperature gradients of 5°R and 194°R were developed in the liquid and ullage, respectively, during the 5,360 second period. These gradients are necessarily a result of convective boundary layer development at the tank sidewall. The distribution of the absorbed heat input also contributed to the increased pressure rise rate as compared to the homogeneous model. For ease of comparison with heat transfer data obtained at other times during the flight, a detailed analysis and discussion of the change in thermodynamic conditions in the closed tank is presented in Section VII-A.

A simplified propellant tank thermodynamic model was devised to predict a pressure rise rate in the closed container based upon measured initial thermodynamic conditions and experimentally derived liquid and ullage heating rates. The simplified model assumed a homogeneous liquid and a homogeneous ullage and allowed mass transfer but not heat transfer across the liquid-vapor interface. The pressure rise rate predicted in this manner is shown in figure VI-6 and is compared to the measured pressure rise rate and the pressure rise rate based upon a homogeneous model with liquid heating only. As shown, the predicted pressure determined from the simplified model (including ullage heating), is still not conservative from a design standpoint, however, it is considerably better than the homogeneous model with liquid heating only. Any general thermodynamic model having a single node liquid and a single node ullage will yield conservative pressure if there is significant ullage heating in comparison to the liquid heating. This is because the ullage heating alone will cause the tank pressure to increase more rapidly than the liquid vapor pressure increases thereby suppressing mass transfer to the ullage. For this reason it becomes obvious that accurate pressure predictions will require a thermodynamic model capable of treating stratification as well as ullage heating.

The importance of this particular experiment is that it verified the theory that very low accelerations are sufficient to support convective motion in both liquids and gases.

2. Common Bulkhead Rupture

As a result of the closed fuel tank experiment, data were also obtained on the rupture of the common bulkhead under orbital flight conditions. At the beginning of the fourth revolution the LOX tank vent was opened and the continuous vent system was closed for the remainder of the flight. Fluid heating caused the fuel tank pressure to rise, but the pressure was to be maintained below 42 psia by the fuel tank pressure relief system. The

hydrogen and LOX tank pressures were approximately 39.9 psia and 5 psia, respectively, at the time KSC lost the telemetry signal at the beginning of the fifth revolution. The loss of signal was a normal below the horizon signal loss. At this time, the data showed that the vehicle was intact and functioning normally. Approximately two minutes after loss of signal at KSC, the vehicle was acquired by radar at the Trinidad tracking station. The radar showed a number of pieces and indicated that the vehicle had exploded during the two-minute period between KSC and Trinidad. The most probable explanation of this occurrence is that the common bulkhead ruptured and a spark or impact detonated the propellants. This conclusion is supported by the conditions existing in the propellant tanks at the time of rupture. Ground tests at the Douglas Aircraft Company, Sacramento Test Operation Facility, had resulted in a collapse of the Ground Test Common Bulkhead at a ΔP of 34.7 psi. The ΔP across the AS-203 common bulkhead at the time of rupture was approximately 34.9 psi. Figure VI-7 summarizes the common bulkhead pressure and temperature conditions at rupture for both the ground and flight test conditions and illustrates the approximate point of rupture during the ground tests. The exact point of failure during the flight could not be determined.

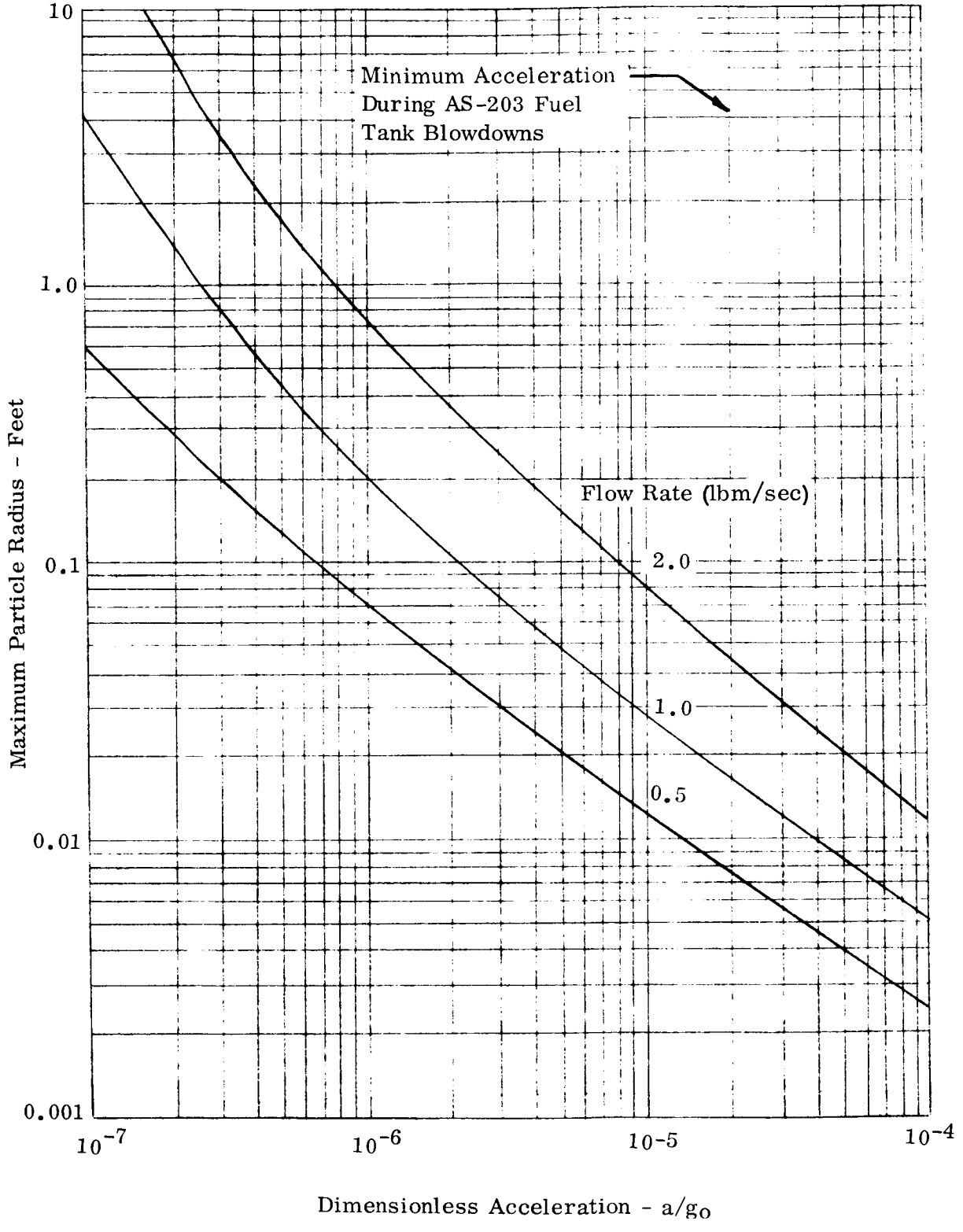

FIGURE VI-1 CALCULATED MAXIMUM SIZE OF PARTICLES ENTRAINED DURING VENTING OF S-IVB FUEL TANK

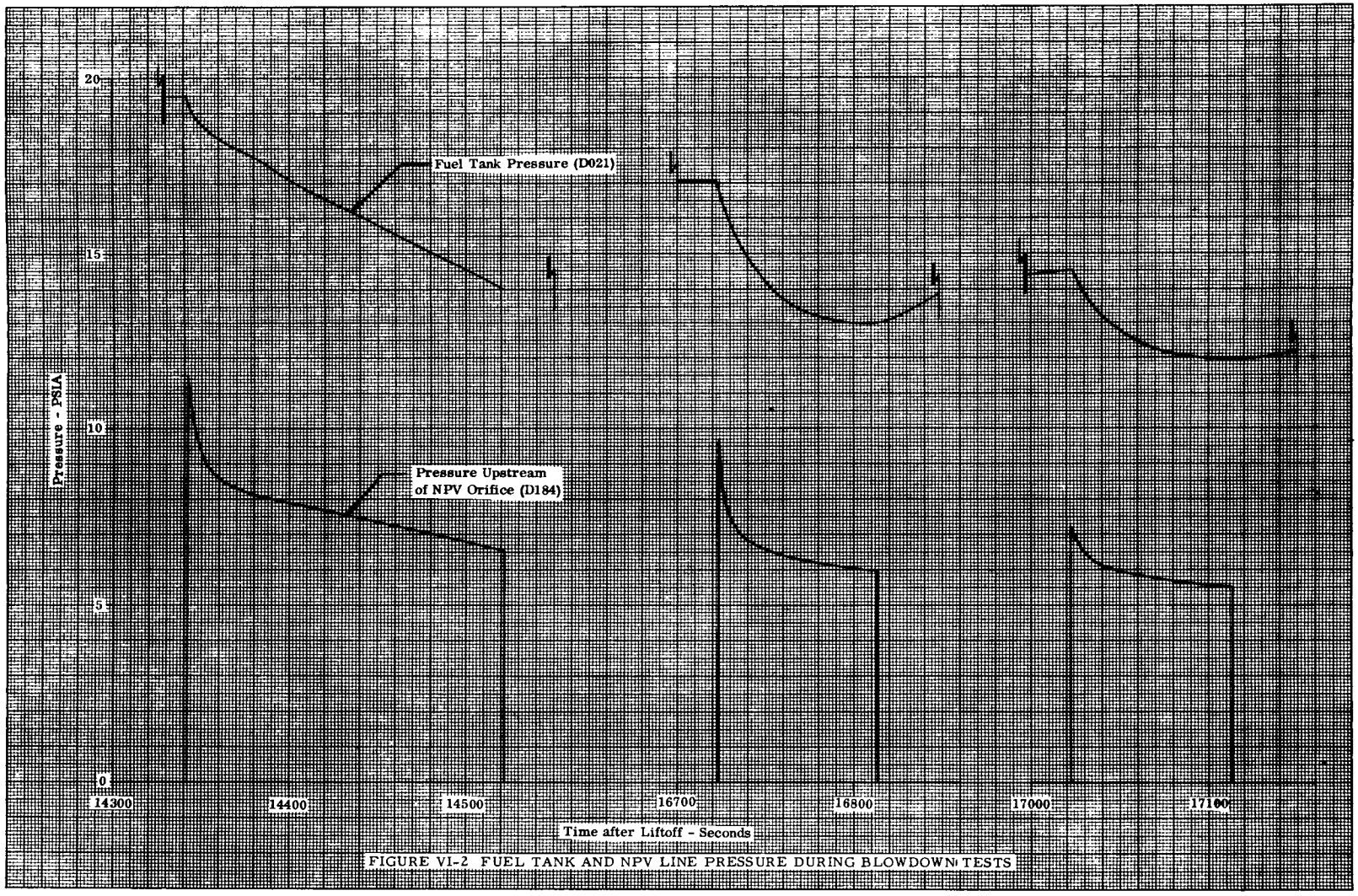

FIGURE VI-2 FUEL TANK AND NPV LINE PRESSURE DURING BLOWDOWN TESTS

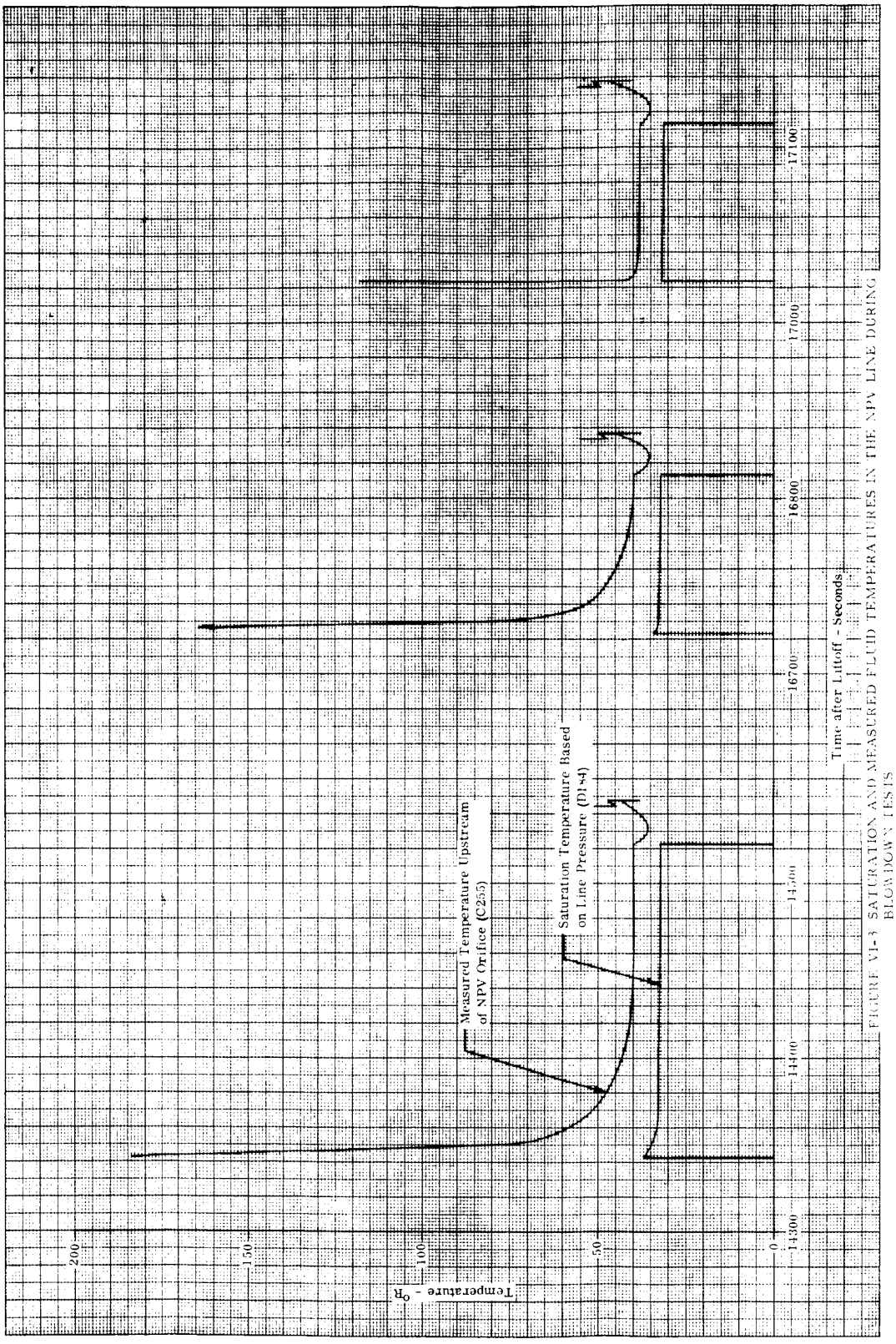

FIGURE VI-3 SATURATION AND MEASURED FLUID TEMPERATURES IN THE NPV LINE DURING BLOWDOWN TESTS

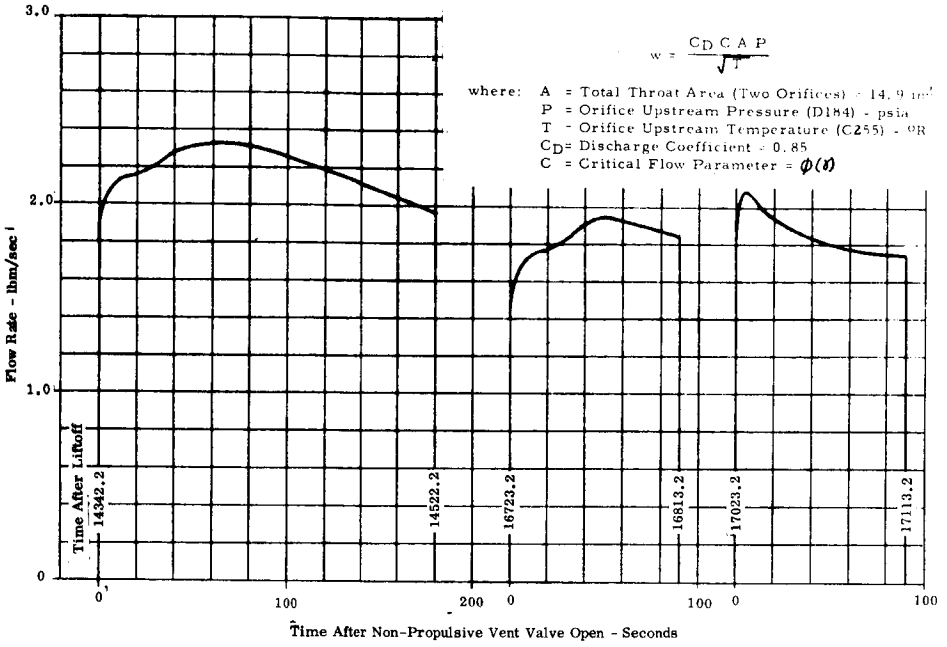

FIGURE VI-4 TRANSIENT MASS FLOW FROM NPV SYSTEM DURING BLOWDOWN TESTS

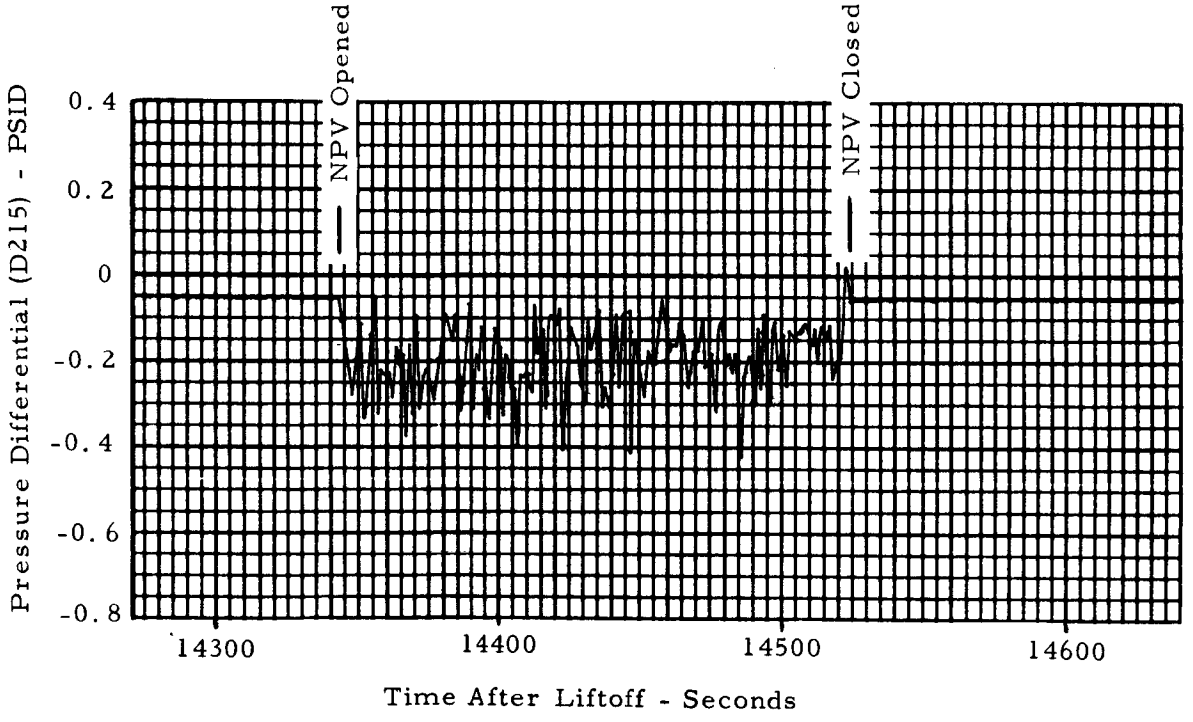

FIGURE VI-5 NON-PROPULSIVE VENT SYSTEM PRESSURE UNBALANCE DURING FIRST BLOWDOWN TEST

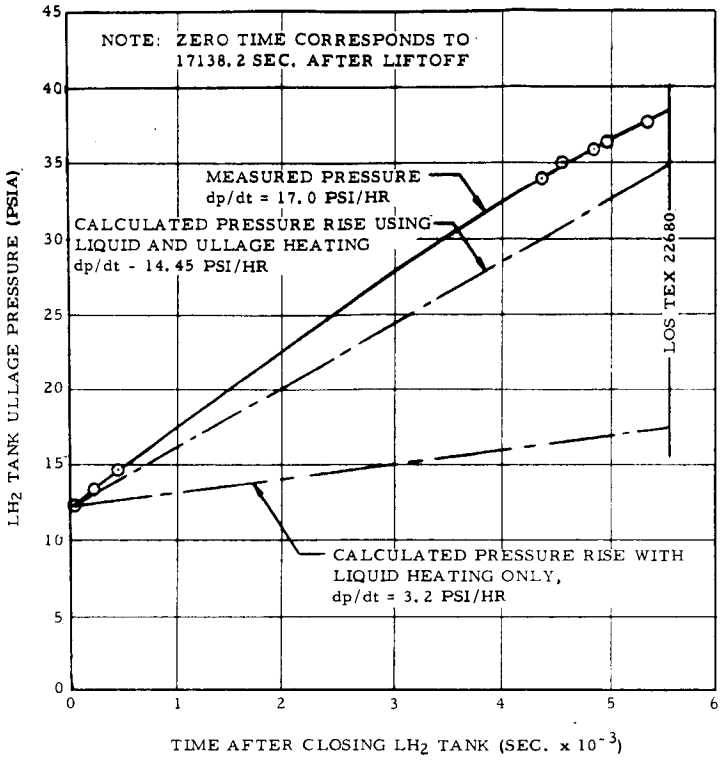

FIGURE VI-6 PRESSURE RISE DURING CLOSED FUEL TANK EXPERIMENT

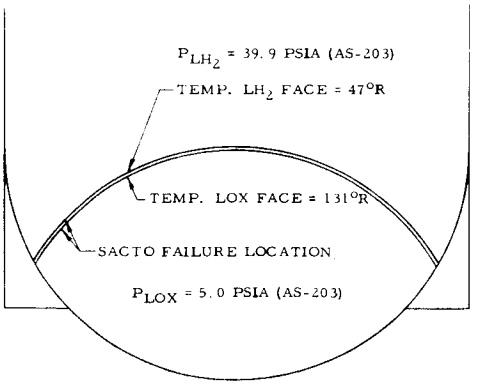

	AS-203	SACTO TEST
FAIL ΔP (PSID)	34.9	34.7
TEMP LH_2 FACE	47°R	37°R
TEMP LOX FACE	131°R	140°R

FIGURE VI-7 COMMON BULKHEAD RUPTURE CONDITIONS

SECTION VII. PROPELLANT TANK HEATING CONDITIONS

The heat transferred to the fluid in the S-IVB fuel tank during the flight was determined so that the adequacy of the tank insulation and the effects of the low gravity environment could be evaluated. Two approaches were employed in utilizing the flight data to determine the heat transfer characteristics of the tank. The first approach was to use the measured changes in fluid conditions in the tank to evaluate heat and mass transfer. The second approach used the measured temperature differences across the tank walls and the thermal properties of the wall material for calculating heat transfer into the tank. The results from the two methods were then compared.

A. CHANGES IN FLUID CONDITIONS

The heat entering the liquid hydrogen during the time interval from 40 seconds before liftoff until S-IB cutoff, 184 seconds later, was calculated from the change in the liquid temperature and the heat of vaporization of the liquid boiloff.

$$Q_f = c_p M_f \Delta T_m + M_{bo} h_{fg} \qquad \text{(VII-1)}$$

where:

Q_f -Total heat entering liquid hydrogen - Btu

c_p -Specific heat of liquid hydrogen (2.6) - $Btu/lb_m\ ^oR$

M_f -Mass of liquid hydrogen (42, 300) - lb_m

ΔT_m -Mean liquid temperature rise during time interval - ^oR

M_{bo} -Mass addition to ullage by evaporation during time interval - lb_m

h_{fg} -Heat of vaporization - Btu/lb_m

A mass balance on the ullage gas using initial and final gas temperatures and pressures indicates that there was no significant mass transfer between the liquid and ullage during this particular 184 second time period. Therefore, the mass transfer term ($M_{bo}\ h_{fg}$) in equation VII-1 becomes zero. It should be noted that both the temperature difference between the wall and liquid bulk,

and the estimated heat flux at this time indicate that nucleate boiling was occurring. Since no mass was being added to the ullage gases, the vapor apparently recondensed in the subcooled liquid bulk.

Figure VII-1 shows the measured liquid hydrogen temperature versus S-IVB tank height at 40 seconds before liftoff, at S-IB cutoff, and at S-IVB cutoff. The thermal boundary layer at the tank sidewall was too thin to be detected by the temperature sensors. However, a rise in the mean liquid temperature was obtained. The mean liquid temperature rise during ground hold and S-IB burn was approximately $0.35^{\circ}R$. Using this temperature rise and equation VII-1, the increase in sensible heat of the liquid was calculated to be 38,500 Btu, or an average of 209 Btu/sec.

In order to determine the actual liquid temperatures, it was necessary to adjust the temperature measurements. A correction factor was determined for each temperature sensor beneath the liquid surface by comparing the indicated temperature of each sensor to the liquid hydrogen saturation temperature at times during the flight when the liquid was known to be saturated at tank pressure. The measured fluid temperatures employed in the heat and mass transfer analyses were corrected by the values shown in table VII-1. Ullage temperature sensors could not be corrected and it was necessary to use the actual readout values. This is not a particularly critical fact since relatively small sensor inaccuracies do not introduce the magnitude of error in calculating the ullage conditions that they would in the case of the liquid.

Because of the varying liquid hydrogen level and rapidly changing ullage gas conditions in the fuel tank during S-IVB burn, considerable error could be introduced in calculating liquid or ullage heating rates. Therefore, heating values were not calculated for this time interval.

The heat input to the liquid hydrogen during orbital coast was determined by evaluating the heat required to vaporize the mass of hydrogen being vented overboard through the continuous vent system (see figure IV-10) during periods when quasi-steady state thermodynamic conditions existed in the fuel tank. Figure VII-2 shows the calculated total liquid hydrogen heating rate during the first three orbits. In addition to heating of the liquid, it was determined that there was also a considerable degree of ullage heating throughout the orbital period. The rate of ullage heating with time is plotted in figure VII-3. The ullage heating rate was determined from the enthalpy change of the vaporized hydrogen gas between the liquid surface (saturated vapor) and the overboard nozzle. This method of analysis is valid only when the tank has reached quasi-steady thermodynamic conditions. The data points shown are for such conditions. This method assumes no heating of the vapor in the vent lines. The ullage temperature data and a radiation heat balance on the continuous vent lines were both used to substantiate the validity of this assumption.

TABLE VII - 1

LIQUID HYDROGEN TEMPERATURE MEASUREMENT CORRECTION FACTORS

Meas. No.	Correction Factor (C)	Meas. No.	Correction Factor (C)
C012	+0.90	C331	+0.10
C052	+0.02	C332	+0.08
C053	-0.05	C333	+0.05
C054	-0.07	C334	-0.05
C092	-0.22	C335	+0.35
C093	-0.22	C339	-1.12
C094	-0.17	C341	-0.02
C095	-0.07	C342	+0.34
C096	-0.02	C343	+0.28
C330	-0.15	C344	+0.22
		C345	-0.22

NOTE: $T_{actual} = T_{measured} + C$

Because steady state conditions did not exist between the first and second blowdown experiments, the total heat addition to both the liquid and ullage masses was calculated by combining the heat input determined from the continuous vent flow with that calculated from changes in fluid conditions in the tank. The calculated mean liquid and ullage heating rates during this period were 21.0 and 6.6 Btu/sec, respectively.

Since no fluid was being vented from the tank during the closed tank experiment, the liquid and ullage heating rates were calculated entirely on the bases of changes in internal fluid conditions. When the tank was closed (17,138 seconds after liftoff) the liquid was saturated throughout at 12.4 psia (35.5°R) and the ullage gas was superheated approximately 5°R. The temperature variation in the liquid hydrogen at the end of the closed tank experiment was

established by correcting (see table VII-1) all liquid temperature sensors and assuming no circumferential variation within the liquid. The isotherms in the liquid at the end of the fourth orbit are shown in figure VII-4. Because the temperature of the liquid in the boundary layer was varying erratically (see figure VII-5), it was necessary to average the temperature values over a 200-300 second time interval in order to obtain a mean value for use in constructing the liquid temperature map. The temperature differential between the liquid hydrogen and the tank walls was greater than the critical value, so that nucleate boiling at the walls occurred throughout the closed fuel tank experiment. Since there were insufficient temperature sensors in the ullage to establish a boundary layer profile, it was necessary to assume that the only temperature variations were in the axial direction and boundary layer gradients were neglected. Figure VII-6 shows the initial and final ullage gas temperatures. By employing the data in figures VII-4 and VII-6 a complete thermal map of the fluid in the tank at the end of the closed tank experiment was constructed and is shown in figure VII-7.

Knowing the initial and final temperature gradients along with initial and final tank pressures it was possible to calculate the mean liquid and ullage gas heating rates during the closed tank experiment. The heat input to the ullage gas was calculated by considering the general energy equation for the ullage.

$$Q_g = (M_{gF}\, U_{gF} - M_{gi}\, U_{gi}) - (M_{gF} - M_{gi})\, h_{fg} \qquad \text{(VII-2)}$$

where:

Q_g	- Heat added to ullage gas	- Btu
M_g	- Mass of ullage gas	- lb_m
U_g	- Internal energy of gas	- Btu/lb_m
h_{fg}	- Heat of vaporization	- Btu/lb_m

Subscripts

F	- Final condition (at 22,498 seconds)
i	- Initial condition (at 17,138 seconds)

The mass and internal energy terms were determined by dividing the ullage volume into nodes or layers having finite thickness as measured along the tank centerline. The specific volume and internal energy of each node were evaluated at the tank pressure and the average temperature of each node as determined from the temperature profiles shown in figure VII-6. These were summed to yield the mass and internal energy of the ullage. The results of this procedure indicate a net liquid evaporation of approximately 250 lb_m. This vaporized liquid was assumed to be added to the ullage at saturation

conditions, and the total heat input to the ullage was subsequently determined to be approximately 31,500 Btu, corresponding to an average heating rate of 5.9 Btu/sec.

The heat added to the liquid during the closed tank experiment was calculated using the following equation.

$$Q_f = c_p M_f \Delta T_m - \frac{M_f v_f \Delta P \times 144}{778} + M_{bo} h_{fg} \qquad \text{(VII-3)}$$

where:

Q_f	- Total heat added to liquid	- Btu
c_p	- Constant pressure specific heat of liquid (2.6)	- $Btu/lb_m\ ^oR$
ΔT_m	- Mean liquid temperature rise during experiment	- ^oR
v_f	- Average specific volume of liquid (0.228)	- ft^3/lb_m
ΔP	- Tank pressure rise during experiment (25.3)	- psi
M_f	- Mass of liquid hydrogen (15,660)	- lb_m
M_{bo}	- Mass of liquid evaporated during experiment	- lb_m
h_{fg}	- Heat of vaporization	- Btu/lb_m

A mean liquid temperature rise during the closed tank experiment of 3.2^oR was obtained by volumetrically averaging the liquid temperatures from a thermal map similar to the one shown in figure VII-7. Using equation VII-3, along with the above data and the previously determined 250 lb_m boiloff, the total heat added to the liquid during the closed fuel tank experiment was calculated to be 160,600 Btu, for an average heating rate of 29.9 Btu/sec.

B. WALL TEMPERATURE DIFFERENCE

The heat input to the fuel tank during the flight was calculated from the steady one-dimensional heat conduction equation using measured internal and external wall temperatures and a previously established wall thermal conductivity. The fuel tank was instrumented with 40 wall temperature sensors (see figures II-3 and II-4). There were four fuel side and two LOX side skin temperature sensors on the common bulkhead; two internal and two external sensors on both the forward and aft domes, and eight internal and eighteen external sensors on the cylindrical sidewall.

Figures VII-8 and VII-9 show the range of measured external sidewall temperatures for the wetted portion of the fuel tank during boost and orbital flight respectively. Figures VII-10 and VII-11 show typical circumferential and axial temperature variations during the boost and orbital phase of the flight. A mean external sidewall temperature was obtained at various times during the flight by plotting the measured values on graphs similar to figure VII-11 and integrating beneath the curves. The mean external sidewall temperature is shown on figures VII-8 and VII-9 for boost and orbital flight, respectively. The range of wetted internal wall temperatures measured during the flight is shown on figure VII-12. The saturation and bulk liquid hydrogen temperatures are also shown on this figure.

The wetted sidewall mean heat flux was calculated from the one-dimensional heat conduction equation using the mean wall temperatures from figures VII-8, VII-9, and VII-12 along with the nominal effective sidewall thermal conductivity shown in figure VII-13. These calculated boost and orbital sidewall heat fluxes are shown in figures VII-14 and VII-15 respectively.

Figure VII-16 shows the measured common bulkhead skin temperatures on both the fuel and oxidizer tank sides. Using this temperature data along with an effective common bulkhead heat transfer coefficient of 0.034 Btu/hr-ft^2-^oR, the mean heat flux across the common bulkhead was calculated and is shown in figure VII-17 versus orbital time. Because of the small number of temperature sensors on the common bulkhead, the accuracy of the calculated heat flux is poor. However, since the heating from the common bulkhead was small compared to total LH_2 heating, no significant error in total LH_2 heating can be introduced from this source.

Figure VII-18 shows both the internal and external fuel tank aft dome skin temperatures during the flight. Using this temperature data and the effective wall thermal conductivity shown in figure VII-13, a mean heat flux across the aft dome was calculated and is shown in figure VII-19.

The heat fluxes determined were used to calculate the liquid heating rates. In order to calculate the liquid heating rate from the sidewall it was first necessary to determine the wetted sidewall area. The quantity of liquid hydrogen in the tank at given times was calculated by subtracting the accumulated vented mass (see figure IV-12) from the liquid mass at orbital insertion (19,100 lb_m). The wetted sidewall area was then determined by assuming that the liquid in the tank remained settled. The area calculated included a meniscus effect which was calculated by the "ellipsoidal approximation" method proposed by Satterlee (reference 4). The calculated wetted sidewall area for the S-IVB-203 fuel tank is shown in figure VII-20. Using this wetted sidewall area and the sidewall heat flux from figure VII-15, the liquid heating rate through the sidewall was calculated and is shown in figure VII-21.

The heating rates through the common bulkhead and the aft dome were calculated from the heat flux data shown on figures VII-17 and VII-19 and are presented in figure VII-22 as a function of the orbital time. Also shown on this figure are estimated heating rates from the aft flange joint and the various lines penetrating the tank. These estimated heating rates were based on analytical calculations and data from reference 15.

The total liquid heating rate, which is shown in figure VII-21, was obtained by summing the heating rates from the common bulkhead, fuel tank aft dome, aft flange joint, suction duct and recirculation return lines, fill and drain lines and fuel tank sidewall.

The heat flux into the ullage gas was also determined from the wall temperature difference. Temperature sensors were located at only one station (545) along the dry portion of the fuel tank sidewall. Therefore, no well defined dry sidewall temperature profiles could be established. The measured internal and external skin temperatures obtained for the dry sidewall portion of the fuel tank are plotted in figure VII-23 versus orbital time. Figure VII-24 shows the circumferential variation of the dry sidewall external temperature for times when the vehicle was in the earth's shadow and in the sun (quasi-steady state vent conditions also existed at the times shown). The mean external sidewall temperature, also shown in figure VII-23, was obtained by circumferentially integrating beneath curves similar to figure VII-24 for each time period that data were available. The calculated heat flux, based on the temperature data in figure VII-23 and thermal conductivity from figure VII-13, is shown in figure VII-25.

The fuel tank upper dome had only two skin temperature sensors on each side of the wall, therefore, only rough estimates can be made as to the wall temperature difference during the orbital period. The available internal and external upper dome temperature data are plotted in figure VII-26. Using this temperature data the upper dome heat flux was calculated and is shown in figure VII-27.

C. COMPARISON OF CALCULATION METHODS

A comparison of the total liquid hydrogen orbital heating rates calculated from the change in fluid properties and from the tank wall temperature difference are shown in figure VII-28. It can be seen from this figure that the heating rate calculated from the change in fluid properties is approximately 50 percent greater than that from the measured wall temperature difference. This large difference in calculated liquid heating rates can be explained only if the effective thermal conductivity of the sidewall is actually greater than that employed in the temperature difference calculation (see figure VII-13). Other factors such as measurement errors, calculation of wetted sidewall

area, estimations of heat losses through secondary sources, and heat transfer between the ullage gas and liquid could have caused some difference in the results. However, the maximum estimated errors that could be introduced from these factors could not account for the differences obtained from the two methods of calculations.

By assuming that the liquid heating calculated from the continuous vent flow is correct, an effective wall thermal conductivity may be calculated. By subtracting the secondary heating rates (common bulkhead, flange joint, etc.) shown on figure VII-22 from the total heating rate given in figure VII-2, the heating rate through the aft dome and the wetted sidewall was determined. Since the maximum and minimum orbital heating rates calculated from continuous vent data occur approximately 600 seconds later than the maximum and minimum wall temperature differences (see figures VII-9, VII-12, and VII-28), it was necessary to adjust the continuous vent data by 600 seconds to correspond to the wall temperature data (this 600 seconds is the thermal lag and includes the time between the heat addition to the tank and its discharge overboard through the CV system). Using these calculated heating rates and the prevailing wall temperature differences from figures VII-9, VII-12, and VII-18 together with the calculated wetted sidewall areas (figure VII-20), the effective wall thermal conductivity was determined. The values of effective thermal conductivity obtained in this manner are shown on figure VII-29. Also shown on this figure are the thermal conductivities of gaseous parahydrogen and gaseous helium, and the range of effective thermal conductivity of the internal insulation as determined from DAC's 8 ft scale tank and Banjo tests (reference 16). Such factors as cracking of insulation, absorption of gaseous hydrogen or gaseous helium by the insulation material, unaccounted for tank penetration, and effects of insulation bonding and filler materials could have caused the effective thermal conductivity of the sidewall to be greater than expected based on the 8 ft scale and Banjo tests data.

The total ullage gas heating rate based on wall temperature differences was calculated using the heat flux of the upper dome and dry sidewall (figures VII-25 and VII-27, respectively) along with the dry sidewall area determined from figure VII-20. The total ullage heating rate calculated by both the wall temperature differences and change in fluid properties methods are shown in figure VII-30. Because of the small number of skin temperature sensors on the upper portion of the fuel tank and the suspected large axial temperature gradient along the sidewall, the heating rates claculated by the wall temperature difference method have questionable accuracy. The total ullage heating rates calculated from continuous vent data during the first two orbits are felt to be more accurate than the heating rates claculated by the change in fluid properties during the third and fourth orbits. However, all heating rates calculated from the continuous vent data are felt to be more reliable than the heating rates calculated by the wall temperature difference method.

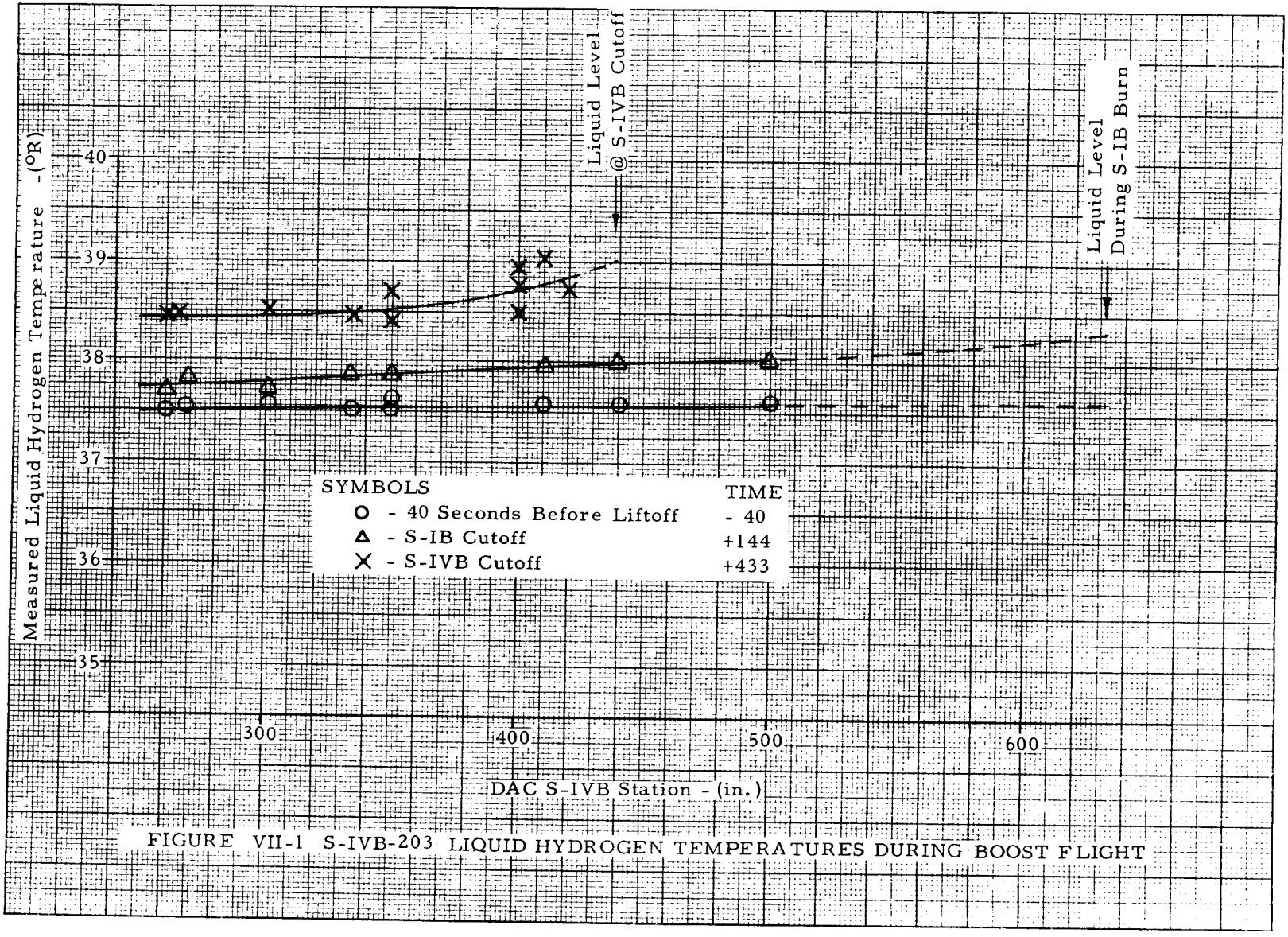

FIGURE VII-1 S-IVB-203 LIQUID HYDROGEN TEMPERATURES DURING BOOST FLIGHT

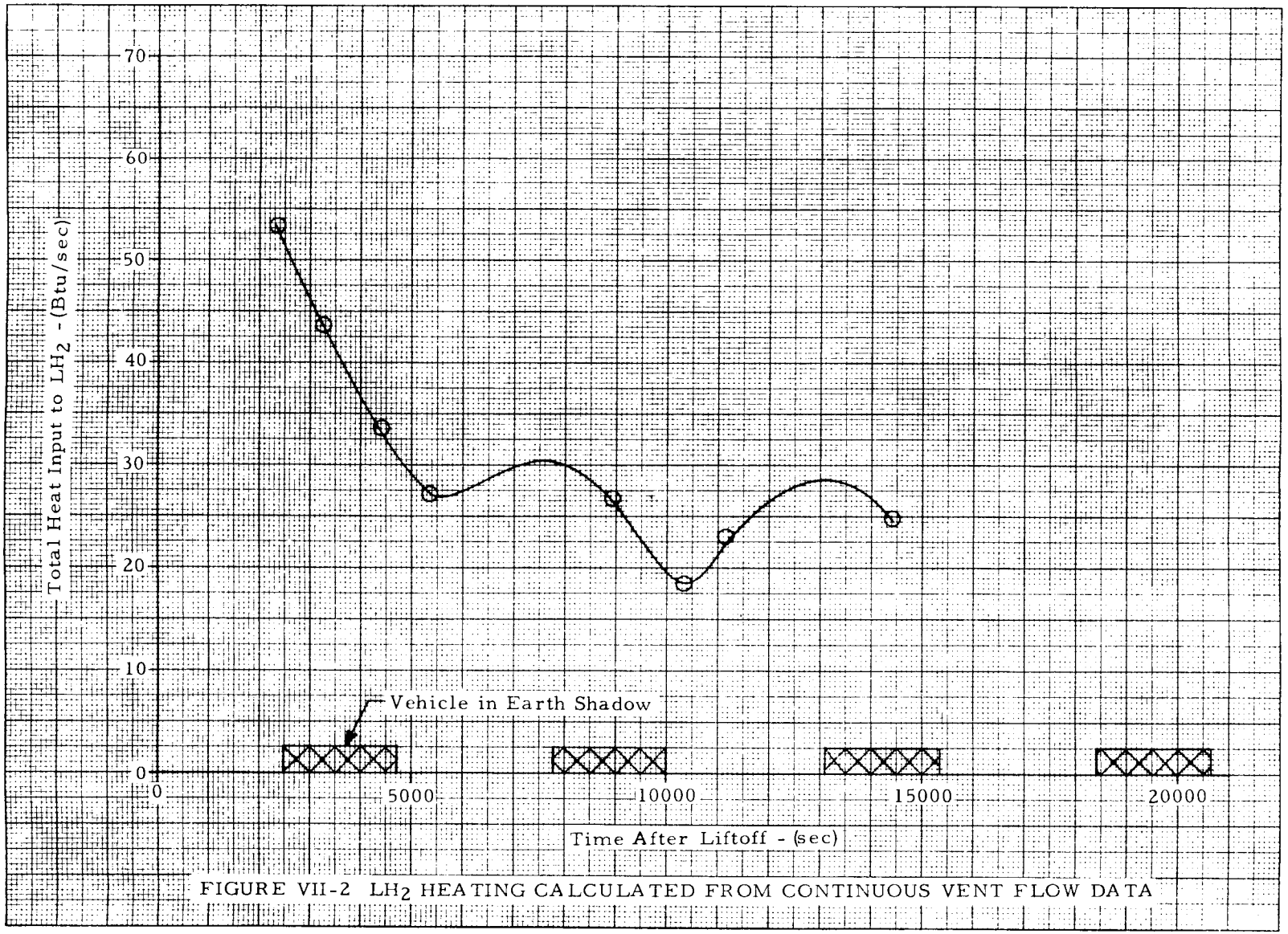

FIGURE VII-2 LH_2 HEATING CALCULATED FROM CONTINUOUS VENT FLOW DATA

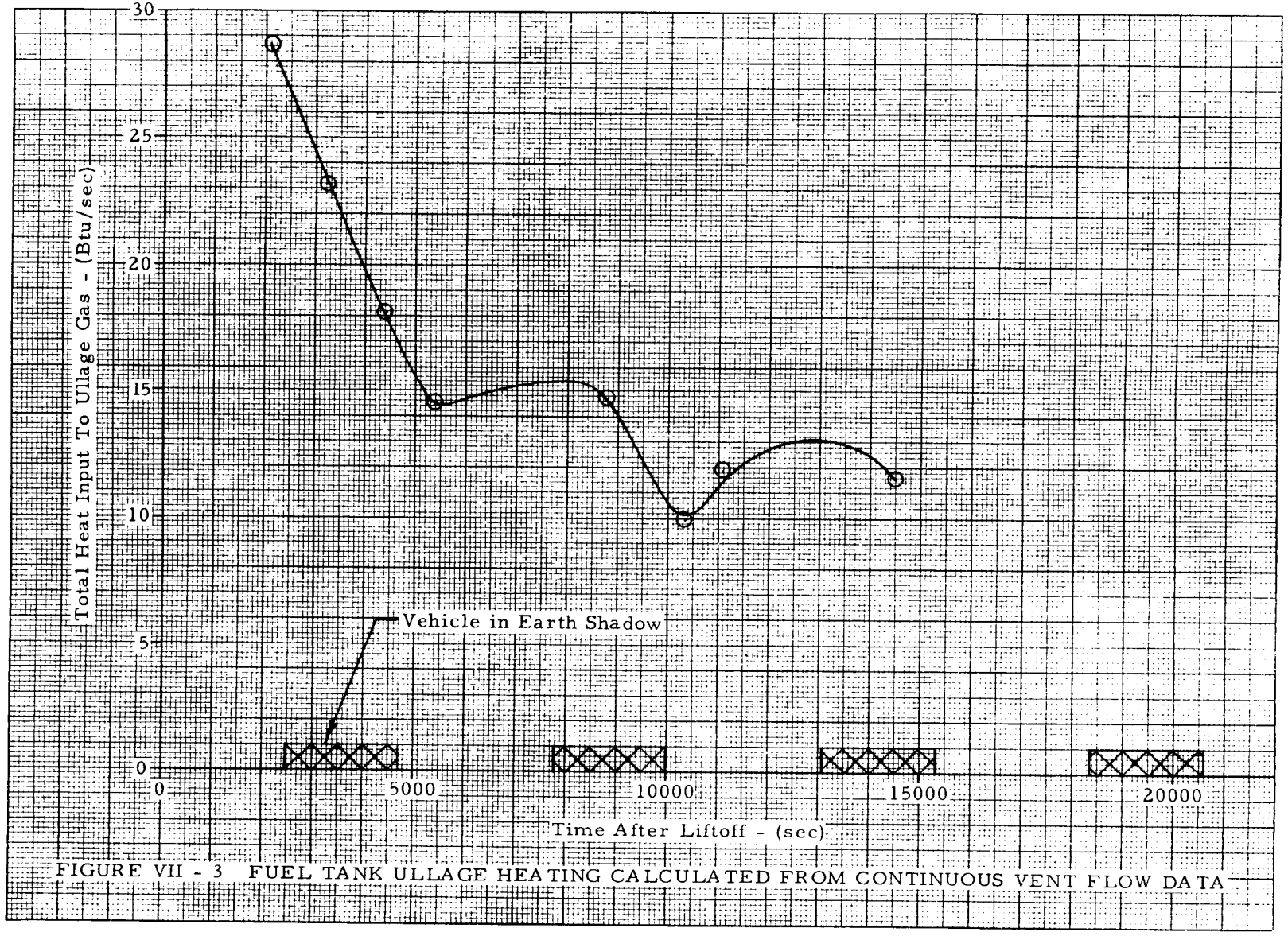

FIGURE VII - 3 FUEL TANK ULLAGE HEATING CALCULATED FROM CONTINUOUS VENT FLOW DATA

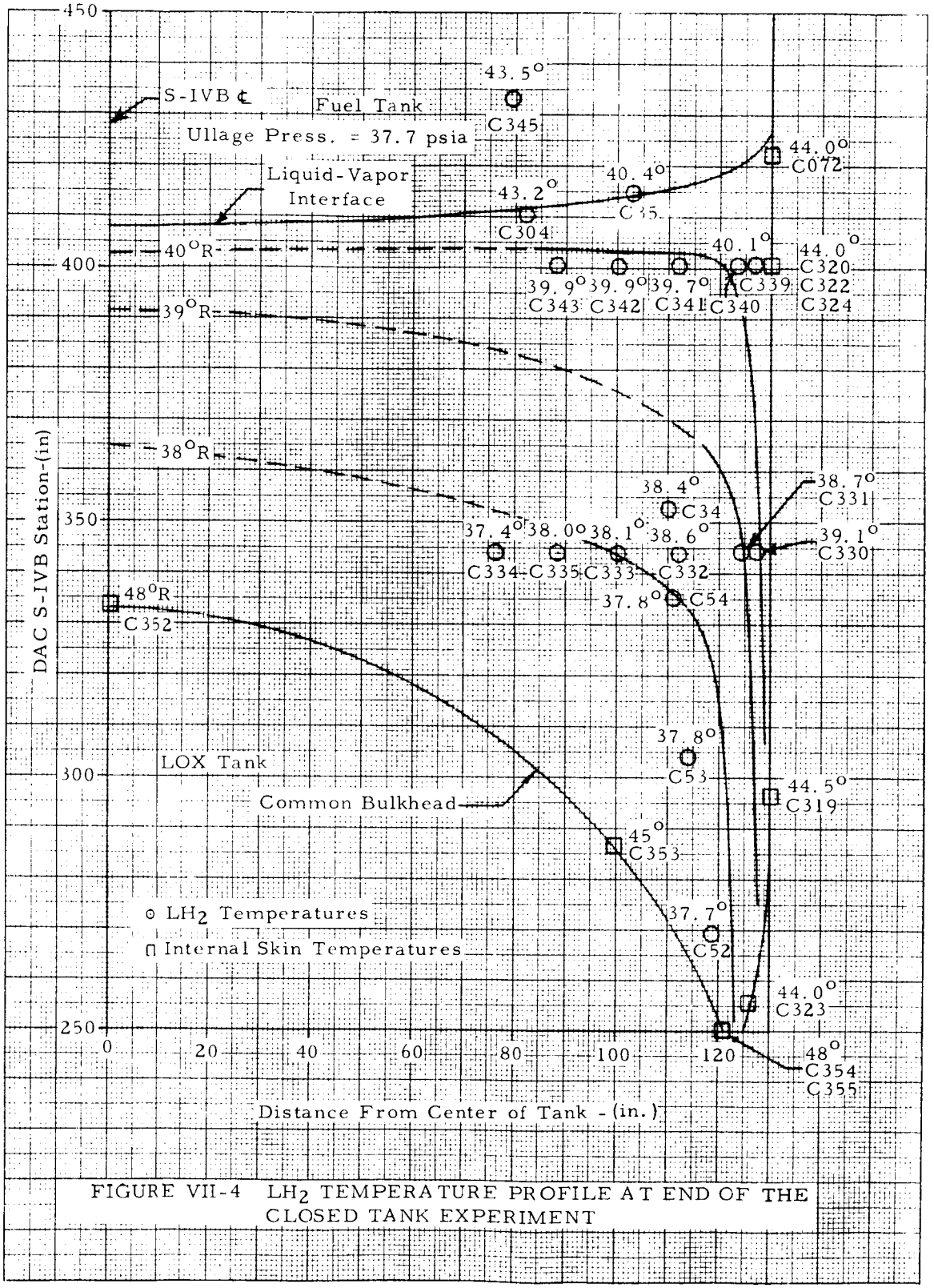

FIGURE VII-4 LH_2 TEMPERATURE PROFILE AT END OF THE CLOSED TANK EXPERIMENT

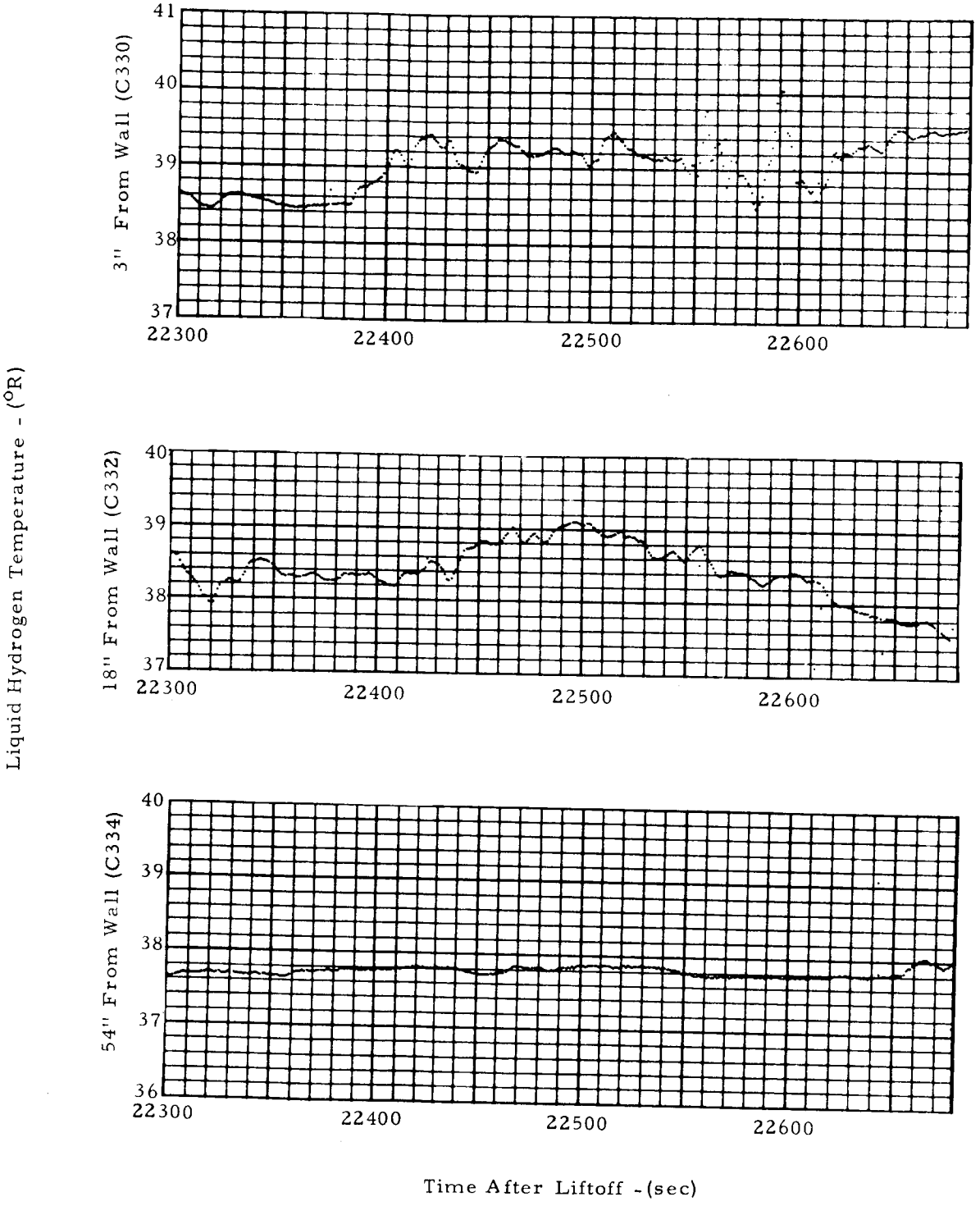

FIGURE VII - 5 TYPICAL LH_2 BOUNDARY LAYER TEMPERATURE MEASUREMENTS AT END OF CLOSED TANK EXPERIMENT

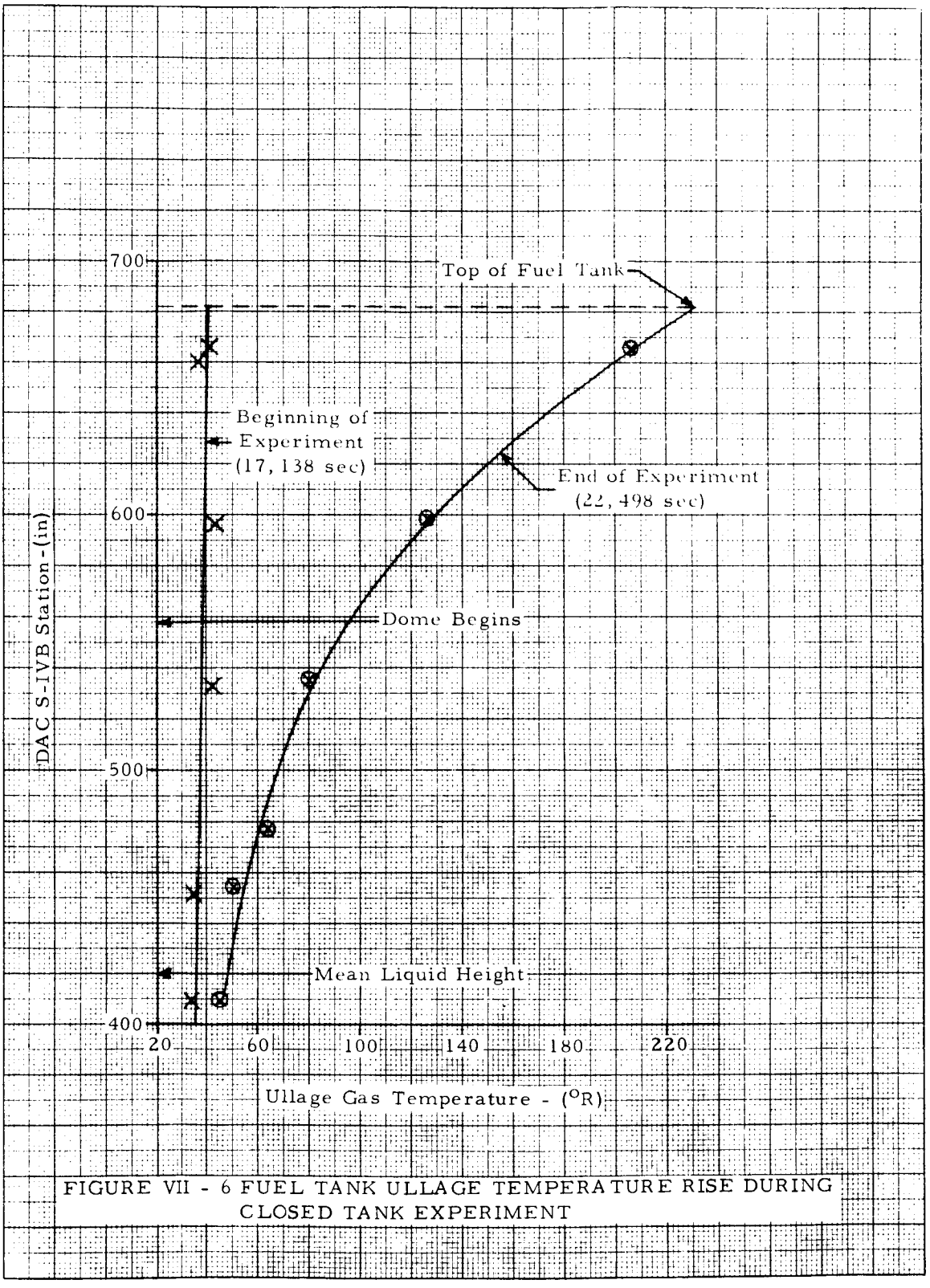

FIGURE VII - 6 FUEL TANK ULLAGE TEMPERATURE RISE DURING CLOSED TANK EXPERIMENT

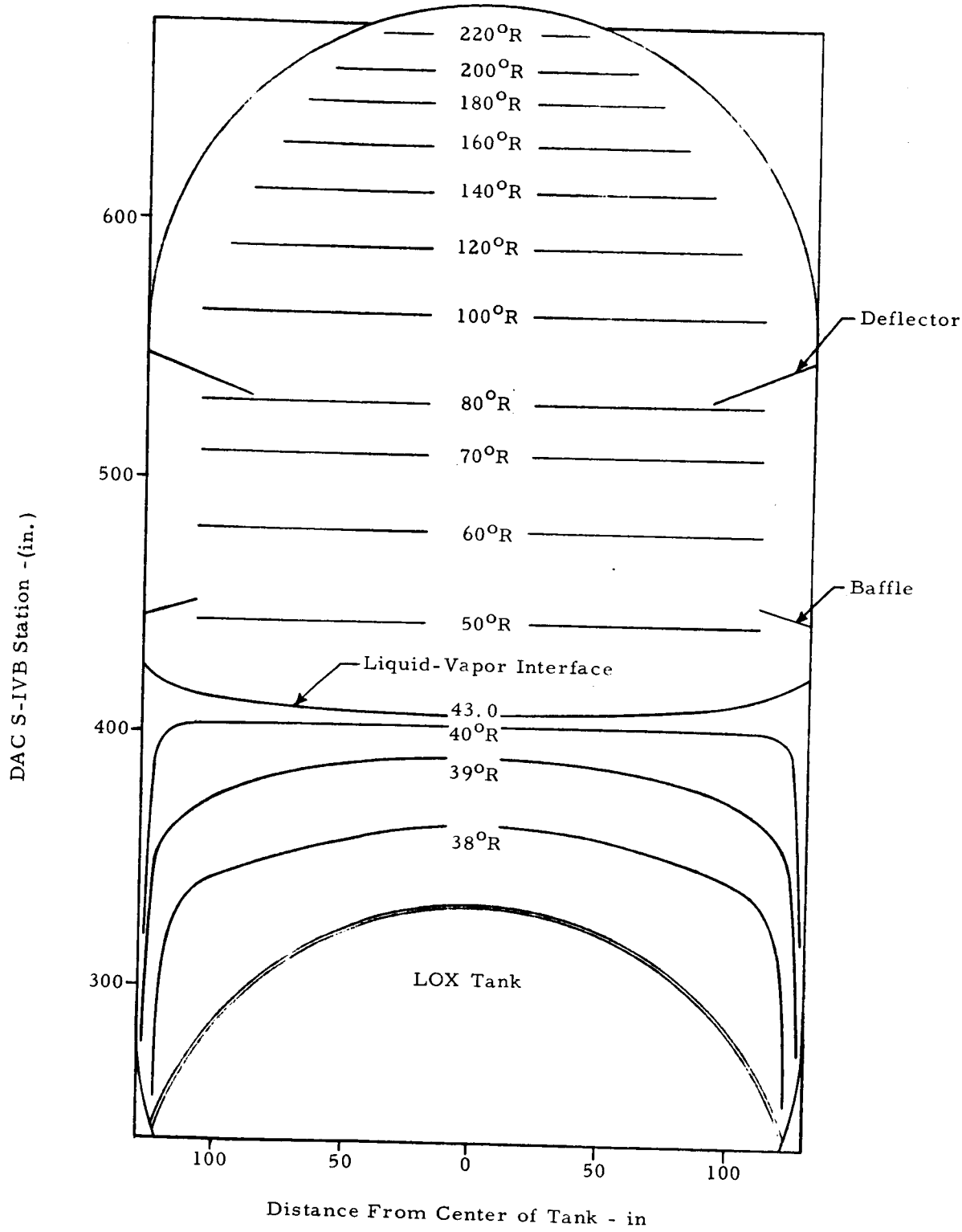

FIGURE VII-7 S-IVB FUEL TANK TEMPERATURE MAP AT END OF CLOSED TANK EXPERIMENT

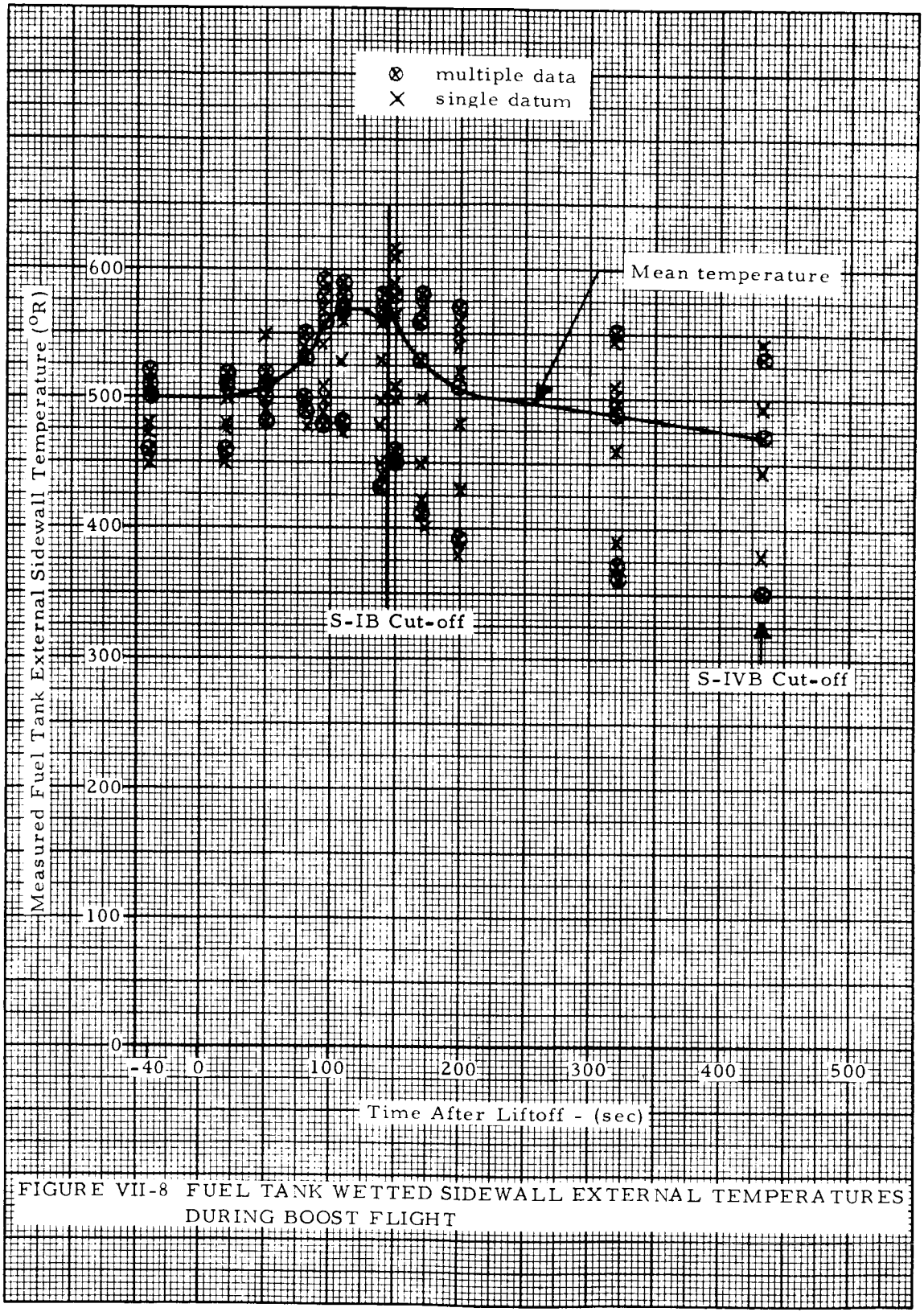

FIGURE VII-8 FUEL TANK WETTED SIDEWALL EXTERNAL TEMPERATURES DURING BOOST FLIGHT

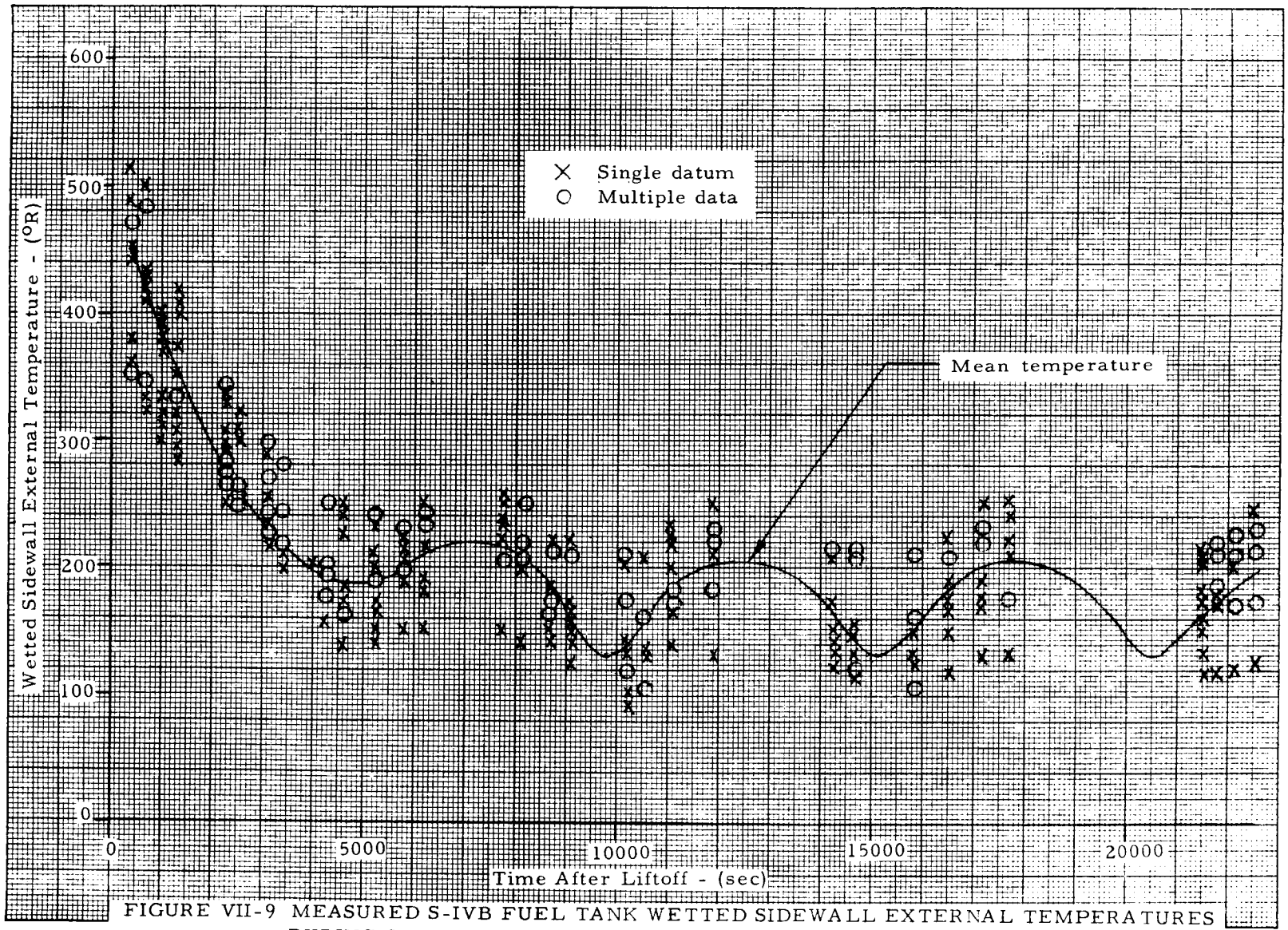

FIGURE VII-9 MEASURED S-IVB FUEL TANK WETTED SIDEWALL EXTERNAL TEMPERATURES DURING ORBITAL FLIGHT

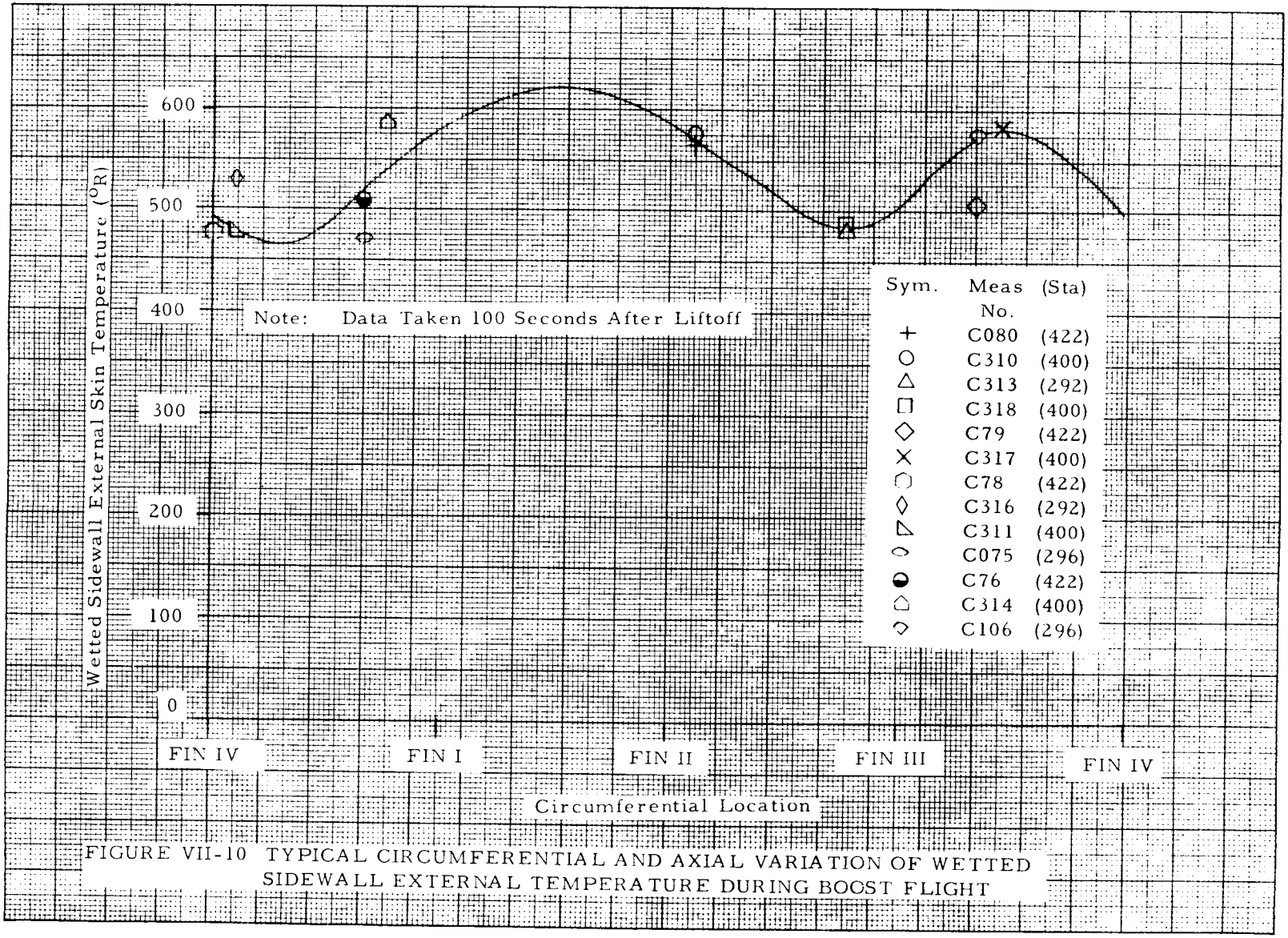

FIGURE VII-10 TYPICAL CIRCUMFERENTIAL AND AXIAL VARIATION OF WETTED SIDEWALL EXTERNAL TEMPERATURE DURING BOOST FLIGHT

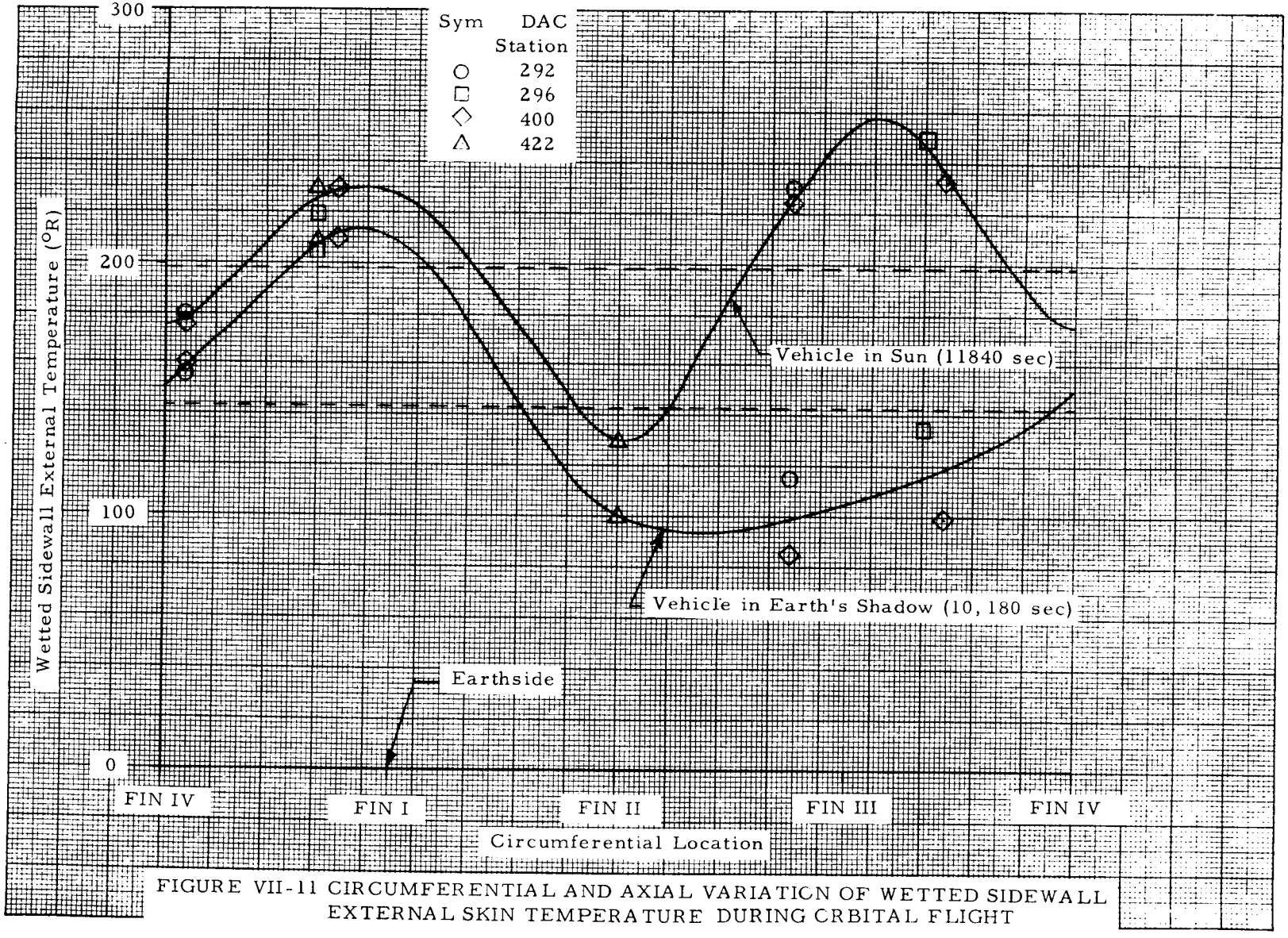

FIGURE VII-11 CIRCUMFERENTIAL AND AXIAL VARIATION OF WETTED SIDEWALL EXTERNAL SKIN TEMPERATURE DURING ORBITAL FLIGHT

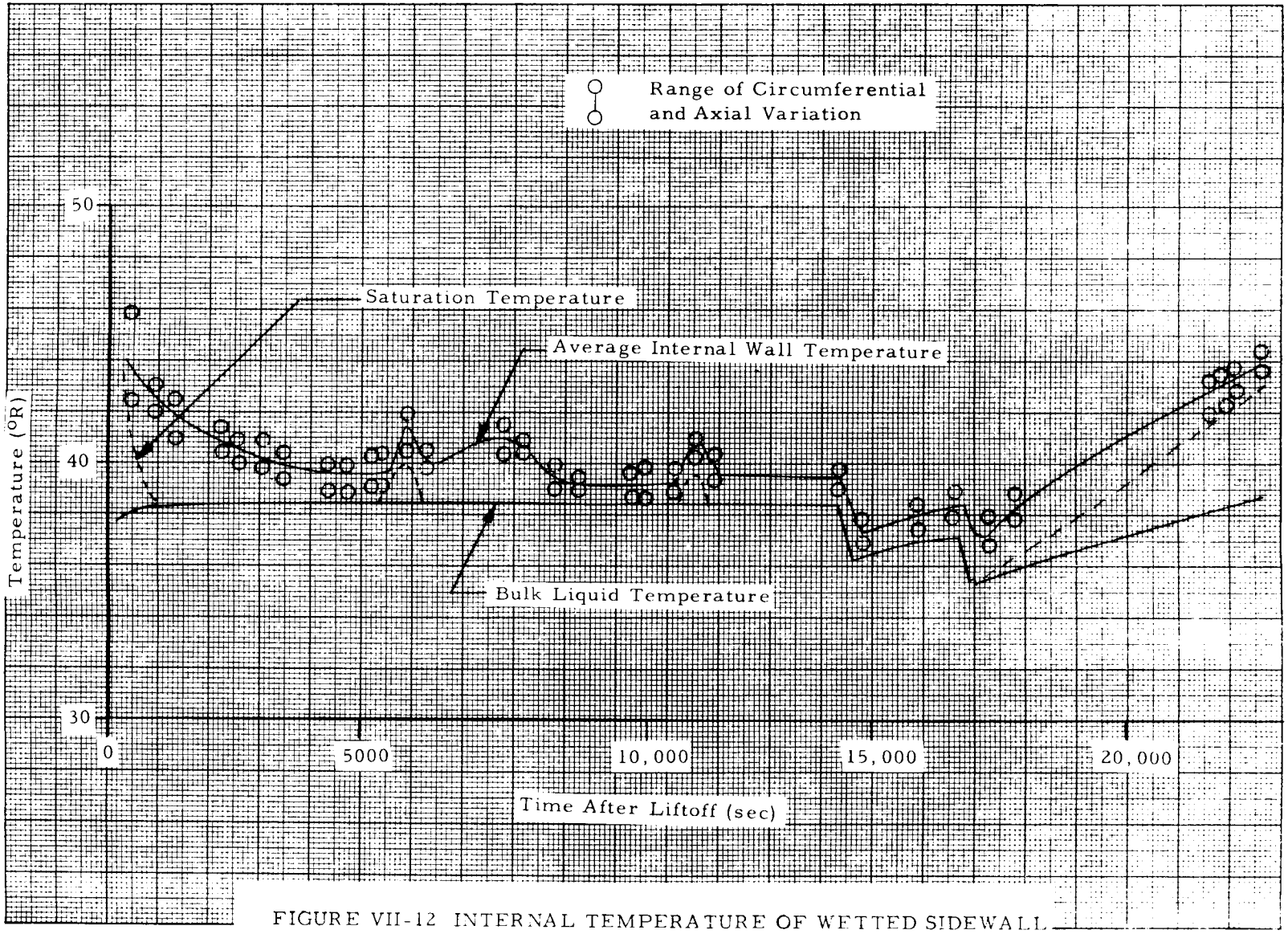

FIGURE VII-12 INTERNAL TEMPERATURE OF WETTED SIDEWALL

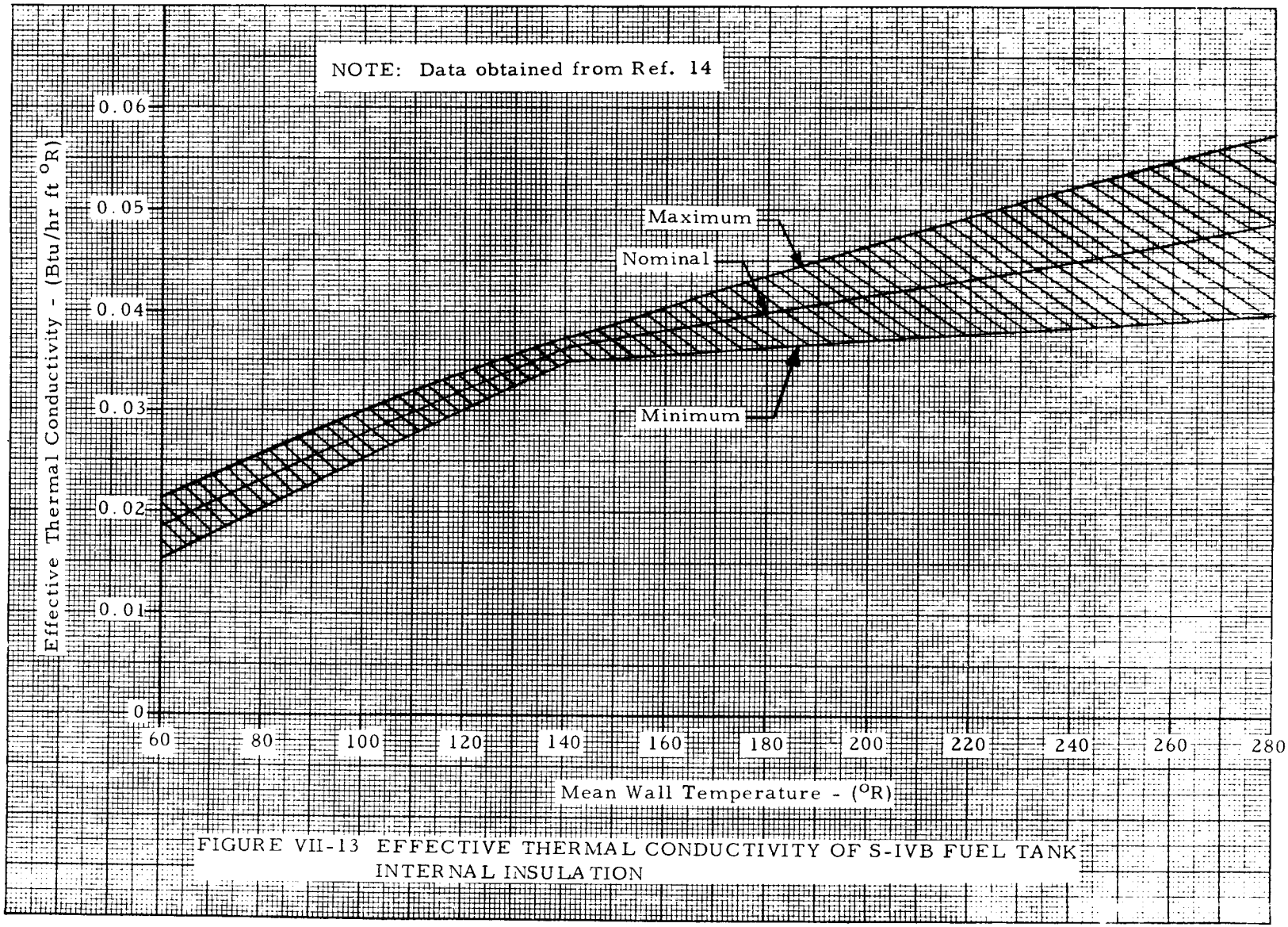

FIGURE VII-13 EFFECTIVE THERMAL CONDUCTIVITY OF S-IVB FUEL TANK INTERNAL INSULATION

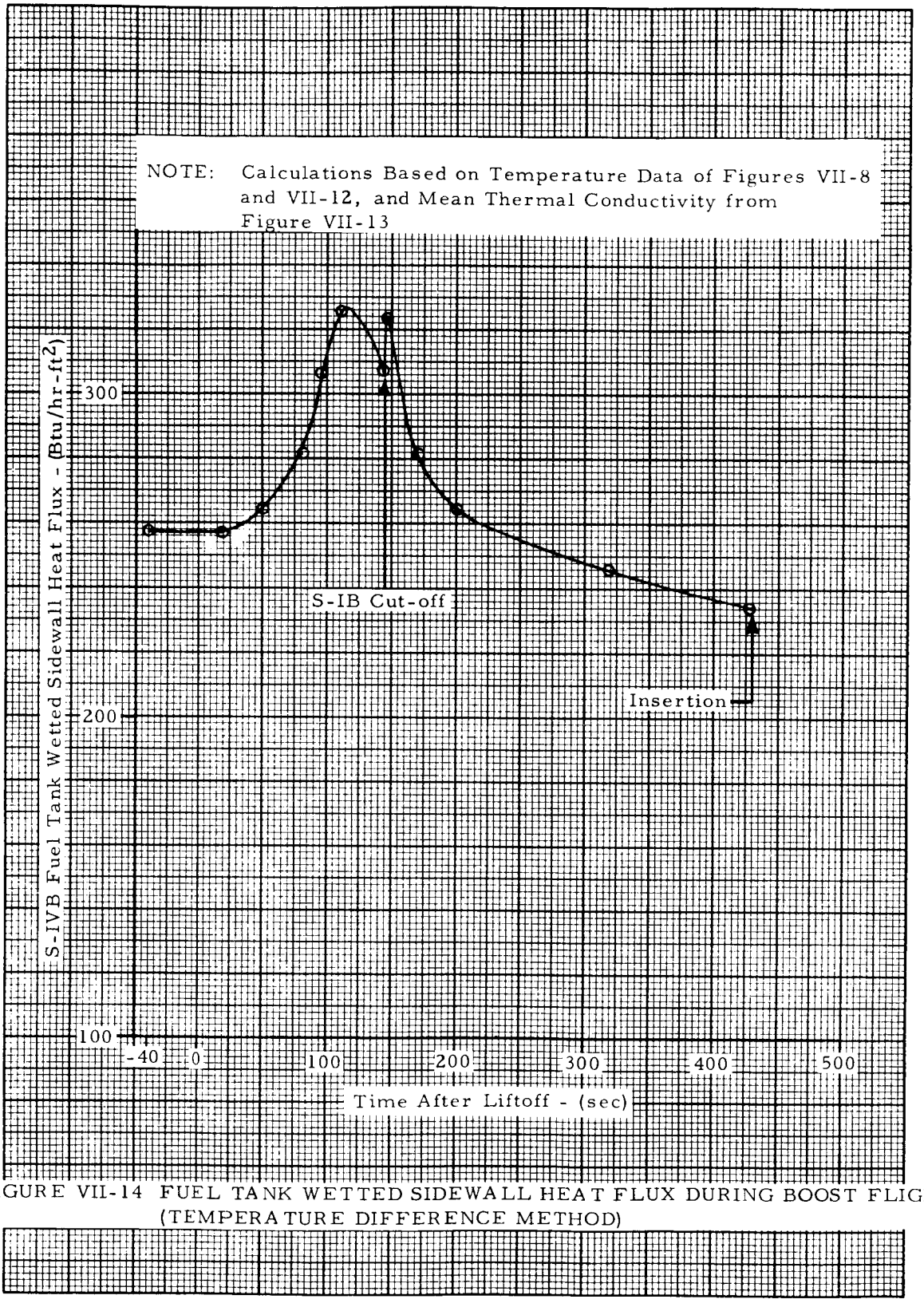

FIGURE VII-14 FUEL TANK WETTED SIDEWALL HEAT FLUX DURING BOOST FLIGHT (TEMPERATURE DIFFERENCE METHOD)

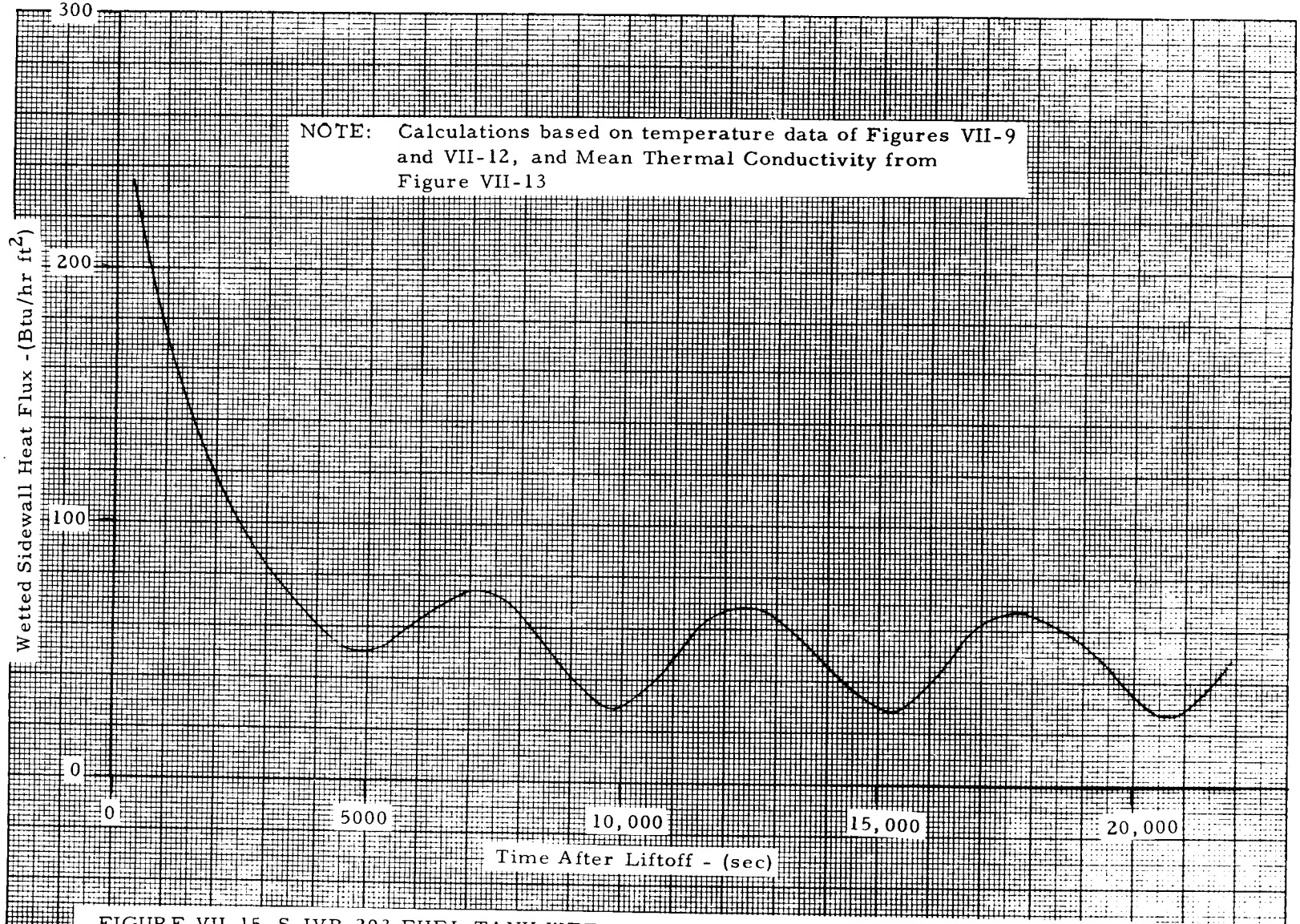

FIGURE VII-15 S-IVB-203 FUEL TANK WETTED SIDEWALL HEAT FLUX DURING ORBITAL PERIOD

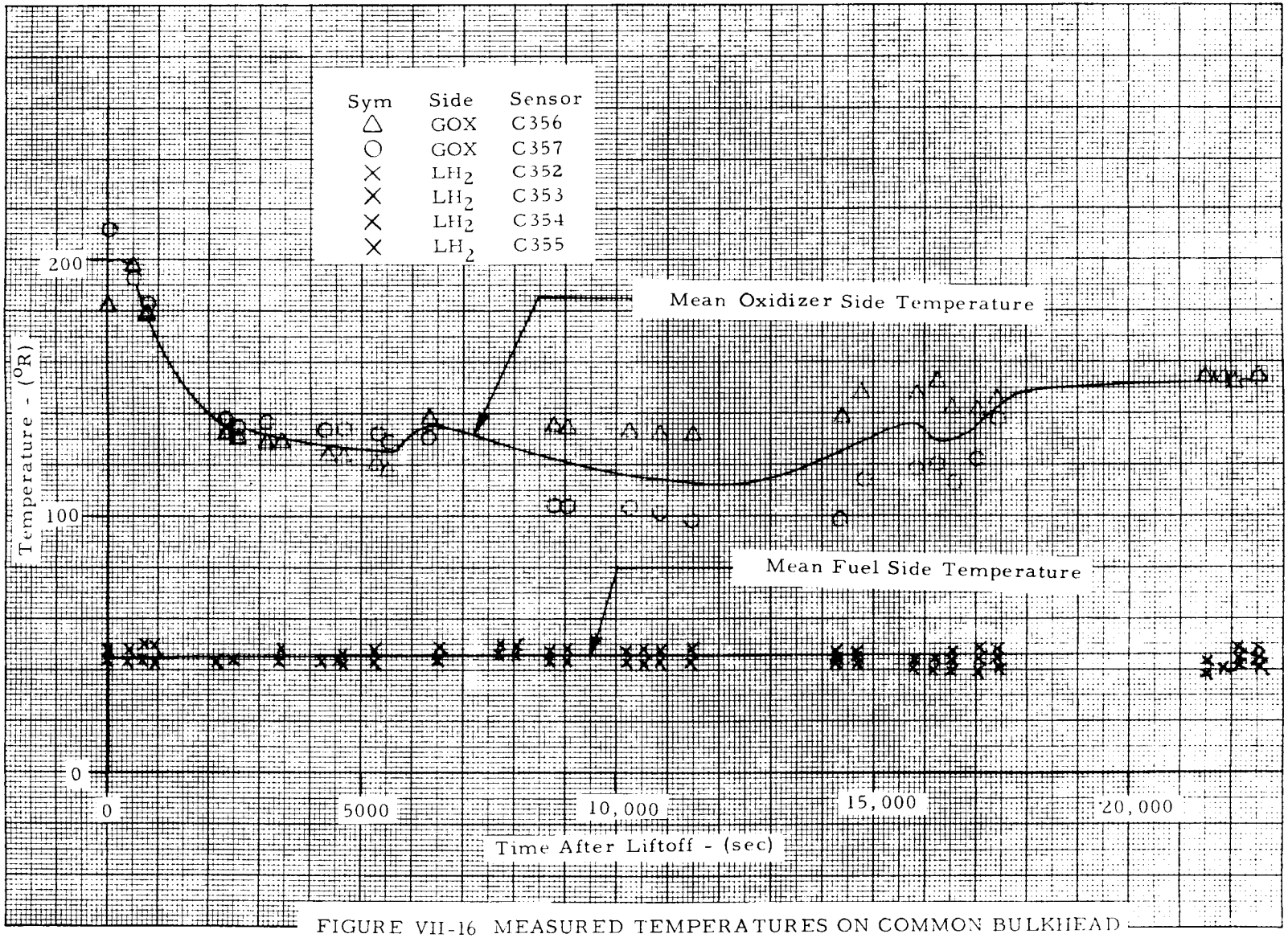

FIGURE VII-16 MEASURED TEMPERATURES ON COMMON BULKHEAD

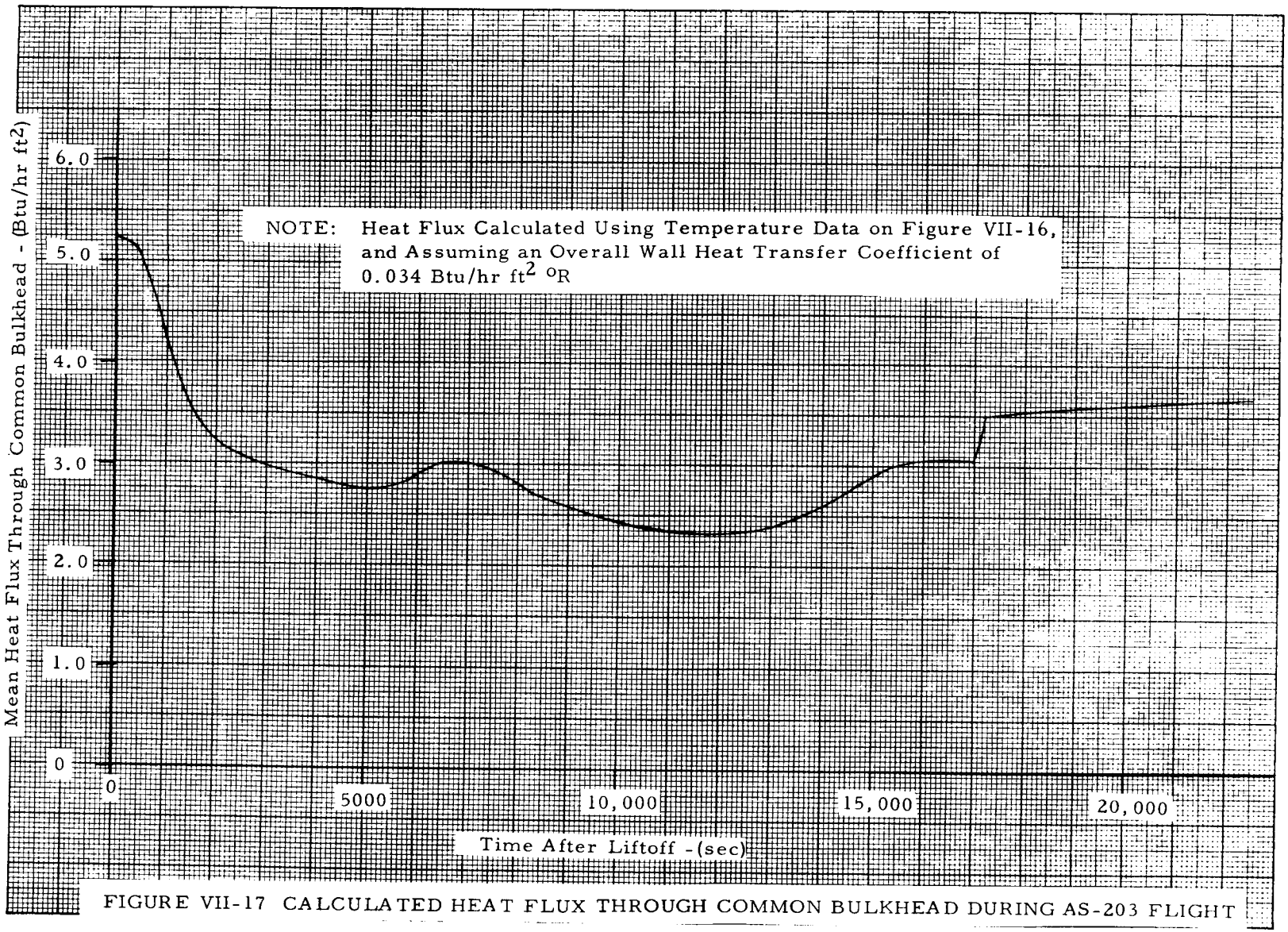

FIGURE VII-17 CALCULATED HEAT FLUX THROUGH COMMON BULKHEAD DURING AS-203 FLIGHT

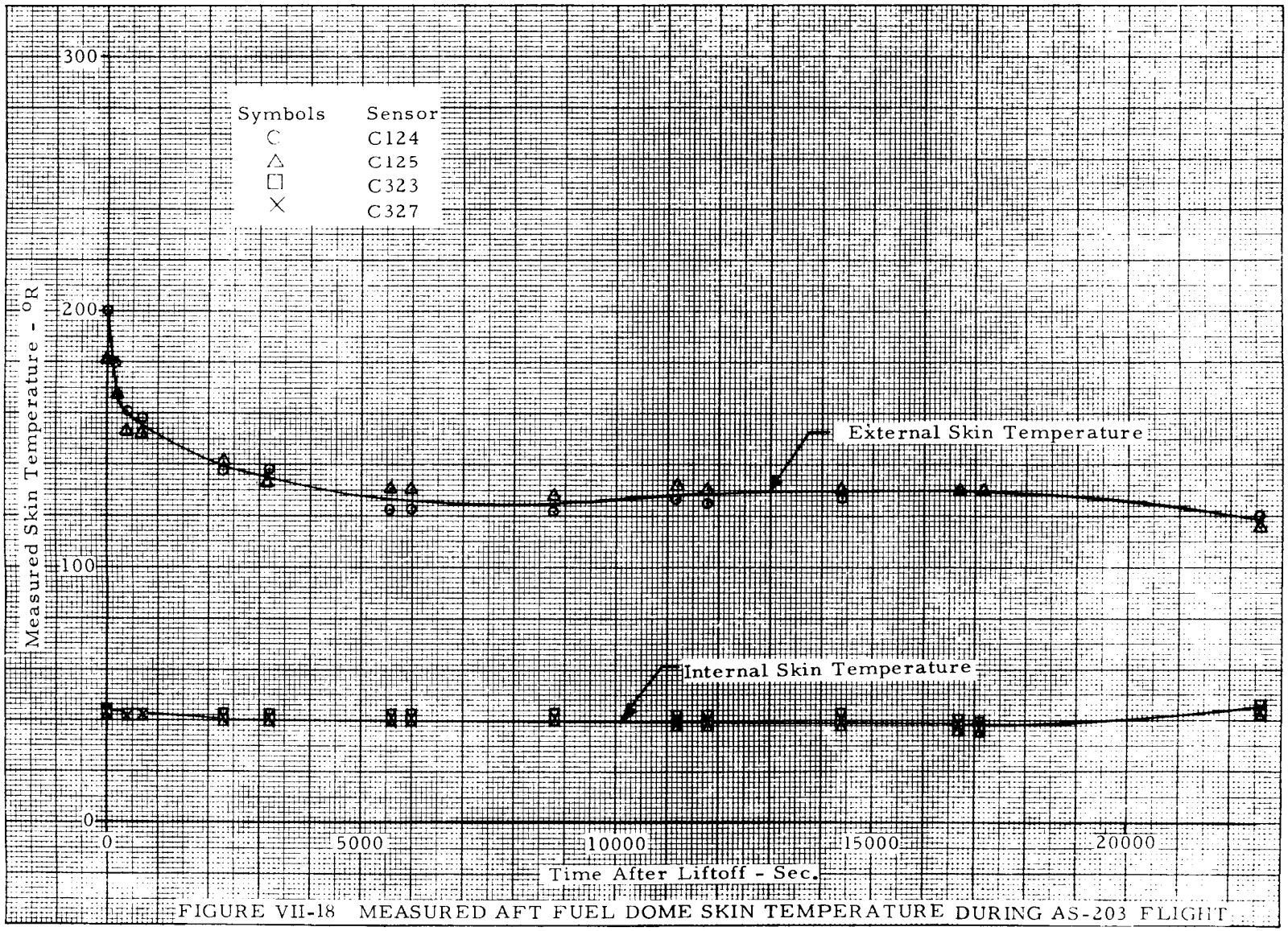

FIGURE VII-18 MEASURED AFT FUEL DOME SKIN TEMPERATURE DURING AS-203 FLIGHT

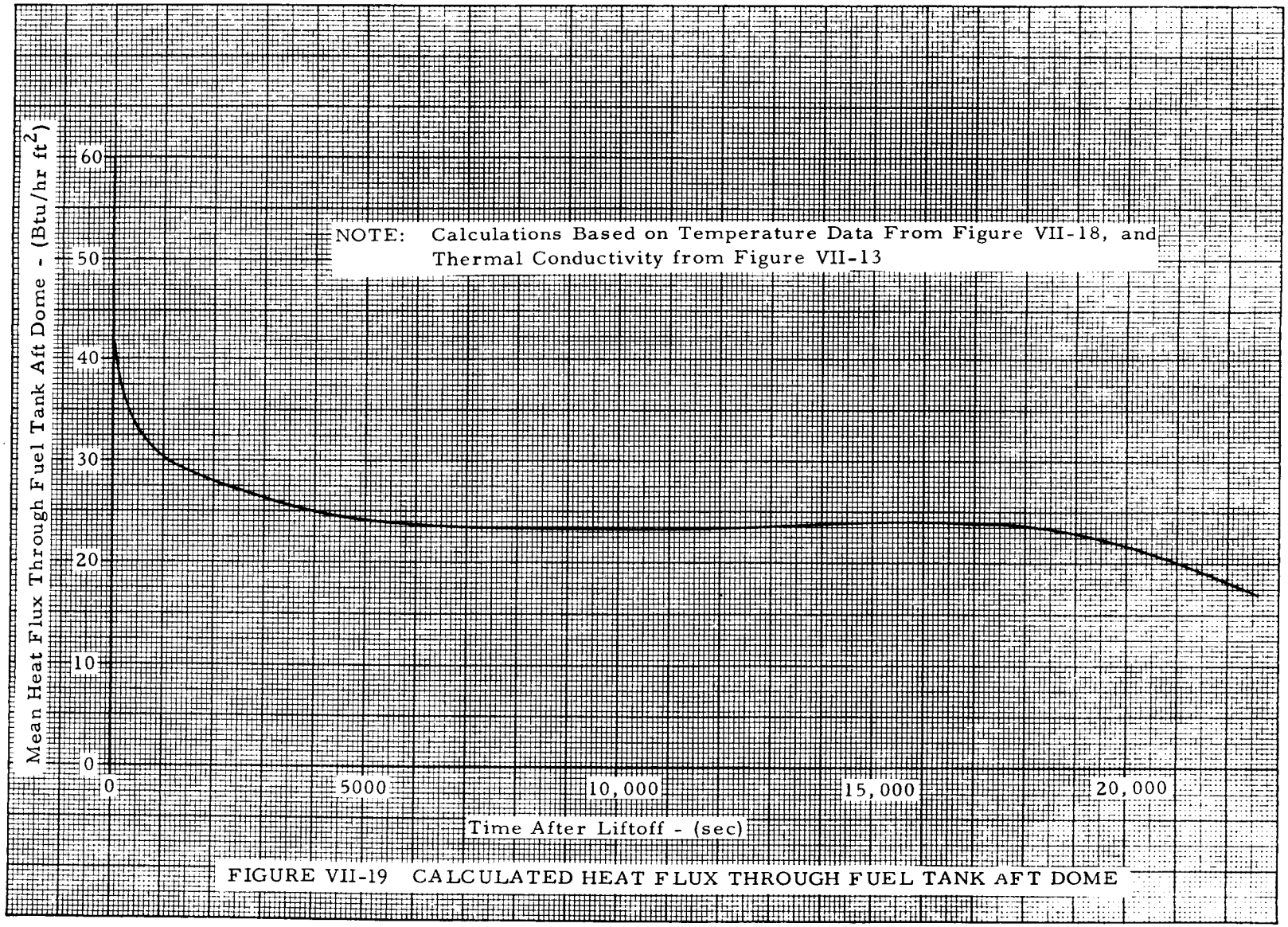

FIGURE VII-19 CALCULATED HEAT FLUX THROUGH FUEL TANK AFT DOME

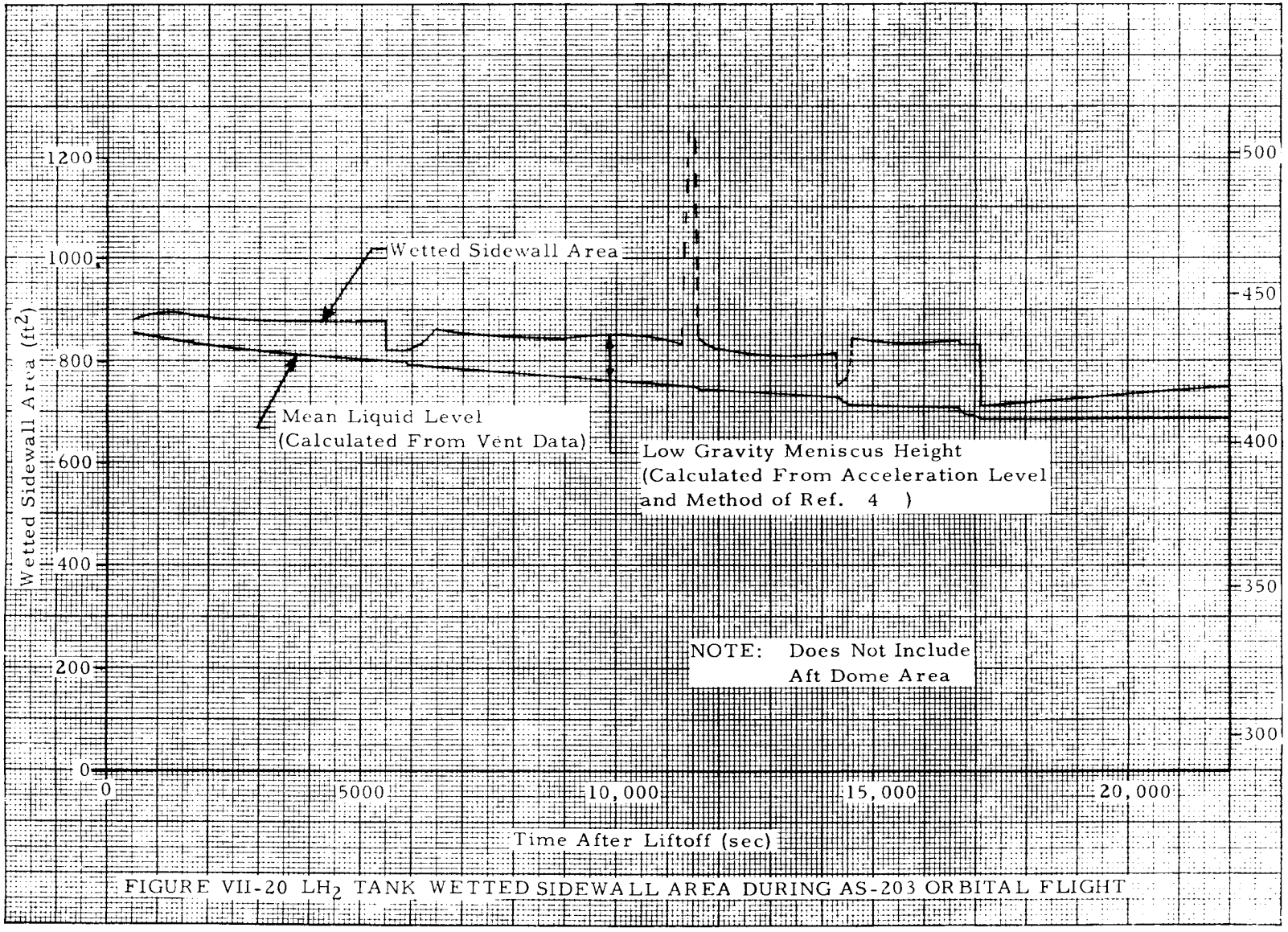

FIGURE VII-20 LH_2 TANK WETTED SIDEWALL AREA DURING AS-203 ORBITAL FLIGHT

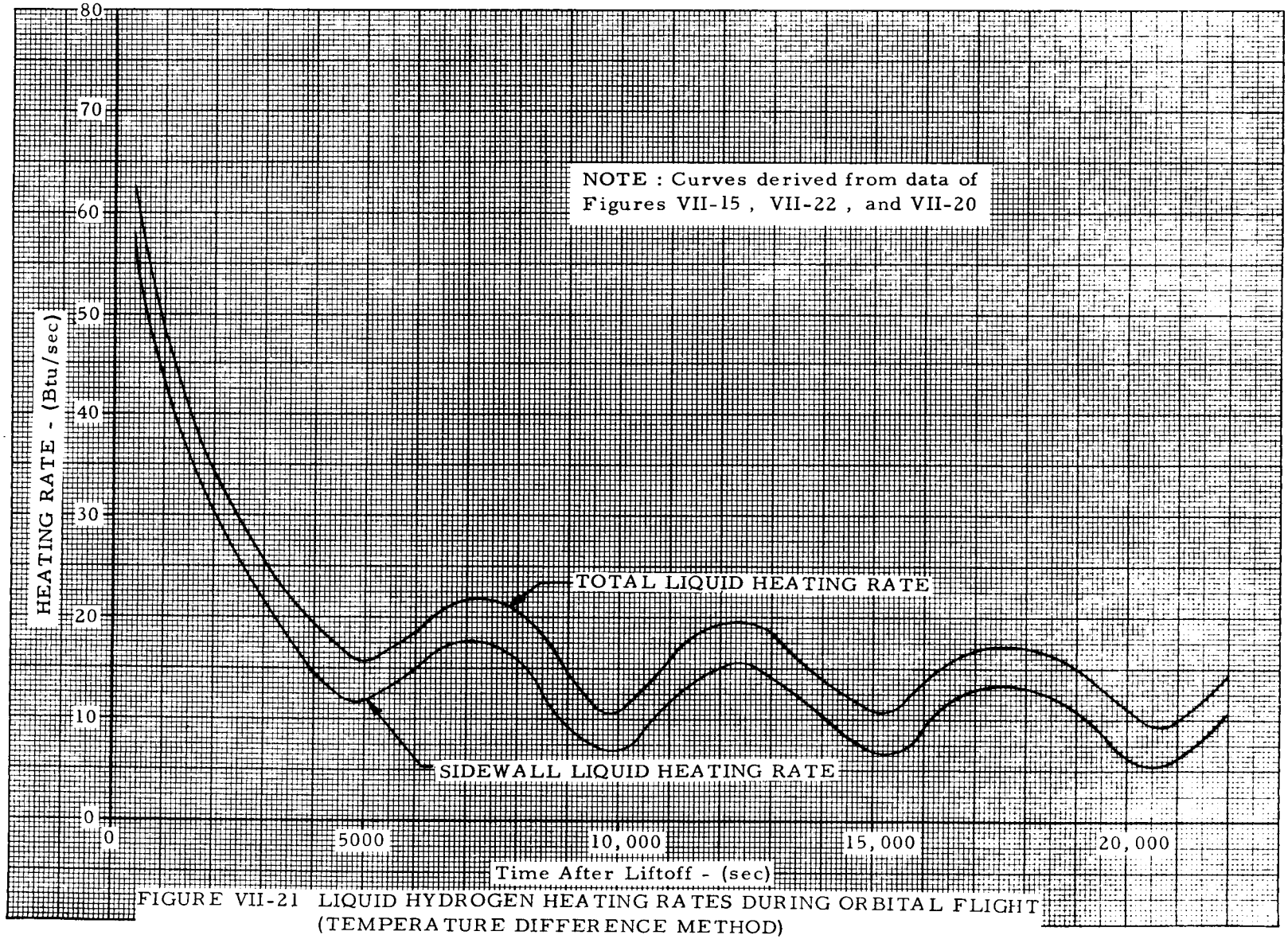

FIGURE VII-21 LIQUID HYDROGEN HEATING RATES DURING ORBITAL FLIGHT (TEMPERATURE DIFFERENCE METHOD)

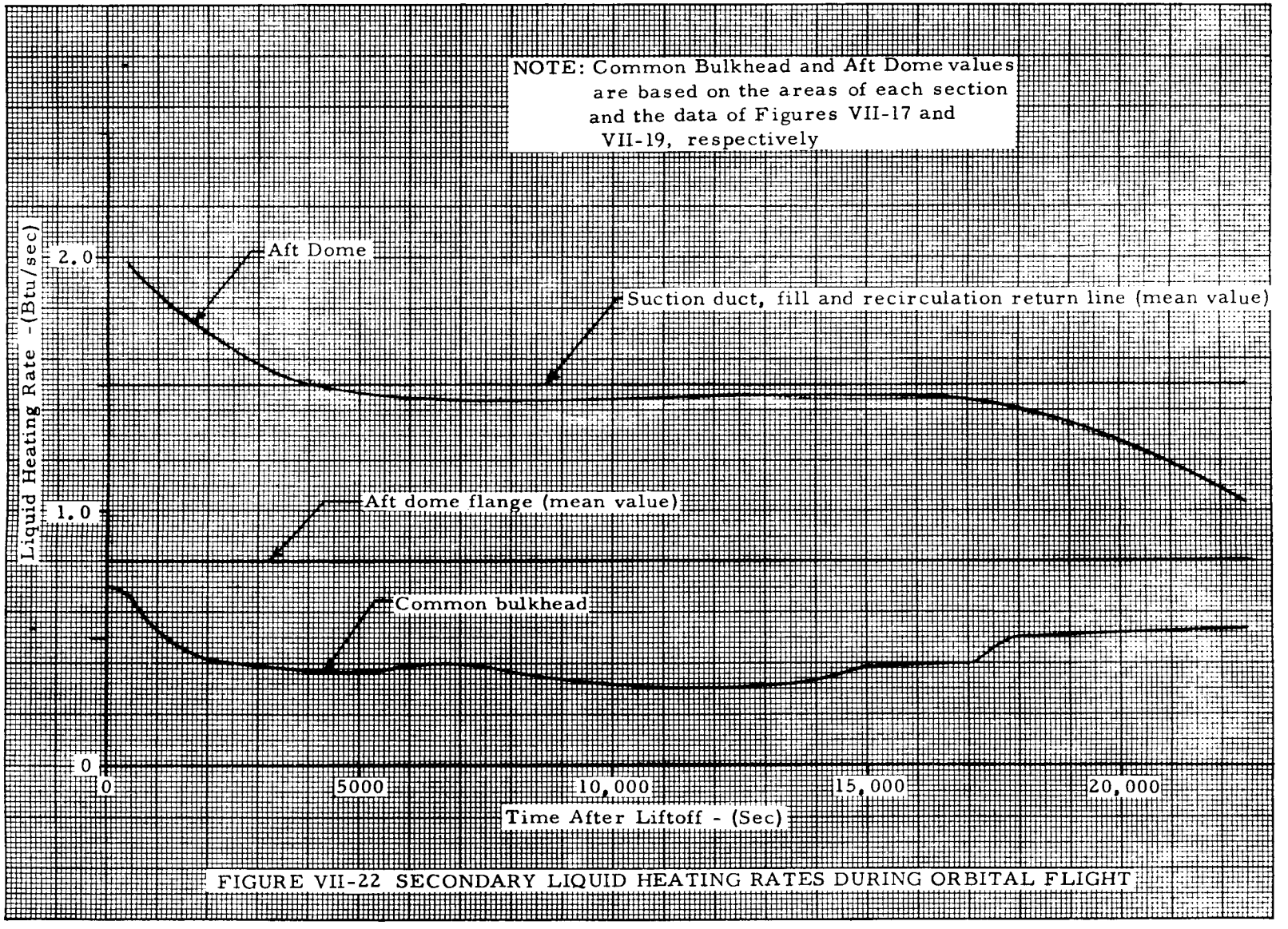

FIGURE VII-22 SECONDARY LIQUID HEATING RATES DURING ORBITAL FLIGHT

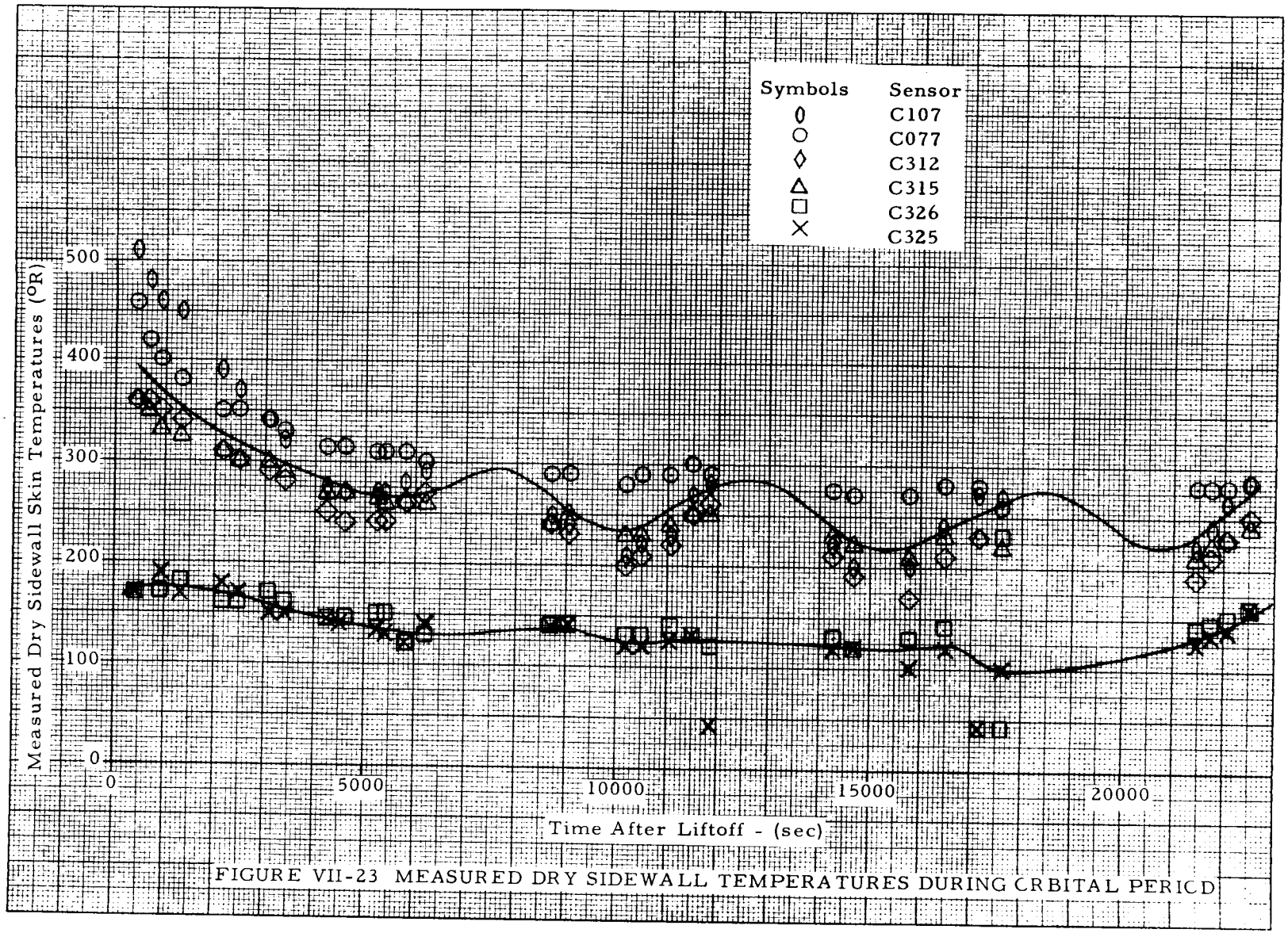

FIGURE VII-23 MEASURED DRY SIDEWALL TEMPERATURES DURING CRBITAL PERICD

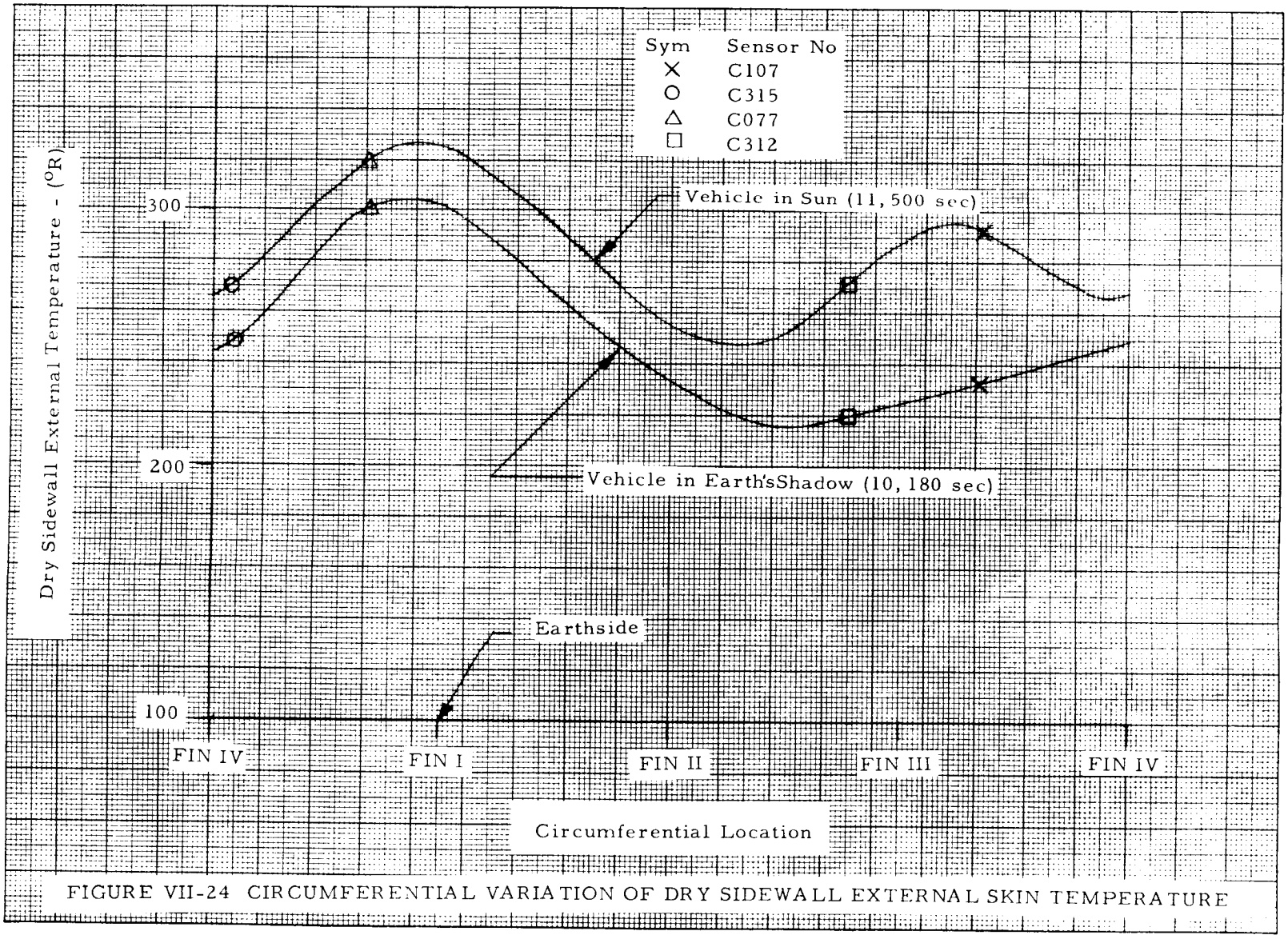

FIGURE VII-24 CIRCUMFERENTIAL VARIATION OF DRY SIDEWALL EXTERNAL SKIN TEMPERATURE

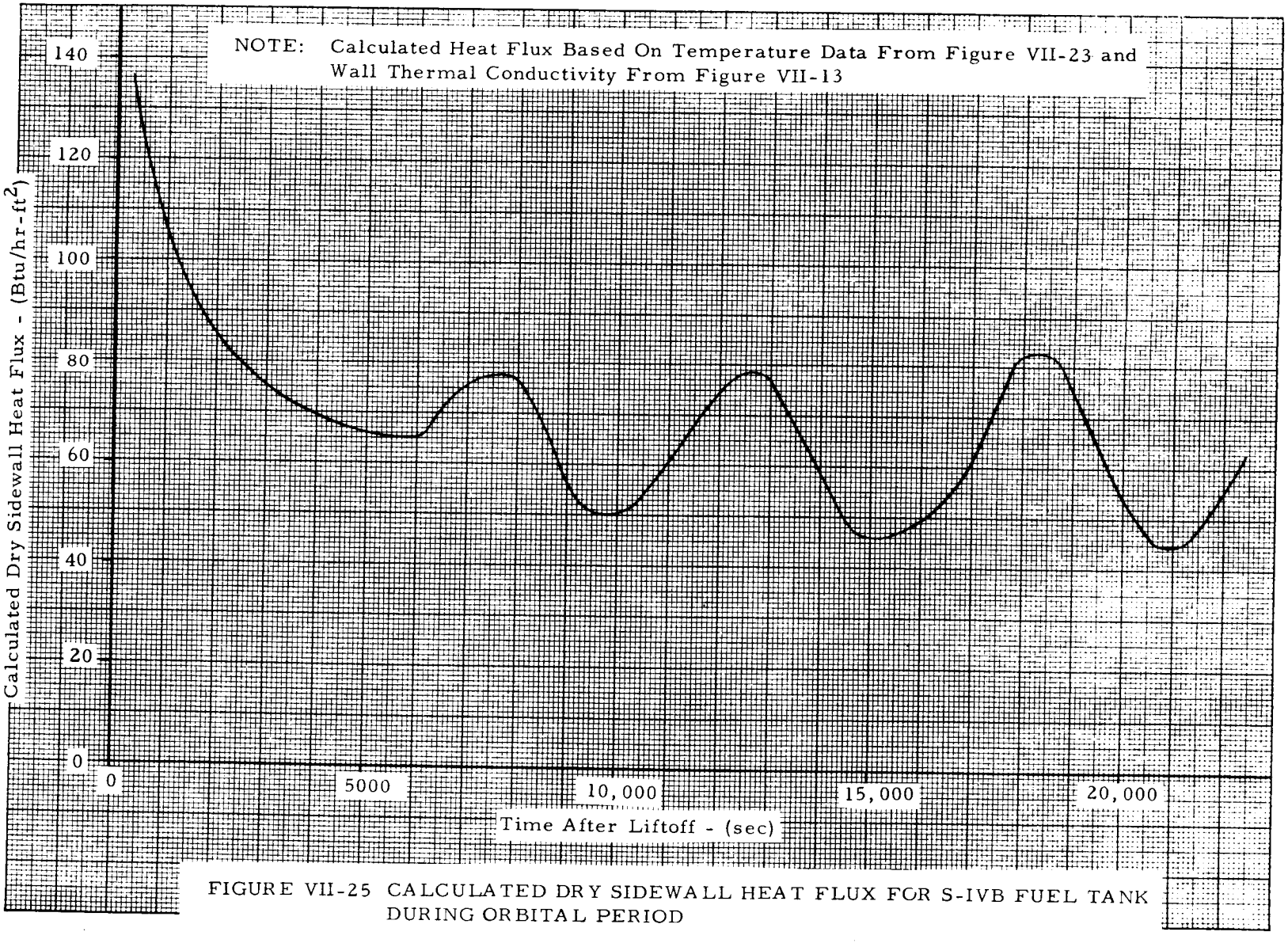

FIGURE VII-25 CALCULATED DRY SIDEWALL HEAT FLUX FOR S-IVB FUEL TANK DURING ORBITAL PERIOD

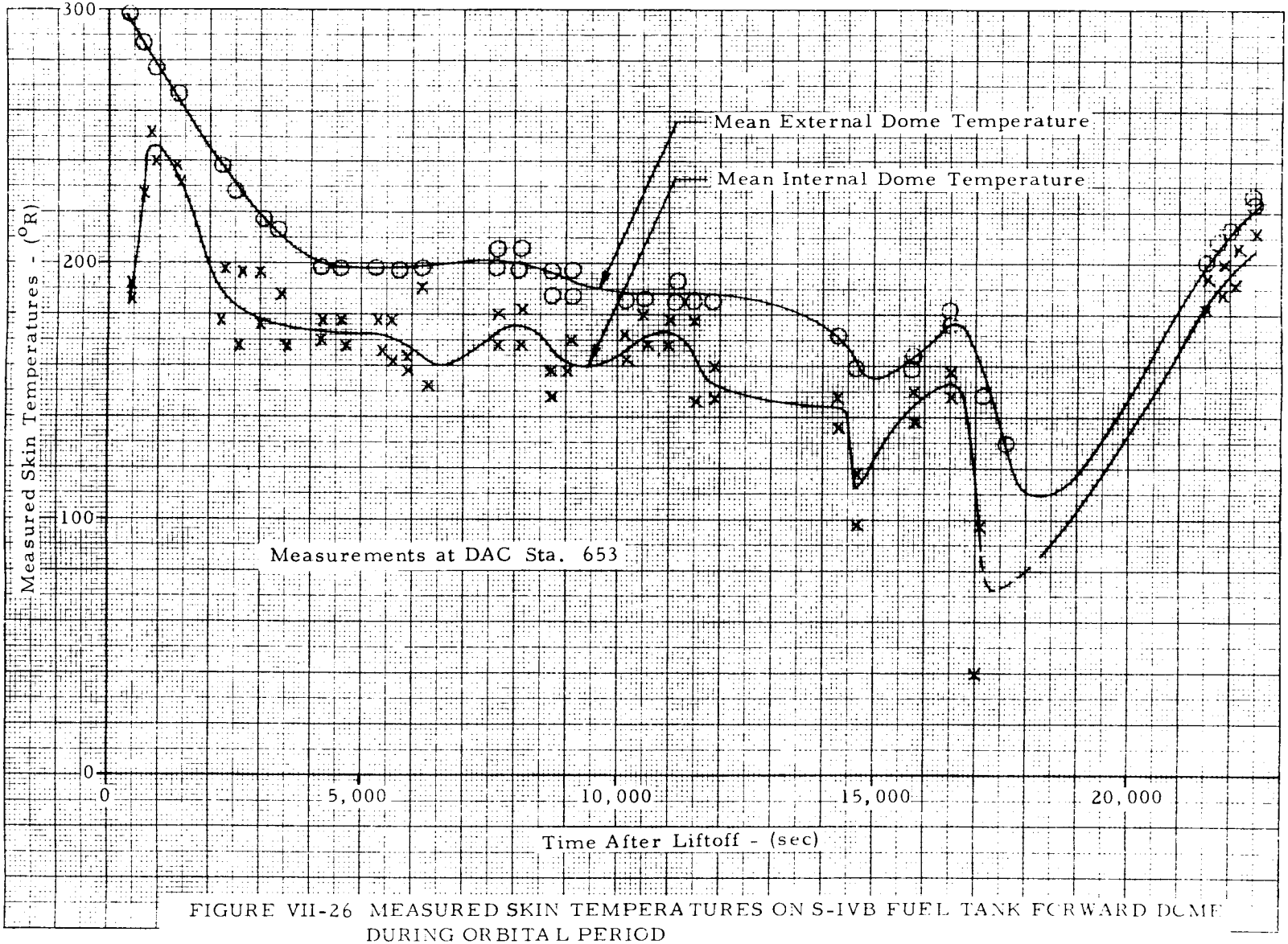

FIGURE VII-26 MEASURED SKIN TEMPERATURES ON S-IVB FUEL TANK FORWARD DOME DURING ORBITAL PERIOD

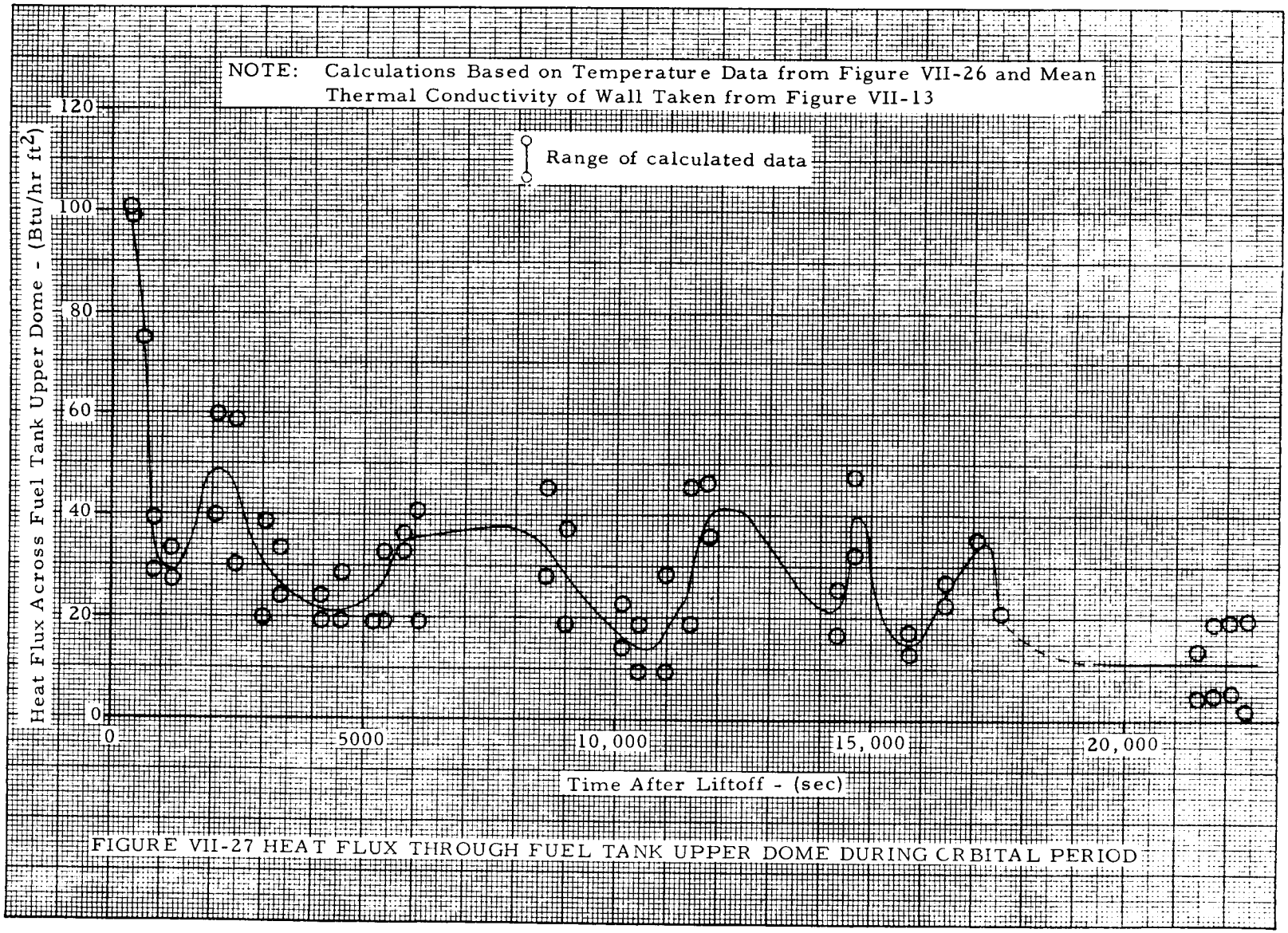

FIGURE VII-27 HEAT FLUX THROUGH FUEL TANK UPPER DOME DURING ORBITAL PERIOD

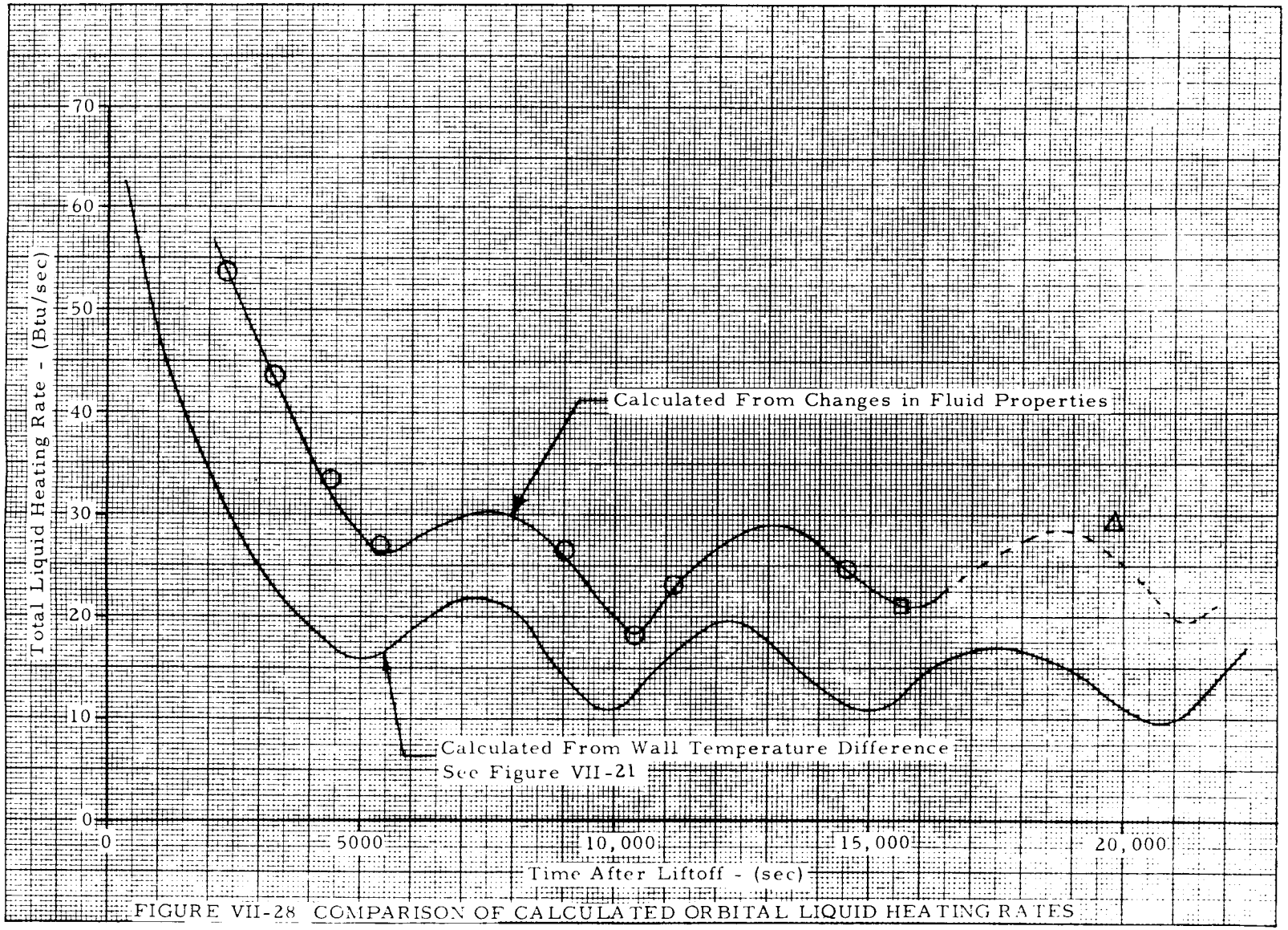

FIGURE VII-28 COMPARISON OF CALCULATED ORBITAL LIQUID HEATING RATES

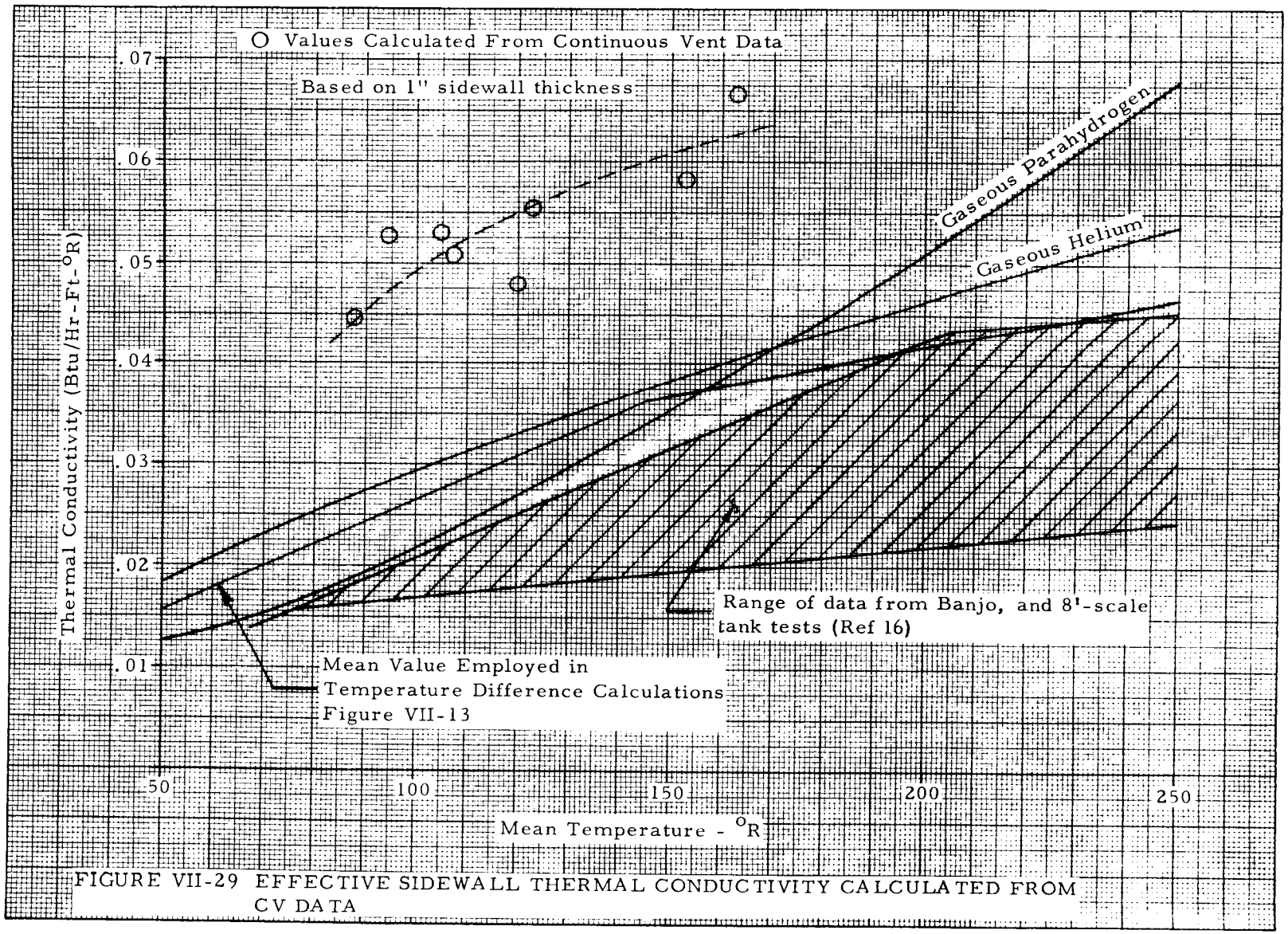

FIGURE VII-29 EFFECTIVE SIDEWALL THERMAL CONDUCTIVITY CALCULATED FROM CV DATA

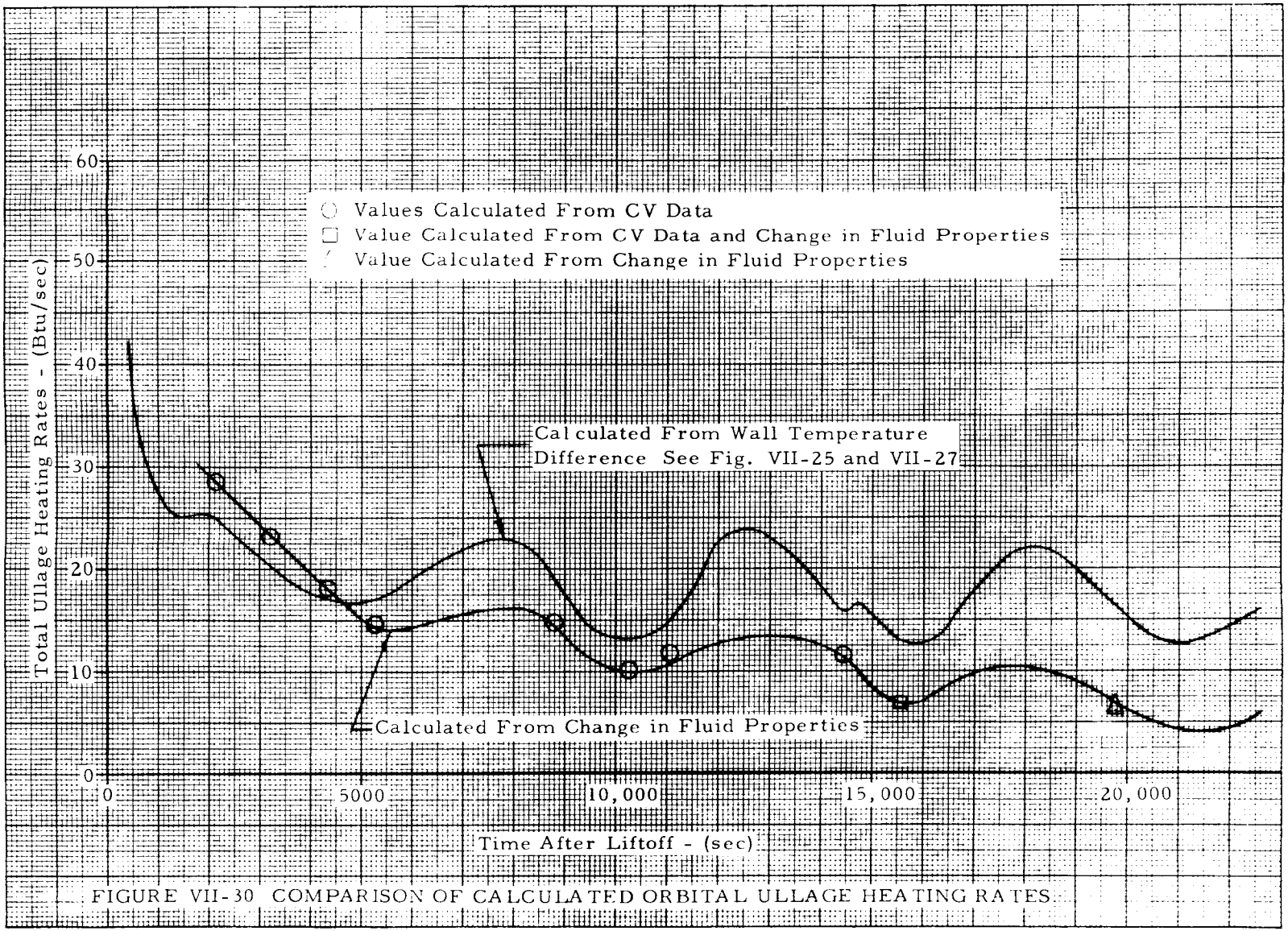

FIGURE VII-30 COMPARISON OF CALCULATED ORBITAL ULLAGE HEATING RATES

SECTION VIII. INSTRUMENTATION AND SUBSYSTEM PERFORMANCE ANOMALIES

In addition to low gravity fluid behavior and heat transfer data, the flight also provided valuable data on the performance of certain types of instrumentation in a low gravity cryogenic environment and indicated performance anomalies of various vehicle subsystems that merit more detailed investigation. The purpose of this section is to discuss the performance of some of the special measuring instruments and vehicle subsystems.

A. TV PERFORMANCE - LIQUID APPARITIONS

Two television cameras were installed in the hydrogen tank manhole cover to provide visual monitoring of the liquid hydrogen behavior during the experiment. TV camera number two performed exceptionally well throughout the mission. However, camera number one failed prior to liftoff. During the mission there were two instances when an optical illusion gave the appearance of liquid hydrogen in the forward end of the tank (above the deflector). The first occurrence was over Texas on the first orbit, and the second was near the end of the third orbit over Bermuda. Although the TV picture seemed to indicate that the liquid surface was above the deflector, none of the other instrumentation indicated the presence of liquid in that region. A careful study of the data showed that large density gradients in the ullage gas gave the appearance of light reflections from a liquid surface. The cause of these density gradients during the first orbit was the partial repressurization of the "cold" hydrogen tank by "hot" gaseous helium. The helium at an average temperature of approximately 200°R was introduced into the hydrogen tank ullage region that had an average temperature of approximately 53°R. The resulting density gradients created a visual image very similar in appearance to that of a Schlieren photograph. On the third revolution the density gradients were created when large particles of liquid were vaporized upon impact with the internal surfaces of the forward dome. These liquid particles were thrown forward as the liquid was resettled in the bottom of the tank at the end of the free coast experiment.

B. LEAKAGE FROM COLD HELIUM STORAGE BOTTLES

The S-IVB LOX tank pressurization system consists of eight interconnected 4.5 cu ft helium storage bottles located in the fuel tank. During S-IVB powered flight helium is bled from these bottles, heated (by a heater on the J-2 engine), and injected into the LOX tank to maintain the required pressure.

On the AS-203 flight the system was required only during boost flight. On Saturn V/S-IVB vehicles the system will be required during boost and for the second J-2 burn after a 4.5 hour orbital coast period.

On the S-IVB-203 stage the helium storage bottles were instrumented internally with one pressure and five temperature sensors (D016, C005, C207, C208, C209, and C210). The recorded temperatures were averaged and employed with the measured pressure (considering compressibility effects) to determine the mass of helium in the bottles at various times during the flight. Measurement C210 was not used in calculating the average temperature because of its limited accuracy (0 to 560°R range).

The AS-203 LOX tank pressurization system functioned normally during boost flight and was closed at J-2 engine cutoff. The system was programmed to retain the remaining pressurant throughout the orbital phase of the flight. The measured helium transient temperatures at J-2 engine cutoff are shown in figure VIII-1. The helium pressure and average temperature at this time are given in figure VIII-2. Based on these values the mass in the helium system was found to decrease from 400 lb_m at engine cutoff to 330 lb_m 120 seconds later. Following this 70 lb_m loss the mass in the system remained essentially constant until the fourth orbit. Figure VIII-3 shows the average temperature, pressure, and calculated mass in the helium storage bottles during the orbital coast period following the mass loss at cutoff. The figure shows that the helium mass remained constant until about 19,000 seconds at which time the system again began losing pressurant. A total of 120 lb_m was lost between 19,000 seconds and 22,400 seconds. No explanation can be offered as to the specific cause of the pressurant losses.

Since an actual J-2 engine restart was not attempted on AS-203, the loss of mass from the pressurant system was not critical. Similar losses on a Saturn V/S-IVB stage could be detrimental to the success of the flight. The cause of the pressurant loss should be investigated and corrected.

C. CONTINUOUS VENT REGULATOR VALVE OSCILLATIONS

The continuous vent regulator valve is designed to maintain the fuel tank at a given pressure level by regulating the mass flow discharged through the continuous vent system. A schematic of the regulator valve is shown in figure VIII-4. When the fuel tank pressure (P_1 in the schematic) is above 20.5 psia, the main poppet should be completely retracted with the vent flow being controlled by the bypass orifice and the cross-sectional area, A_1, beneath the main poppet. (For valve specifications see DAC Drawing 1B56547.) At tank pressures below 20.0 psia the main poppet should be completely closed and the vent flow is then controlled by the bypass orifice. At pressures between 20.0 and 20.5 psia, the main poppet should be partially opened.

During the AS-203 flight the regulator valve operated properly when the main poppet was completely opened ($P_1 > 20.5$ psia) or completely closed ($P_1 < 20.0$ psia). However, during the time the tank pressure was in the regulating region ($20.5 > P_1 > 20.0$ psia), the main poppet oscillated from the fully opened to fully closed position at frequencies from 2 to 30 cycles per minute. Figure VIII-5 shows the continuous vent line pressure, P_2, at various times in the orbital period. The pressure oscillations shown are caused by the varying flow rates through the regulator valve.

The oscillations occurring in the regulator valve were probably caused by a pressure feed back between the controller sensing bellows and the continuous vent line pressure, P_2. See figure VIII-4. The controller sensing bellows is activated by the pressure difference between the fuel tank and the continuous vent line ($P_1 - P_2$). When ($P_1 - P_2$) becomes great enough to overcome the spring loading on the controller sensing bellows, the pilot poppet opens, thereby decreasing the pressure behind the main poppet (P_3). As P_3 decreases, the main poppet opens, thereby increasing the flow through the vent system and, thus, rapidly increasing the vent line pressure, P_2. This increase in P_2 decreases the pressure differential across the controller sensing bellows ($P_1 - P_2$) thus causing the pilot poppet to close. When the pilot poppet closes, P_3 increases due to the bleed flow through the adjustable orifice. This increase in P_3 causes the main poppet to close, thereby decreasing the vent flow rate and the continuous vent line pressure, P_2. As P_2 decreases, the controller sensing bellows again opens the pilot poppet and the cycle repeats.

Two approaches may be taken to improve the operation of the continuous vent regulator valve. First, the frequency of the valve oscillations may be decreased by reducing the bleed flow through the adjustable orifice. Second, to completely eliminate the oscillations, it will probably be necessary to sense a constant pressure on the low pressure side of the controller sensing bellows. One possible place to sense a constant pressure is in the non-propulsive vent (NPV) line (see Proposed Modification on figure VIII-4). The small flow rate through the pilot poppet will not cause any measurable pressure increase in the NPV line, and no force unbalance problems should be encountered.

D. QUALITY METER PERFORMANCE

A quality meter employing a gamma ray scattering technique was located in the S-IVB-203 continuous vent line. This meter was designed to measure the quality of the vented fluid in the range of 50 to 100% with an accuracy of ±5%. The meter was required to indicate qualities below 50%, however, no specified accuracy was required in this range. A more complete discussion on the quality meter operation and meter specifications is given in reference 1 and 17, respectively.

The flight results indicate that it was possible for a two-phase fluid mixture to be present in the continuous vent system at only two time periods during the flight. These times occurred in the third revolution during the first fuel tank blowdown test over Carnarvon, Australia, and over the North American continent during the second and third tank blowdown tests. At all other times during the flight the vapor being vented was superheated at least $20^{\circ}R$. Figure VIII-6 shows a typical meter readout during a time when the fuel tank was under quasi-steady state continuous vent operation. Figure VIII-7 shows the temperature of the ullage gas in the fuel tank both above and below the tank vent outlet, as well as the fluid temperature in the vent line during the same time interval as the quality meter readings shown by figure VIII-6. It is apparent from figure VIII-7 that superheated vapor was being vented, yet the quality meter output indicated values ranging from 20% to 100% fluid quality. This false reading, as explained by the meter manufacturer, was caused by a readout voltage "loop-over" which resulted when the vapor entering the vent system was superheated (see reference 18). Figures VIII-8 through VIII-11 show the quality meter readout and vented fluid temperatures at times when nearly saturated vapor was passing through the vent system. It can be seen from these figures that the quality meter continued to read values ranging from 15 to 100% quality. However, there was a noticeable change in the quality measurement as the vented fluid temperature approached the saturation temperature. During the period when nearly saturated fluid was being vented, the meter indicated a quality ranging from 15% to 25%. This reading is felt to be erroneous because the measured fluid temperature (C256 and C257) upstream of the continuous vent nozzles was slightly superheated during this entire time period (see figure VI-3). A heat balance on the vent line indicates that it would be impossible to completely evaporate all of the liquid in a fluid mixture of less than 90% quality between the vent inlet and discharge nozzle.

No information that was useful in the evaluation of the fluid quality being vented from the S-IVB fuel tank was obtained from the quality meter measurement. However, the meter did respond to changes in fluid density and if the meter can be modified to eliminate the voltage signal "loop-over" problem occurring with superheated vapor, useful information could possibly be obtained from such a meter.

E. LIQUID-VAPOR SENSORS

Seven liquid-vapor sensors were added in the liquid hydrogen tank. Four of the sensors (N047, N048, N049, N050) were Douglas Aircraft designed concentric ring capacitance type transducers. Two additional sensors (N051 and N053) were capacitance type transducers of a different design produced by Transonics. This configuration was designed to minimize the effect on capacitance of small quantities of liquid that might cling to the sensor under

low gravity conditions. One sensor (N052) was a variable resistance type transducer. This unit is basically the same sensor that has been used on the Centaur vehicle. All units were designed for operation in a reduced gravity environment. Additional details on the mechanical and operating characteristics of the instruments are given in reference 1. The purpose for using the various designs was to obtain a relative performance evaluation of the different types and to assist in descriminating between liquid and vapor at various locations in the tank. To obtain a relative performance comparison, a Douglas sensor, an experimental sensor, and a thermocouple were each mounted at the same location on the instrumentation probe. Three such combinations were installed. The fourth Douglas instrument was located on the existing instrumentation probe. The following table indicates the specific sensor locations.

TABLE VIII-1
LIQUID-VAPOR SENSOR LOCATIONS

Douglas Sensor	Experimental Sensor	Temperature Sensor	S-IVB Station
N047	N051	C344	410.3
N048	N052	C347	479
N050			570
N049	N053	C348	650

1. Performance During Powered Flight and Orbital Insertion

During S-IVB powered flight, all three sensors at any given location gave the same indication, i.e., wet or dry, at any given time. The combination of sensors at STA 650 indicated dry and the combination at STA 410.3 indicated wet throughout powered flight. N050 and all sensors at STA 479 responded sharply from wet to dry as the liquid level drained past them. Following orbital insertion, all sensors at STA 479 indicated contact with the deflected slosh wave (figure III-3) at about 450 seconds after liftoff. At 470 seconds the temperature sensor (C347) again indicated gas, and at about 475 seconds N052 indicated gas. Instrument N048 (Douglas design) continued to indicate liquid until Bermuda lost telemetry signal at approximately 700 seconds. The response of C347, N048, and N052 from liftoff until the loss of telemetry signal at Bermuda is shown by figure VIII-12. The output of N052 has been erroneously processed and presented as degrees Rankine instead of volts. However, the use of the output to indicate wet or dry appears valid. From the data shown by figure VIII-12, it appears that N048 and N052 both responded rapidly from wet to dry during powered flight

(acceleration greater than one "g"). In the low gravity environment following orbital insertion, both responded rapidly from dry to wet as substantiated by comparison with the temperature sensor. N052 also responded satisfactorily from wet to dry as evidenced by comparison with C347. However, N048 apparently trapped liquid and never again indicated dry while in range of the Bermuda tracking station.

2. End Rev 1, Begin Rev 2

Sensor N048 was still indicating liquid when the vehicle was tracked at Carnarvon, Australia, and continued to indicate liquid over the United States at the end of the first revolution. N052 was off scale indicating dry. Until 5,540 seconds, it was impossible to determine whether C347 was sensing liquid or gas because the tank was saturated. However, at 5,540 seconds, C347 responded instantaneously with a slight temperature increase concurrent with the fuel tank repressurization indicating that it was definitely in the vapor region. At approximately 5,800 seconds, N048 finally indicated dry. This time does not correspond to any particular event. Apparently the higher acceleration imposed by the LOX ullage thrusting system during the chilldown sequence, together with the higher ullage gas temperature, was adequate to vaporize, or otherwise remove, the liquid from the sensing unit. All other instruments indicated wet or dry at all times consistent with their location relative to the settled liquid.

3. End Rev 2, Begin Rev 3

When the vehicle was again tracked over Carnarvon and the United States, N048 was again indicating wet. C347 was obviously 2 - 3°R above saturation temperature and N052 was off scale indicating dry in both cases. N048 continued to indicate wet during the entire duration over the United States and Bermuda.

4. First Fuel Tank Blowdown

When the non-propulsive vent valve was opened at 14,342 seconds to initiate the first fuel tank blowdown sequence, C347 responded immediately by gradually decreasing from 2°R superheated to saturation temperature. N048 indicated wet at all times. N052 was initially dry. However, 40 seconds after initiating the test, N052 indicated wet and appeared to intermittently wet and dry during the remainder of the blowdown sequence. After the termination of the blowdown, the sensor continued to alternately wet and dry with decreasing frequency. In the instrument cluster at STA 650, the temperature sensor (C348) decreased rapidly from 55°R to saturation temperature at the initiation of the blowdown. Both liquid-vapor sensors indicated dry throughout the test.

5. Second and Third Fuel Tank Blowdowns

The second and third blowdown tests provided the first information on the response characteristics of the Transonics produced instruments. Figure VIII-13 shows the response of N048, N049, N050, N052, and N053 during and following the second and third blowdowns. Of these, N052 apparently produced the only realistic indication of both wetting and drying. N053 (Transonics) and N050 (Douglas) both indicated wet between the second and third tests and both remained wet until loss of telemetry signal even though N052 finally indicated dry at 17,300 seconds. By the time the vehicle reached Hawaii on the fourth orbit (22,400 seconds), all sensors were indicating dry. Any trapped liquid was apparently evaporated by the superheated ullage gases during the fourth orbit.

All of the liquid-vapor sensor designs responded rapidly from wet to dry during operation in a high gravity environment and from dry to wet in a low gravity environment. From the data reviewed at various times during the orbital phase of the flight, it appears that the Douglas and Transonic sensors, once wetted, trap sufficient liquid to continue indicating wet when other data suggest that the sensors should be dry. Sensor N052 responded rapidly from wet to dry and dry to wet and correlated closely with the adjacent temperature sensor at all times during the flight.

F. PRESSURE SENSORS

For the liquid hydrogen orbital experiment, nine additional pressure sensors complemented the normal S-IVB stage R&D pressure measurements. Three of these nine sensors were unique pressure differential sensors (D211, D215, and D214) installed to determine if any imbalance existed between the discharge ports of the continuous vent, non-propulsive vent, and LOX ullage thruster systems. The remaining six sensors were of standard design.

Table VIII-2 identifies the pressure sensors whose performance was not entirely normal. Three of the sensors (D078, D082, and D105) failed prior to liftoff. The LOX tank inlet pressure (D055) was at an incorrect level and did not respond correctly to the tank pressure changes. Several other sensors (see table VIII-2) were not properly zeroed. A forward skirt external pressure measurement (D116) remained at 14.7 psia throughout the entire flight. The fuel tank inlet pressure (D054) failed 148 seconds after liftoff, and the LOX ullage thrusting system differential pressure (D214) failed at 292 seconds.

The fuel tank continuous vent exit #2 pressure (D182) had a slow response to pressure changes during the flight. This is shown in a comparison with the continuous vent exit #1 pressure (D181) when the CV system was opened after the first orbital chilldown (figure VIII-14). The CV system differential

pressure measurement (D211) was mounted on the same measurement line as measurement D182. The differential pressure measurement (D211) was off scale during transient periods, indicating a large pressure differential between the exits. Since the existence of a 15 psi pressure differential (figure VIII-14) was highly unlikely, it is probable that the measurement line from the transducers to the continuous vent duct was almost completely blocked, thereby preventing the transducers from measuring the transient pressure within the vent duct.

The fuel pump inlet pressure (D002) apparently failed only during S-IVB powered flight, since the reading was an abnormal 11 psi below the fuel tank ullage pressure (see figure V-47). This measurement did, however, operate under the higher acceleration levels of the S-IB boost and also throughout the orbital coast period (see figures V-11 and V-42). A complete explanation of this peculiar failure should be determined since the actual existance of the lower pressure would violate engine operating requirements.

G. TEMPERATURE SENSORS

Fifty-seven temperature sensors were added to the S-IVB-203 stage in addition to the normal R&D flight instrumentation. Twenty-three of the added sensors were of modified designs. Fifteen of the instruments (C322 through C335, C339 through C344, C346 through C349, and C373) were modified to reduce the tendency for liquid to cling and thus cause an erroneous signal. The temperature sensors normally consist of a solid cylindrical rod that is surrounded by a perforated barrel for protection. Because the barrel could act as a capillary trap in the low gravity environment, it was removed and the rod was reinforced for strength. The removal of the perforated barrel did provide a better sensor in the low gravity environment. Figure VIII-15 compares the insertion transients recorded from a modified sensor (C347) with those recorded from an unmodified sensor (C036). Under the higher acceleration of boost flight (about 3 g's) both sensors quickly dried as the liquid level dropped below the sensor (about 375 seconds). This was indicated by the increase from the subcooled liquid temperature to the ullage gas temperature. Following J-2 engine cutoff (at 432 seconds) both C036 and C347 were wetted by the deflected slosh wave (figure III-3). As determined from the TV coverage the liquid subsequently settled in the tank. The modified sensor (C347) indicated liquid for only 18 seconds (from 452 to 470 seconds). Then, as the liquid settled the sensor became dry and returned to the ullage gas temperature. The unmodified sensor (C036) indicated the presence of liquid in the ullage space beginning at 502 seconds. However, liquid was apparently trapped by the barrel and contrary to the television observation it still indicated the presence of liquid 185 seconds later when the telemetry signal was lost.

Another modified sensor, C345, was near the liquid surface during the first orbital chilldown. As the liquid surface sloshed the sensor was alternately in the ullage gas and beneath the liquid surface. This is shown in figure VIII-16. When in the ullage gas the sensor indicated the higher temperature of the ullage gas. As the subcooled liquid covered the sensor the temperature decreased to the temperature of the subcooled liquid. When the liquid surface again dropped below the sensor, the sensor became dry and indicated the temperature of the warmer ullage gas. These examples clearly indicate the favorable performance of the modified sensor in the low gravity environment and the apparent tendency of the unmodified designs to trap liquid. Of the remaining modified sensors, six were surface temperature sensors on the common bulkhead (C352 through C357), and two were combined as a dual element sensor (C363 and C364) in a single transducer.

Table VIII-3 identifies the temperature measurement anomalies which occurred. Two of the sensors (C340 and C349) failed prior to liftoff, and two others (C127 and C154) were never on scale. Four sensors in the LOX tank and one at the LOX pump inlet had an insufficient measurement range since the minimum LOX temperature during the flight was above the maximum of the measurement range. Three fuel tank external measurements failed during the flight, C078 at 2,390 seconds, C079 between 2,480 and 3,080 seconds, and C310 at 3,330 seconds. The engine LH_2 pump wall temperature (C150) failed at 253 seconds and the APS injector valve wall temperature (C177) failed during the fourth orbit. Data from the J-2 engine fuel injector temperature measurement (C200) were received, however, the data were erroneously reduced in Btu/ft^2 second instead of ^oR.

TABLE VIII-2

S-IVB-203 PRESSURE SENSOR PERFORMANCE ANOMALIES

Meas. No.	Name	Remarks
D002	Press. - Fuel Pump Inlet	Apparent failure during S-IVB Powered flight.
D054	Press. - LH_2 Tank Inlet	Failed at 148 sec.
D055	Press. - LOX Tank Inlet	Unexpected level, incorrect response
D062	Press. - LH_2 Recirc. Return Line Tank Inlet	Inoperative 0 to 15 sec and 40 to 160 sec.
D078	Press. - Attitude Control Chamber 1-1 (I,v)	Failed prior to launch
D082	Press. - Attitude Control 2-2 (IIIp)	Failed prior to launch
D087	Press. - Helium Repress. Sphere	Dropped below 0 psia at 5565 sec.
D105	Press. - LOX Tank Press Mod Helium	Failed prior to launch
D116	Press. - Forward Skirt External 8	Remained at 14.7 psia
D182	Press. - Fuel Tank Continuous Vent 2	Slow Response
D211	Press. - Differential - Cont. Vent Exit	Slow response, exceeded limits
D214	Press. - Diff. - LOX Ullage Thrust System	Failed at 292 sec
D215	Press. - Diff. - Non-Prop. Vent Exit	Reading .06 psid too low
D219	Press. - Diff. - LOX Chilldown Pump	Reading 2 psi too low

TABLE VIII-3

S-IVB-203 TEMPERATURE SENSOR PERFORMANCE ANOMALIES

Meas. No.	Name	Remarks
C004	Temp. - LOX Pump Inlet	Insufficient range, off scale high
C040	Temp. - Oxidizer Tank Pos 1	Insufficient range, off scale high
C041	Temp. - Oxidizer Tank Pos 2	Insufficient range, off scale high
C042	Temp. - Oxidizer Tank Pos 3	Insufficient range, off scale high
C043	Temp. - Oxidizer Tank Pos 4	Insufficient range, off scale high
C078	Temp. - Fuel Tank External-4	Failed at 2390 sec
C079	Temp. - Fuel Tank External-5	Failed Approx 2700 sec
C127	Temp. - LH_2 Duct 2	Never Came on Scale
C150	Temp. - Eng. LH_2 Pump Wall	Failed at 253 sec - off scale high
C154	Temp. - LOX Prevalve B/P Line Wall	Never came on scale
C177	Temp. - APS Inj Valve Wall Eng 2 & 3	Off scale, high - fourth orbit
C200	Temp. - Fuel Injector	Data reduction error
C310	Temp. - Fuel Tank External	Failed at 3330 sec - off scale, high
C340	Temp. - LH_2 Pos -31	Failed prior to launch
C349	Temp. - LH_2 Ullage Gas 5	Failed prior to launch

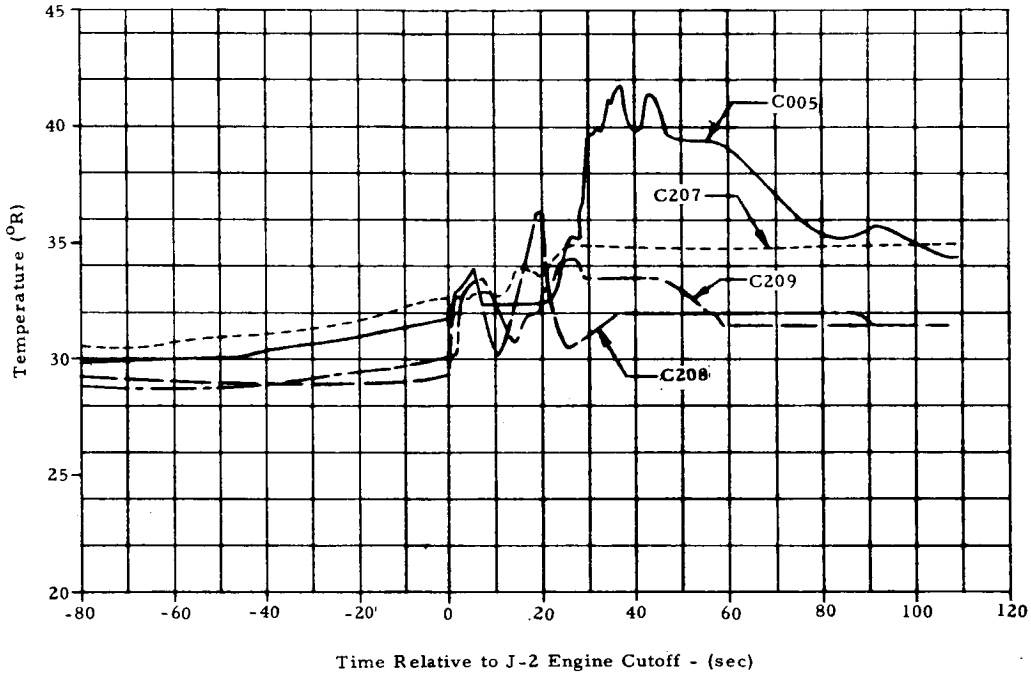

FIGURE VIII-1 HELIUM TEMPERATURES IN STCRAGE BOTTLES AT J-2 ENGINE CUTOFF

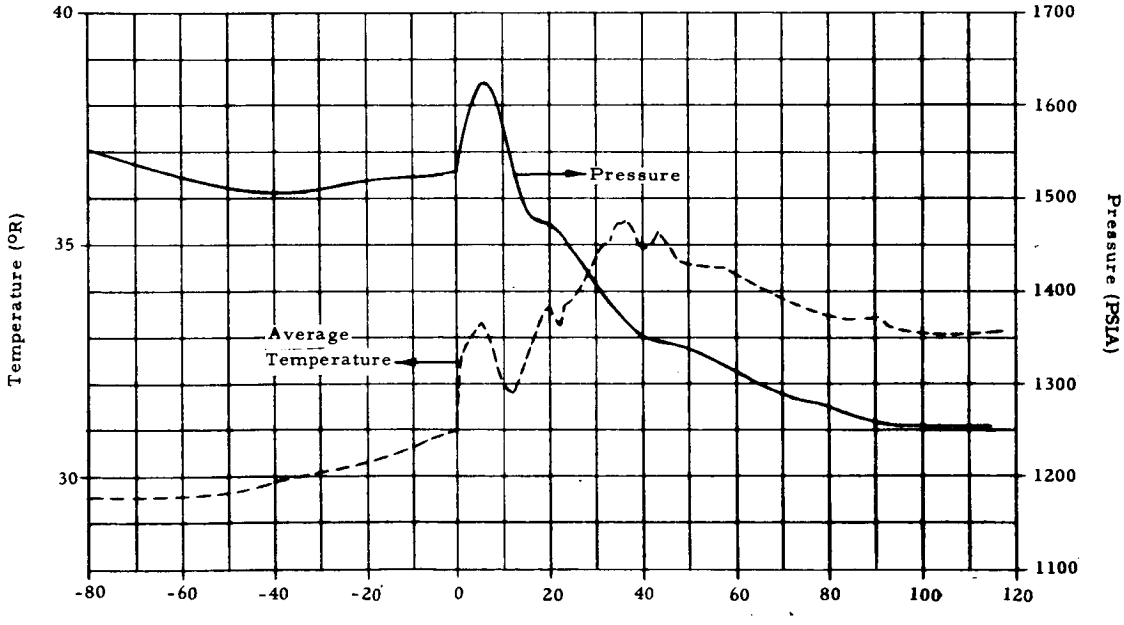

FIGURE VIII-2 HELIUM PRESSURE AND AVERAGE TEMPERATURE IN STORAGE BOTTLES AT J-2 ENGINE CUTOFF

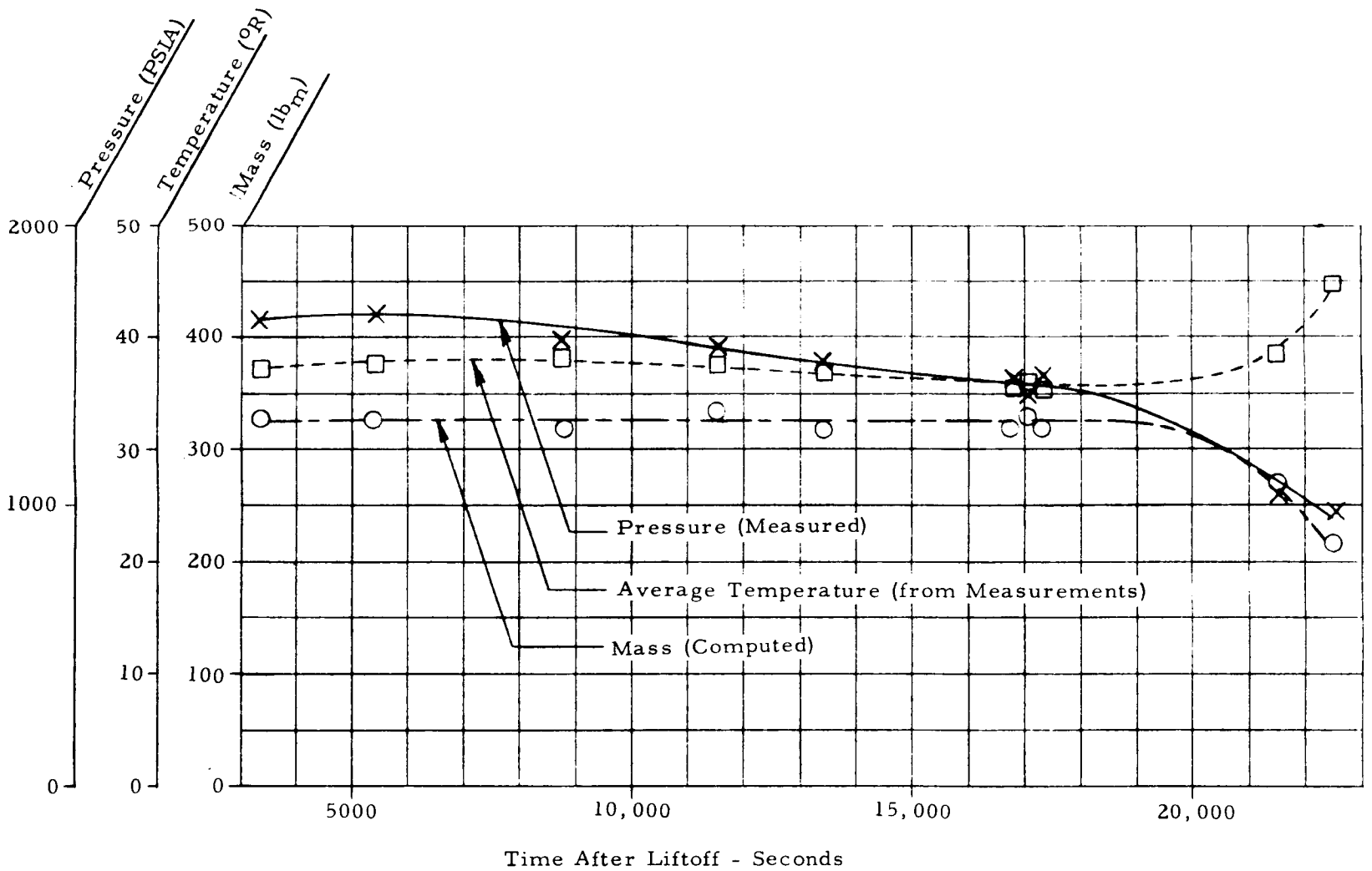

FIGURE VIII-3 MASS, PRESSURE, AND AVERAGE TEMPERATURE IN THE HELIUM STORAGE BOTTLES DURING ORBITAL COAST

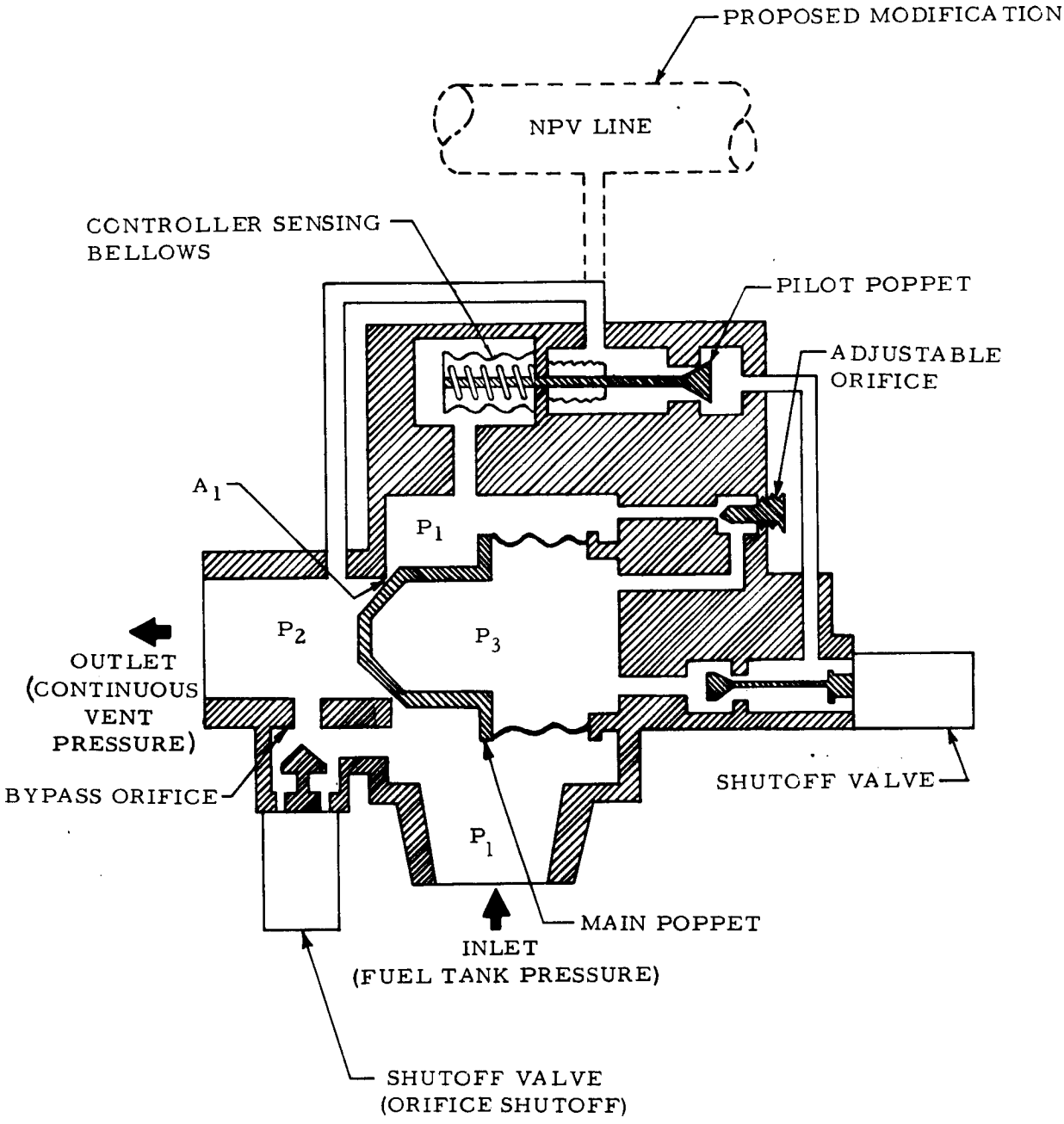

FIGURE VIII - 4 SCHEMATIC OF CONTINUOUS VENT REGULATOR VALVE

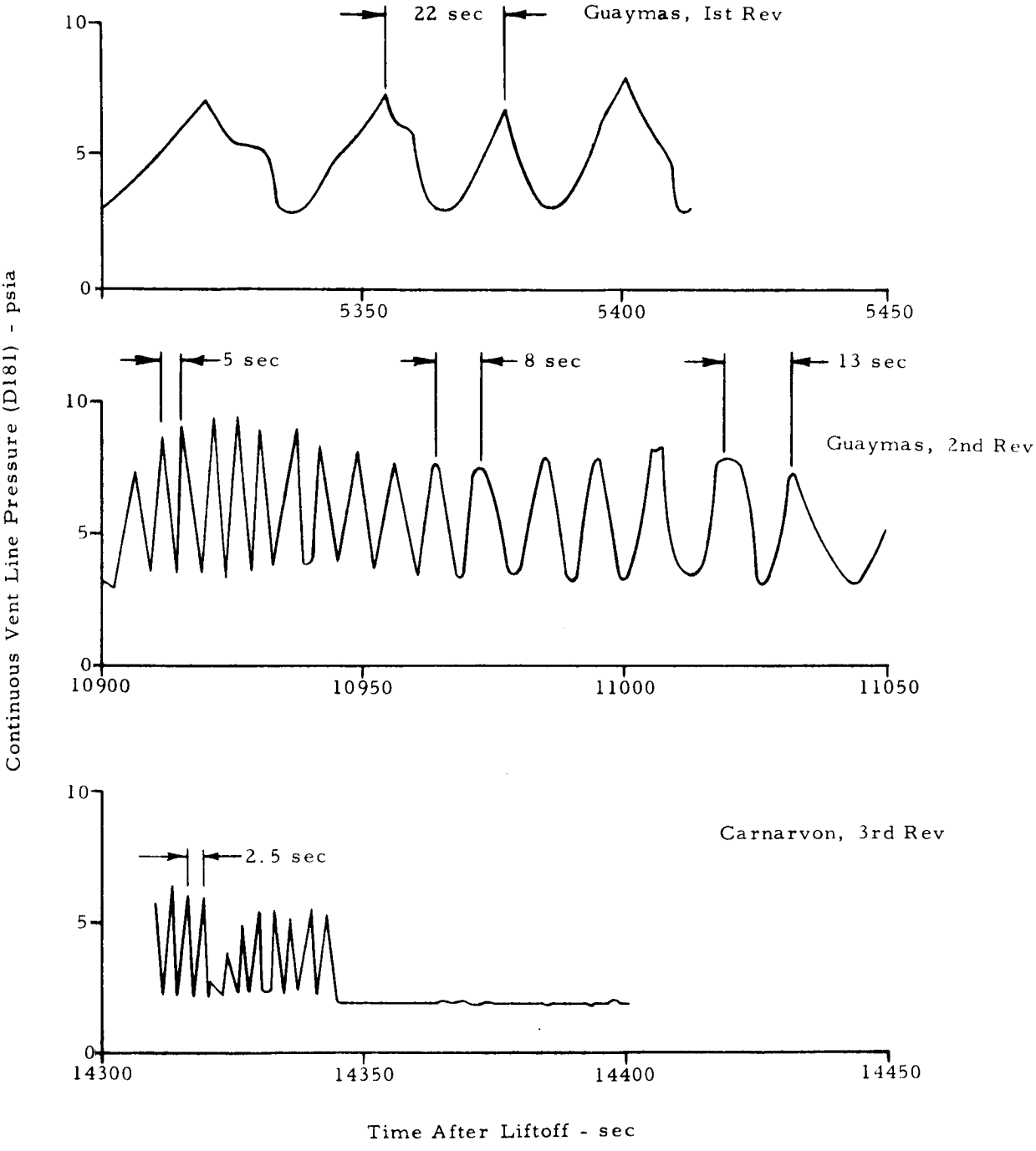

FIGURE VIII - 5 TYPICAL REGULATOR VALVE OSCILLATION FREQUENCIES

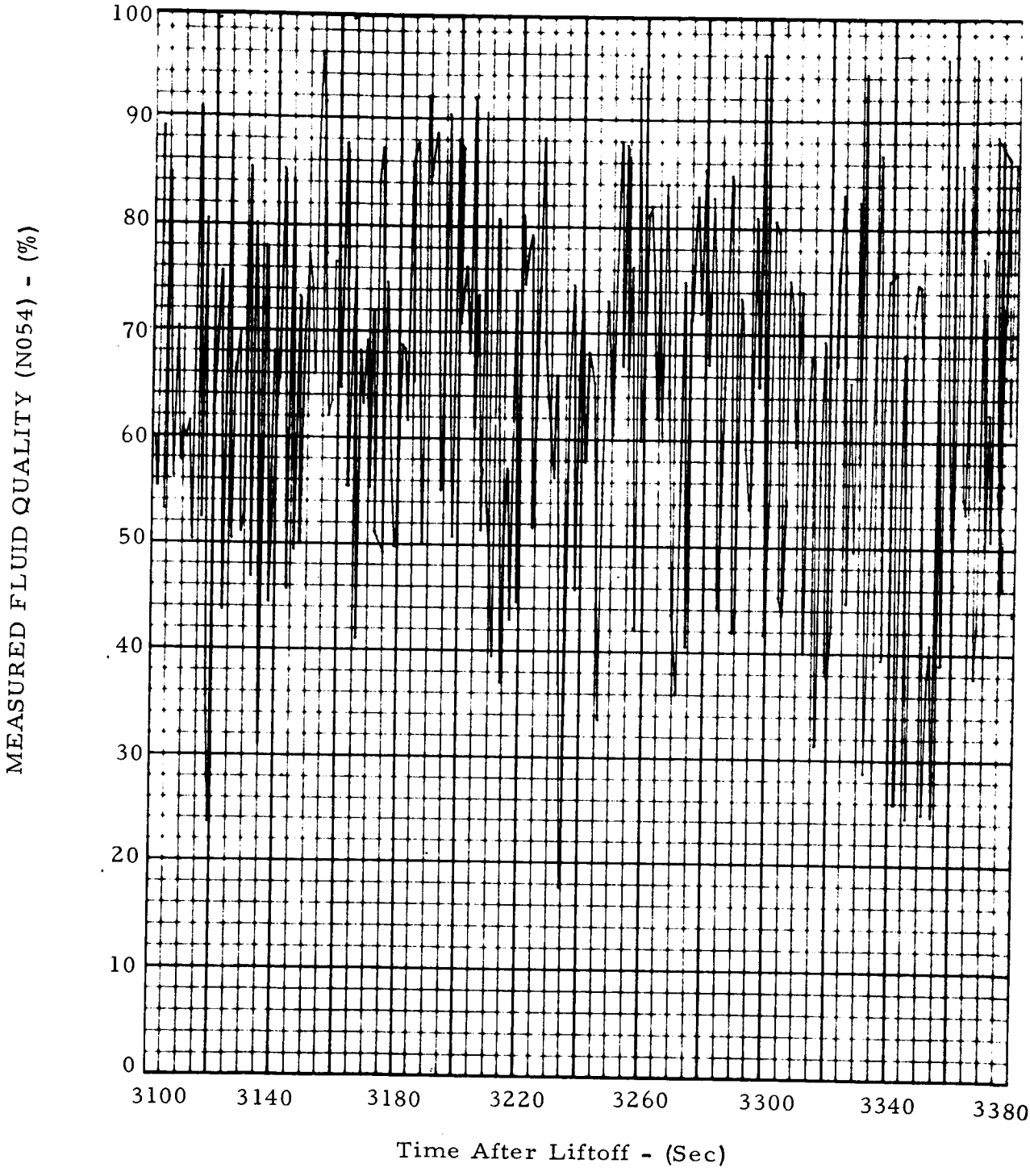

FIGURE VIII-6 TYPICAL QUALITY METER READOUT DURING STEADY STATE CONTINUOUS VENT OPERATION

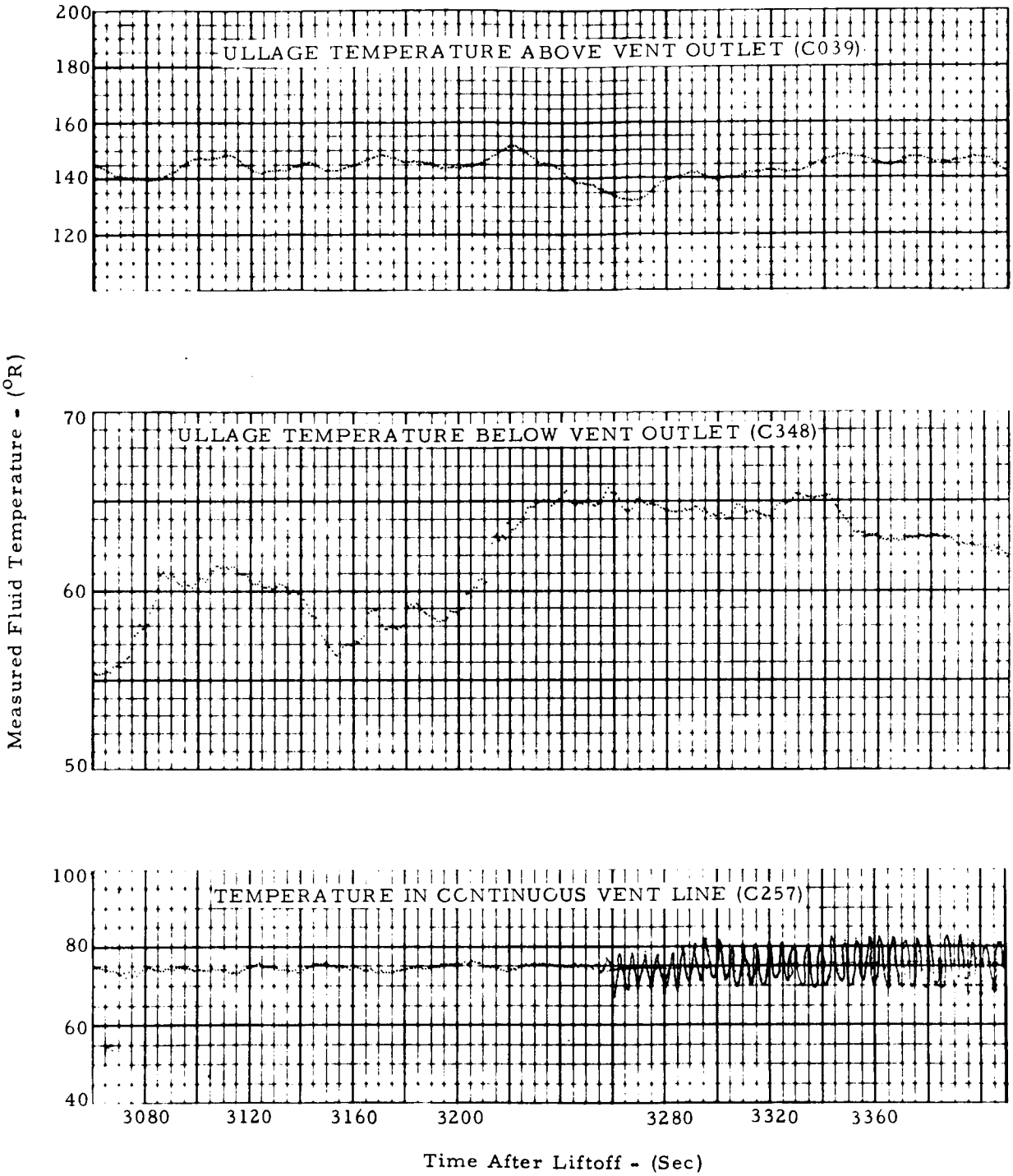

FIGURE VIII-7 TYPICAL VENTED FLUID TEMPERATURES DURING STEADY STATE CONTINUOUS VENT OPERATION

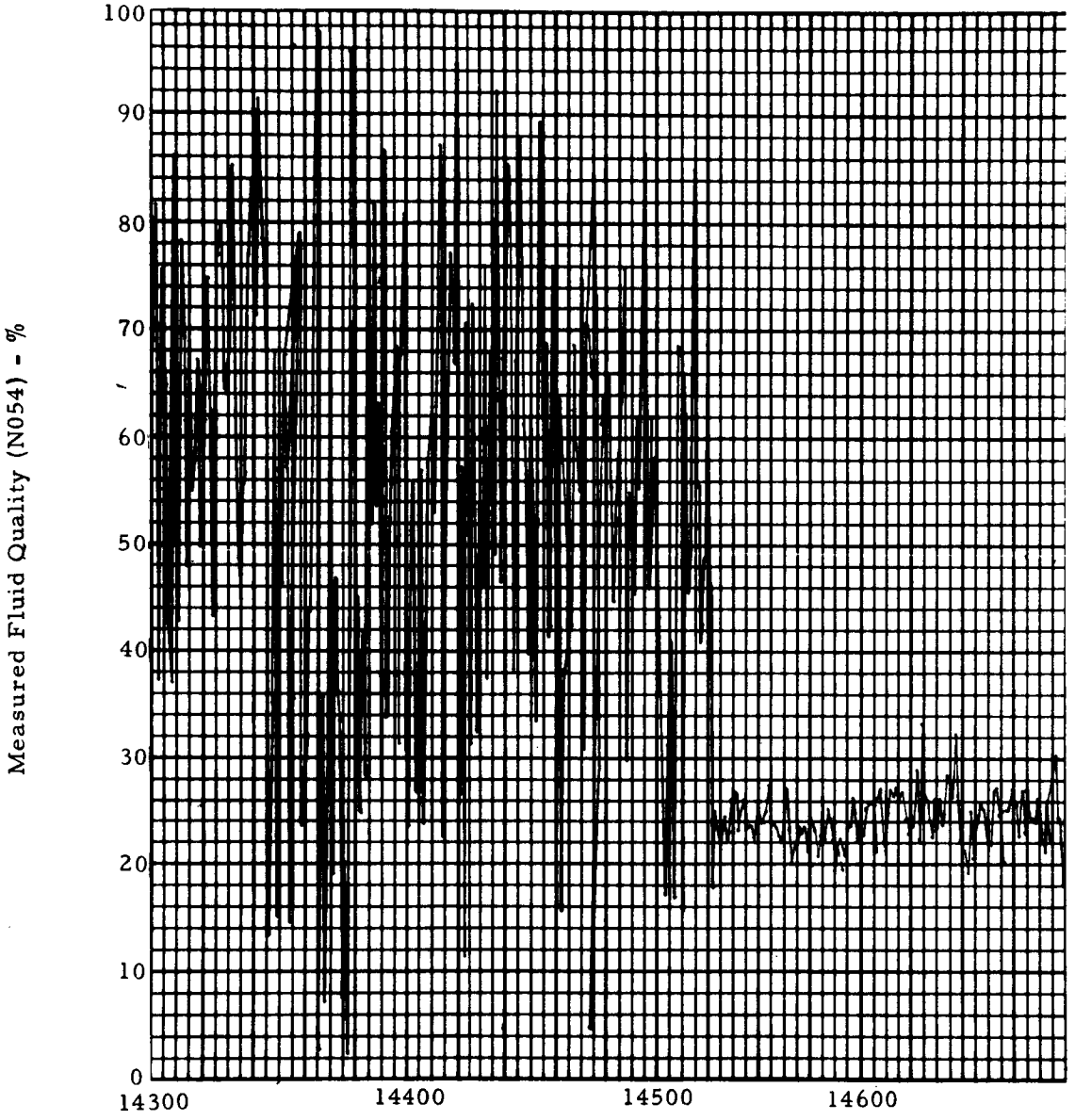

FIGURE VIII-8 VENTED FLUID QUALITY MEASUREMENT DURING FIRST TANK BLOWDOWN TEST

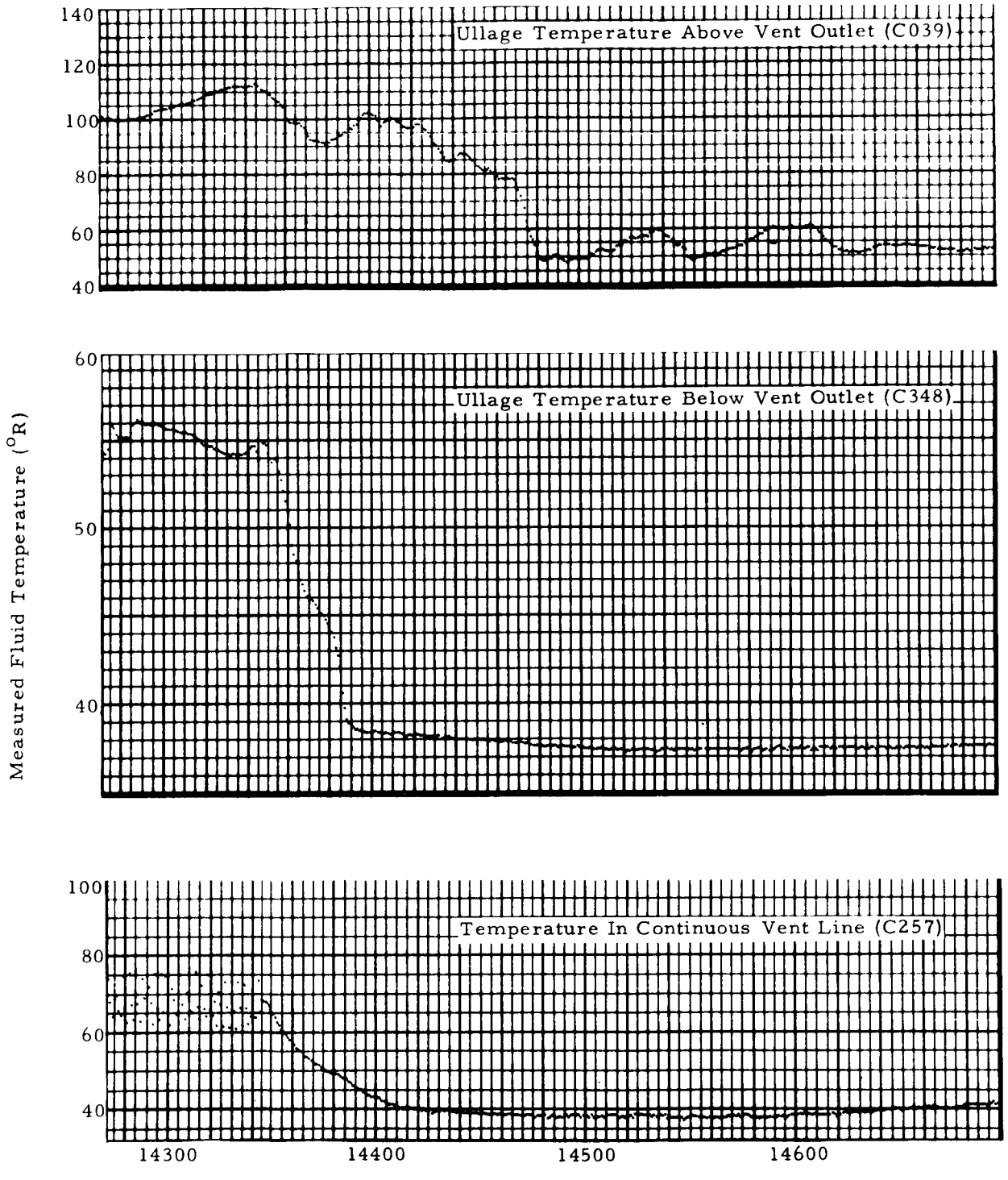

FIGURE VIII-9 VENTED FLUID TEMPERATURE MEASUREMENTS DURING FIRST TANK BLOWDOWN TEST

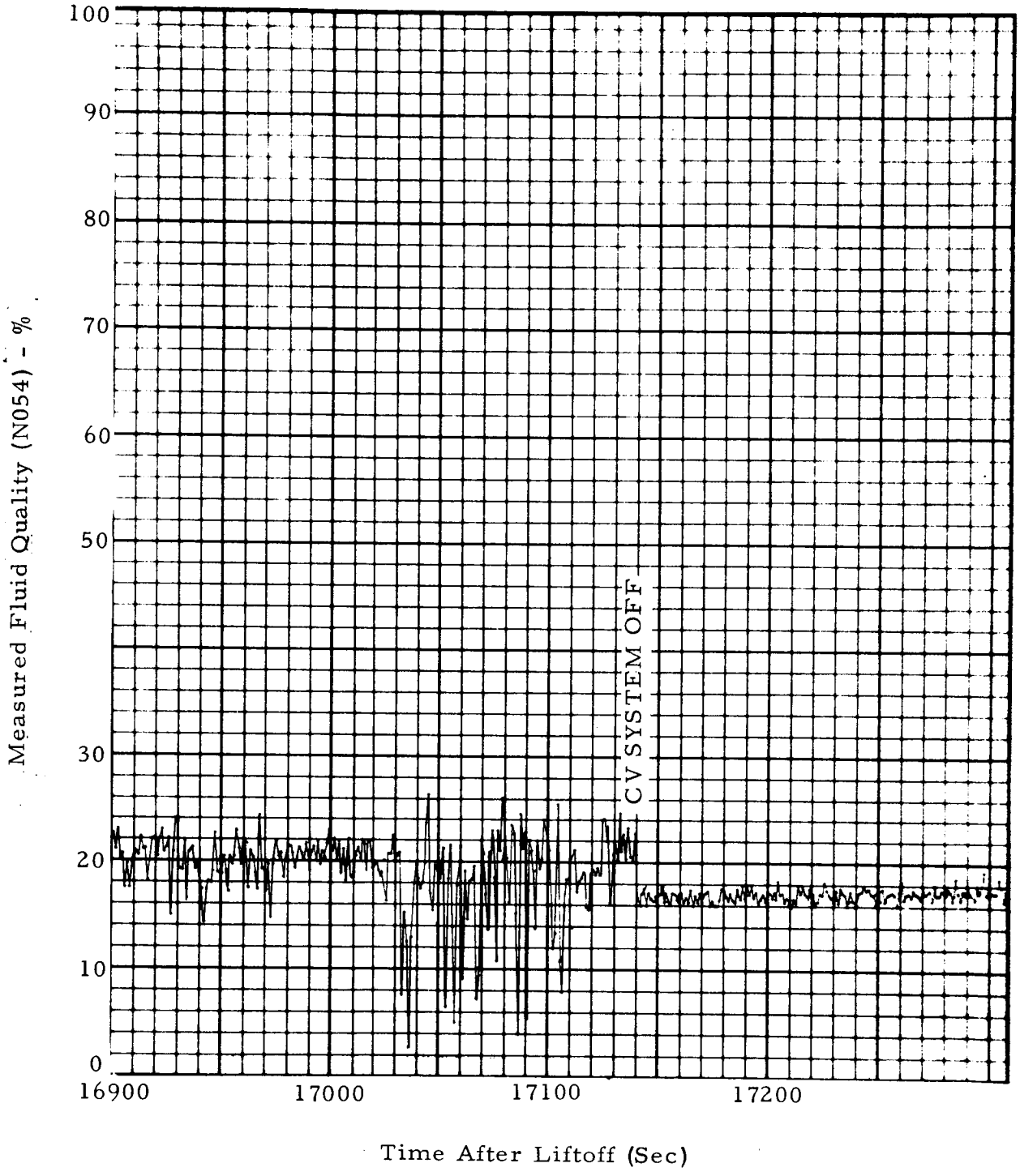

FIGURE VIII-10 VENTED FLUID QUALITY MEASUREMENT DURING THIRD TANK BLOWDOWN TEST

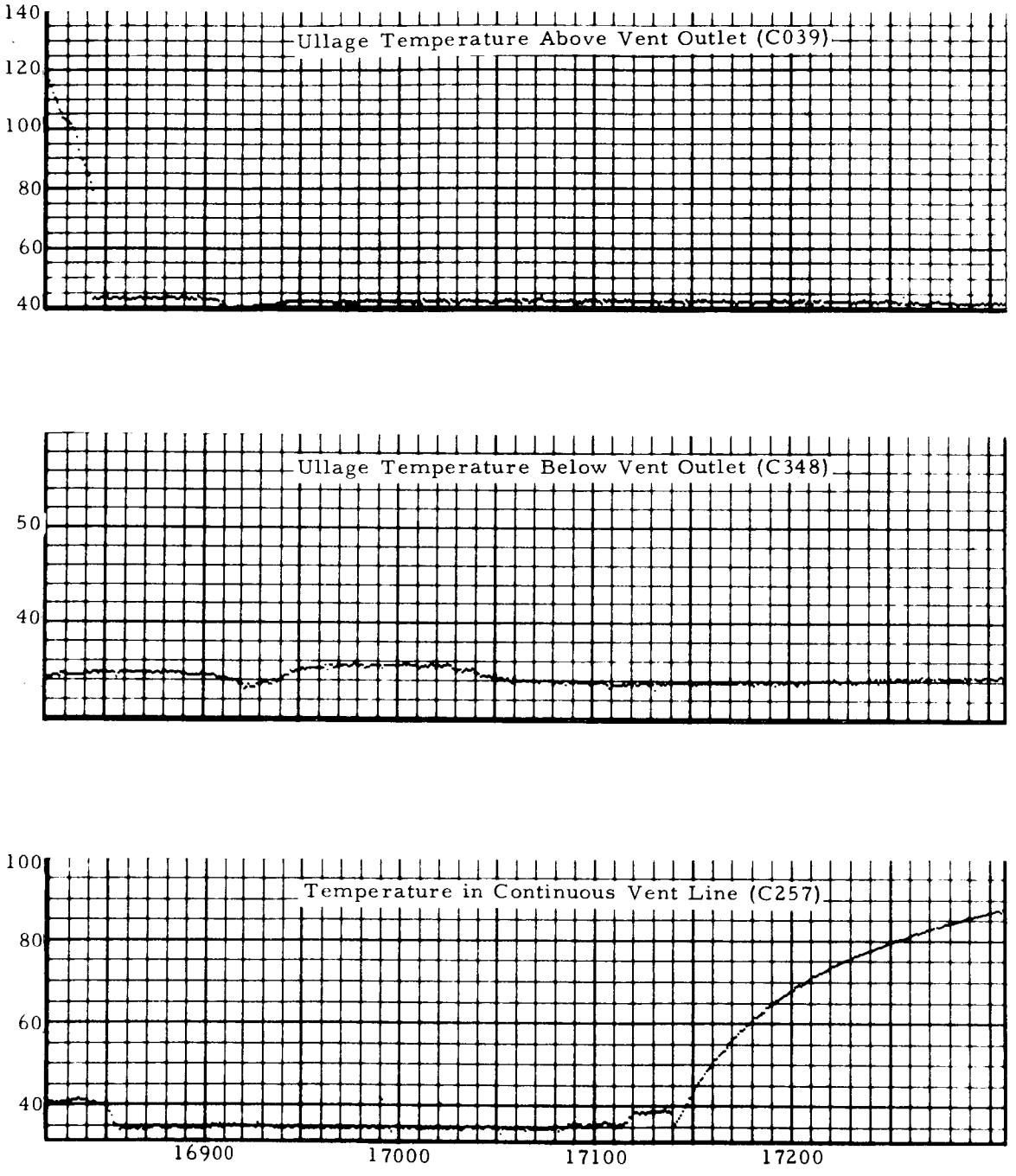

FIGURE VIII-11 VENTED FLUID TEMPERATURE MEASUREMENTS DURING THIRD TANK BLOWDOWN TEST

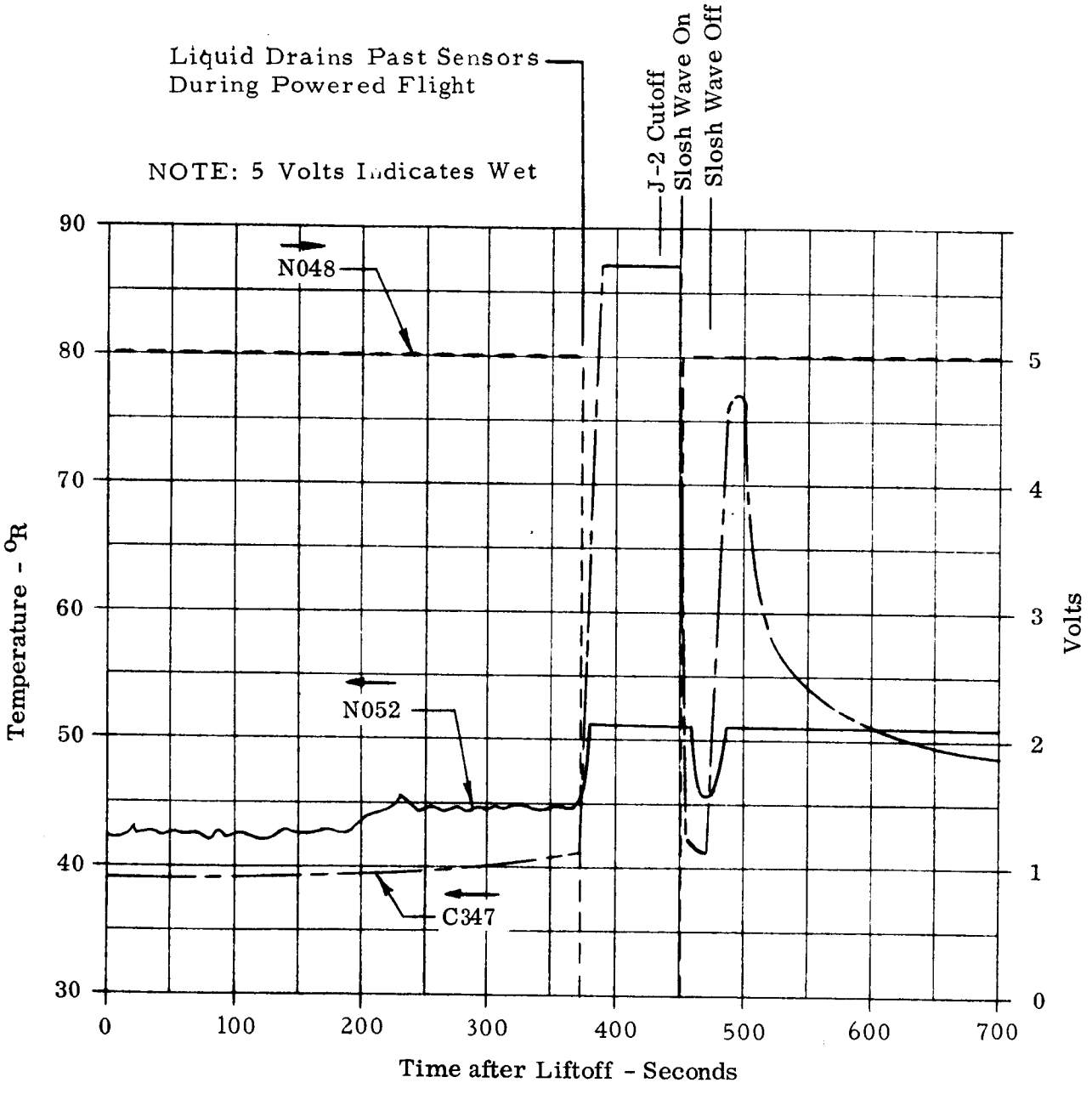

FIGURE VIII-12 LIQUID-VAPOR SENSOR RESPONSE FROM LIFTOFF TO BERMUDA LOS

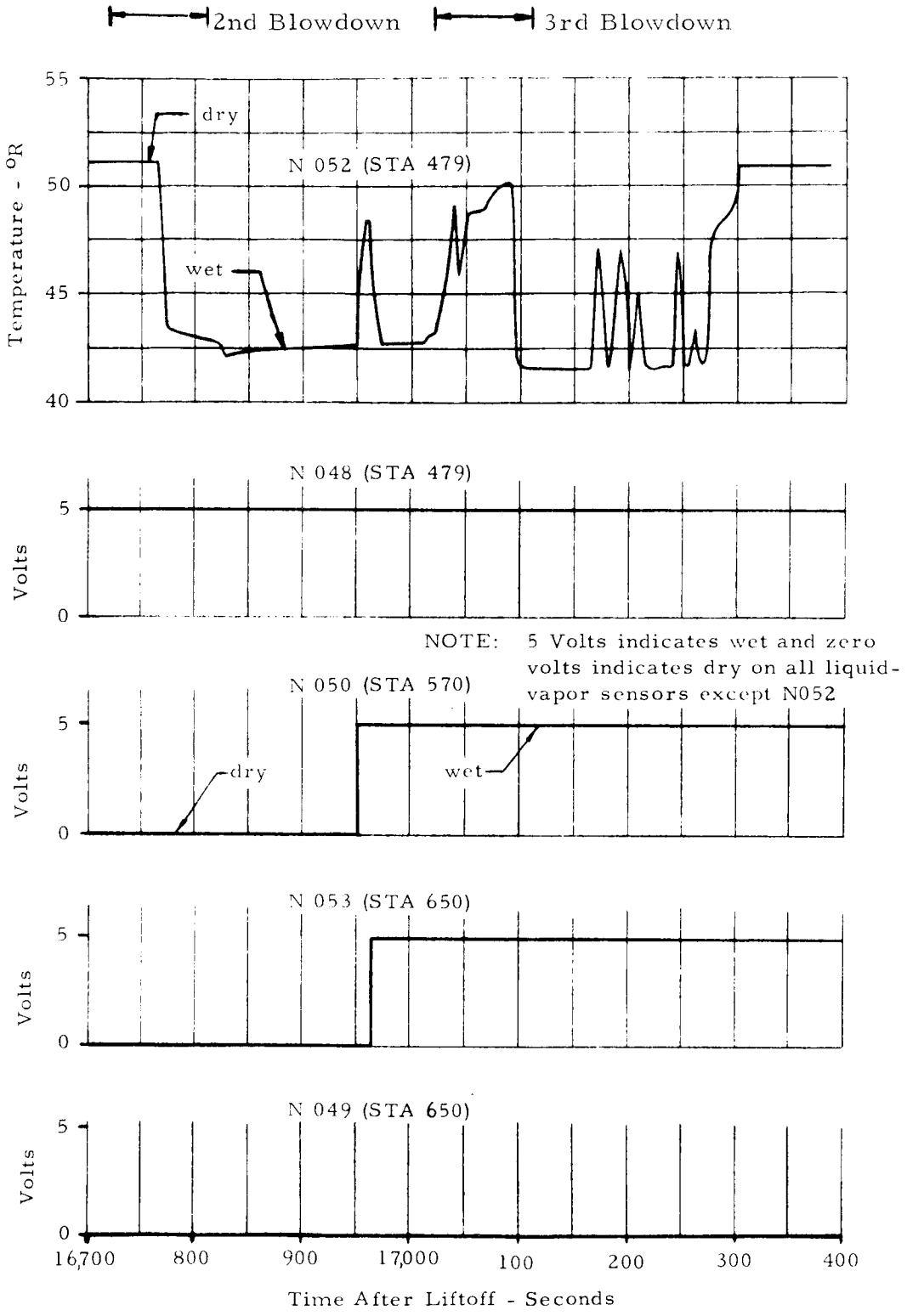

FIGURE VIII-13 LIQUID-VAPOR SENSOR RESPONSE DURING SECOND AND THIRD BLOWDOWNS

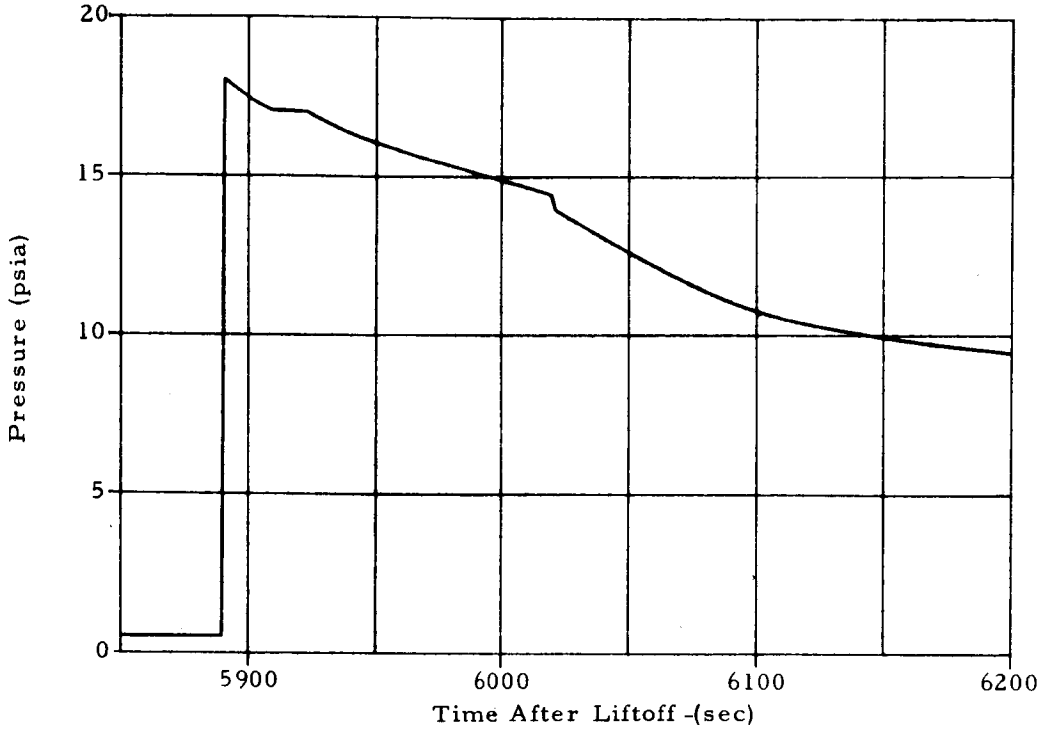

D181 - FUEL TANK CONTINUOUS VENT EXIT (#1) PRESSURE

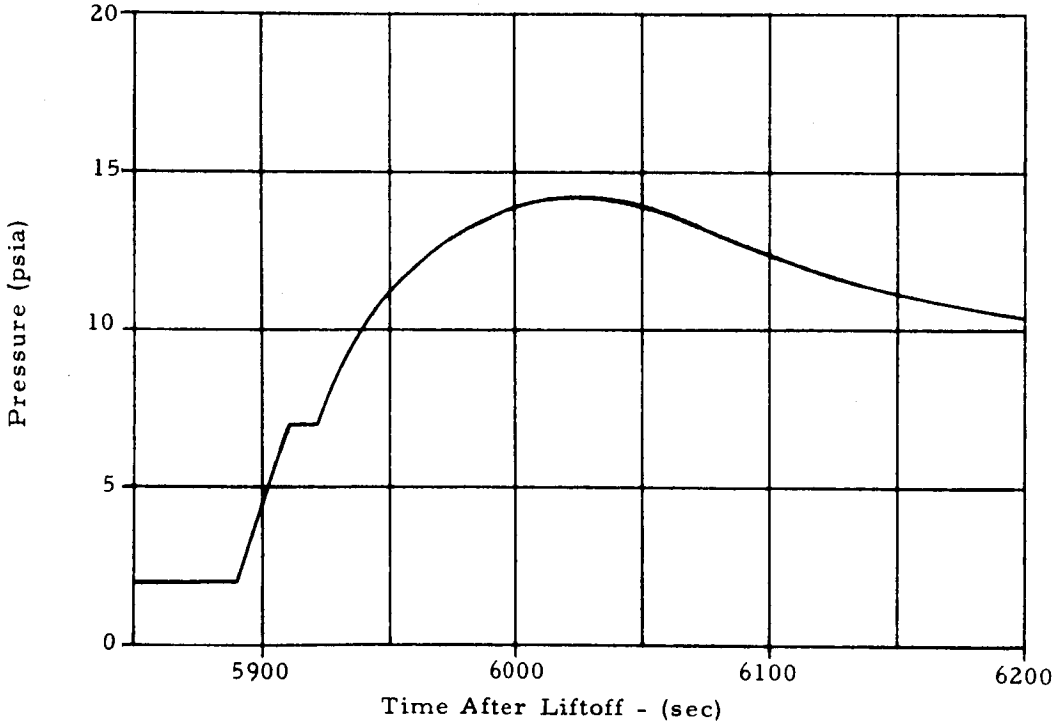

D182 - FUEL TANK CONTINUOUS VENT EXIT (#2) PRESSURE

FIGURE VIII-14 COMPARISON OF CONTINUOUS VENT SYSTEM EXIT PRESSURES

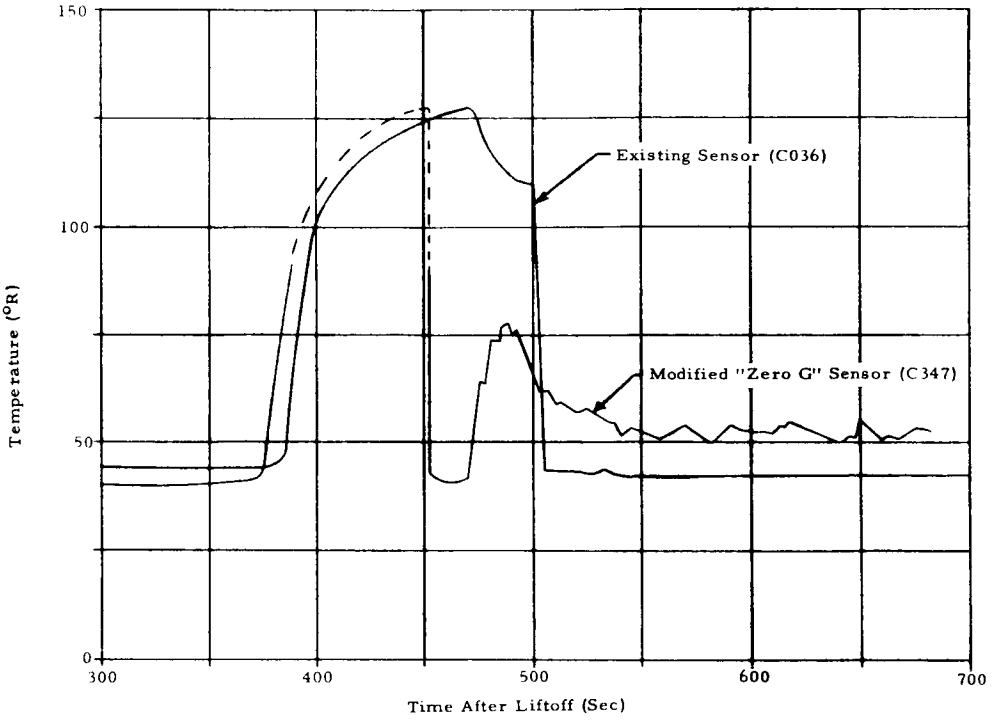

FIGURE VIII-15 PERFORMANCE OF TEMPERATURE SENSORS DURING INSERTION TRANSIENTS

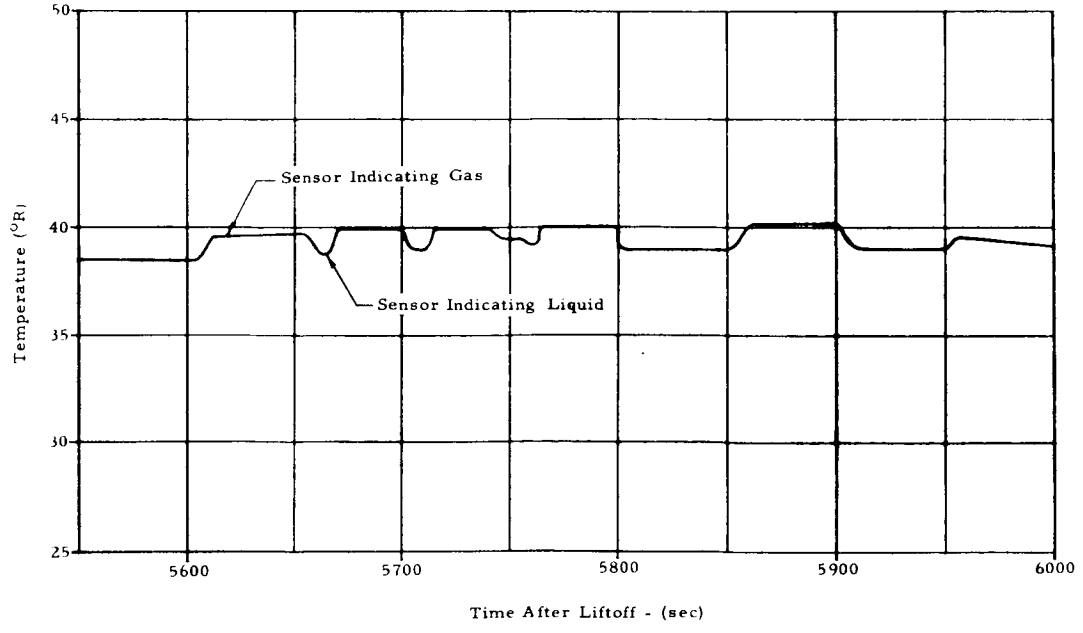

FIGURE VIII-16 PERFORMANCE OF MODIFIED SENSOR (C345) UNDER LOW GRAVITY CONDITIONS

REFERENCES

1. D. Talley, "Instrumentation for the Liquid Hydrogen Experiment, AS-203," R-ASTR-IM, April 1, 1966.

2. Saturn IB/SA-203 Flight Sequence, MSFC Drawing No. 10M30153, Revision B, May 4, 1966.

3. Saturn V/S-IVB Stage Modifications for Propellant Control During Orbital Venting, Douglas Aircraft Report SM-47177, April 1, 1965.

4. H. M. Satterlee and W. C. Reynolds, "The Dynamics of the Free Liquid Surface in Cylindrical Containers Under Strong Capillary and Weak Gravity Conditions," Stanford University Technical Report LG-2, Stanford, California, May, 1964.

5. W. D. Ward, "Calculations of Mass-Flow and Thrust Produced for A Two-Phase Fluid Mixture Passing Through A Choked Nozzle," NASA-TM-X-53269, August 4, 1965.

6. Chrysler Technical Note HSM-N819, "Predicted Orbital Thermodynamics and Venting Characteristics of the SA-203 Propellant Tanks," June 22, 1966.

7. Chrysler Memorandum HSM-M412, "Evaluation of the AS-203 Fuel Tank Repressurization System Data," October 5, 1966.

8. Chrysler Memorandum HSM-M02-66, "Evaluation of the S-IVB-17 Battleship Test LH_2 Chilldown Data," July 1, 1966.

9. Chrysler Memorandum HSM-M408, "Evaluation of LH_2 Chilldown Data From S-IVB Battleship Tests 21 and 25X," September 9, 1966.

10. Chrysler Memorandum HSM-M409, "Evaluation of LOX Chilldown Data From S-IVB Battleship Tests 21 and 25X," September 23, 1966.

11. Chrysler Memorandum HSM-M746, "Chilldown Test Data From S-IVB-203 Acceptance Firing," June 20, 1966.

12. Chrysler Memorandum HSM-M03-66, "Simplified Analytical Model for Determining S-IVB/J-2 Engine Chilldown Time," July 7, 1966.

13. T. E. Bowman, "Cryogenic Liquid Experiments in Orbit, Final Report, Volume I, Liquid Settling and Interface Dynamics," Martin Report CR-66-25 (Volume I), July, 1966.

14. Discussion with J. L. Vaniman, R-P&VE-PT (MSFC), December 12, 1966.

15. Heat Transfer Dispersion Study on the S-IVB Liquid Hydrogen (LH_2) Tank (Preliminary Copy), Douglas Aircraft Report SM-46745, November 23, 1964.

16. "S-IVB Liquid Hydrogen Tank Internal Insulation Effective Thermal Conductivity," Douglas Aircraft Figure prepared by E. F. Flores, September 30, 1965 (Evaluation of Banjo Tests, 8' scale tank tests, and acceptance firing tests).

17. Cryogenic Quality Meter, Douglas Aircraft Specification Control Drawing 1B52861.

18. Results of the Second Saturn IB Launch Vehicle Test Flight AS-203, NASA-MSFC Confidential Report MPR-SAT-FE-66-12, September 22, 1966.

13. T. E. Bowman, "Cryogenic Liquid Experiments in Orbit, Final Report, Volume I, Liquid Settling and Interface Dynamics," Martin Report CR-66-25 (Volume I), July, 1966.

14. Discussion with J. L. Vaniman, R-P&VE-PT (MSFC), December 12, 1966.

15. Heat Transfer Dispersion Study on the S-IVB Liquid Hydrogen (LH_2) Tank (Preliminary Copy), Douglas Aircraft Report SM-46745, November 23, 1964.

16. "S-IVB Liquid Hydrogen Tank Internal Insulation Effective Thermal Conductivity," Douglas Aircraft Figure prepared by E. F. Flores, September 30, 1965 (Evaluation of Banjo Tests, 8' scale tank tests, and acceptance firing tests).

17. Cryogenic Quality Meter, Douglas Aircraft Specification Control Drawing 1B52861.

18. Results of the Second Saturn IB Launch Vehicle Test Flight AS-203, NASA-MSFC Confidential Report MPR-SAT-FE-66-12, September 22, 1966.

BB-3.4.3-5-101

EVALUATION OF AS-203 LOW GRAVITY ORBITAL EXPERIMENT

Contributors: W. D. Ward
L. E. Toole
C. A. Ponder
M. E. Meadows
C. W. Simmons
J. H. Lytle
J. M. McDonald
B. M. Kavanaugh

Approved: O. S. Messner

O. S. Messner, Supervisor
Heat Transfer and Fluid Mechanics Group

Approved: M. C. Ziemke

M. C. Ziemke, Managing Engineer
Fluid Mechanics and Thermodynamics Research Section

Approved: W. M. Cannizzo

W. M. Cannizzo, Manager
Systems Simulation and Integration Branch

DISTRIBUTION

NATIONAL AERONAUTICS AND SPACE ADMINISTRATION

Marshall Space Flight Center

Mr. Wood	R-P&VE-PT	25
Mr. Cantrell	I-I/IB-E	1

CHRYSLER CORPORATION SPACE DIVISION

1. Huntsville Operations

J. D. Clifford	Dept. 4000	1
H. Bader, Jr.	Dept. 4800	1
W. M. Cannizzo	Dept. 4810	1
B. Maddox	Technical Library	2

2. Michoud Operations

A. F. Carlsen	Dept. 2732	1
R. W. Loomis	Dept. 2732	1
D. N. Buell	Dept. 2760	1
R. Ross	Dept. 2780	1
B. F. Elam	Dept. 2782	1
M. Holmes	Technical Library	2

3. Florida Operations

F. Morey	Technical Library	2